

University of South Bohemia in České Budějovice



Faculty of Science

Ph.D. Thesis

**Formation of Fe-S clusters in the mitochondrion of
*Trypanosoma brucei***

Piya Changmai

Supervisor: Prof. RNDr. Julius Lukeš, CSc.

Co-supervisor: RNDr. Eva Horáková, Ph.D.

Institute of Parasitology

Biology Centre of the Academy of Sciences of the Czech Republic

České Budějovice 2013

Changmai P. (2013) **Formation of Fe-S clusters in the mitochondrion of *Trypanosoma brucei***
Ph.D. thesis, in English - 144 pages, University of South Bohemia, Faculty of Science, České
Budějovice, Czech Republic

ANOTATION

This thesis focuses on iron sulfur (Fe-S) cluster biogenesis by the ISC machinery in the mitochondrion of *Trypanosoma brucei*. Most of proteins in the pathway show conserved functions, while some features are distinct from their counterparts in other organisms. We also show here the essentiality of the ISC machinery in bloodstream stage despite the fact that the parasites contain the rudimentary mitochondrion in this stage. The key player for the ISC export machinery, which is indispensable in the maturation of extra-mitochondrial Fe-S proteins, shows some extraordinary phenomena which may imply the moonlighting function of the protein. I also show preliminary data of an ongoing project concerning a putative heme transporter. The results indicate role in heme uptake of the protein, but further study is required to confirm the function of the protein.

DECLARATION

I hereby declare that I did all the work presented in this thesis by myself or in collaboration with co-authors of the presented papers and only using the cited literature.

České Budějovice, 5 September 2013

Piya Changmai

PROHLÁŠENÍ

Prohlašuji, že svoji disertační práci jsem vypracoval samostatně pouze s použitím pramenů a literatury uvedených v seznamu citované literatury. Prohlašuji, že v souladu s § 47b zákona č. 111/1998 Sb. v platném znění souhlasím se zveřejněním své disertační práce, a to - v úpravě vzniklé vypuštěním vyznačených částí archivovaných Přírodovědeckou fakultou - elektronickou cestou ve veřejně přístupné části databáze STAG provozované Jihočeskou univerzitou v Českých Budějovicích na jejích internetových stránkách, a to se zachováním mého autorského práva k odevzdanému textu této kvalifikační práce. Souhlasím dále s tím, aby toutéž elektronickou cestou byly v souladu s uvedeným ustanovením zákona č. 111/1998 Sb. zveřejněny posudky školitele a oponentů práce i záznam o průběhu a výsledku obhajoby kvalifikační práce. Rovněž souhlasím s porovnáním textu mé kvalifikační práce s databází kvalifikačních prací Theses.cz provozovanou Národním registrem vysokoškolských kvalifikačních prací a systémem na odhalování plagiátů.

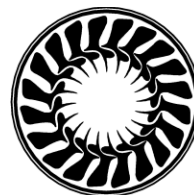
V Českých Budějovicích, 5. Zář 2013

Piya Changmai

This thesis originated from a partnership of Faculty of Science, University of South Bohemia, and Institute of Parasitology, Biology Centre of the ASCR, supporting doctoral studies in the Molecular and cell biology study program.



Přírodovědecká
fakulta
Faculty
of Science



Statement regarding contribution

The thesis is based on the following papers (listed chronologically):

- I. Paris, Z., Changmai, P., Rubio, M.A.T., Zíková, A., Stuart, K.D., Alfonzo, J.D., and Lukeš, J. (2010) The Fe/S cluster assembly protein Isd11 is essential for tRNA thiolation in *Trypanosoma brucei*. *J Biol Chem* **285**: 22394–22402. (IF = 4.651)

Piya Changmai participated in growth curve analysis, western blot analysis for localization, confirmation of RNAi and stabilization of the ISC proteins and membrane potential measurement. He also analyzed data, prepared figures for publication and revised the manuscript.

- II. Long, S., Changmai, P., Tsaousis, A.D., Skalický, T., Verner, Z., Wen, Y.-Z., *et al.* (2011) Stage-specific requirement for Isa1 and Isa2 proteins in the mitochondrion of *Trypanosoma brucei* and heterologous rescue by human and *Blastocystis* orthologues. *Mol Microbiol* **81**: 1403–1418. (IF = 4.961)

Piya Changmai participated in cloning and electroporation, growth curve analysis, western blot analysis, the aconitase and fumarase activities measurement in the human Isa rescue cell lines. He also did western blot analysis to confirm the down-regulation of both Isa proteins in the bloodstream stage. He analyzed the data and revised and prepared figures for the manuscript.

- III. Changmai, P., Horáková, E., Long, S., Černotíková-Stříbrná, E., McDonald, L.M., Bontempi, E.J., and Lukeš, J. (2013) Both human ferredoxins equally efficiently rescue ferredoxin deficiency in *Trypanosoma brucei*. *Mol Microbiol* **89**: 135-151. (IF = 4.961)

Piya Changmai did most of the experiments. He analyzed the data and wrote the manuscript.

- IV. Kovářová, J., Horáková, E., Changmai, P., Vancová, M., and Lukeš, J. Mitochondrial and nucleolar localization of cysteine desulfurase Nfs and the scaffold protein Isu in *Trypanosoma brucei*. *Eukaryot Cell* (submitted) (IF = 3.586)

Piya Changmai participated in western blot analysis (comparative amount of proteins in two stages and confirmation of Isu RNAi cells) and fumarase and aconitase activities measurement. Furthermore, he analyzed the data and revised the manuscript.

Julius Lukeš, the corresponding author of all mentioned papers, approves the contribution of Piya Changmai in these papers as described above.

.....
Prof. RNDr. Julius Lukeš, Csc.

Acknowledgements

I would like to thank Prof. Julius Lukeš, not only for the great opportunity to work in his lab, but also for his patience and valuable advice concerning science and life. It is one of the greatest things in my life. I very much appreciate the great guidance and favors of Eva Horáková, my life would be much more difficult without her. I also would like to thank all of the members in Jula's and Alča's labs for the friendship and the fabulous atmosphere in the lab, it is a great fun working and partying with you guys. I also thank all my friends for their friendships. I thank Jára Cimrman for an inspiration to live in České Budějovice. I would like to express my deep sense of gratitude to my family for love, understanding and supports. Last but not least, my thanks go to the Czech government for granting me a scholarship to learn the Czech language and to study here.

Contents

1. Summary	1
2. Overview	4
2.1 <i>Trypanosoma brucei</i>.....	4
2.1.1 Life cycle of <i>T. brucei</i>	4
2.1.2 <i>T. brucei</i> as a model organism for functional genomics	6
2.2 Iron-sulfur (Fe-S) cluster.....	7
2.2.1 Iron uptake in <i>T. brucei</i>	8
2.2.2 Fe-S cluster biogenesis by the ISC machinery.....	9
2.2.3 The ISC export machinery	11
2.2.4 The CIA machinery.....	12
2.3 Heme	13
2.3.1 Heme biosynthesis	14
2.3.2 Heme uptake	16
3. Results	
3.1 The Fe/S Cluster Assembly Protein Isd11 Is Essential for tRNA Thiolation in <i>Trypanosoma brucei</i>.....	18
3.2 Stage-specific requirement for Isa1 and Isa2 proteins in the mitochondrion of <i>Trypanosoma brucei</i> and heterologous rescue by human and <i>Blastocystis orthologues</i>	28
3.3 Both human ferredoxins equally efficiently rescue ferredoxin deficiency in <i>Trypanosoma brucei</i>	45
3.4 Mitochondrial and nucleolar localization of cysteine desulfurase Nfs and the scaffold protein Isu in <i>Trypanosoma brucei</i> (submitted to <i>Eukaryotic cell</i>).....	57

3.5	Functional analysis of putative heme transporter <i>TbHrg</i> in <i>T.brucei</i> (unpublished data)	101
3.6	Functional analysis of putative heme transporter <i>TbHrg</i> in <i>T.brucei</i>	127
4.	Conclusions	134
5.	References	135
6.	Curriculum vitae	144

Summary

Trypanosoma brucei, causative agent of sleeping sickness in humans and nagana in animals, is among important model organisms which are widely used by researchers. We take advantage of the availability of genome database and various molecular and genetic methods to explore functions of proteins and cellular mechanisms. While not available in flagellates such as *T. cruzi* and *Leishmania*, RNAi approach is feasible in *T. brucei*. Its convenience and effectiveness made it a method of choice for functional genomics. We exploit RNAi methodology in majority of this works, in order to get insight into the functions of the targeted genes.

Iron-sulfur (Fe-S) clusters are ancient cofactors which are essential for all domains of life. The number of studies of Fe-S clusters is rapidly growing, with newly discovered Fe-S proteins reported regularly each year. Eukaryotes have inherited the Fe-S biogenesis from their ancestral endosymbionts, namely the mitochondrial and plastidial part of ISC and SUF machineries. The cytosolic CIA machinery for maturation of extra-mitochondrial Fe-S proteins requires a key factor, which is produced by the ISC machinery in mitochondria and subsequently exported to the cytosol. My work concerns studies on the ISC machinery in *T. brucei* with Fe-S clusters maturation in the mitochondrion and subsequent export on unknown component(s) to the cytosol. Another project in progress is the study of a putative heme transporter in *T. brucei*. Heme is a prosthetic group which is an essential part of hemoproteins. Most organisms are able to synthesize heme, but not *T. brucei*, which as a heme auxotroph obtains it from the environment.

The cysteine desulfurase (Nfs) is a key player in the ISC machinery. It functions as a sulfur donor to the scaffold IscU. We studied functions of Isd11, a binding partner of Nfs, which is unique to eukaryotes. We showed tight interaction between Isd11, Nfs and IscU, with Isd11 stabilizing both Nfs and IscU. We demonstrated that Isd11 is essential for Fe-S clusters biosynthesis, as well as for the cytosolic and mitochondrial tRNA thiolation, unlike Mtu1, which affects only the latter one. **(Result 3.1- Paris *et al.*, 2010 JBC)**

Isa proteins are homologs of prokaryotic IscA, which are required for the maturation of mitochondrial [4Fe-4S] proteins such as aconitase and fumarase. Two homologs of Isa proteins were identified in *T. brucei* (*TbIsa1* and *TbIsa2*). Our results show that the depletion

of either *TbIsa1* or *TbIsa2* reduced cell proliferation. The defect was even more pronounced by simultaneous depletion of *TbIsa1* and *TbIsa2*, which indicated their functional redundancy. We showed that *TbIsa1* and *TbIsa2* are essential for maturation of mitochondrial [4Fe-4S] proteins, but not the cytosolic. The only known homologue of Isa in *Blastocystis hominis* was able to rescue growth and enzymatic activity of Fe-S proteins in *T. brucei*. Moreover, the expression of human Isa1, Isa2 and Isa1/2 was able to partially rescue enzymatic activities of the mitochondrial Fe-S proteins in *T. brucei*. **(Result 3.2 – Long *et al.*, 2011 MM)**

Fe-S cluster assembly on IscU requires electrons most likely from ferredoxin for the reduction of S⁰ to S²⁻. We identified two homologs of ferredoxin in *T. brucei*, designated *TbFdxA* and *TbFdxB*. Both ferredoxins are localized in the mitochondrion, but only *TbFdxA* has a role in the Fe-S clusters biosynthesis. The depletion of *TbFdxA* was lethal, while the depletion of *TbFdxB* was not. There was a discrepancy in previous studies about the relevance of human Fdx2 for the Fe-S clusters assembly. We expressed ectopic copies of both human ferredoxins (Fdx1 and Fdx2) in *TbFdxA* RNAi *T. brucei*, and showed their import into the mitochondrion and subsequent restoration of the growth together with the Fe-S protein activities. These data indicate that both human proteins are capable of functioning in the Fe-S clusters biogenesis. **(Result 3.3 – Changmai *et al.*, 2013 MM)**

T. brucei in bloodstream stage (BS) contains a rudimentary mitochondrion, which lacks most of the functions known for the organelle of the procyclic stage (PS). No data on the Fe-S clusters biogenesis in the BS stage were available, and Fe-S proteins in this compartment are either rare or overall missing. We overexpressed ectopic copies of aconitase and fumarase and found that the enzymatic activities of both enzymes were almost as high as in the PS. The result indicates that the Fe-S biogenesis functions effectively in this rudimentary organelle of the BS cells. As expected, Fe-S assembly proteins ferredoxin, frataxin, Isu and Nfs are localized in the mitochondrion, where the ISC machinery takes place. Unexpectedly, Isu and Nfs also localized in the nucleolus, where their function(s) remain unknown yet. It is probably not tRNA thiolation, since it was not affected in the Isu-depleted BS cells. **(Result 3.4 - Kovářová *et al.*, submitted to *Eukaryotic Cell*)**

Extra-mitochondrial Fe-S proteins require CIA machinery for their maturation. The machinery relies on an unknown compound (X), which is produced by the ISC machinery in mitochondria and exported to the cytosol, where it seems to function as a precursor for the pathway. The putative key player for the export machinery is Atm1, an ATP binding cassette (ABC) transporter. In this study we also investigate function(s) of Mdl, another ABC transporter which in *S. cerevisiae* exports the degraded polypeptides from the mitochondrial matrix. The overexpressed Mdl1 is able to reduce iron accumulation in the mitochondria of yeast Atm1 mutant. The depletion of either Atm1 or Mdl in *T. brucei* caused growth defect, but when Atm1 and Mdl were depleted simultaneously, the cells proliferate normally. Atm-depleted cells had compromised enzymatic activities of the Fe-S proteins in the cytosolic but not the mitochondrial fraction. While the ablation of Mdl had no effect on the Fe-S cluster proteins, the data suggest a role in an intermediate step between the ISC and the CIA machinery. Interestingly, the simultaneous depletion of Atm1 and Mdl did not alter enzymatic activities either. We are currently further analyzing this intriguing phenomenon also in yeasts by generating the double Δ Atm1+Mdl2. **(Result 3.5 – Changmai *et al.*, manuscript in prep.)**

Since *T. brucei* is a heme auxotroph, it needs to take up heme from an external source. Heme acquisition mechanism in the procyclic stage of *T. brucei* is still unknown. We have chosen a *T. brucei* homolog of the putative heme transporter from *Leishmania amazonensis* and designated it *TbHrg*. We employed RNAi to investigate his its function in both life cycle stages of *T. brucei*. In PS the depletion of *TbHrg* did not cause growth defect when cells were grown in high heme medium, but in low heme medium cells exhibited reduced proliferation. Heme B was decreased in both the high as well as low heme medium, with more pronounced phenotype in the latter one. This project is still in progress, more experiments are required to get insight the function(s) of *TbHrg* in both life cycle stages of *T. brucei*. **(Result 3.6– Changmai *et al.*, unpublished data.)**

2. Overview

2.1. *Trypanosoma brucei*

T. brucei is a parasitic protist that causes African trypanosomiasis, namely sleeping sickness in humans and nagana in animals. There are three sub-species that cause variants of trypanosomiasis in Africa.

i./ *T. brucei gambiense* is found in west and central Africa. This sub-species causes chronic trypanosomiasis in humans, which makes up over 98 % of the reported cases of sleeping sickness. People can be infected for years without any symptoms. The symptoms can emerge when the parasite has already passed through the blood-brain barrier to invade and damage the central nervous system.

ii./ *T. brucei rhodesiense* is found in eastern and southern Africa. *T. b. rhodesiense* causes acute trypanosomiasis in humans, which constitutes under 2% of the report cases of sleeping sickness. Symptoms emerge after a few weeks or months of infection.

iii./ *T. brucei brucei* causes nagana or animal African trypanosomiasis. This particular sub-species is not able to infect humans due to Trypanosome lytic factor which is present in humans and some other primates as innate immunity. *T. b. brucei* is widely used as a model organism in laboratory.

African trypanosomiasis is transmitted by an insect vector the tsetse fly. There are around 70 million people who live in the risk area of infection. In 1998, there were around 40,000 reported cases, but the actual number of infections was estimated to be 300,000. In 2005 after active surveillance and the Pan African Tsetse and Trypanosomiasis Eradication Campaign, the newly reported decreased to 17,616, and the actual number of cases was estimated to be between 50,000 – 70,000. Newly reported cases in 2012 reached 7,197. Nowadays, in many countries like Gambia, Namibia, Niger, Togo and more, transmission has apparently been stopped. Tight regulation and surveillance has resulted in shrinking the number of new infection cases (<http://www.who.int/mediacentre/factsheets/fs259/en/>).

2.1.1 Life cycle of *T. brucei*

During the digenetic lifecycle in the mammalian bloodstream and in the insect vector, *T. brucei* undergoes a change in morphology and biochemical mechanisms in

order to adapt itself to the significantly different environment (Fig. 1.). In the procyclic stage (PS; in the midgut of tsetse fly), *T. brucei* relies mainly on carbon sources from amino acids, especially L-proline, for energy production, even though it prefers glucose in a glucose rich environment (Bringaud *et al.*, 2006). Since its mitochondrion at this stage is fully active, the organelle accommodates both substrate-level and oxidative phosphorylation for production of ATP. In the bloodstream stage (BS), the parasite relies on glycolysis for ATP production. Although in this stage the morphology and most functions of the mitochondrion are repressed, the trypanosome alternative oxidase (TAO) is fully active (Besteiro *et al.*, 2005; Chaudhuri *et al.*, 2006). The ATP synthase complex (mitochondrial respiratory complex V) in this stage has an unconventional function, it pumps protons out of the matrix at the expense of ATP hydrolysis in order to maintain the mitochondrial membrane potential (Schnauffer *et al.*, 2005).

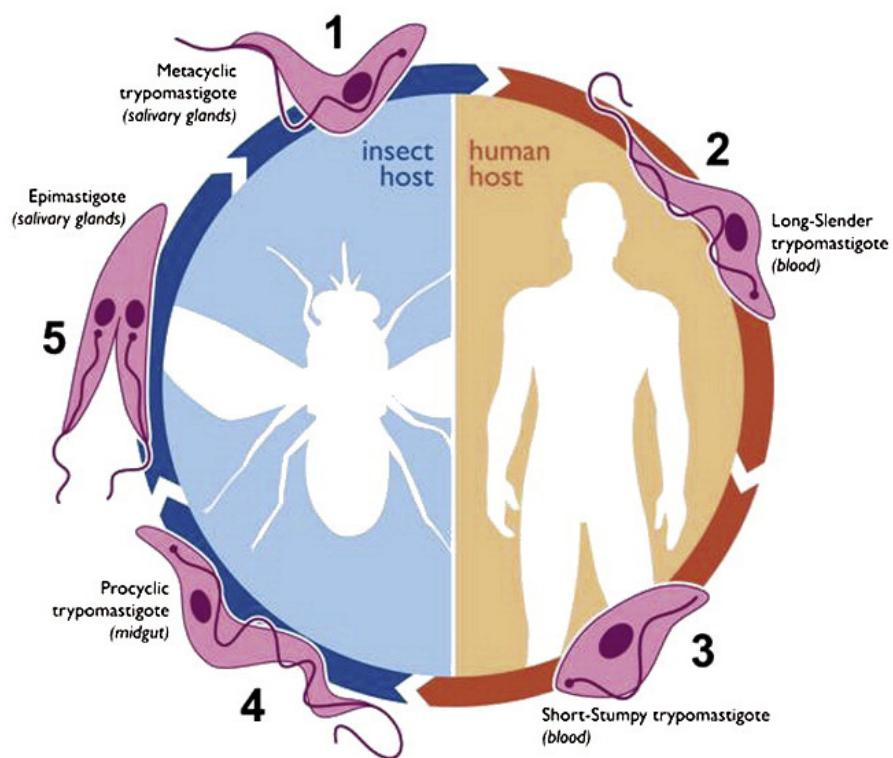


Fig. 1. Life cycle of *T. brucei* (Cuervo *et al.*, 2010)

T. brucei along with other trypanosomatids has several distinctive features. They contain a single large mitochondrion with a complex network of circular DNA. More than half of mitochondrial mRNAs undergo post-transcriptional RNA processing, so called RNA-editing, which an enormous number of uridine residues

(Us) is inserted or deleted in order to generate start/stop codons and translatable sequences (Lukeš *et al.*, 2005). Apart from these unusual features in the mitochondrion, trypanosomatids nuclear DNA is uniquely transcribed in clusters of genes as polycistronic pre-mRNA which subsequently undergo *trans*-splicing and polyadenylation in order to generate translatable mRNA (Clayton, 2002). Another notable feature is the ability to produce a Variant Surface Glycoprotein (VSG) coat which helps the parasites to evade the host's immune system (Thon *et al.*, 1990; Pays, 2005).

2.1.2 *T. brucei* as a model organism for functional genomics

The completion of the *T. brucei* genome sequencing and freely available data have allowed us to study the organism with various methods. Gene knockout by homologous recombination is a powerful approach to study the function of target genes (Gaud *et al.*, 1997). Yet, due to technical complications and limitations, this gene knockout technique may not be the first method to choose for the study of the gene of interest. *T. brucei* is diploid and multicopy genes require different combinations of selectable markers and multiple rounds of transfection. When the gene of interest is essential for cell survival, its regulatable ectopic expression is needed before disruption of the second allele. When the expression of the ectopic copy is not sufficient, the cells with disruption of two alleles are not available. Gene knockdown by RNAi overcomes these complications and some limitations of the homologous recombination gene knockout method. The RNAi approach is able to down regulate many different genes at the same time and an expression of multicopy genes can be eliminated at once. Moreover, RNAi cell lines are easy to generate and the down regulation is slow enough to let us study the intermediate phenotype before the death of the cells. The cell lines that are widely used for RNAi generation and ectopic copy expression are the strain 29-13 in procyclic stage (PS) and the strain Lister 427 (cell line 90-13) in bloodstream stage (BS) (Wirtz *et al.*, 1999). These cell lines constitutively express T7 polymerase and the tetracycline repressor genes (Wickstead *et al.*, 2002). These cell lines are used in combination of RNAi vectors containing the T7 opposing promoters under the control of tetracycline operators. When tetracycline is absent, the tet repressor binds to the tet operators downstream of the opposing T7 promoters and transcription does not occur. In the presence of

tetracycline, the tetracycline repressor is released from the tetracycline operator and binds to tetracycline. This event results in transcription of double stranded RNA by T7 polymerase, followed by the RNAi mechanism which degrades the mRNA of the target gene(s) (Wang, 2000).

2.2. Iron-sulfur (Fe-S) cluster

Iron-sulfur (Fe-S) clusters are ancient prosthetic groups which are essential for many forms of life. In a typical cell, there are more than a hundred proteins, so called iron-sulfur proteins (Fe-S) proteins, which require one or more Fe-S clusters for their function. Iron-sulfur proteins have different roles in cellular processes, such as DNA replication (DNA polymerases (Netz *et al.*, 2011), primase (Klinge *et al.*, 2007)), tricarboxylic acid cycle (aconitase (Suzuki *et al.*, 1976)), oxidative phosphorylation (mitochondrial respiratory complexes I-III (R Cammack, 1977; Mauro Degli Esposti, 1985), tRNA modification (Alfonzo and Lukeš, 2011) and many more (for review see Stehling and Lill, 2013). Iron-sulfur clusters have a variety of functions such as electron transfer, due to ability of iron to switch oxidation state Fe^{2+} (Ferrous) and Fe^{3+} (Ferric) (Beinert, 1997), they act as a Lewis acid in aconitase (Beinert *et al.*, 1996), as sulfur donor (Booker *et al.*, 2007) and have probably other as yet undescribed functions.

Ferredoxin from *Clostridium pasteurianum* was the first known Fe-S protein to be investigated (Mortenson *et al.*, 1962; Flannery *et al.*, 2011). The most common structure of Fe-S clusters are rhombic [2Fe-2S] and cubane [4Fe-4S] (Beinert, 1997; Goldberg *et al.*, 2008). Iron sulfur clusters are able to assemble into apoproteins spontaneously in a constructive chemical condition *in vitro* (Malkin and Rabinowitz, 1966), however, Fe-S biogenesis in living organisms require complex mechanisms and regulation.

In prokaryotes, there are three machineries of Fe-S cluster biogenesis; i/ the NIF (**n**itrogen **f**ixation) machinery, which is found in nitrogen-fixing bacteria, ii/ the SUF (**s**ulfur mobilization) machinery and iii/ the ISC (**i**ron-**s**ulfur **c**luster) machinery (Py and Barras, 2010). Both ISC and SUF machineries are present in *Escherichia coli*, where the ISC machinery is used under normal conditions, while the SUF machinery is used when cells are under oxidative stress and also in iron depleted conditions. When each ISC or SUF is disrupted, major defects cannot be observed, but

spontaneous loss of both machineries causes cell death (Takahashi and Tokumoto, 2002). *E. coli* lacking ISC and SUF were rescued by heterogeneous expression of nifSU-like operon genes from *Helicobacter pylori* (Tokumoto, 2004). In eukaryotes, mitochondria have inherited the ISC machinery from their α -proteobacterial endosymbiotic ancestor. Eukaryotes which contain mitochondrion-derived organelles, such as hydrogenosomes (for example *Trichomonas vaginalis*) and mitosomes (for example *Giardia intestinalis*), have also retained Fe-S biogenesis. As eukaryotes with fully functional mitochondria, most of them harbor α -proteobacterial ISC machinery. The exceptions known so far are *Entamoeba histolytica* and *Mastigamoeba balamuthi*, in which orthologous proteins of the ISC and SUF machineries are absent (Ali *et al.*, 2004; Gill *et al.*, 2007). Instead, they contain orthologs from the NIF machinery which is believed to have been acquired by lateral gene transfer from an ancestor of ϵ -proteobacteria (Ali *et al.*, 2004; Nývltová *et al.*, 2013). Plastids have retained SUF machinery. Since apicoplast is a secondary endosymbiont which originated from engulfed green algae, it has inherited SUF machinery. The SUF machinery most likely provide the clusters to Fe-S proteins in variant biochemical pathways such as IspG and IspH in the isoprenoid biosynthesis pathway and ferredoxin in Fe-S cluster biogenesis itself (Seeber and Soldati-Favre, 2010). The function of SUF machinery is needed to be proved experimentally. SufB, a putative scaffold protein of the SUF machinery, is predicted to be encoded in apicoplast. A nuclear encoded protein SufC, a putative component of SUF machinery, was shown to be targeted to apicoplast. The protein is shown to interact with a nuclear encoded protein SufC. SufC was reported to have ATPase activity and interacts with SufB (Kumar *et al.*, 2011).

2.2.1 Iron uptake in *T. brucei*

T. brucei BS acquires iron through transferrin-receptor mediated endocytosis, while it uses different mechanism in PS (Ligtenberg *et al.*, 1994). *T. brucei* PS uptakes iron from complexes by electrochemically reducing ferric (Fe^{3+}) iron to ferrous (Fe^{2+}) iron, then the ferrous iron is transported to the cells (Mach *et al.*, 2013). The exact iron transporter in PS is still unknown. Mach *et al.*, (2013) identified putative divalent metal transporters with ZIP (ZRT, IRT-like Protein) domain (Guerinot, 2000) (TritypDB accession numbers Tb11.01.0720; Tb11.01.0770;

Tb11.01.0760; Tb11.01.0730; Tb11.01.0725) and a ferric reductase homolog (Tb11.02.1990). In *Leishmania amazonensis*, the plasma membrane ferric reductase (LFR1) electrochemically reduces extracellular ferric iron to ferrous iron, which is subsequently transported into the cells by the ZIP family transporter LIT1 (*Leishmania* iron transporter 1) (Huynh *et al.*, 2006). This mechanism of iron uptake is likely to be active under iron deprived condition, since LFR1 and LIT1 are not needed when iron is excess (Flannery *et al.*, 2011).

2.2.2 Fe-S clusters biogenesis by the ISC machinery

In eukaryotes the ISC machinery is confined in mitochondrion. Nevertheless some of the ISC proteins have been found in the cytosol of *Trachipleistophora hominis* (Goldberg *et al.*, 2008) and mammalian cells (Tong and Rouault, 2006). In mammalian cells, cytosolic IscU (see below) is able to recover cytosolic Fe-S protein maturation after oxidative damage and iron chelation (Tong and Rouault, 2006). However, its role in *de novo* Fe-S synthesis is unlikely, since expression of its binding partner Nfs (see below) in the cytosol in the absence of the mitochondrial counterpart can maintain Fe-S protein activities neither in the cytosol nor the mitochondria (Biederbick *et al.*, 2006).

In the ISC synthetic pathway (Fig. 2.), Fe-S clusters are assembled on the scaffold proteins IscU (bacteria) or Isu1 (*S. cerevisiae*). Cysteine desulfurase usually termed IscS in bacteria and Nfs in eukaryotes represents the sulfur donor. This enzyme converts cysteine to alanine in order to release sulfur, which then forms a disulfide bond on a conserved cysteine residue of the enzyme and is subsequently transferred to the scaffold protein (Kispal *et al.*, 1999). In mitochondria, cysteine desulfurase exists as a complex of Nfs and Isd11. The latter being a eukaryotic invention with no homolog in prokaryotes. Isd11 is present in all eukaryotic supergroups, including protists with mitosomes or hydrogenosomes. These data further support the widely accepted view of a shared ancestor between mitochondria and mitochondrion-like organelles (Adam *et al.*, 2006; Richards and van der Giezen, 2006). Even though Nfs has desulfurase activity and is able to function solely without Isd11 *in vitro*, Isd11 is needed for the assembly of Fe-S clusters on the scaffold protein *in vivo* (Wiedemann *et al.*, 2006). The relevance of Isd11 to cysteine

desulfurase activity is unknown, but Isd11 clearly has a role in stabilizing Nfs (Paris *et al.*, 2010).

The exact iron donor of the ISC machinery remains unclear. frataxin or a complex of glutathione and glutaredoxin was proposed to be the source of iron for the Fe-S cluster assembly (Yoon and Cowan, 2003; Qi *et al.*, 2012). Studies *in vitro* indicate that frataxin has a regulatory role in the Fe-S cluster formation, as bacterial frataxin (CyaY) acts as their inhibitor (Iannuzzi *et al.*, 2011) while human frataxin acts as an enhancer (Tsai and Barondeau, 2010). Ferredoxin, labeled Fdx in bacteria and or Yah1 in *S. cerevisiae*, is a putative electron donor of electrons for reduction of S^0 in cysteine to S^{2-} in the Fe-S clusters. Ferredoxin receives electrons from ferredoxin reductase where NADH is original source of electrons (Kakuta *et al.*, 2001; Mühlhoff, 2003).

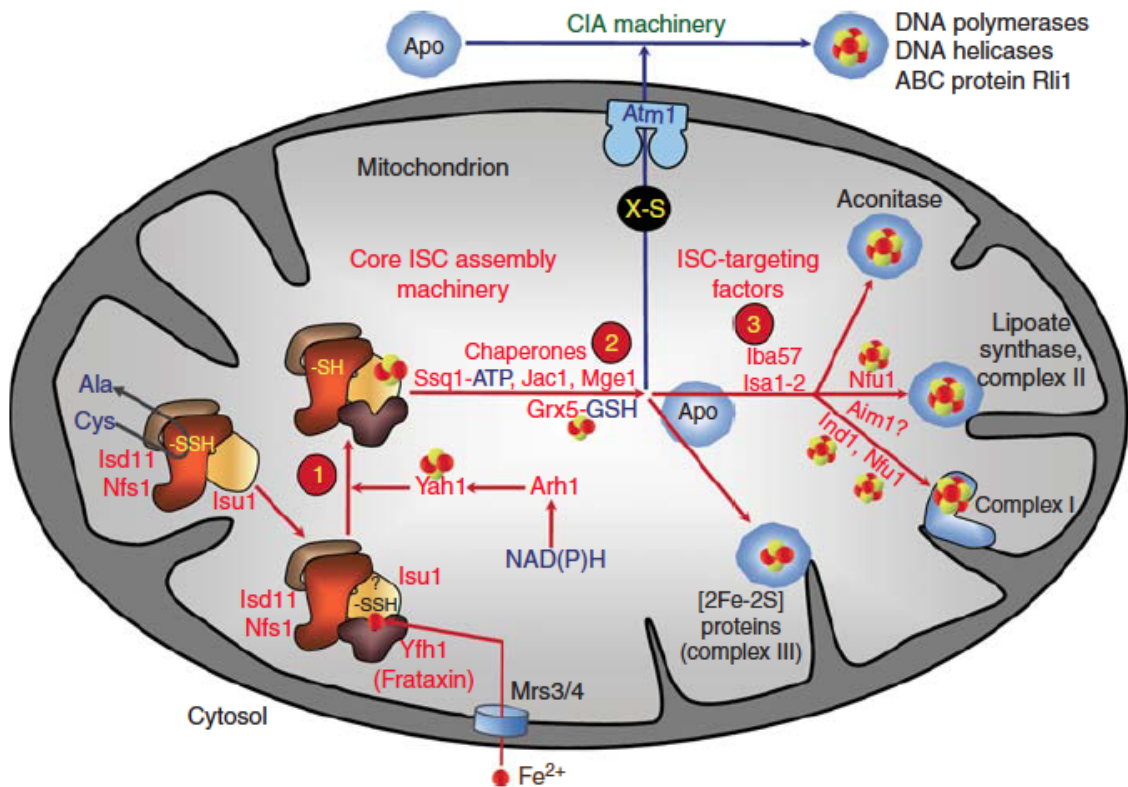


Fig. 2. Scheme of ISC machinery in *S. cerevisiae* (Stehling and Lill, 2013)

Fe-S proteins require incorporation of clusters from the scaffold to their apo forms. In mitochondria of *S. cerevisiae*, Jac1 (DnaJ-like cochaperone; in bacteria HscB) binds to Isu1 and subsequently recruits the ATP-bound Ssq1 (Hsp70 ATPase; in bacteria HscA) to interact at the conserved LPPVK loop of Isu1. Next, ATP on

Ssq1 is hydrolyzed, which is followed by dissociation of the Fe-S cluster from Isu1. The nucleotide exchange factor Mge1 exchanges on Ssq1 ADP with ATP, then the ATP-bound Ssq1 is disassembled from apo-Isu1, which is ready for the next round. The dissociated Fe-S cluster from Isu1 may be directly transferred to apoprotein or to mitochondrial monothiol glutaredoxin Grx5. The Fe-S cluster may transiently bind to Grx5, and is then transferred to apo-proteins. Grx5 is not essential for viability in *S. cerevisiae*, but it is indispensable in humans and zebrafish (Wingert *et al.*, 2005; Camaschella *et al.*, 2007; Rodríguez-Manzanares *et al.*, 2002; Ye *et al.*, 2010). Some Fe-S proteins, especially those that contain the [4Fe-4S] cluster, require additional factors for its transfer Fe-S cluster to apoproteins. The tetrahydrofolate-binding protein Iba57 as well as Isa1 Isa2 are responsible for the maturation of Fe-S proteins in the aconitase superfamily. How these proteins help in the conversion of [2Fe-2S] clusters to [4Fe-4S] cluster and which mechanism they use for integration of [4Fe-4S] cluster into apoproteins is still unclear.

2.2.3 The ISC export machinery

Cytosol and the nucleus house innumerable Fe-S proteins, which are essential for viability and involved in crucial metabolic functions. In spite of the presence of a eukaryote-only cytosolic iron-sulfur protein assembly (CIA) machinery dedicated to the maturation of extra-mitochondrial Fe-S proteins, it still requires an unknown sulfur containing substrate “X” from mitochondria. The key player, Atm1, an ATP-binding cassette transporter localized in the mitochondrial inner membrane, links the mitochondrial and cytosolic Fe-S assembly. The C-terminal end and the nucleotide binding domain are exposed to the mitochondrial matrix which is the site for ATP binding and hydrolysis (Chaloupková *et al.*, 2004). It has been shown *in vitro* that thiol-containing compounds are able to stimulate the ATPase activity of Atm1 which implies that the “X” component probably contains sulfur (Kuhnke *et al.*, 2006). Apart from the role in Fe-S clusters biogenesis, “X” might have a role in iron sensing and homeostasis, since the depletion of Atm1 causes a hyperaccumulation of iron in mitochondria of humans, mice and *S. cerevisiae* in aerobic condition (Pondarre, 2006; Cavadini *et al.*, 2007; Miao *et al.*, 2009). In contrast to these organisms, depletion of Atm1 homolog in *S. cerevisiae* in anaerobic condition and in *Arabidopsis thaliana* does not elevate level of iron in mitochondria (Bernard *et al.*, 2009; Miao *et al.*,

2009). Based on these results it is evident that the role of Atm1 in iron homeostasis is species specific and cultivating condition-dependent. The sulfhydryl oxidase Erv1 and the tripeptide glutathione were suggested to assist Atm1 in export, since the depletion of Erv1 and/or glutathione disrupts the maturation of extra-mitochondrial Fe-S proteins and triggers hyperaccumulation of iron in mitochondria of *S. cerevisiae* which mimics the phenotype in Atm1 depleted cells (Lange *et al.*, 2001; Sipos, 2002).

2.2.4 CIA machinery

The CIA machinery initiates with a transiently assembled [4Fe-4S] cluster on the P-loop NTPase Cfd1 and Nbp35 forming a heterotetrameric scaffold complex. The [4Fe-4S] cluster bridge Cfd1 and Nbp35 at the conserved C-terminal motif (Netz *et al.*, 2012). This step requires sulfur from the ISC machinery via the ISC export machinery. The nucleotide binding domains of these scaffold proteins are also crucial for the integration of the clusters to the Cfd1-Nbp35 complex (Netz *et al.*, 2012). *Arabidopsis thaliana* possesses the Nbp35 homolog but not Cfd1. Nbp35 homolog of *A. thaliana* is able to partially complement growth of *S. cerevisiae* lacking Cfd1, but not the Nbp35 (Bych *et al.*, 2008). Nbp35 has another [4Fe-4S] cluster which is constantly bound at the amino terminus. This binding requires an electron from the Fe-S protein Dre2. The electron is transferred from the electron source NADPH to Dre2 through a flavin-containing oxidoreductase Tah18. When yeast was exposed to H₂O₂, the GFP tagged version of Tah18 was relocalized to mitochondria and caused cell death. GFP-tagged Tah18 itself, under normal condition, did not trigger cell death, as cells were viable when the protein was artificially localized to mitochondria in the absence of H₂O₂. Overexpression of Dre2-Tah18 fusion protein reduced susceptibility to H₂O₂ (Vernis *et al.*, 2009). The Cfd1-Nbp35 complex assists the maturation of Nar1, which contain a Fe-S cluster itself. Nar1 acts as an intermediate between the scaffold Cfd1-Nbp35 complex and the CIA targeting complex (Cia1, Cia2 and Mms19) since the depletion of Nar1 does not affect the integration of Fe-S clusters on the Cfd1-Nbp35 complex, but the depletion of either Cfd1 or Nbp35 interrupts binding of Fe-S clusters to Nar1 (Netz *et al.*, 2007). The depletion of Cia1 does not alter the assembly of Fe-S clusters into Nar1 (Balk *et al.*, 2005) proving the downstream position of Cia1 in the pathway. Humans have two homologs of Nar1, namely IOP1 and IOP2. IOP1 has a role in the CIA machinery, while IOP2 most

likely not (Song and Lee, 2008). IOP2 is localized in the nucleus and interacts with prelamin A, but its exact function is still unknown (Barton and Worman, 1999). Subsequently, Fe-S clusters require the CIA targeting complex in order to be conveyed to the target apoproteins. Cia1 is essential for the maturation of all extramitochondrial Fe-S proteins which were examined so far, apart from the Fe-S proteins involved in the previous steps of the CIA machinery (Balk *et al.*, 2005). Cia1, the human homolog of Cia1, is able to complement its homolog in *S. cerevisiae* in the maturation of Fe-S proteins (Srinivasan *et al.*, 2007). Mms19 has an influence on RNA polymerase II transcription and nucleotide excision repair by regulating level of subunit Rad3 of the transcription factor II H (Kou *et al.*, 2008; Lauder *et al.*, 1996). In humans, Mma19 forms complex with XPD (human homolog of Rad3), MIP18, Cia1 and ANT2 contributing in chromosome segregation (Ito *et al.*, 2010). Mms19 interacts with various Fe-S proteins and also incorporates Fe-S clusters to the proteins associated to DNA metabolism (Gari *et al.*, 2012; Stehling *et al.*, 2012). Cia2 is a component of the CIA targeting complex required for maturation of Fe-S proteins. Humans have two homologs of Cia2, namely CIA2A (FAM96A) and CIA2B (FAM96B). The complex of CIA2B-CIA1-MMS19 has a role behind the maturation of most extramitochondrial Fe-S proteins, while CIA2A-CIA assists the maturation of iron regulatory protein 1 engaged in iron homeostasis. Additionally, CIA2A also binds and stabilizes the iron regulatory protein 2 which is not an Fe-S protein (Stehling *et al.*, 2013).

2.3. Heme

Heme is an important prosthetic group, which consists of a porphyrin ring with tightly bound iron in the center. Proteins that contain heme group, known as hemoproteins, participate in many different cellular processes. Due to the presence of heme iron in either oxidized or reduced state, they can participate in electron transport and redox reactions. Hemoglobin belongs to one of the best known hemoproteins, which has a role in oxygen transport in vertebrates (Perutz, 1942). Heme, is also a cofactor of the mitochondrial respiratory complexes II thru IV including cytochrome *c*. Further than cytochrome P450, which participate in drug metabolism and sterol biosynthesis (Anzenbacher and Anzenbacherova, 2001; Schenkman and Jansson, 2003), catalase converting hydrogen peroxide to water and oxygen (Chelikani *et al.*,

2004) to name just a few from many existing hemoproteins. Heme itself is toxic since it is triggering oxidative stress (Toh et al., 2010). Parasites which feed on blood or live in bloodstream requires some mechanism for detoxification, because the excess of heme is lethal for them (Pal and Joshi-Purandare, 2001). Heme oxygenase is able to degrade heme to biliverdin, iron and carbon monoxide, which are less reactive. Heme oxygenase-like protein was found in *Plasmodium falciparum*, which is likely one of mechanisms that protects cells from heme oxidative damage (Okada, 2009). In humans, heme has an ability to regulate its biosynthesis by feedback inhibition. It represses ALA synthase 1 by reducing its transcription and translation, destabilizing mRNA and inhibiting mitochondrial transportation of the protein. Heme also stimulates its degradation by expressing heme oxygenase 1 (for review see Furuyama et al., 2007). The only known eukaryote, which does not require heme for viability is *Phytomonas serpens* (Kořený et al., 2012). The lack of heme does not affect level and enzymatic activity of respiratory complex II. Moreover, the ergosterol, which requires heme for its biosynthesis, is not formed and lanosterol is instead incorporated into the membrane.

2.3.1 Heme biosynthesis

The heme biosynthesis pathway is conserved in all domains of life and most organisms are able to synthesize heme. Eukaryotes have obtained the heme biosynthesis pathway from bacterial endosymbiotic ancestor. The heme biosynthesis pathways differ in the substrates of the first precursor δ -aminolevulinic acid (ALA). α -proteobacteria and most non-photosynthetic eukaryotes produce ALA from glycine and succinyl-CoA by ALA-synthase (Duncan et al., 1997), while in photosynthetic eukaryotes and most prokaryotes, ALA is synthesized from glutamate (Beale, 1999). The remaining steps of the pathway are conserved in all organisms. In humans, heme biosynthesis pathway takes place in both cytosol and mitochondria. ALA is synthesized in mitochondria, then is exported by an unknown mechanism to cytosol probably by ABCB10 transporter (Bayeva et al., 2013). After several enzymatic steps, coproporphyrinogen III is imported back to mitochondria probably via ABCB6 (Krishnamurthy et al., 2006). Later protoporphyrin IX is formed and in the next step iron is added by ferrochelatase to form heme., The whole pathway is confined to

chloroplasts in most of the photosynthetic eukaryotes (Beale, 1999). In *Chromera velia*, ALA is produced in the mitochondrion, then transported to the photosynthetic plastid where the rest of the pathway takes place. In apicomplexans, the initial step takes place in the mitochondrion, the further steps are in apicoplast followed by cytosol and the last step is back in the mitochondrion (Kořený *et al.*, 2011).

T. brucei fully lost enzymes from the heme biosynthesis pathway, unlike *Leishmania*, which retains last three enzymes. It allows them to grow in the medium lacking heme, but with the addition of protoporphyrin IX (Sah *et al.*, 2002). It was proposed that *Leishmania* has obtained the last three enzymes by horizontal gene transfer from γ -proteobacterium (Kořený *et al.*, 2010).

Some insect Trypanosomatids such as *Blastocrithidia culicis* and *Crithidia oncopelti* have endosymbiotic bacteria, which synthesize and provide heme for them and allow them to grow in a chemically defined medium without heme. The flagellates lacking bacterial endosymbionts require an additional heme or protoporphyrin IX for their growth (K P Chang, 1975). Heme auxotroph organisms have evolved mechanisms to acquire heme from the environment (see below, section 1.3.2).

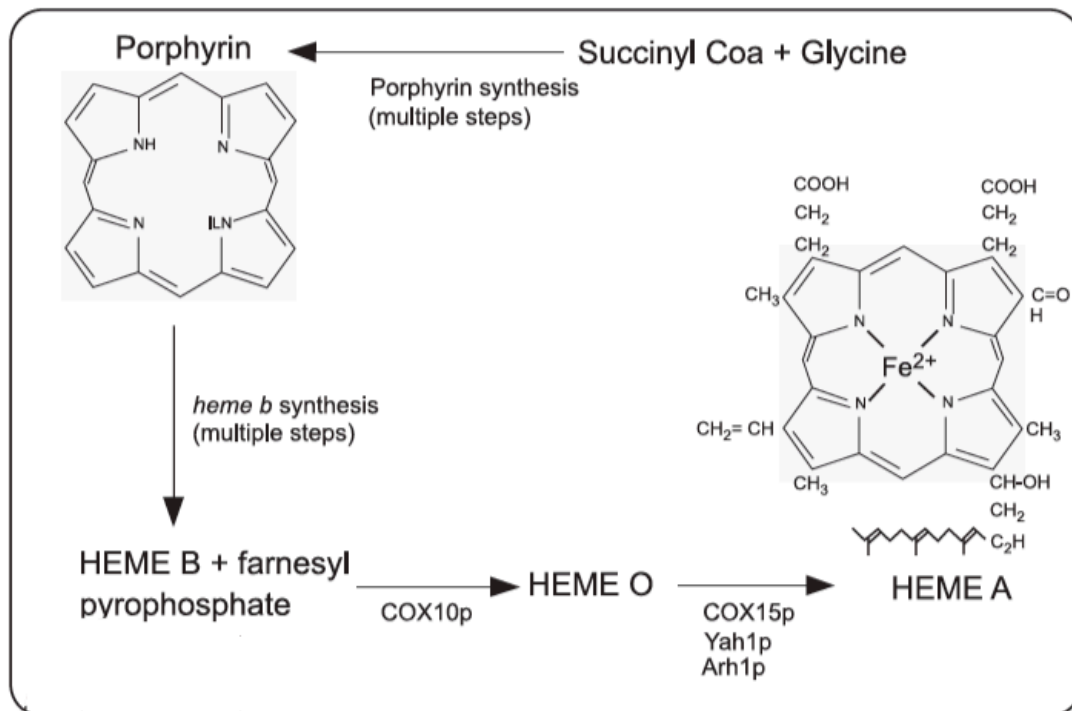


Fig. 3. Heme A synthesis in *S. cerevisiae* (Moraes *et al.*, 2004)

Heme A is an essential cofactor of cytochrome *c* oxidase (respiratory complex IV) and its biosynthesis is confined to the mitochondrion. The pathway starts after heme B is synthesized/imported, then Cox10 converts the vinyl group on pyrrole ring A into a 17-hydroxyethylfarnesyl moiety, resulting in heme O (Saiki *et al.*, 2002.). In the next step, Cox15 along with ferredoxin and ferredoxin reductase converts the methyl group on pyrrole ring D into an aldehyde, resulting in heme A (Fig. 3.) (Barros, 2002; Changmai *et al.*, 2013).

2.3.2 Heme uptake

There are organisms which completely or partially lost the heme biosynthesis pathway, such as *Caenorhabditis elegans* (Rao *et al.*, 2005), tick (Braz *et al.*, 1999) or Trypanosomatids (for review see Kořený *et al.*, 2010).

Free-living worm *C. elegans* acquires heme from soil bacteria in nature or from dietary source (Rao *et al.*, 2005). Heme is also an iron source for *C. elegans* in low iron environment (Rao *et al.*, 2005). **H**eme **r**esponsive **g**ene-4 (Hrg-4) along with its three paralogs (Hrg-1, Hrg-5 and Hrg-6) was identified by genome search. Hrg-4 and Hrg-1 are up-regulated in low heme condition, while Hrg-5 and Hrg-6 express constitutively (Rajagopal *et al.*, 2008). Hrg-1 has orthologs in vertebrates, but the others are nematode-specific. All paralogs are able to rescue the growth of *hem1Δ S. cerevisiae*, a yeast strain which lacks first enzyme of heme biosynthesis pathway, meaning they all can transport heme (Yuan *et al.*, 2012). According to their localization, Hrg-4 was proposed to take up heme through plasma membrane, while Hrg-1 transports heme from endosome/lysosome related organelle (Rajagopal *et al.*, 2008). The human homolog of Hrg-1 has an important role in heme and iron recycling. Human Hrg-1 is located on the phagolysosomal membrane transports free heme, from phagolysosomal lumen to the cytosol (White *et al.*, 2013). Heme can be further incorporated into hemoglobin, exported or degraded by heme oxygenase 1 and 2 in order to release iron (White *et al.*, 2013).

Leishmania donovani seems to have another mechanism to acquire heme. Hemoglobin (Hb) is endocytosed through a 46-kDa receptor on the flagellar pocket, and then degraded in lysosomes to release heme for intracellular use (Sengupta *et al.*, 1999; Krishnamurthy *et al.*, 2005). *L. donovani* with defective LdRab7 regulating Hb transport to the late degradative compartment, was rescued by the addition of hemin

(Patel *et al.*, 2008). These data implies, that *L. donovani* may acquire heme by two different mechanisms. In other words, it may import free heme through a heme transporter or internalizes Hb through endocytosis.

The BS *T. brucei* flagellates takes up heme through a haptoglobin-hemoglobin receptor (TbHpHbR), a glycoprotein receptor which is exclusively expressed in BS (Vanhollebeke *et al.*, 2008). TbHpHbR is localized close to the flagellar pocket and kinetoplast. In primates, there is a haptoglobin-related protein (Hpr) which can also bind to hemoglobin (Hb). Hp-Hb or Hpr-Hb complexes bind TbHpHbR and are subsequently internalized to serve as a heme source of hemoproteins in *T. brucei* (Vanhollebeke *et al.*, 2008). This mechanism is like a double-edged sword, although it acquires heme for the cell, it also takes up trypanosome lytic factor 1 (TLF-1) which kills the parasite.

The mechanism of heme uptake in *T. brucei* PS is still elusive. In this study we have chosen a putative candidate, which is a homolog of heme transporter from *Leishmania amazonensis*, LHR1 (Huynh *et al.*, 2012).

3. Results

3.1 The Fe/S Cluster Assembly Protein Isd11 Is Essential for tRNA Thiolation in *Trypanosoma brucei*

(reprint of The Journal of Biological Chemistry 285: 22394-22402)

The Fe/S Cluster Assembly Protein Isd11 Is Essential for tRNA Thiolation in *Trypanosoma brucei*^{*,§}

Received for publication, November 10, 2009, and in revised form, April 13, 2010. Published, JBC Papers in Press, May 4, 2010, DOI 10.1074/jbc.M109.083774

Zdeněk Paris[‡], Piya Changmai[‡], Mary Anne T. Rubio[§], Alena Zíková^{‡¶}, Kenneth D. Stuart[¶], Juan D. Alfonzo[§], and Julius Lukeš^{‡¶1}

From the [‡]Biology Centre, Institute of Parasitology, Czech Academy of Sciences, and Faculty of Sciences, University of South Bohemia, 37005 České Budějovice (Budweis), Czech Republic, the [§]Department of Microbiology and Ohio State University Center for RNA Biology, The Ohio State University, Columbus, Ohio 43210, and the [¶]Seattle Biomedical Research Institute, Seattle, Washington 98109

Fe/S clusters are part of the active site of many enzymes and are essential for cell viability. In eukaryotes the cysteine desulfurase Nfs (IscS) donates the sulfur during Fe/S cluster assembly and was thought sufficient for this reaction. Moreover, Nfs is indispensable for tRNA thiolation, a modification generally required for tRNA function and protein synthesis. Recently, Isd11 was discovered as an integral part of the Nfs activity at an early step of Fe/S cluster assembly. Here we show, using a combination of genetic, molecular, and biochemical approaches, that Isd11, in line with its strong association with Nfs, is localized in the mitochondrion of *T. brucei*. In addition to its involvement in Fe/S assembly, Isd11 also partakes in both cytoplasmic and mitochondrial tRNA thiolation, whereas Mtu1, another protein proposed to collaborate with Nfs in tRNA thiolation, is required for this process solely within the mitochondrion. Taken together these data place Isd11 at the center of these sulfur transactions and raises the possibility of a connection between Fe/S metabolism and protein synthesis, helping integrate two seemingly unrelated pathways.

Every extant archaeal, bacterial, and eukaryotic cell contains proteins whose functions depend on iron-sulfur (Fe/S) clusters. In a typical eukaryotic cell these ancient co-factors are part of more than 100 different proteins, the assembly of Fe/S clusters is invariably essential for viability. In particular, several mitochondrial proteins involved in electron transport, such as subunits of respiratory complexes I, II, and III, and ferredoxin contain numerous Fe/S clusters. Moreover, nuclear and cytosolic proteins, including the ribosomal protein Rli1, primase Pri2, and xanthine oxidoreductase, to name just a few, depend functionally on these co-factors (for recent reviews, see Refs. 1 and 2).

A key component of the Fe/S cluster assembly (ISC) machinery is the cysteine desulfurase (Nfs), which removes sulfur from cysteine, converting it into alanine (3). Nfs binds to a highly conserved scaffold protein termed IscU, forming a complex,

upon which the Fe/S cluster is assembled with the sulfur provided by Nfs and iron coming from an additional protein, likely frataxin (4, 5). However, the exact mechanism of cluster formation has yet to be fully understood. Somewhat unexpectedly, a third component of this Fe/S cluster assembly complex, a small protein named Isd11, was identified as a stable and essential binding partner of the eukaryotic Nfs protein (6–9). Based on *in vitro* experiments, Nfs was originally thought to catalyze sulfur transfer by itself (10), but it was recently shown to require the assistance of Isd11 for the formation of Fe/S clusters on the IscU scaffold (6, 7). Co-expression in *Escherichia coli* of Nfs and Isd11 from the microsporidian *Trachipleistophora hominis* confirmed that it is indeed a complex of both tightly bound proteins that represents the functional cysteine desulfurase (11).

The *Isd11* gene has also been found in the ancestral protists that contain hydrogenosomes and mitosomes (12, 13). Isd11 belongs to the LYR family (9) and in yeast stabilizes mitochondrial Nfs1, which is in its absence prone to aggregation. Although in yeast Isd11 seems to be confined to the mitochondrion (6, 7), it is equally abundant in the mitochondrion and nucleus of human cells, where its depletion resulted in inactivation of Fe/S cluster-containing cytosolic and mitochondrial aconitases. Furthermore, its down-regulation in human cells disrupts iron homeostasis (9).

Moreover, an interconnection between Fe/S cluster biogenesis and 2-thiouridine (^s2U) modification of tRNAs has been found in yeast and human cells. In these organisms, tRNA thiolation occurs in two places: the cytoplasm and mitochondria. In both compartments, modification of mitochondrial and cytosolic tRNAs requires the participation of components of the mitochondrial (ISC) and cytosolic Fe/S cluster assembly machineries (CIA), respectively (1). This is likely due to the direct involvement of some of these proteins in tRNA modifications and by the fact that Tyw1 and Elp3 proteins themselves need Fe/S clusters for their function (14). However, thiolation of tRNAs in both cellular compartments of the yeast cell was shown to directly depend on mitochondrial Nfs1 (15–17) but does not require the involvement of Fe/S-containing enzymes. This suggests a role for this desulfurase in sulfur-relay, independent of its function in Fe/S cluster assembly.

The factors that relay the sulfur from Nfs1 to tRNAs differ in the two compartments. In mitochondria, Mtu1, a homolog of bacterial MnmA, acts as the tRNA-specific 2-thiouridylase (17). Disruption of this gene in yeast not only eliminated the thiola-

* This work was supported, in whole or in part, by National Institutes of Health Grants AI065935 (to K. D. S.) and GM084065 and National Science Foundation Grant MCB-0620707 (to J. D. A.), Czech Science Foundation Grant 204/09/1667, Ministry of Education of the Czech Republic Grants LC07032, 2B06129, and 6007665801, and a Praemium Academiae award (to J. D. L.).

§ The on-line version of this article (available at <http://jbc.org>) contains **supplemented Figs. S1–S4**.

¹ To whom correspondence should be addressed: Branišovská 31, 370 05, České Budějovice, Czech Republic. E-mail: jula@paru.cas.cz.

tion of mitochondrial tRNAs but also led to reduced respiratory activity and impaired mitochondrial protein synthesis. Furthermore, the down-regulation of the human homologue of MTU1 in HeLa cells by RNA interference (RNAi)² resulted in a phenotype observed in patients afflicted with myoclonus epilepsy associated with ragged-red fibers (17).

In the cytoplasm, Urm1p, the earliest-diverging ubiquitin-like protein, was shown to act as a sulfur carrier in tRNA thiolation, providing a possible evolutionary link between ubiquitin-like proteins and sulfur transfer. Specifically, five genes (URM1, UBA4, NCS2, NCS6, and YOR251c) have been identified in a genome-wide screen of *Saccharomyces cerevisiae* to be responsible for 2-thiouridine synthesis (18–20). *In vitro* assays indicate that Ncs6p binds to tRNA, whereas Uba4p first adenylates and then directly transfers sulfur onto Urm1p (18). However, tRNA thiolation still cannot be efficiently reconstituted *in vitro* in any of these systems, suggesting the involvement of additional components.

Trypanosoma brucei and related flagellates are responsible for human African sleeping sickness and numerous other serious diseases that afflict millions in tropical regions. Within the last decade this early branching eukaryote also became approachable by numerous methods of forward and reverse genetics. In these cells, both the mitochondrion-targeted Nfs and a nucleus-localized Nfs-like protein have cysteine desulfurase and selenocysteine lyase activities. However, of these two proteins only Nfs is essential for ISC (21, 22). Due to the complete loss of tRNA genes from its organellar DNA, the single mitochondrion of *T. brucei* imports all tRNAs from the cytoplasm (23). We have recently shown that in the insect stage of the parasite Nfs is indispensable for thiolation of both cytosolic and mitochondrial tRNAs. Furthermore, thiolation has important implications for cytoplasmic tRNA stability of normally thiolated tRNAs and mitochondrial C to U editing of tRNA^{Trp} (24).

In this work we demonstrate that Isd11 is essential for Fe/S cluster assembly of both mitochondrial and cytosolic proteins of *T. brucei*, like in other eukaryotes (6, 7, 9, 11, 13). We also show for the first time that Isd11 is required for thiolation of both cytosolic and mitochondrial tRNAs and that Isd11 is not solely an Nfs chaperone for Fe/S cluster assembly, whereas Mtu1 is essential for mitochondrial tRNA thiolation only. Taken together, these findings provide further evidence for the association of the two pathways and suggest a possible link between Fe/S cluster assembly and translation mediated by tRNA thiolation. The involvement of Isd11 in tRNA thiolation also provides yet another missing key component in the complex tRNA thiolation pathway of eukaryotic cells.

EXPERIMENTAL PROCEDURES

Plasmid Constructs, Transfections, Cloning, RNAi Induction, and Cultivation—A 300-nucleotide long part of the *Isd11* gene (Tb10.389.1785) was PCR amplified using primers Isd-F (5'-CTCGAGATGACAAACACCGTCAAACACT) and Isd-R (5'-ACTAGTTTACTCTTCTTCTTCTTGCGTCAC) (added

XhoI and SpeI restriction sites are underlined) from total genomic DNA of *T. brucei* strain 29-13. The amplicon was cloned into the p2T7-177 vector, which was upon NotI-mediated linearization introduced into procyclic *T. brucei* 29-13 cells and selected as described elsewhere (25). The same strategy was used to prepare cells in which the Mtu1 mRNA was targeted by RNAi. A 501-nucleotide long fragment of the *Mtu1* gene (Tb927.8.1830) was amplified via primers Mtu-F (5'-CTCGAGGCAACACGCTCAACGTTG) and Mtu-R (5'-GGATCCCCGCGTGAACACCTTCTC) (added XhoI and BamHI restriction sites are underlined), cloned, and stably integrated into the *T. brucei* 29-13 PF cells as described above. RNAi was triggered by the addition of 1 μg/ml of tetracycline to the SDM-79 medium. Cell density was measured every 24 h using the Beckman Z2 Coulter counter over a period of 8 (Isd11)/14 (Mtu1) days after the induction of double-stranded RNA synthesis. The inducibly expressed C-terminal tandem affinity purification (TAP)-tagged Isd11 protein was created by PCR amplification of the full-size *Isd11* gene and inserted into the pLew-79-MHTAP plasmid (26). Similarly, to obtain cells expressing TAP-tagged IscU and frataxin proteins, the full-size genes encoding the scaffold protein IscU (Tb09.21.2830) and frataxin (Tb927.3.1000) were PCR-amplified as described above. The NotI-linearized constructs were electroporated into the 29-13 cells and phleomycin-resistant clones were selected following a protocol described previously (25). The bloodstream *T. brucei* strain 920 was cultured at 37 °C as described elsewhere (27).

Northern Blot Analyses—Total RNA was isolated using TRIzol (Sigma) from procyclic cells cultivated in SDM-79 medium. Approximately 10 μg/lane of total RNA was loaded on a 1% agarose-formaldehyde gel, blotted, and cross-linked. Hybridization was performed in NaP_i solution using probes labeled by random priming with [α-³²P]dATP (MP Biomedicals) overnight at 55 °C. Membranes were washed and the radioactive signal was detected as described previously (28).

Expression and Purification of Recombinant Isd11—The full-size *Isd11* gene was amplified by PCR with primers IsdE-F (5'-CACCATGACAAACACCGTCAAAA) and IsdE-R (5'-ACTAGTTTACTCTTCTTCTTCTTGCGTCAC) (containing the stop codon (underlined)). The amplicon was gel-purified and cloned into the pET100 expression vector (Invitrogen). The resulting expression plasmid encoding His₆-tagged *Isd11* was transformed into the *E. coli* strain BL21(DE3) (Novagen). Insoluble protein was obtained from induced bacterial cells (incubation at 30 °C for 2 h) under denaturing conditions using affinity chromatography.

Digitonin Fractionation and Immunolocalization—Digitonin fractionation was performed following a protocol described elsewhere (21). Subcellular localization of the expressed tagged proteins within the cell was determined by IFA using polyclonal anti-Myc antibodies (Invitrogen) as described previously (29). Co-localization analysis was performed using monoclonal antibody mAB61 against the MRP1/2 complex (30) coupled with Texas Red X-conjugated secondary antibody (Invitrogen).

Preparation of Antibodies and Western Blot Analyses—Polyclonal antibody was prepared by immunizing rabbits at 2-week

² The abbreviations used are: RNAi, RNA interference; TAP, tandem affinity purification; APM, [(N-acryloylamino)-phenyl]mercuric chloride.

tRNA Thiolation and Fe/S Cluster Assembly

intervals with four subcutaneous injections of 0.5 mg of purified recombinant Isd11 protein emulsified with complete (1st injection) and incomplete (following injections) Freund's adjuvant. Another polyclonal antibody was raised by immunizing a rat at 2-week intervals by Cocalico Biologicals Inc. (Reamstown, PA). Cell lysates corresponding to 5×10^6 cells/lane were separated on 15% SDS-polyacrylamide gel, blotted, and probed. The rabbit serum (1:1,000) against Isd11 was used for further experiments because it contained more specific antibodies. The polyclonal rabbit antibodies against the *T. brucei* frataxin (31), Nfs and IscU (21), Gap1 (27), and enolase (kindly provided by P. A. M. Michels) were used at 1:500, 1:1,000, 1:1,000, 1:1,000, and 1:100,000 dilutions, respectively.

TAP Purification and Mass Spectrometry Analysis—The TAP protocol was adapted from the published method (32). The tagged complexes were purified from 1×10^9 cells lysed with 0.25% Nonidet P-40, cleared by low speed centrifugation, and the supernatant was further lysed with 1.25% Nonidet P-40 and cleared by high speed centrifugation ($40,000 \times g$ at 4°C in a Sorvall SW-55 rotor for 40 min). The tagged complexes were isolated by sequential binding to IgG and calmodulin affinity columns. This method was adapted from the published protocol (33). Purified complexes were analyzed by mass spectrometry basically as described previously (32).

Measurement of Mitochondrial Membrane Potential—After centrifugation, exponentially growing procyclic cells were resuspended in 1 ml of fresh SDM-79 medium (at a concentration 5×10^6 cells/ml) and mitochondrial inner membrane potential was measured by the uptake of 0.4% tetramethylrhodamine ethyl ester (Molecular Probes) for 20 min at 27°C . After staining, the cells were resuspended in a dye-free medium and instantly measured by flow cytometry using an Epics XL flow cytometer (Coulter).

Measurement of Enzymatic Activities—The activities of fumarase and aconitase were measured in total cell lysates, as well as in subcellular fractions obtained by digitonin treatment, the purity of which was controlled by compartment-specific antibodies. Fumarase activity was determined in procyclic cells resuspended in Hanks' balanced salt solution (Invitrogen) containing 0.1% Triton X-100 and incubated for 5 min on ice. After centrifugation, the activity was measured spectrophotometrically at 240 nm as the rate of production of fumarate. The activities of aconitase and threonine dehydrogenase were established as described elsewhere (34).

APM Gel Electrophoresis and Northern Blot Analysis—Thiolation of different tRNAs was analyzed using the [(N-acryloylamino)-phenyl]mercuric chloride (APM) gel, and blotted as described elsewhere (35). In the control reactions the thiol group was removed by treatment in 0.4% hydrogen peroxide, 1 mM EDTA, 100 mM phosphate buffer (pH 8.0) for 1 h at room temperature. The percentage of thiolation was established using the volume of band(s) corresponding to the thiolated and non-thiolated species. To determine ratios of total tRNA in each sample the volume of the whole lane was used and compared between RNA isolated from the non-induced and RNAi-induced cells. Ratios were then standardized using tRNAs that do not get thiolated.

RESULTS

Isd11 Is a Mitochondrial Protein—We have used the Isd11 protein sequence of *S. cerevisiae* as a query to search the *T. brucei* genome. We have identified three putative Isd11 homologues, Isd11-1, Isd11-2, and Isd11-3 (calculated molecular masses 11.77, 23.69, and 18.79 kDa, respectively) (Fig. S1). Although all three genes contain the LYR/K domain, only Isd11-1 (hence Isd11) shares high sequence similarity with Isd11 proteins from plants, human, and other eukaryotes (Fig. S2). Disruption of Isd11-2 by RNAi was not lethal and preliminary results indicate its association with respiratory complexes rather than with Fe/S cluster assembly.³ Isd11-3 was not studied further.

On the basis of its N-terminal leader sequences, MitoProt predicted mitochondrial localization of Isd11 with a 0.879 (~88%) probability. The predicted cleavage site of the *T. brucei* mitochondrial processing peptidase was at position 13 (Figs. S3 and S4). To further assess its predicted localization, Isd11 was expressed in *E. coli* and rabbit polyclonal antibodies were raised against the purified recombinant protein. Fractionation by treatment with the detergent digitonin allowed us to obtain cytosolic and mitochondrial fractions of the *T. brucei* procyclics, the purity of which was confirmed by antibodies against compartment-specific markers enolase (cytoplasmic) and the Gap1 protein (mitochondrial) (Fig. 1). In agreement with the *in silico* predictions, the Isd11 protein was localized to the mitochondrion (Fig. 1A, left panel). Next, we were interested on whether Isd11 is also present in the bloodstream (=mammalian) stage of *T. brucei*, whose single mitochondrion is largely down-regulated in terms of size and activity. Indeed, also in the bloodstream stage, all detectable Isd11 protein appears to be confined to the mitochondrion (Fig. 1A, right panel). Immunofluorescence assays using anti-Myc polyclonal antibodies showed that tagged IscU and Isd11 localize to the reticulated mitochondrion and that both proteins are equally distributed throughout the organelle (Fig. 1B). These results also showed that the TAP tags did not interfere with mitochondrial import and thus provide validity for purifying the Isd11-Nfs-IscU complex.

Isd11 Forms a Stable Complex with Nfs and IscU—In yeast, microsporidian, and human cells, Isd11 was shown to be associated with the Nfs protein (6, 7, 9, 11, 13). To explore whether similar interactions of Isd11 occur in trypanosomes, a TAP-tagged version of this protein was generated and expressed under control of a tetracycline-inducible promoter. Clarified cell lysate obtained from these cells was subjected to tandem affinity purification. SYPRO Ruby staining of an aliquot of a TAP eluate containing Isd11, separated by SDS-PAGE, revealed the presence of only two visible protein bands (data not shown). Mass spectrometry analysis of the tagged Isd11 complex identified, besides Isd11, Nfs, and IscU, both with at least two unique doubly tryptic peptides (Fig. 1C). To exclude the possibility of nonspecific protein association, IscU was selected for reciprocal TAP tagging. Reassuringly, the TAP-tagged IscU pulled down Isd11 and Nfs, confirming that these

³ Z. Vávrová and J. Lukeš, unpublished results.

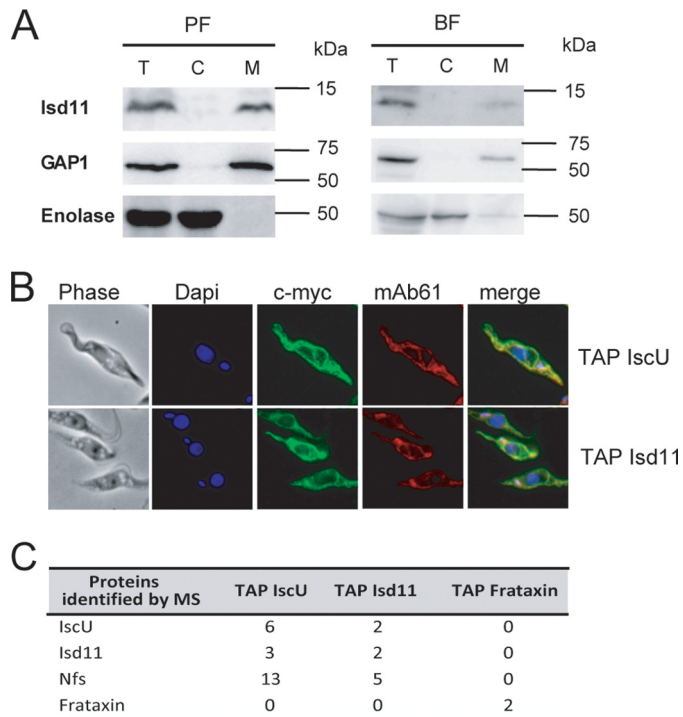


FIGURE 1. *A*, Lsd11 is localized in the mitochondrion of the procyclic (PF) and bloodstream stages (BF). Cytosolic and mitochondrial fractions were obtained from both developmental stages by fractionation using digitonin. Upon resolution by SDS-PAGE the lysates were blotted and immunoprobed with α -Lsd11 antibodies. Antibodies against enolase and GAP1 proteins were used as cytosolic and mitochondrial markers, respectively. Total cell lysates (T), cytosolic (C), and mitochondrial (M) fractions were screened in both stages. Positions of the protein markers are indicated on the right. *B*, tagged Lsd11 and IscU were visualized by fluorescence microscopy using polyclonal anti-c-Myc antiserum coupled with fluorescein isothiocyanate-conjugated secondary antibody. Co-localization immunofluorescence was performed with monoclonal antibody mAb61 against the mitochondrial MRP1/2 complex (30). The first column (phase) shows phase-contrast light microscopy of the *T. brucei* procyclic cells; the second column (Dapi) shows staining of nuclear and mitochondrial (=kinetoplast) DNA with 4,6-diamidino-2-phenylindole (DAPI); the third column (c-Myc) shows localization of the TAP-tagged proteins using the polyclonal α -Myc antibody; the fourth column (mAb61) shows co-localization of the mitochondrial MRP1/2 complex using monoclonal α -mAb61 antibody; the last column (merge) documents merged fluorescence images. *C*, proteins were identified by mass spectrometry analysis of TAP tags from cells expressing TAP-tagged Lsd11, IscU, or frataxin. Only proteins identified in both IscU and Lsd11 TAP tag purifications and at least by two unique peptides are shown. The number indicates the total number of unique peptides identified.

three proteins form a stable complex. Finally, we have also TAP-tagged frataxin to assay its putative interaction with the above proteins. As shown in Fig. 1C, under the conditions used, mass spectrometry analysis of the purified TAP-tagged frataxin did not reveal the presence of any other protein, implying that in *T. brucei* frataxin does not form a stable complex with the above proteins.

Lsd11 Is Required for Fe/S Cluster Assembly—To establish the role of Lsd11 in *T. brucei* procyclics, we performed RNAi-mediated knockdown of the transcript using a tetracycline-inducible RNAi construct. Upon the addition of the antibiotics, proliferation of the clonal cell line was markedly inhibited starting with day 3 (Fig. 2A), which is in good agreement with the decrease in the levels of the target protein (see below). The growth inhibition persisted for 8 days post-induction when the growth curve was terminated (Fig. 2A). Northern blotting

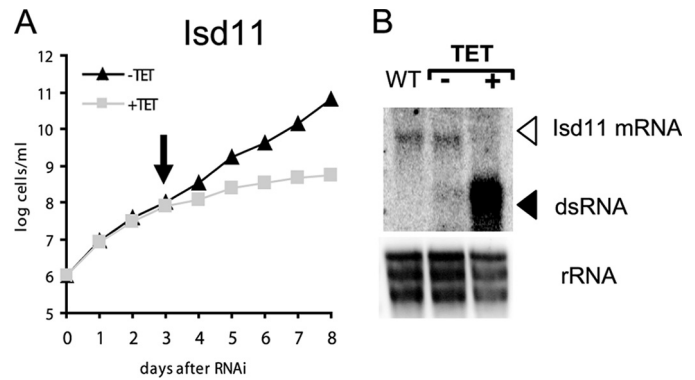


FIGURE 2. *A*, effects of Lsd11 RNAi on the growth of the parasite. Growth curves of non-induced (*TET*⁻; triangles) and induced (*TET*⁺; squares) knockdown for Lsd11. The y axis is labeled by a log scale and represents the products of the measured cell densities and total dilutions. Cell densities were measured using the Beckman Z2 cell counter. The arrow indicates the sampling time point for the latter experiments. *B*, Lsd11 mRNA levels were analyzed by blotting total RNA extracted from non-induced cells (-) and cells harvested 3 days of RNAi induction against Lsd11 (+). The position of the targeted mRNA and double-stranded RNA synthesis following induction are indicated with open and closed arrows, respectively. As a loading control, the gel was stained with ethidium bromide to visualize rRNA bands. WT, wild type.

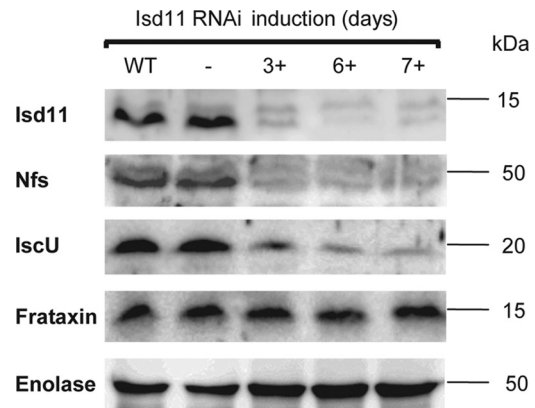


FIGURE 3. Silencing of Lsd11 affects stability of other Fe/S cluster assembly proteins in procyclic *T. brucei*. Expression level of Lsd11, cysteine desulfurase (Nfs), scaffold protein (IscU), and frataxin as determined by immunoblot analysis of whole cell lysates of the parental 29-13 cell line (wt), non-induced cells (-), and cells 3, 5, and 7 days of RNAi induction. Enolase was used as a cytosolic loading control. Positions of the protein markers are indicated on the right.

after 72 h of RNAi induction showed depletion of the target Lsd11 mRNA (Fig. 2B). This result was also confirmed by Western blot analysis that showed a dramatic decrease in Lsd11 protein levels by day 3 of RNAi induction. The protein was virtually eliminated by day 5 and became almost undetectable in lysates isolated from cells 1 week after RNAi induction (Fig. 3). From the Western blot it is also apparent that no leaky transcription occurred, as the level of Lsd11 remained unchanged and at comparable levels in the 29-13 wild type as well as the non-induced cells (Fig. 3).

The observed association between Lsd11, Nfs, and IscU revealed by TAP tag analysis led us to assess the levels of each of these proteins in cells depleted of Lsd11 by RNAi. Indeed, as its general binding partner, Nfs followed the expression pattern of Lsd11, becoming substantially down-regulated 3 days of RNAi induction, although it does not seem to be totally eliminated in cells collected in the studied time points (Fig. 3). A very similar result was obtained using the anti-IscU antibody, whereas the

tRNA Thiolation and Fe/S Cluster Assembly

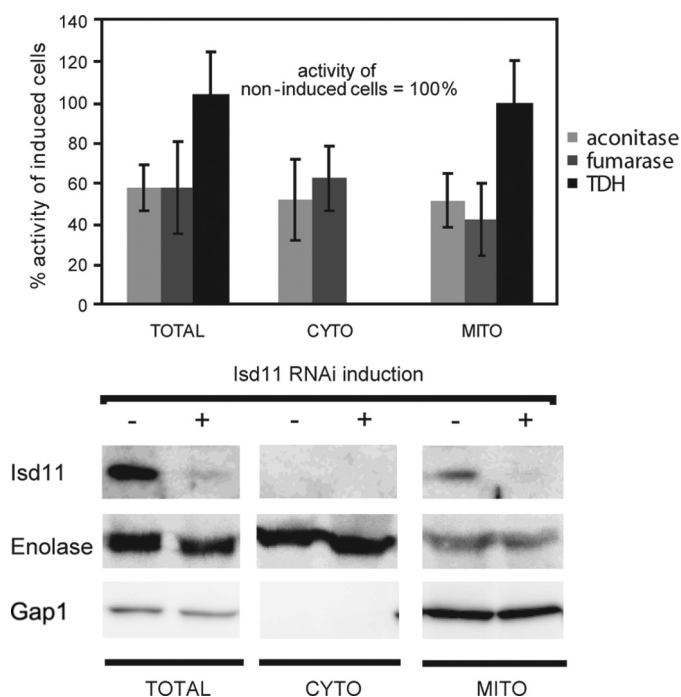


FIGURE 4. Activity of fumarase and aconitase (Fe/S cluster-containing proteins) is significantly reduced after down-regulation of Isd11. The percentage of specific aconitase and fumarase activity in total cell lysate (*total*), cytosol (*cyto*), and mitochondrion (*mito*) in the non-induced and RNAi-induced cells is shown. Values for the non-induced cells were considered as 100% activity. The mean \pm S.D. values of six independent induction experiments are shown. The purity of cellular fractions obtained by digitonin fractionation from the non-induced (-) and RNAi-induced cells (+) was controlled with the α -enolase (cytosolic marker) and α -Gap1 antibodies (mitochondrial marker).

levels of frataxin, which does not interact with the other three proteins (Fig. 1C), remained unaltered in the Isd11 knockdowns (Fig. 3).

To assess the putative role of Isd11 in the Fe/S cluster assembly, we have measured the activities of marker Fe/S cluster-containing aconitase and fumarase. Both enzymes have a dual localization in the *T. brucei* procyclics (31, 34), which allows separate evaluation of the impact of RNAi against Isd11 on cytosolic and mitochondrial proteins. The purity of cytosolic and mitochondrial fractions obtained from the non-induced and RNAi-induced procyclic *T. brucei* by digitonin treatment was first assessed by Western blot analysis using antibodies against Gap1 and enolase, as described above (Fig. 4). When compared with the non-induced cells, activities of both metabolic enzymes dropped by 45 to 60% in cells depleted for Isd11 (Fig. 4). The activity of mitochondrial threonine dehydrogenase, a protein lacking Fe/S clusters, remained unaltered in both the non-induced and RNAi-induced cells (Fig. 4).

Isd11 Is Essential for Cytosolic and Mitochondrial tRNA Thiolation—Besides playing a role in Fe/S assembly, the Nfs protein is also the key desulfurase for tRNA thiolation in *E. coli*, as well as in *S. cerevisiae* and *T. brucei* (15, 24, 36). These observations raised the question of whether Isd11 is also essential for tRNA thiolation. Because Isd11 is a binding partner for Nfs, we decided to explore its possible role in tRNA metabolism further. Total RNA was isolated from the non-induced cells and from cells depleted for Isd11 (collected 72 h after RNAi induc-

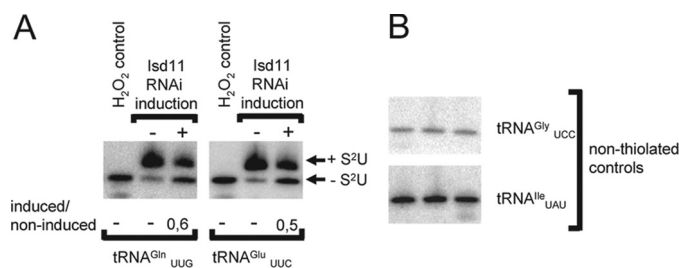


FIGURE 5. Isd11 is essential for cytosolic tRNA thiolation. RNA isolated from non-induced (-) and RNAi-induced Isd11 cells (+) was separated on an APM gel followed by Northern blot analysis (A). Bands corresponding to thiolated and non-thiolated tRNAs are indicated. H₂O₂ is used as a control to show complete oxidation of thiolation, eliminating the mobility shift. The ratio of total tRNA isolated from RNAi-induced (+) to non-induced (-) cells after standardizing with non-thiolated tRNAs (B) is shown below each panel, where a ratio of 1 would indicate no change, less than 1 indicates lower steady-state levels of a particular tRNA.

tion). These RNA samples were separated on mercury-containing APM gels (see “Experimental Procedures”). In these gels, the thiolated tRNA species migrate slower than the non-thiolated ones, and the thiolation status of tRNAs is thus reflected in their differential mobility. We performed Northern blots of APM gel-separated RNAs obtained from the non-induced and RNAi-induced cells, using radioactive probes specific for two cytosolic tRNAs (tRNA^{Gln}_{UUG} and tRNA^{Glu}_{UUC}) that get thiolated at the wobble position. In cells with down-regulated Isd11 (+ lanes), thiolation of tRNA^{Gln}_{UUG} and tRNA^{Glu}_{UUC} was reduced by 60 and 50%, respectively (Fig. 5A).

Importantly, the levels of two non-thiolated cytoplasmic tRNA species used as controls, tRNA^{Gly}_{UCC} and tRNA^{Leu}_{UAU}, were unaltered regardless of the amount of Isd11 in the procyclic cells (Fig. 5B). These data indicate that Isd11 is indispensable for the thiolation of cytoplasmic tRNAs.

S. cerevisiae contains two separate pathways involving multiple protein factors that work on the sulfur-relay mechanism essential for tRNA thiolation. In the cytoplasm this pathway requires Nfs1 (the yeast homolog of Nfs) and several additional ubiquitin-like proteins, such as Uba24, Urm1, and Ncs6/Ncs2. The mitochondrial sulfur-relay system requires at least Nfs1 and Mtu1, the latter factor being implicated in the sulfur transfer step onto the tRNA. In light of the mitochondrial localization of Isd11 in *T. brucei* and other eukaryotes, we decided to explore its possible involvement in mitochondrial thiolation using a radioactively labeled probe specific for tRNA^{Trp}, the only known tRNA to undergo mitochondrion-specific thiolation in these cells. We probed Northern blots of total RNA isolated from the mitochondria of the wild type and RNAi-induced cells separated by the APM gels. We found that similar to the cytosolic case for tRNA^{Gln} and tRNA^{Glu}, tRNA^{Trp} thiolation is also down-regulated in cells depleted for Isd11 (Fig. 7A).

Mtu1 Is Essential for Mitochondrial tRNA Thiolation—To assess possible involvement of Mtu1 in the thiolation reaction in trypanosomes, we performed a Blast search, using the *S. cerevisiae* Mtu1 protein as a query, which identified a single homologue for the *Mtu1/Mnma* gene in the *T. brucei* genome (Tb927.8.1830). The Mtu1 protein has a predicted molecular mass of 61.28 kDa, and its inclusion into the alignment of several eukaryotic *Mtu1* genes (17) revealed the presence of virtu-

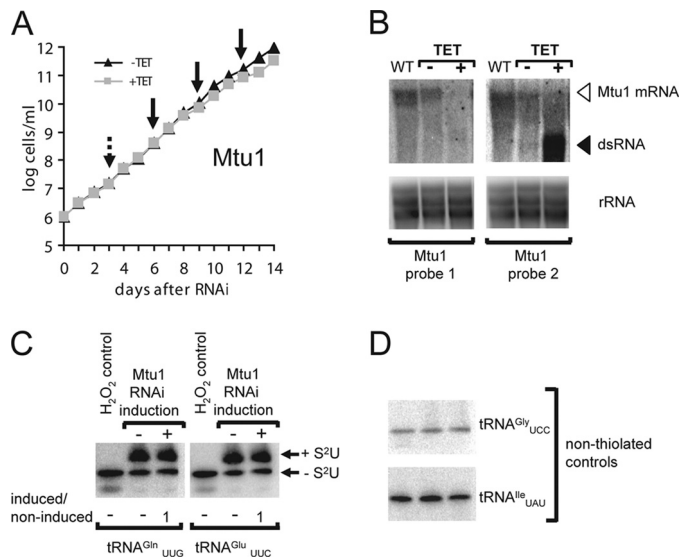


FIGURE 6. Silencing of Mtu1 affects neither growth phenotype nor cytosolic tRNA thiolation. *A*, growth curves of non-induced (TET^- ; triangles) and RNAi-induced (TET^+ ; squares) knockdown for Mtu1 are presented as in Fig. 2A. Dotted and solid arrows indicate time points for RNA isolation and mitochondrial membrane potential measurements, respectively. *B*, Mtu1 mRNA levels were analyzed by blotting total RNA extracted from the non-induced cells ($-$) and cells harvested 3 days of RNAi induction against Mtu1 ($+$). Northern blot and the stained gel are as described in the legend to Fig. 2B. Mtu1 probe 1 was prepared from a fragment of the gene other than the one used for RNAi. Mtu1 probe 2 corresponds precisely to the gene fragment cloned into the RNAi vector. *C*, RNA isolated from the non-induced ($-$) and RNAi-induced Mtu1 cells ($+$) was separated on an APM gel followed by Northern blot analysis. Bands corresponding to thiolated and non-thiolated tRNAs are indicated. H_2O_2 was used as a control to show complete oxidation of thiolation, eliminating the mobility shift. The level of tRNA thiolation is shown below the panel and calculated as described previously. *D*, the tRNA^{Gly} and tRNA^{Ile} were used as loading controls.

ally all conserved residues and 29 and 45% sequence identity and similarity, respectively, with its *S. cerevisiae* homologue (Fig. S3).

Given its essentiality in other systems, we anticipated a similar situation in the *T. brucei* procyclics. The addition of tetracycline induced a massive synthesis of double-stranded RNA, resulting in a significant down-regulation of the targeted Mtu1 mRNA (Fig. 6B). However, cells ablated for Mtu1 grow very well in the SDM-79 medium, their growth curve being virtually indistinguishable from those of the wild type 29-13 cells (data not shown) and the non-induced cells even after 2 weeks of cultivation (Fig. 6A). Nonetheless, we tested whether Mtu1 is also involved in mitochondrial thiolation. We found that Mtu1 RNAi led to a decrease in tRNA^{Trp} thiolation (Fig. 7A) comparable with that caused by the depletion of Isd11. Significantly, the function of Mtu1 is relegated to mitochondrial thiolation, because no decrease in cytoplasmic thiolation was observed with RNA isolated from the Mtu1 RNAi cells (Figs. 6C and 7B). In addition, tRNA^{Gln} and tRNA^{Glu}, which are thiolated in the cytoplasm, show no thiolation following import into the mitochondria (Fig. 7B). Although this observation may seem puzzling, it has been shown very recently that these two tRNAs undergo de-thiolation following import by an as yet unknown mechanism (37).

Taken together, these data demonstrate that unlike Mtu1, which is mitochondrion-specific, Isd11 is essential for both

cytosolic and mitochondrial thiolation. This behavior is similar to that observed with Nfs and leads to the conclusion that both proteins are essential for tRNA thiolation in both the cytoplasm and mitochondria. Significantly, Mtu1 itself does not contain an Fe/S cluster, implying that Isd11 plays a direct role in thiolation beyond its essential role in Fe/S assembly. Therefore the Nfs-Isd11 complex is an integral part of a more general sulfur-relay system not just limited to the Fe/S cluster assembly.

Effect of Isd11 and Mtu1 RNAi on Mitochondrial Membrane Potential—In the procyclic stage, mitochondrial inner membrane potential is maintained by the activity of the cytochrome-mediated respiratory chain (38). Quantification of the uptake of tetramethylrhodamine ethyl ester by flow cytometry enabled us to measure the potential in non-induced and RNAi-induced cells. As shown in Fig. 8A, a dramatic decrease of membrane potential was observed in the Isd11-depleted cells at day 3 of RNAi induction, likely a consequence of the core subunits of respiratory complexes being depleted for the Fe/S clusters. However, numerous measurements of the membrane potential at 3, 6, 9, and 12 days upon the induction of RNAi against Mtu1 did not reveal differences between the non-induced cells and those depleted for Mtu1 (Fig. 8B).

DISCUSSION

Isd11, a eukaryotic invention in the Fe/S cluster assembly pathway, is present in all sequenced eukaryotic genomes as a single-copy gene (6, 7, 12). Interestingly, the model flagellate *T. brucei* represents an exception, because a Blast search identified three putative homologs of Isd11 in its genome. Based on the presence of the LYR/K sequence motif found in subunits of respiratory complex I, Isd11 might originally have served as a subunit of this complex, but was at an early stage of eukaryotic evolution abducted for novel functions. Indeed, whereas the Isd11 protein functionally analyzed in this study is clearly associated with the Fe/S cluster assembly, another homologue (Isd11-2) appears to have a function unrelated with this process.³ In yeasts, microsporidia, and humans, Isd11 is a binding partner of Nfs, essential for its desulfurase activity *in vivo* and thus indispensable for cell survival (6, 7, 11, 13).

Using mass spectrometry and Western analysis, we have shown herein that in the unicellular parasite *T. brucei*, Isd11 also interacts with Nfs and the Fe/S cluster assembly chaperon IscU. Furthermore, we have demonstrated that the studied protein assists in the ISC pathway, because the Fe/S cluster-dependent activities of aconitase and fumarase were significantly decreased in the Isd11-deficient background.

There is one important difference between yeast and human knockdowns for Isd11. Although in human cells, down-regulation of this protein causes destabilization not only of its direct binding partner Nfs1, but also IscU (13), it is only Nfs1 that is eliminated from the Isd11 mutant yeast cells (7). The results obtained in trypanosomes are reminiscent of those obtained with human cells, as both proteins are clearly eliminated in the absence of Isd11. Human and trypanosome cells also share another aspect of the Isd11 function not seen with yeast. Although Isd11 depletion leads to defects of both mitochondrial and cytosolic Fe/S cluster proteins (Ref. 9 and this work),

tRNA Thiolation and Fe/S Cluster Assembly

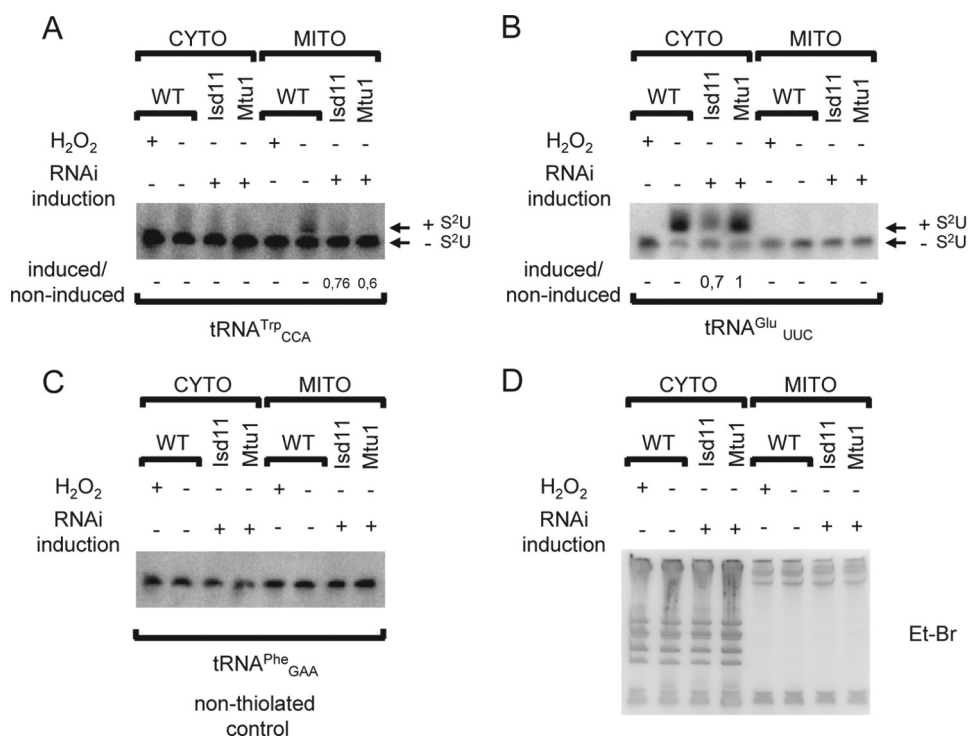


FIGURE 7. Isd11 and Mtu1 are essential for mitochondrial thiolation of tRNA^{Trp}_{CCA}. Cytosolic and mitochondrial RNA from wild type cells (WT) and RNAi-induced cells was separated by APM acrylamide gel electrophoresis. **A** and **B**, Northern blot analysis probing for tRNA^{Trp} and tRNA^{Glu}. Bands corresponding to thiolated and non-thiolated tRNAs are indicated. H₂O₂ is used as a control to show complete oxidation of thiolation, eliminating the mobility shift. The level of tRNA thiolation is shown below the panel and calculated as described previously. The tRNA^{Phe} (**C**) is used as a loading control and ethidium bromide shows the purity of mitochondrial fractions (**D**).

similar experiments in yeast only affect the organellar ISC pathway (6, 7).

Given the mitochondrial localization and strong association of Isd11 with Nfs shown in this work, intuitively, one would expect that Isd11 is also essential for thiolation, as previously suggested (1). We therefore tested this hypothesis further and undertook a detailed analysis of tRNAs in cells depleted for Isd11. Indeed, this protein is indispensable for *T. brucei* tRNA thiolation, a modification that is conserved, widespread, and essential in most organisms. Isd11, however, is needed not only for mitochondrial but also for cytosolic tRNA thiolation, despite the fact that in trypanosomes Isd11, analogous to Nfs, is detectable by Western blotting and immunolocalization only within the organelle (Ref. 24 and this work). The possible presence of Isd11 in the cytosol in amounts that escape selection by Western blot but that are sufficient to generate thiolated tRNAs in the cytoplasm via the cytoplasmic sulfur relay system (18, 39, 40) is highly unlikely for the following reasons. Another component of the Fe/S assembly, Atm1, is in all examined organisms strictly confined to the mitochondrion (1, 2, 41). However, we have shown that the same as Isd11, down-regulation of Atm1 affects thiolation of cytosolic tRNAs in *T. brucei*.⁴ This strongly implies that it is the extrusion, via Atm1, of an unknown sulfur component into the cytoplasm (1, 2) that is decreased in Isd11 RNAi knockdowns, which is responsible for

⁴ P. Flegontov, M. Obornik, P. Changmai, Z. Paris, and J. Lukeš, unpublished results.

the drop in cytosolic tRNA thiolation. Notably, Elp3 is an iron-sulfur containing protein, which was proposed to be one of the components of the sulfur-relay system for thiolation in yeast (18). This creates a scenario in which both proteins may be present in amounts in the cytosol that escape Western detection but are sufficient to generate thiolated tRNAs in the cytoplasm via the cytoplasmic sulfur-relay system (18, 39, 40).

In mitochondria, besides Nfs1 at least one more protein is required for thiolation, namely Mtu1, the eukaryotic homolog of MnmA (20, 37). As expected, we found that down-regulation of Mtu1 in *T. brucei* leads to the loss of mitochondrial but not cytoplasmic thiolation. Mtu1, however, is dispensable for cell growth and the unaltered mitochondrial membrane potential in cells lacking Mtu1 shows that organellar translation in *T. brucei* remains functional even with decreased thiolation, allowing the assembly of respiratory complexes. This is certainly unexpected,

because defects in this gene are thought to be responsible for the serious human disorder myoclonus epilepsy associated with ragged-red fibers (17). Surprisingly, the conserved nucleotide binding motif (SGGVDS), which in other organisms is located in the N-terminal part of the Mtu1 protein, is in the *T. brucei* homologue found within the predicted mitochondrial signal peptide. We can only speculate that in this case the *in silico* prediction is incorrect and that the nucleotide binding motif remains present in the Mtu1 protein.

What then is the function of mitochondrial thiolation? In the *T. brucei* mitochondrion, tRNA^{Trp} undergoes thiolation and contains s²U at an unusual U₃₃ position of the anticodon loop. This modification is commonly found at U₃₄ (the first position of the anticodon) in tRNA^{Glu}, tRNA^{Gln}, and tRNA^{Lys} in bacteria and eukarya (42). tRNA^{Trp} also undergoes C to U editing at the first position of the anticodon. However, less than 100% molecules are edited and both the UCA and CCA anticodon-containing isoacceptors co-exist in the mitochondrion (24). These two tRNAs are then presumably dedicated to decoding the UGA and UGG codons. We hypothesized that thiolation serves to maintain the levels of these two isoacceptors in the organelle. In a previous study (24), we found that down-regulation of Nfs leads to reduced thiolation of tRNAs in both cellular compartments. Surprisingly, low thiolation produces two different phenotypic outcomes: (i) it triggers destabilization of only those specific cytosolic tRNAs, which are normally thiolated; (ii) in the mitochondrion, the lack of thiolation leads to excessive editing of tRNA^{Trp} (24).

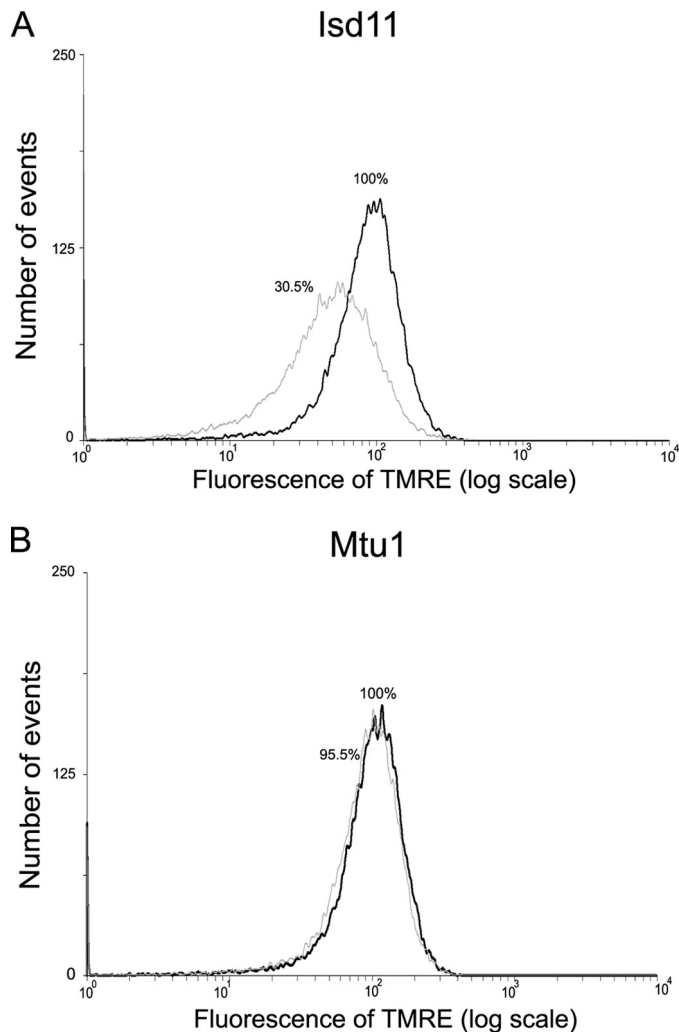


FIGURE 8. Effect of RNAi against either Lsd11 or Mtu1 on mitochondrial membrane potential. Mitochondrial membrane potential was measured in non-induced cells (*thick black line*), as well as in cells with down-regulated Lsd11 (*A*) or Mtu1 (*B*) (*thin gray line*) that were, after incubation with 0.4% tetramethylrhodamine ethyl ester (TMRE), analyzed using flow cytometry. Ablated cell lines were analyzed 3 days of RNAi induction in the case of Lsd11 and 3, 6, 9, and 12 days in case of Mtu1, respectively. The distribution of fluorescence was plotted as frequency histogram.

Interestingly, tRNA^{Trp} is made in the nucleus and transits through the cytoplasm, where a portion of it is maintained for cytoplasmic translation and another portion is imported into the mitochondrion. In the cytoplasm, tRNA^{Trp} is not thiolated but gets the unusual U₃₃ thiolation following mitochondrial import. This suggests that the cytoplasmic system is unable to thiolate U₃₃ and is specific for U₃₄, as in the case of tRNA^{Gln}, tRNA^{Glu}, and tRNA^{Lys} in most organisms (15, 17, 24, 43). This then implies that the mitochondrial thiolation system has gained the capacity to thiolate U₃₃ and this adaptation may either be the result of the need to regulate tRNA editing, differential compartmentalization of enzyme and substrate, or both. To what extent these processes are exploited by these parasites for fine-tuning gene expression and metabolic rates remains an open question, but intracellular compartmentalization played a central role in the evolution of these pathways. It clearly impacts the way the maturation of various substrates is specified, be it for the purpose of assembly of an ancient Fe/S co-

factor or an s²U tRNA modification. We suggest that perhaps the connection between thiolation and Fe/S cluster assembly is not just a moonlighting function for the enzymes involved. Our observations raise the possibility of a cross-talk between these very important pathways in an attempt to coordinate translation with the Fe/S-dependent metabolism.

REFERENCES

- Lill, R., and Mühlhoff, U. (2008) *Annu. Rev. Biochem.* **77**, 669–700
- Lill, R. (2009) *Nature* **460**, 831–838
- Zheng, L., White, R. H., Cash, V. L., and Dean, D. R. (1994) *Biochemistry* **33**, 4714–4720
- Gerber, J., Mühlhoff, U., and Lill, R. (2003) *EMBO Rep.* **4**, 906–911
- Ramazzotti, A., Vanmansart, V., and Foury, F. (2004) *FEBS Lett.* **557**, 215–220
- Adam, A. C., Bornhövd, C., Prokisch, H., Neupert, W., and Hell, K. (2006) *EMBO J.* **25**, 174–183
- Wiedemann, N., Urzica, E., Guiard, B., Müller, H., Lohaus, C., Meyer, H. E., Ryan, M. T., Meisinger, C., Mühlhoff, U., Lill, R., and Pfanner, N. (2006) *EMBO J.* **25**, 184–195
- Marelja, Z., Stöcklein, W., Nimtz, M., and Leimkühler, S. (2008) *J. Biol. Chem.* **283**, 25178–25185
- Shi, Y., Ghosh, M. C., Tong, W. H., and Rouault, T. A. (2009) *Hum. Mol. Genet.* **18**, 3014–3025
- Mühlhoff, U., Balk, J., Richhardt, N., Kaiser, J. T., Sipos, K., Kispal, G., and Lill, R. (2004) *J. Biol. Chem.* **279**, 36906–36915
- Goldberg, A. V., Molik, S., Tsaousis, A. D., Neumann, K., Kuhnke, G., Delbac, F., Vivares, C. P., Hirt, R. P., Lill, R., and Embley, T. M. (2008) *Nature* **452**, 624–628
- Richards, T. A., and van der Giezen, M. (2006) *Mol. Biol. Evol.* **23**, 1341–1344
- Shan, Y., Napoli, E., and Cortopassi, G. (2007) *Hum. Mol. Genet.* **16**, 929–941
- Esberg, A., Huang, B., Johansson, M. J., and Byström, A. S. (2006) *Mol. Cell* **24**, 139–148
- Nakai, Y., Umeda, N., Suzuki, T., Nakai, M., Hayashi, H., Watanabe, K., and Kagamiyama, H. (2004) *J. Biol. Chem.* **279**, 12363–12368
- Nakai, Y., Nakai, M., Lill, R., Suzuki, T., and Hayashi, H. (2007) *Mol. Cell Biol.* **27**, 2841–2847
- Umeda, N., Suzuki, T., Yukawa, M., Ohya, Y., Shindo, H., Watanabe, K., and Suzuki, T. (2005) *J. Biol. Chem.* **280**, 1613–1624
- Leidel, S., Pedrioli, P. G., Bucher, T., Brost, R., Costanzo, M., Schmidt, A., Aebersold, R., Boone, C., Hofmann, K., and Peter, M. (2009) *Nature* **458**, 228–232
- Huang, B., Lu, J., and Byström, A. S. (2008) *RNA* **14**, 2183–2194
- Noma, A., Sakaguchi, Y., and Suzuki, T. (2009) *Nucleic Acids Res.* **37**, 1335–1352
- Smíd, O., Horáková, E., Vilímová, V., Hrdy, I., Cammack, R., Horváth, A., Lukeš, J., and Tachezy, J. (2006) *J. Biol. Chem.* **281**, 28679–28686
- Poliak, P., Van Hoewyk, D., Oborník, M., Zíková, A., Stuart, K. D., Tachezy, J., Pilon, M., and Lukeš, J. (2010) *FEBS J.* **277**, 383–393
- Simpson, A. M., Suyama, Y., Dewes, H., Campbell, D. A., and Simpson, L. (1989) *Nucleic Acids Res.* **17**, 5427–5445
- Wohlgamuth-Benedum, J. M., Rubio, M. A., Paris, Z., Long, S., Poliak, P., Lukeš, J., and Alfonzo, J. D. (2009) *J. Biol. Chem.* **284**, 23947–23953
- Vondrusková, E., van den Burg, J., Zíková, A., Ernst, N. L., Stuart, K. D., Benne, R., and Lukeš, J. (2005) *J. Biol. Chem.* **280**, 2429–2438
- Jensen, B. C., Kifer, C. T., Brekken, D. L., Randall, A. C., Wang, Q., Drees, B. L., and Parsons, M. (2007) *Mol. Biochem. Parasitol.* **151**, 28–40
- Hashimi, H., Čičová, Z., Novotná, L., Wen, Y. Z., and Lukeš, J. (2009) *RNA* **15**, 588–599
- Hashimi, H., Zíková, A., Panigrahi, A. K., Stuart, K. D., and Lukeš, J. (2008) *RNA* **14**, 970–980
- Zíková, A., Panigrahi, A. K., Dalley, R. A., Acestor, N., Anupama, A., Ogata, Y., Myler, P. J., and Stuart, K. (2008) *Mol. Cell. Proteomics* **7**, 1286–1296
- Panigrahi, A. K., Zíková, A., Dalley, R. A., Acestor, N., Ogata, Y., Anupama, A., Myler, P. J., and Stuart, K. D. (2008) *Mol. Cell. Proteomics* **7**,

tRNA Thiolation and Fe/S Cluster Assembly

534–545

31. Long, S., Jirků, M., Ayala, F. J., and Lukeš, J. (2008) *Proc. Natl. Acad. Sci. U.S.A.* **105**, 13468–13473
32. Panigrahi, A. K., Schnauffer, A., Carmean, N., Igo, R. P., Jr., Gygi, S. P., Ernst, N. L., Palazzo, S. S., Weston, D. S., Aebersold, R., Salavati, R., and Stuart, K. D. (2001) *Mol. Cell. Biol.* **21**, 6833–6840
33. Gavin, A. C., Bösche, M., Krause, R., Grandi, P., Marzioch, M., Bauer, A., Schultz, J., Rick, J. M., Michon, A. M., Cruciat, C. M., Remor, M., Höfert, C., Schelder, M., Brajenovic, M., Ruffner, H., Merino, A., Klein, K., Hudak, M., Dickson, D., Rudi, T., Gnau, V., Bauch, A., Bastuck, S., Huhse, B., Leutwein, C., Heurtier, M. A., Copley, R. R., Edlmann, A., Querfurth, E., Rybin, V., Drewes, G., Raida, M., Bouwmeester, T., Bork, P., Seraphin, B., Kuster, B., Neubauer, G., and Superti-Furga, G. (2002) *Nature* **415**, 141–147
34. Saas, J., Ziegelbauer, K., von Haeseler, A., Fast, B., and Boshart, M. (2000) *J. Biol. Chem.* **275**, 2745–2755
35. Crain, P. F., Alfonzo, J. D., Rozenski, J., Kapushoc, S. T., McCloskey, J. A., and Simpson, L. (2002) *RNA* **8**, 752–761
36. Mihara, H., Kato, S., Lacourciere, G. M., Stadtman, T. C., Kennedy, R. A., Kurihara, T., Tokumoto, U., Takahashi, Y., and Esaki, N. (2002) *Proc. Natl. Acad. Sci. U.S.A.* **99**, 6679–6683
37. Bruske, E. I., Sendfeld, F., and Schneider, A. (2009) *J. Biol. Chem.* **284**, 36491–36499
38. Besteiro, S., Barrett, P., Rivière, L., and Bringaud, F. (2005) *Trends Parasitol.* **21**, 185–191
39. Johansson, M. J., Esberg, A., Huang, B., Björk, G. R., and Byström, A. S. (2008) *Mol. Cell. Biol.* **10**, 3301–3312
40. Schlieker, C. D., Van der Veen, A. G., Damon, J. R., Spooner, E., and Ploegh, H. L. (2008) *Proc. Natl. Acad. Sci. U.S.A.* **47**, 18255–18260
41. Zutz, A., Gompf, S., Schägger, H., and Tampé, R. (2009) *Biochim. Biophys. Acta* **1787**, 681–690
42. Agris, P. F., Söll, D., and Seno, T. (1973) *Biochemistry* **12**, 4331–4337
43. Kamenski, P., Kolesnikova, O., Jubenot, V., Entelis, N., Krashennikov, I. A., Martin, R. P., and Tarassov, I. (2007) *Mol. Cell* **26**, 625–637

3.2 Stage-specific requirement for Isa1 and Isa2 proteins in the mitochondrion of *Trypanosoma brucei* and heterologous rescue by human and *Blastocystis orthologues*

(reprint of Molecular Microbiology 81: 1403–1418)

Stage-specific requirement for *Isa1* and *Isa2* proteins in the mitochondrion of *Trypanosoma brucei* and heterologous rescue by human and *Blastocystis* orthologues

Shaojun Long,^{1†} Piya Changmai,^{1,2}
Anastasios D. Tsaousis,³ Tomáš Skalický,^{1,2}
Zdeněk Verner,^{1,2} Yan-Zi Wen,^{1†} Andrew J. Roger³
and Julius Lukeš^{1,2*}

¹Biology Centre, Institute of Parasitology, Czech Academy of Sciences, České Budějovice (Budweis), Czech Republic.

²Faculty of Sciences, University of South Bohemia, České Budějovice (Budweis), Czech Republic.

³Centre for Comparative Genomics and Evolutionary Bioinformatics, Department of Biochemistry and Molecular Biology, Dalhousie University, Halifax, Canada.

Summary

IscA/Isa proteins function as alternative scaffolds for the assembly of Fe-S clusters and/or provide iron for their assembly in prokaryotes and eukaryotes. Isa are usually non-essential and in most organisms are confined to the mitochondrion. We have studied the function of Tblsa1 and Tblsa2 in *Trypanosoma brucei*, where the requirement for both of them to sustain cell growth depends on the life cycle stage. The Tblsa proteins are abundant in the procyclic form, which contains an active organelle. Both proteins are indispensable for growth, as they are required for the assembly of Fe-S clusters in mitochondrial aconitase, fumarase and succinate dehydrogenase. Reactive oxygen species but not iron accumulate in the procyclic mitochondrion upon ablation of the Tblsa proteins, but their depletion does not influence the assembly of Fe-S clusters in cytosolic proteins. In the bloodstream form, which has a downregulated mitochondrion, the Tblsa proteins are non-essential. The *Isa2* orthologue of the anaerobic protist *Blastocystis* partially rescued the growth and enzymatic activities of Tblsa1/2 knock-down. Rescues of single knock-downs as well as heterologous rescues with human

***Isa* orthologues partially recovered the activities of aconitase and fumarase. These results show that the *Isa1* and *Isa2* proteins of diverse eukaryotes have overlapping functions.**

Introduction

Iron–sulphur (Fe-S) proteins are present in all domains of life. Most of them are essential and it is estimated that in a typical eukaryotic cell over 100 proteins containing Fe-S clusters are involved in electron transport, catalysis, sensing and DNA/RNA metabolism. However, this is likely an underestimate because numerous other Fe-S cluster-dependent functions are continuously being elucidated and more proteins than previously appreciated have been shown to possess the evolutionarily ancient Fe-S cofactors (Johnson *et al.*, 2005; Lill and Mühlenhoff, 2005; Fontecave, 2006; Lill, 2009).

The current paradigm holds that most, if not all, Fe-S clusters in eukaryotes are synthesized within their mitochondria by the highly conserved iron–sulphur cluster (ISC) assembly machinery that originated from this organelle's prokaryotic endosymbiont ancestor. While a substantial fraction of the clusters formed *de novo* are integrated into organellar proteins, some of them are exported into the cytosol and the nucleus, where they are incorporated into the target proteins via a eukaryote-specific cytosolic Fe-S cluster pathway (= CIA) (Kato *et al.*, 2002; Lill and Mühlenhoff, 2008). Key components of the ISC system are: (i) cysteine desulphurase (Nfs/IscS) that catalyses desulphurization of L-cysteine into alanine providing sulphur (Zheng *et al.*, 1993); (ii) frataxin (Yfh), which is proposed to deliver iron, although its exact function remains to be established (Lill and Mühlenhoff, 2008; Long *et al.*, 2008a); (iii) ferredoxin (Yah1) that provides electrons for the reduction of sulphur to sulphide in the clusters (Nakamura *et al.*, 1999); and (iv) a metallochaperone (IscU/IscU1), on which the Fe-S cofactors are transiently assembled (Nishio and Nakai, 2000; Mühlenhoff *et al.*, 2003). However, the list of conserved and essential components of the Fe-S cluster assembly pathway is steadily growing and currently includes approximately two dozen proteins (Lill, 2009).

Accepted 6 July, 2011. *For Correspondence. E-mail: jula@paru.cas.cz; Tel. (+420) 387775416; Fax (+420) 385310388. Present addresses: [†]Institute for Cell and Molecular Biosciences, Faculty of Medical Science, Newcastle University, UK; [‡]School of Life Sciences, Sun Yat-Sen (Zhongshan) University, Guangzhou, China.

With the exception of the CIA pathway, all dedicated machineries for Fe-S cluster assembly contain the A-type scaffold component (Lill, 2009). In eukaryotic genomes, the homologue(s) of prokaryotic IscA are the Isa proteins (Zheng *et al.*, 1998; Rouault and Tong, 2005). In the yeast *Saccharomyces cerevisiae*, as well as in numerous other eukaryotes, two Isa homologues labelled Isa1 and Isa2 were recently shown to have an additional binding partner Iba57, also involved in Fe-S cluster assembly (Gelling *et al.*, 2008). Isa1 is found in all multicellular model organisms, while it may be poorly conserved or even missing in protists with reduced mitochondria or mitosomes, such as *Encephalitozoon cuniculi*, *Cryptosporidium parvum*, *Entamoeba histolytica* and *Trichomonas vaginalis* (Lill and Mühlenhoff, 2005; Vinella *et al.*, 2009).

It was proposed that the rather small IscA and SufA (member of the bacterial SUF operon) proteins serve in prokaryotic Fe-S cluster biosynthesis as alternative scaffold proteins (Krebs *et al.*, 2001; Ollagnier-de-Choudens *et al.*, 2001; Wollenberg *et al.*, 2003; Lu *et al.*, 2008) and a similar function was also suggested for their eukaryotic homologues (Wu *et al.*, 2002). Furthermore, IscA may provide iron for the Fe-S cluster assembly in *Escherichia coli*, especially under limited iron conditions (Ding *et al.*, 2004), a role consistent with its very strong iron-binding affinity (Ding and Clark, 2004). These features were recently demonstrated also for the human Isa1 (hIsa1) (Lu *et al.*, 2010). Deletion of IscA or SufA causes only a minor growth phenotype in *E. coli* (Djaman *et al.*, 2004), while the simultaneous elimination of both proteins is lethal (Tan *et al.*, 2009) and can be partially rescued by hIsa1 (Lu *et al.*, 2010).

Two independent crystallographic studies of the *E. coli* IscA revealed a monodimeric or monotetrameric form with a novel fold and a pocket that can accommodate an iron atom or a Fe-S cluster (Bilder *et al.*, 2004; Cupp-Vickery *et al.*, 2004). Moreover, Mossbauer spectroscopical analysis was instrumental in showing that IscA can bind both [2Fe-2S] and [4Fe-4S] clusters, although it remains to be established whether the former cluster type is an intermediate step in the construction of [4Fe-4S] cluster, or a derivative thereof (Ollagnier-de-Choudens *et al.*, 2004).

Although the IscA/Isa proteins are widely distributed across the tree of Life, they do not seem to be essential, since their elimination in *E. coli* leads to only a mild phenotype (Tokumoto and Takahashi, 2001; Djaman *et al.*, 2004). Two different explanations for this result have been put forward: (i) IscA/Isa proteins from different Fe-S cluster machineries can, to some extent, complement each other, or (ii) they are essential only under specific growth conditions (Fontecave and Ollagnier-de-Choudens, 2008). The latter possibility gained some support from the observation that IscA in *E. coli* is indispensable in the presence of high

concentrations of oxygen (Johnson *et al.*, 2006) but is non-essential under anaerobic conditions (Wang *et al.*, 2010). The Isa proteins are also dispensable in *S. cerevisiae* (Jensen and Culotta, 2000; Pelzer *et al.*, 2000), where they function as substrate-specific assembly factors required for proper function of biotin and lipoic acid synthases, as well as in the maturation of mitochondrial aconitase (Mühlenhoff *et al.*, 2007; Gelling *et al.*, 2008). The hIsa1 protein is expressed in multiple tissues (Córcaz-Castellano *et al.*, 2004) and was recently shown to have dual localization in human cells (Song *et al.*, 2009). Even though the majority of the protein in HeLa cells was localized in the mitochondrial matrix, a fraction was also consistently found in the cytosol and it was proposed that hIsa1 might serve as a scaffold for the delivery of Fe-S clusters to aconitase in both cellular compartments (Song *et al.*, 2009). In any case, the Isa1 deficiency in yeast was rescued by its human orthologue (Córcaz-Castellano *et al.*, 2004), while hIsa1 can rescue the IscA and SufA mutant in *E. coli* (Lu *et al.*, 2010). Furthermore, a large-scale computational analysis uncovered a strong co-expression between the Isa1 and Isa2 proteins and the synthesis of haem (Nilsson *et al.*, 2009). Still, too little is currently known about the potential cross talk between Fe-S cluster and haem biosynthetic processes (Wingert *et al.*, 2005) to draw further conclusions.

In order to further clarify the function of the Isa proteins, we undertook their functional analysis in *Trypanosoma brucei*, a parasitic protist responsible for the highly pathogenic African sleeping sickness and other diseases. Trypanosomatids are evolutionarily distant from other eukaryotes that have been well studied, and represent the only excavate protists amenable to functional analyses. Moreover, trypanosomes are very interesting model organisms, in which the fully active mitochondrion of the procyclic stage transforms into a downregulated organelle that retains only basic functions in the bloodstream stage (Lukeš *et al.*, 2005). We reasoned that functional analyses in these two different forms of mitochondria in trypanosomes may shed additional light on the still rather enigmatic function of the Isa proteins in the eukaryotic cell.

Results

Identification and phylogenetic analyses of Isa1 and Isa2

The available kinetoplastid genomes were searched for homologues of the yeast Isa1 and Isa2 proteins. A BLAST search identified two homologues in the *T. brucei* genome, here labelled TbIsa1 (Tb927.8.5540) and TbIsa2 (Tb927.5.1030). We identified similar Isa orthologues in the *Trypanosoma cruzi*, *Leishmania major*, *Leishmania*

braziliensis and *Leishmania infantum* genomes (Fig. S1A and B). Alignment of their deduced amino acid sequences with numerous prokaryotic and eukaryotic homologues revealed high conservation of both proteins among kinetoplastid flagellates, including the three cysteine residues predicted to be involved in the ligation of Fe or Fe-S clusters. From the sequence alignment it is apparent that the characteristic architecture of the *E. coli* *IscA* protein, composed of two α -helices and seven β -sheets (Bilder *et al.*, 2004), is likely conserved in its *T. brucei* homologues, and this prediction was confirmed by structural modelling (data not shown). The *TbIsa1* and *TbIsa2* genes code for 272 and 173-amino-acid-long proteins with calculated molecular weights of 29.5 kDa and 19.0 kDa, respectively, and their overall identity is 23% at the amino acid level. Both proteins are predicted to contain a cleavable mitochondrial import signal, with probability 0.3733 and 0.9748 for *TbIsa1* and *TbIsa2*, respectively (MitoProtII), and similarly high probabilities predicted by pSORT.

To investigate the phylogenetic distribution of the *Isa1* and *Isa2* proteins (*ISA1/2*) we used a previously published alignment from a genome wide search on these proteins (Vinella *et al.*, 2009). To this alignment, we added the sequences of *Isa1* and *Isa2* from all available identified homologues but also some additional eukaryotic sequences recently available from genomic and transcriptomic projects. Maximum likelihood and Bayesian phylogenetic analyses demonstrated that *Isa1* and *Isa2* sequences from two clades (Fig. S1A). Interestingly, while most eukaryotes have both isoforms, all homologues from parasites such as *T. vaginalis* and *Giardia lamblia* cluster within the *Isa2* clade, while the diatom *Thalassiosira pseudonana* homologues group within the *Isa1* cluster. The genome of another parasite, *E. histolytica*, appears to be completely devoid of either *Isa* homologue (Fig. S1A).

Expression, subcellular localization and interaction of TbIsa

In order to establish the subcellular localization, and to follow the sedimentation properties and depletion of the *TbIsa* proteins, we have overexpressed the full-size *Isa1* protein in *E. coli*, from which the abundantly expressed insoluble protein has been purified (data not shown). Specific polyclonal antibodies generated against *TbIsa1* in a rat were used for further experiments. The polyclonal antibodies against *TbIsa2* were generated against a synthetic oligopeptide derived from the *T. brucei* protein (see *Experimental procedures*). In order to verify the predicted mitochondrial localization of both proteins, we have obtained cytosolic and mitochondrial fractions from the procyclic form (PF) (strain 29–13) cells of *T. brucei*. The

purity of both fractions, obtained by digitonin fractionation was confirmed by compartment-specific cytosolic and mitochondrial markers enolase and mitochondrial RNA binding protein (MRP) 2 respectively. As shown in Fig. 1A, all detectable *TbIsa1* and *TbIsa2* proteins are indeed confined to the organelle.

Based on the crystal structure of *IscA* it was predicted that in *E. coli* this protein forms one of the two alternative tetrameric oligomers (Bilder *et al.*, 2004). We wondered whether the two trypanosome *Isa* proteins form a complex or bind the *Iba57* protein, their interacting partner in yeast (Gelling *et al.*, 2008). First, we tested possible interaction by sedimentation in glycerol gradients. Western analysis on the fractions showed that both proteins co-sediment in fractions 4–6 (Fig. S2), suggesting that *Isa* proteins may be in a complex. Sedimentation of mitochondrial proteins *TbRGG1* and *KREL1*, used as controls, was in agreement with previously reported data (Hashimi *et al.*, 2008). However, mass spectrometry analysis of proteins pulled down via TAP-tagged *TbIsa1* and *TbIsa2* did not identify *TbIba57* (data not shown). Next, co-immunoprecipitations in the cell lysates with anti-*TbIsa1* or anti-*TbIsa2* antibodies, under physiological or high salt conditions, did not reveal mutual interactions between these two proteins (data not shown). It remains plausible though that, like the *E. coli* *IscA*, the *TbIsa* proteins form homo-dimers.

Expression of both TbIsa genes is essential in procyclic trypanosomes

In order to assess the function of individual *Isa* proteins in the PF of *T. brucei*, we used RNAi to selectively down-regulate the mRNA levels of *TbIsa1* and/or *TbIsa2*. A fragment of the *TbIsa1* gene or the entire *TbIsa2* gene was cloned into the p2T7-177 vector containing opposing tetracycline-regulatable promoters. Moreover, another cell line was transfected with a *NotI*-linearized p2T7-177 vector containing fragments of the *TbIsa1* and *TbIsa2* genes cloned in tandem, which allowed their parallel ablation. For each construct, several clonal cell lines have been obtained by limiting dilution using phleomycin as a selectable marker. In representative clones RNAi was induced by the addition of 1 $\mu\text{g ml}^{-1}$ tetracycline to the medium and the growth was monitored using cell counter. Upon RNAi induction, the growth of the *TbIsa* knock-downs was identical with the non-induced cells until day 3. Thereafter, the growth of the RNAi-induced *TbIsa1* and *TbIsa2* cells slowed significantly down (Fig. 1B and C). A cumulative effect occurred in the induced double knock-down cells, which virtually stopped dividing on day 4 post induction (Fig. 1D), and did not recover even after 12 days. The depletion of the target proteins was monitored by Western blot analysis using specific antibodies. In cells in which the *TbIsa1* mRNA was targeted, a very strong

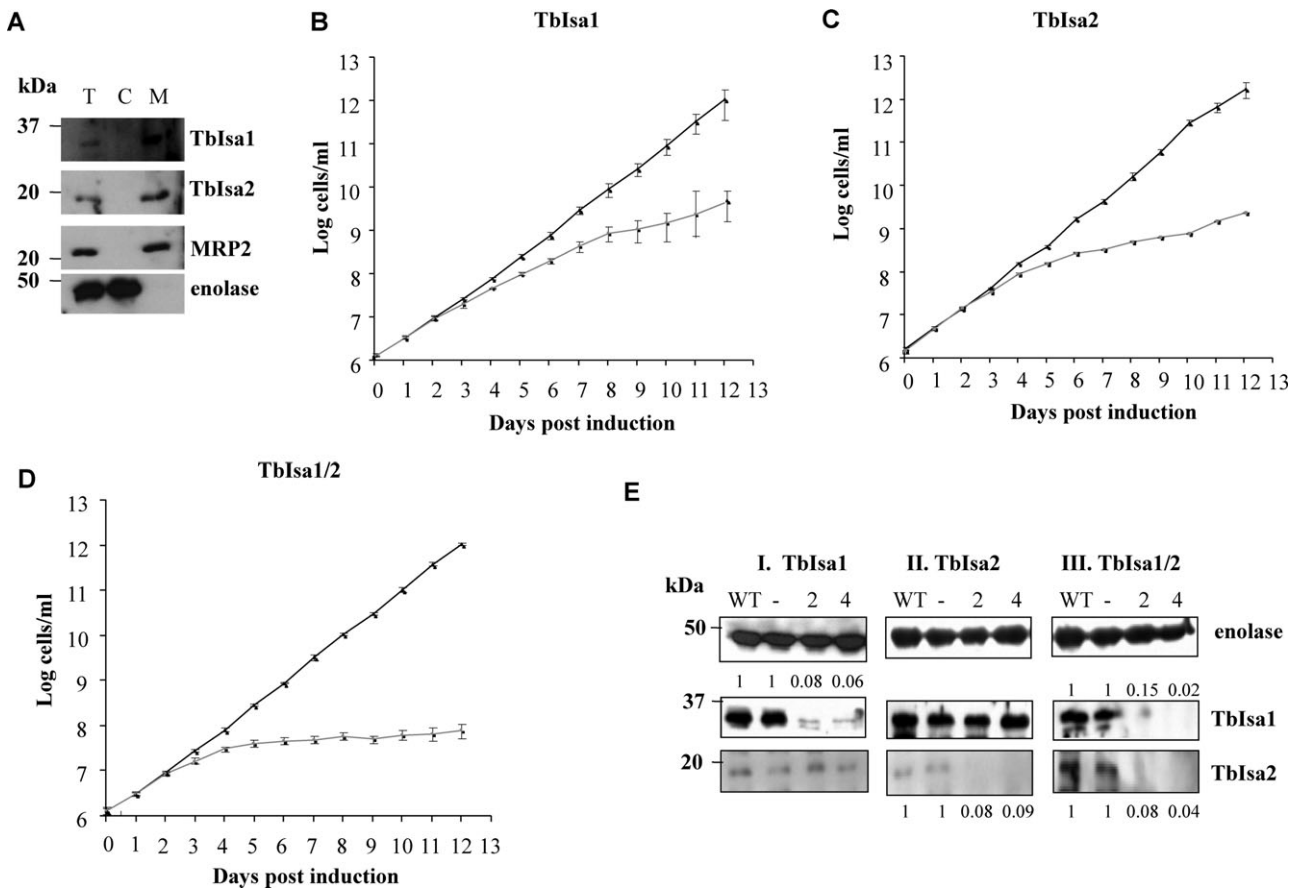


Fig. 1. Tblsa proteins are essential for growth of PF *T. brucei* and RNAi is specific for target Tblsa.

A. Western blot analysis of Tblsa1 and Tblsa2 in total lysates (T) and purified cytosolic fractions (C) and mitochondrial (M). Mitochondrial RNA binding protein 2 (MRP2) and enolase were used as mitochondrial and cytosolic markers respectively.

B–D. Growth inhibition following RNAi induction against Tblsa1 (B), Tblsa2 (C) and Tblsa1/2 (D). Cell numbers were measured using cell counter. The numbers of non-induced cells (squares; black line) and those after RNAi induction (circles; grey line) are indicated. The y-axis is labelled by a log scale and represents the product of cell densities measured and total dilution. The mean and the SD values represent the average of three independent RNAi experiments after selecting of *T. brucei* RNAi cell lines by Northern and Western blots.

E. Protein levels were analysed by Western blot analysis with α -Tblsa1 and α -Tblsa2 antibodies in whole-cell extracts from wild-type (WT) PF cells, non-induced (-) and RNAi-induced single (I, Tblsa1; II, Tblsa2) and double (III, Tblsa1/2) knock-downs after 2 and 4 days of induction. The band densities of Tblsa1 and Tblsa2 in the RNAi-induced cells are indicated above the bands, as compared with the bands in the non-induced cells. α -Enolase antibody was used as a loading control. Protein size marker positions are indicated.

decrease of the Tblsa1 protein occurred already by day 2 of RNAi induction (Fig. 1E). While more than 90% of the protein was eliminated at this early time point, residual Tblsa1 protein remained present at a stable level even by day 4.

In the Tblsa2 knock-downs, the anti-Tblsa2 antibody allowed observing the virtual disappearance of the target protein by day 2 (Fig. 1E). In both cell lines, Western analysis was instrumental to show that both antibodies and RNAi knock-downs are specific for their targets, as the levels of the non-interfered Tblsa protein remained unaltered even after 4 days of RNAi induction. Western analysis with the anti-Tblsa1/Isa2 antibodies confirmed a very efficient elimination of both proteins in the double knock-downs (Fig. 1E) and the lack of their mutual interaction.

Tblsa are required for the assembly of mitochondrial Fe-S clusters only

While early studies implicated the yeast Isa proteins with the assembly of both cytosolic and mitochondrial Fe-S clusters (Jensen and Culotta, 2000; Pelzer *et al.*, 2000), according to more recent data their function is associated only with the mitochondrion (Mühlenhoff *et al.*, 2007). We have tested the effect of individual and parallel depletion of the Tblsa proteins on selected enzymes in both cellular compartments of the PF trypanosomes. The Fe-S cluster-containing aconitase (encoded by one gene) and fumarase (encoded by two different genes) have dual localization in trypanosome cells, with 30 and 50% of aconitase and fumarase activities in the mitochondrion respectively (Saas *et al.*, 2000; Coustou *et al.*, 2006),

allowing us to measure their activities separately in the mitochondrion and cytosol (Fig. 2A and B). The purity of each compartment fraction was assessed by Western blot analysis using antibodies against mitochondrial MRP2 and cytosolic enolase (Fig. 2E). As shown in Fig. 2A, in all three RNAi knock-downs, 2 days upon the addition of tetracycline into the medium the mitochondrial aconitase activity dropped by 60%. Following additional 48 h, only about 25% of the activity persisted (Fig. 2A). The depletion of any of the *TbIsa* proteins had an even more dramatic effect on mitochondrial fumarase, which on day 2 decreased by between 60 to 75%, while on day 4 only 10–25% residual activity remained (Fig. 2B). A parallel measurement of the activities of aconitase and fumarase in pure cytosolic fractions obtained from the non-induced

and RNAi-induced *TbIsa* knock-downs revealed that neither of these activities was decreased (Fig. 2A and B). The activity of succinate dehydrogenase (complex II), an Fe-S cluster containing enzyme that is exclusively mitochondrial, followed a pattern very similar to both above-mentioned enzymes. Its activity dropped most in the double knock-downs, with only 15% of its activity remaining after 4 days of RNAi induction (Fig. 2C). The activity of threonine dehydrogenase, an enzyme lacking Fe-S clusters, was used as a control; its activity remained unaffected in both the non-induced and RNAi-induced cells (Fig. 2D).

In order to evaluate possible associations of the *TbIsa* proteins with other components of the mitochondrial Fe-S cluster assembly machinery, we have followed the levels

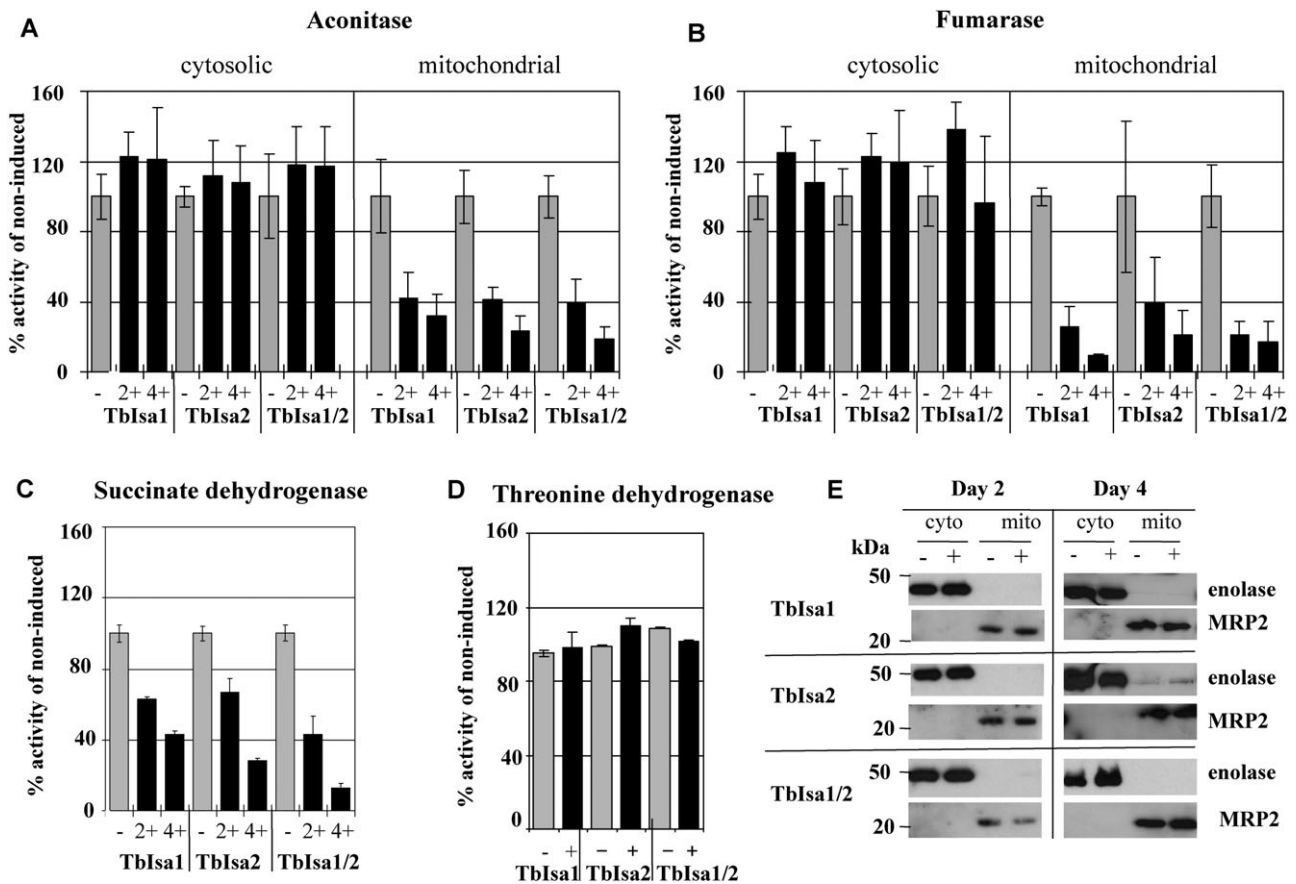


Fig. 2. Biochemical consequences of RNAi-mediated downregulation of *TbIsa* proteins in PF *T. brucei*.

A. The effect of RNAi against *TbIsa1*, *TbIsa2* and *TbIsa1/2* on the activity of the Fe-S cluster-containing cytosolic (left panel) and mitochondrial (right panel) aconitase. Enzymatic activities were measured in non-induced cells (grey columns) (-) and cells 2 and 4 days of RNAi induction (black columns) (+). Specific activities are shown as percentage of activities in non-induced cells; the mean and the SD values represent the average of three independent RNAi experiments.

B. Enzymatic activities of Fe-S cluster-containing fumarase are shown same as in (A).

C. Enzymatic activities of Fe-S cluster-containing mitochondrial succinate dehydrogenase (= complex II) are shown same as in (A).

D. Enzymatic activities of Fe-S cluster lacking threonine dehydrogenase are shown same as in (A).

E. The purity of the cellular fractions (cyto – cytosolic; mito – mitochondrial) obtained for the above enzymatic measurements from non-induced (-) cells, as well as from *TbIsa1*, *TbIsa2* and *TbIsa1/2* knock-downs after 2 and 4 days upon RNAi induction (+) was verified by Western analysis using α -enolase and α -MRP2 antibodies, which served as cytosolic and mitochondrial markers respectively. Protein size marker positions are indicated.

of the cysteine desulphurase Nfs, metallochaperone IscU and frataxin in the interfered cells 2, 4 and 6 days of RNAi induction. However, in both the single and double knock-downs the abundance of all of these proteins remained unaltered (Fig. S3).

Reactive oxygen species is elevated but iron content remains unaltered in the mitochondrion

We were interested to determine if the disturbance of mitochondrial Fe-S cluster-containing enzymes had a more general impact on functions of the organelle. Using dihydroethidium we have shown that all Tblsa RNAi-induced cells accumulate ROS (Fig. 3A–C). In yeast, disruptions of the ISC pathway, such as the depletion of the Isa proteins, frequently lead to iron accumulation in the mitochondrion. We wondered whether the same effect will also occur in the trypanosome cells. The concentration of iron was followed in mitochondrial fractions by the ferene

method, which detects all intracellular iron except the one bound by haem (Pieroni *et al.*, 2001). The measurement revealed an unaltered iron level in the organelle of RNAi-induced double knock-downs when compared with the non-induced cells (Fig. 3D).

Both Tblsa are non-essential in bloodstream trypanosomes

Since the depletion of Tblsa's exhibited an effect on the mitochondrial Fe-S cluster-containing proteins in the PF cells, we also generated RNAi knock-downs in the bloodstream form (BF), which parasitizes mammalian blood. These cells are known to have a largely downregulated organelle, as compared with the PF cells (Schneider, 2001; Lukeš *et al.*, 2005; Tielens and van Hellemond, 1998). First, using the anti-Tblsa1 and anti-Tblsa2 antibodies, the levels of the Tblsa proteins in total lysates of the BF cells purified from the blood of a rat were shown to

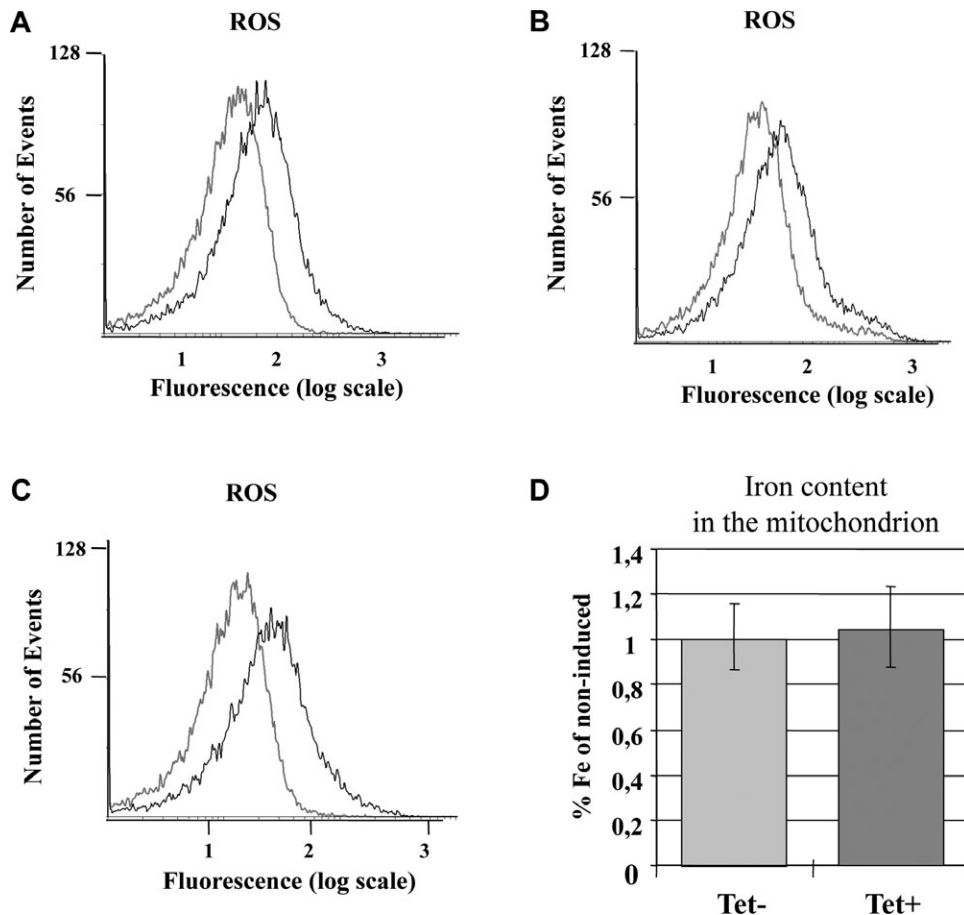


Fig. 3. Measurement of ROS and iron content in mitochondrion of PF *T. brucei* RNAi cell lines.

A–C. ROS were measured using dihydroethidium in Tblsa1 RNAi cells (A), Tblsa2 RNAi cells (B) and Tblsa1/2 RNAi cells (C) after 4 days of RNAi induction (black line), as compared with the respective non-induced cells (grey line). Representative data from three independent experiments are shown.

D. The concentration of iron was quantified by the ferene method for mitochondrial fraction obtained from the non-induced cells (–) and cells, in which Tblsa1/2 were ablated (4 days of RNAi induction) (+). Experiments were performed for three independent RNAi inductions.

be substantially lower than in the PF cells (Fig. 4A). Signal quantification revealed that there is about 4× and 6.2× less of *TbIsa1* and *TbIsa2*, respectively, in the BF than in the PF cells. Next, the *TbIsa1*, *TbIsa2* and *TbIsa1/2* RNAi constructs used to deplete the target proteins in the PF cells were electroporated into the *T. brucei* 427 BF cells

grown in HMI-9 medium. The growth of phleomycin-resistant non-induced and RNAi-induced clones was then followed for one week, with cells diluted on a daily basis. Unexpectedly, no or only a very weak growth phenotype was observed in either of the transfectants (Fig. 4B–D). The target *TbIsa* transcripts were undetectable in the BF

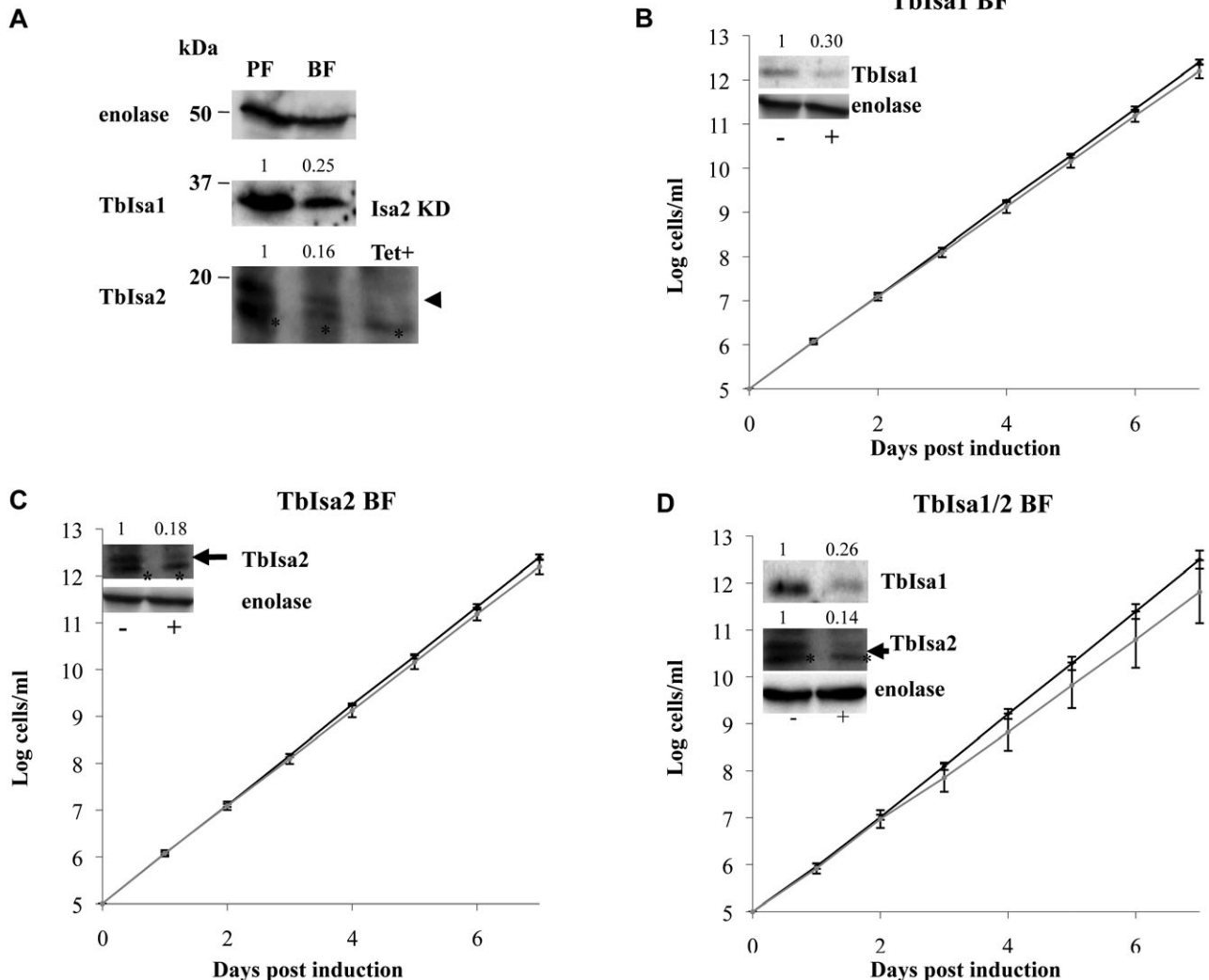


Fig. 4. *TbIsa* proteins are non-essential for BF *T. brucei*.

A. *TbIsa1* and *TbIsa2* are much less abundant in the BF cells (strain 920) than in the PF cells (strain 29–13), as shown by Western blot analysis with the α -*TbIsa1* and α -*TbIsa2* antibodies. The specific and non-specific bands recognized by the α -*TbIsa2* antibodies are labelled with an arrow and asterisk respectively. Induced PF *Isa2* RNAi cells were used as a control for the *TbIsa2*-specific band. Numbers above the bands indicate their relative density in the RNAi-induced cells as compared with the non-induced ones. Cytosolic enolase was used as a loading control. Protein size marker positions are indicated.

B–D. Growth curves of *TbIsa1* (B), *TbIsa2* (C) and *TbIsa1/2* double knock-down (D) cells over 7 days showed that RNAi silencing altered only very weakly the growth of the BF cells. Cells were diluted every 24 h to a density of 10^5 cells ml^{-1} and their numbers were measured using cell counter. The numbers of non-induced cells (black line) and those after RNAi induction by the addition of $1 \mu\text{g ml}^{-1}$ tetracycline (grey line) are indicated. The y-axis is labelled by a log scale and represents the product of cell densities measured and total dilution. The mean and the SD values represent the average of three independent RNAi experiments after selecting RNAi cell lines by Northern and Western blots. The arrow indicates a sampling point for Western blot analysis. Western blot analysis of total protein extracted from the non-induced (–) cells, and knock-down cells 4 days of RNAi induction (+) are shown as insets. Numbers above the bands indicate their relative density in the RNAi-induced cells as compared with the non-induced ones. The α -*TbIsa1* and α -*TbIsa2* antibodies followed the target proteins, the α -enolase antibody was used as a loading control. The specific and non-specific bands recognized by α -*TbIsa2* antibodies are indicated by arrow and asterisk respectively.

cells assayed by Northern blot analysis (data not shown), yet Western blot analysis with anti-TbIsa1/Isa2 antibodies confirmed a decrease by 70% and 85% of the targeted protein upon RNAi induction in the respective single knock-down (Fig. 4B and C). Equally efficient downregulation of both proteins was documented in the double knock-down cells (Fig. 4D).

Functional rescues with human Isa homologues

While human Isa1 has been intensely studied and can rescue *E. coli* (Lu *et al.*, 2010) and yeast cells depleted for its homologues (Córcaz-Castellano *et al.*, 2004), nothing is known about the function of human Isa2. Here we have attempted to use the trypanosome model to study the human Isa proteins using a complementation assay. Based on our observation that TbIsa1 can to some extent substitute for TbIsa2, and vice versa, since both proteins have similar biochemical properties, we prepared various rescue combinations with the human Isa genes. To this end, the following rescue cell lines were generated: (i) TbIsa1 + hIsa1; (ii) TbIsa2 + hIsa2; (iii) TbIsa1 + hIsa2; (iv) TbIsa2 + hIsa1; (v) TbIsa1/2 + hIsa1; (vi) TbIsa1/2 + hIsa1/2; and (vii) TbIsa1/2 + hIsa2.

In both the human and *T. brucei* cells, most mitochondrion-targeted proteins are synthesized as precursors that are, upon import, proteolytically matured by mitochondrial processing peptidase. We have shown recently that the signal peptide on the human frataxin will efficiently target the downstream protein into the trypanosome organelle (Long *et al.*, 2008b). Therefore, the coding sequence for the human frataxin signal peptide (1–54 residues) was introduced to replace the predicted signal peptide (1–13 residues) of hIsa1 gene obtained from the human cDNA library, after an attempt with full-length hIsa1 failed due to the lack of its import into the *T. brucei* mitochondrion (data not shown). The full-length hIsa2 with its genuine import signal inserted in the pFC4 vector was used in all rescue experiments with this protein. Import of these heterologous proteins was followed using antibody against the HA₃-tag attached to the C-termini of hIsa1 protein and with a specific antibody against hIsa2. As shown in Fig. 5A, all tagged hIsa1 was imported into the single mitochondrion of PF cells, while the situation was more complex in the case of hIsa2, which was equipped with its genuine import signal. Western blot analysis detected two forms, apparently representing the pre-processed (arrow) and processed (arrowhead) hIsa2, while no signal was detected in cell lines lacking the hIsa2 construct (Fig. 5C). Therefore, we resorted to Western blot analysis of cellular fractions from the TbIsa2 + hIsa2 cells. As expected, the resulting mitochondria contained only the shorter processed form of hIsa2, whereas the most abundant species in the cytosol

was the pre-processed protein. In the total cell lysate, the processed hIsa2 protein predominated, although the processing of this alien protein was apparently less efficient relative to the genuine trypanosome mitochondrial proteins (Fig. 5B).

Next, we measured the activities of aconitase and fumarase in the mitochondrion, as activities of these proteins in the cytosol were not influenced by the status of the TbIsa proteins (Fig. 2). Comparative measurement of these activities in the above-described PF cell lines, as well as in cells with ablated TbIsa2 and TbIsa1/2 showed that both activities are, to some extent, rescued in all cases (Fig. 6). Particularly efficient is the rescue of TbIsa2 by hIsa2, while the other combinations resulted in less efficient rescues, especially when aconitase is considered (Fig. 6A). The activity of fumarase was restored to almost wild-type levels even in both cross-rescues (TbIsa1 + hIsa2 and TbIsa2 + hIsa1) (Fig. 6B), strongly indicating that the functions of the human Isa proteins are overlapping in *T. brucei*. However, although the cell growth was not recovered by the human Isa proteins (data not shown), high level of enzymatic activities were measured in the rescue cells.

Rescue with Blastocystis Isa2

So far, no information is available on the function of the Fe-S cluster assembly proteins identified in the anaerobic mitochondrion-related organelles (MROs) of *Blastocystis hominis*. Since MROs display a mixture of mitochondrial and hydrogenosomal features, they are functionally and evolutionarily distinct from the canonical aerobic mitochondria of yeast and mammals (Stechmann *et al.*, 2008). Being the only Isa homologue identified in *B. hominis* (Fig. S1), BhIsa2 was used to rescue the TbIsa deficiency in *T. brucei*. The full-length BhIsa2 gene amplified from a cDNA molecule was cloned into the pABPURO vector and introduced into the PF *T. brucei* inducible for RNAi against the *T. brucei* Isa1/2 double knock-down. The empty pABPURO vector and TbIsa1/2 RNAi knock-down were used as controls. The growth phenotype triggered by the depletion of TbIsa1/2 was partially rescued by the expression of BhIsa2 (data not shown). Furthermore, the activities of mitochondrial fumarase (Fig. 7A), aconitase (Fig. 7B), as well as succinate dehydrogenase (Fig. 7C), almost reached the wild-type levels.

Discussion

Trypanosoma brucei and related flagellates are responsible for devastating diseases of humans and other vertebrates in most tropical regions. These parasites are also the most genetically tractable excavate protists, and as a consequence, they are the only representatives of this

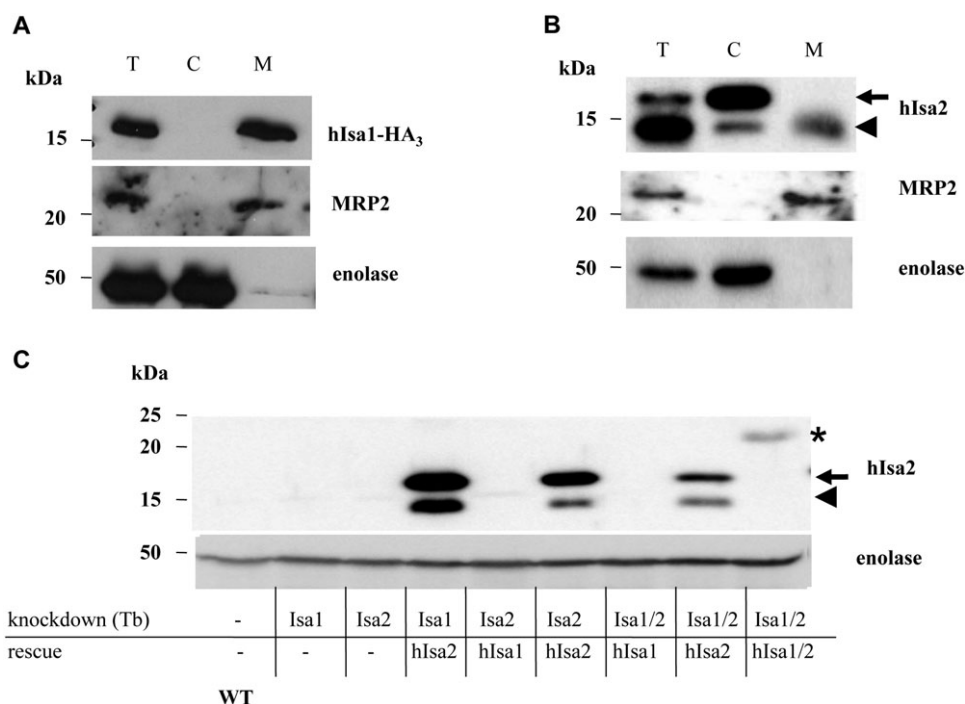


Fig. 5. Human Isa proteins are expressed, processed and efficiently targeted into the mitochondrion of PF *T. brucei*.

A. Western blot analysis of the expression and targeting of the HA₃-tagged human frataxin signal peptide lead hIsa1. Total cell lysate (T), cytosolic (C) and mitochondrial (M) fractions isolated by digitonin fractionation were probed with antibody against the HA₃ tag. α -MRP2 and α -enolase antibodies were used as mitochondrial and cytosol-specific markers respectively.

B. Western blot analysis of the expression, processing and targeting of hIsa2. Total cell lysate (T), cytosolic (C) and mitochondrial (M) fractions isolated by digitonin fractionation were probed with antibody against human Isa2. α -MRP2 and α -enolase antibodies were used as mitochondrial and cytosolic markers respectively. The pre-processed and processed forms of hIsa2 are indicated with an arrow and arrowhead respectively.

C. Western blot analysis of the expression and processing of hIsa2 in various PF cell lines. The table below describes which Tblsa protein was downregulated (knockdown-Tb) by RNAi, and which human (h) Isa protein was used to complement the RNAi knock-down cells (rescue). Total lysate was obtained from the following cells: 29–13 PF cells (WT), Tblsa1 knock-down, Tblsa2 knock-down, Tblsa1 knock-down transfected with pFC4-hIsa2, Tblsa2 knock-down transfected with pABPURO-hIsa1, Tblsa2 knock-down transfected with pFC4-hIsa2, Tblsa1/2 double knock-down transfected with pABPURO-hIsa1, Tblsa1/2 double knock-down transfected with pFC4-hIsa2, Tblsa1/2 double knock-down transfected with both pABPURO-hIsa1 and pFC4-hIsa2-HA. The pre-processed and processed forms of hIsa2 are indicated with an arrow and arrowhead respectively. The HA₃-tagged hIsa2 corresponds to the pre-processed form and is labelled with an asterisk. α -Enolase antibody was used as loading control.

eukaryotic super-group, in which functional studies are routinely made. We are interested in investigating how Fe-S clusters are generated in this deeply divergent and medically highly relevant protist.

So far, we have demonstrated that several key components of the pathway are present in *T. brucei* and their function seems to be conserved with respect to the well-studied eukaryotes, such as *S. cerevisiae*, *Arabidopsis thaliana* and humans. A preliminary search for genes encoding members of the ISC and CIA pathways in the *T. brucei* genome revealed not only the presence of all conserved components but in a few cases even the existence of several homologues of otherwise single-copy genes (S.L and J.L., unpubl. results). Therefore, it is reasonable to assume that the complexity of the Fe-S cluster assembly in this unicellular eukaryote will be similar to that of the sophisticated machinery emerging from the studies of multicellular organisms.

Proper assembly of the Fe-S clusters in trypanosomes clearly requires the function of cysteine desulphurase Nfs, its interaction partner Lsd11 and the metallochaperone IscU, the bulk of which is localized in the single reticulated mitochondrion (Smid *et al.*, 2006; Paris *et al.*, 2010). More recently, we have shown that, although undetectable by Western blot analysis, a tiny amount of Nfs is also present in the cytosol/nucleus and the same seems to apply for selenocysteine lyase, which has overlapping functions with the above-mentioned protein (Poliak *et al.*, 2010). Furthermore, the *T. brucei* Nfs is indispensable for the thiolation of tRNAs in both mitochondrial and cytosolic compartments (Wohlgamuth-Benedum *et al.*, 2009). Another core ISC component, frataxin, is essential for Fe-S clusters incorporated not only in the mitochondrial proteins, but also in the cytosolic ones, although for survival of the trypanosome, mitochondrial localization of frataxin is mandatory (Long *et al.*, 2008a,b).

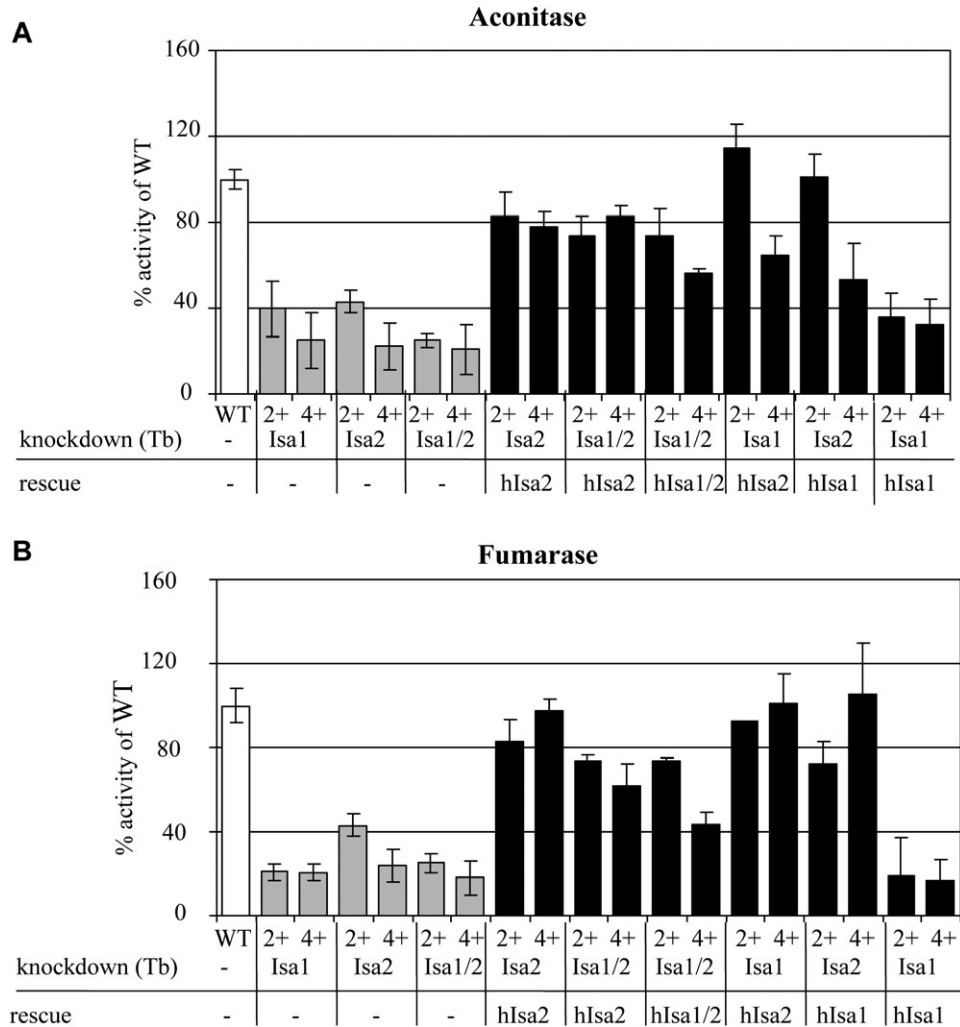


Fig. 6. Biochemical consequences of *TbIsa* knock-downs (cross) rescued with human *Isa* proteins in PF *T. brucei*.

A. Enzymatic activity of aconitase was measured for mitochondrial fractions obtained with digitonin fractionation. Its activity in 29–13 PF cells represents 100% (white column), activities in *TbIsa1*, *TbIsa2* and *TbIsa1/2* double knock-down 2 and 4 days upon RNAi inductions (+) (grey columns). Activities shown in black columns are from the following cells: *TbIsa2* knock-downs transfected with pFC4-*hIsa2*, *TbIsa1/2* double knock-down transfected with pFC4-*hIsa2*, *TbIsa1/2* double knock-down transfected with pABPURO-*hIsa1* and pFC4-*hIsa2*, *TbIsa1* knock-down transfected with pFC4-*hIsa2*, *TbIsa2* knock-down transfected with pABPURO-*hIsa1*, *TbIsa1* knock-down transfected with pABPURO-*hIsa1*+HA_s; the mean and the SD values represent the average of measurements of three independent RNAi inductions. The table below describes which *TbIsa* protein was downregulated (knockdown-Tb) by RNAi, and which human (h) *Isa* protein was used to complement the RNAi knock-down cells (rescue).

B. Enzymatic activity of Fe-S cluster-containing mitochondrial fumarase. Cell lines are same as in (A).

Here we have focused on the role of the eukaryotic *Isa* proteins, functionally studied so far mostly in *S. cerevisiae*. Until recently, they were affiliated with the Fe-S cluster assembly of mitochondrial proteins such as aconitase and biotin synthase (Pelzer *et al.*, 2000; Mühlenhoff *et al.*, 2007). This view was, however, recently challenged, as human *Isa1* was proposed to play an important role in both mitochondrial and cytosolic Fe-S cluster assembly in HeLa cells (Song *et al.*, 2009). We have therefore inspected activities of the Fe-S cluster-containing fumarase and aconitase, which have a dual localization in the PF trypanosomes (Saas *et al.*,

2000; Coustou *et al.*, 2006) and are thus particularly suitable for assessing the impact on different cellular compartments. Whereas activities of both enzymes invariably dropped in both the mitochondrion and cytosol of the PF cells upon the depletion of Nfs, *IscU*, *Isc11* or frataxin (Smid *et al.*, 2006; Long *et al.*, 2008a; Paris *et al.*, 2010), the consequence of depletion of the *Isa* proteins was different, as it impacts only on the organellar Fe-S cluster-containing enzymes. Moreover, the activity of succinate dehydrogenase was strongly depleted in all *TbIsa* knock-downs, a phenomenon which went unnoticed in other eukaryotes (Jensen and Culotta, 2000;

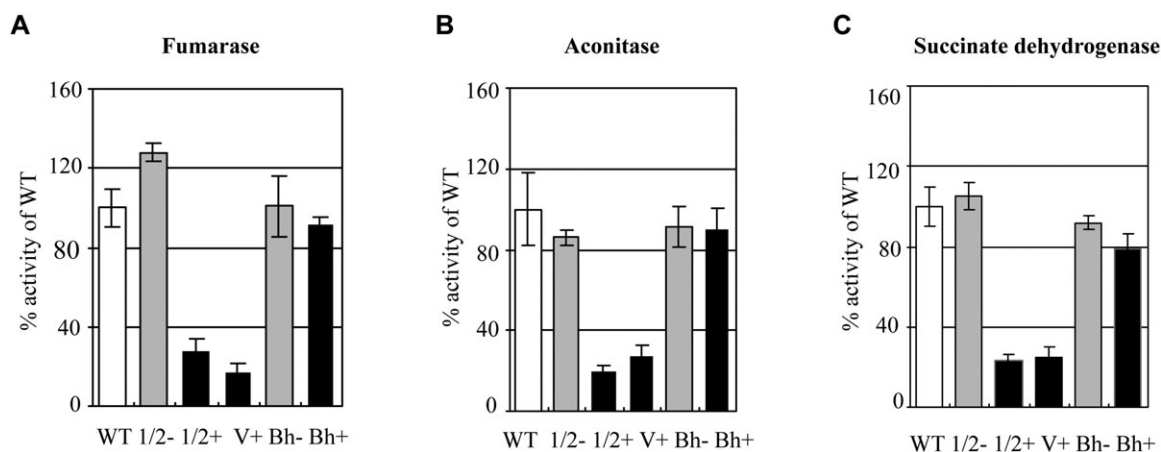


Fig. 7. Biochemical consequences of *Tblsa1/2* double knock-down rescued with *B. hominis* *Isa2* proteins in PF *T. brucei*. Enzymatic activities of fumarase (A), aconitase (B) and succinate dehydrogenase (C) were measured in the digitonin isolated mitochondria. A given activity in 29–13 PF cells represents 100% (white column). Activity in non-induced *Tblsa1/2* cells (1/2–) and the same cell transfected with *Bhlsa2* (Bh–) is shown in grey columns. Activity in RNAi-induced *Tblsa1/2* (1/2+), *Tblsa1/2* with an empty pABPURO vector (V+), and those transfected with *Bhlsa2* (Bh+) after 4 days of RNAi induction is shown in black columns; the mean and the SD values represent the average of measurements from three independent RNAi induction.

Kaut *et al.*, 2000; Pelzer *et al.*, 2000; Mühlenhoff *et al.*, 2007; Gelling *et al.*, 2008).

It is likely that this drop in activities of all three inspected mitochondrial Fe-S proteins is responsible for the observed lethal phenotype. Moreover, the ablation of the *Tblsa* proteins caused a dramatic increase of ROS in all RNAi-induced cell lines, particularly in the double knock-down. We attribute this effect to the disruption of the respiratory chain due to the shortage of Fe-S clusters needed for its components, not to the Fenton reaction, since iron did not accumulate in the *Tblsa*-depleted organelle. Particularly telling is the apparent lack of importance of *Tblsa* in the BF cells, in which both proteins can be ablated with no impact on cell growth. It is well known that the BF mitochondrion is considerably reduced and lacks respiratory complexes, yet it still efficiently imports proteins, maintains membrane potential, and replicates and transcribes its mitochondrial DNA, the transcripts of which are properly edited and translated (Schneider, 2001; Hashimi *et al.*, 2010). This organelle lacks most if not all Fe-S cluster-containing proteins such as respiratory complexes I thru III (Besteiro *et al.*, 2005; Lukeš *et al.*, 2005; Tielens and van Hellemond, 1998), fumarase (Coustou *et al.*, 2006) and aconitase (P.C and J.L., unpubl. results). The only currently known [2Fe-2S] cluster-containing mitochondrial protein in the BF *T. brucei*—monothiol glutaredoxin 1 is, however, non-essential (Comini *et al.*, 2008). Our results provide indirect, but rather strong evidence that except for a very low amount of aconitase, no other proteins containing the [4Fe-4S] clusters are made in this downregulated organelle, rendering the two *Tblsa* proteins fully dispensable for this life stage. Moreover, non-

essentiality of the *Tblsa* proteins for the BF *T. brucei* further confirmed that they do not participate in Fe-S cluster export and cytosolic Fe-S cluster assembly. It is reasonable to assume that both these pathways are required also at the BF stage, since numerous cytosolic Fe-S proteins, such as Rli1 are essential for yeast (Kispal *et al.*, 2005) as well as trypanosomes (Estévez *et al.*, 2004). Still, the low amount of *Tblsa* in BF cells may reflect the existence of as yet unidentified [4Fe-4S] proteins in their mitochondrion.

Recently, Song *et al.* (2009) showed that in HeLa cells the majority of *hlsa1* is located in the mitochondrion, while a miniscule but functionally important amount of this protein is also present in the cytosol. Although we cannot entirely rule out a similar situation in the studied flagellates, two lines of evidence presented in this study – the lack of an effect of *Tblsa* ablation on the cytosolic Fe-S cluster proteins and the non-essentiality of these proteins in the BF cells – indicate that the *Tblsa* proteins only have a functional role in the mitochondrion of *T. brucei*. In *E. coli* *IscA* was shown to be required for maturation of the [4Fe-4S] enzymes (Tan *et al.*, 2009). The non-essentiality of *Tblsa* for cytosolic Fe-S proteins indicates that ferredoxin, an [2Fe-2S] protein and electron donor for the ISC machinery (Lill and Mühlenhoff, 2008) indeed remains unaffected by the lack of the *Tblsa* proteins in the organelle. It thus appears that in *T. brucei* the *Isa* proteins specifically function for mitochondrial [4Fe-4S] proteins, such as fumarase, aconitase and succinate dehydrogenase. However, the cofactor of *IscA/Isa* proteins, whether it is iron (Ding and Clark, 2004; Ding *et al.*, 2004; Lu *et al.*, 2010) or Fe-S cluster (Ollagnier-de-Choudens *et al.*, 2004), remains elusive. Our

attempts to identify it in the Tblsa proteins failed due to low expression of the tagged proteins in *T. brucei*.

It is also worth noting that haem is not synthesized in trypanosomes (Kořený *et al.*, 2010), so the association of Isa1 with haem synthesis, supported by the data obtained in mouse and zebra fish (Nilsson *et al.*, 2009), is certainly not contributing to its essentiality in trypanosomes. Furthermore, the [4Fe-4S] cluster-carrying biotin synthase, which requires the assistance of Isa proteins for the synthesis of biotin in the *S. cerevisiae* mitochondria (Mühlhoff *et al.*, 2007), is not encoded in the *T. brucei* genome and thus cannot contribute to the observed growth phenotype.

We have demonstrated that Tblsa1 and Tblsa2 have similar functions in mitochondrion-confined Fe-S cluster assembly, the essentiality of which is particularly visible in PF RNAi double knock-downs, a situation unlike yeast (Jensen and Culotta, 2000; Pelzer *et al.*, 2000). It was shown recently that human Isa1 was able to partially rescue the growth of the *E. coli* IscA and SufA double knock-out (Lu *et al.*, 2010), but no characterization of hlsa2 rescues has been provided so far. Here we demonstrate the capacity of hlsa1 and/or hlsa2 to partially cross-rescue the activities of mitochondrial aconitase and fumarase in both single and double Tblsa1 and/or Tblsa2 knock-downs, proving their overlapping function. Ablation of Tblsa2 and complementation of the *T. brucei* cell line with hlsa2 seems to have a stronger effect on mitochondrial Fe-S proteins than that of their counterparts. However, in none of the various rescue combinations cell growth was fully recovered, indicating that hlsa failed to replace an as yet unknown activity of the Tblsa proteins.

The fact that both Tblsa proteins are essential components of the mitoproteome of PF *T. brucei*, their function being conserved as confirmed by rescue with orthologues from evolutionarily very distantly related anaerobic unicellular and aerobic multicellular eukaryotes, testifies to the unique and indispensable role of the Isa proteins in the Fe-S cluster assembly.

Experimental procedures

Phylogenetic analysis

For Isa1/2 sequences, multiple sequence alignments were created using MAFFT (Katoh *et al.*, 2002) based on a seed alignment of ATC sequences kindly provided by Celine Brochier-Armanet (Vinella *et al.*, 2009). The complete multiple sequence alignment was trimmed using MANUEL (Blouin *et al.*, 2009) and phylogenetic trees were estimated from alignments by using RAxML 7.04 (Stamatakis *et al.*, 2005) with the LG+F model of amino acid substitution and a γ model of rate heterogeneity. Bayesian phylogenetic analysis was carried out using MrBayes with the same model settings.

RNAi constructs, transfections, cloning and RNAi induction

To downregulate the Isa1 and Isa2 mRNAs by RNAi, 530-nt- and 522-nt-long fragments of the Isa1 and Isa2 genes were amplified using primer pairs Isa1-FP and Isa1-RP, and Isa2-FP and Isa2-RP (Table S1), respectively, from total genomic DNA of the *T. brucei* strain 29–13. Both amplicons were separately cloned into the p2T7-177 vector, which was, upon NotI-mediated linearization, introduced into procyclic (PF) *T. brucei* 29–13 cells using a BTX electroporator and selected as described elsewhere (Vondrušková *et al.*, 2005). The double knock-down was prepared by cloning the same fragment of the Isa2 gene, into the p2T7-177 + Isa1 construct, which was stably integrated into the *T. brucei* 29–13 PF cells as described above. All three RNAi constructs were introduced into the 427 BF *T. brucei* cells using the Amaxa Nucleofector II electroporator, with transfectants kept in the HMI-9 medium and selected following a protocol described elsewhere (Hashimi *et al.*, 2008).

Parasite cell culture

PF *T. brucei* (cell line 29–13) was cultivated at 27°C in SDM-79 medium containing G418 and hygromycin (Vondrušková *et al.*, 2005). BF *T. brucei* (strain 427) was grown *in vitro* in HMI-9 medium supplemented with hygromycin (Hashimi *et al.*, 2008). Wild-type BF (strain 920) were harvested from the blood of an infected rat by cardiac exsanguination when the parasitaemia reached 1×10^9 cell ml⁻¹. Blood was placed onto a DE52 DEAE cellulose (Whatman) column, washed with PSG buffer (38 mM Na₂HPO₄, 2 mM KH₂PO₄, 80 mM glucose, 29 mM NaCl, pH 8.0), eluted parasites were collected by centrifugation and the pellet was stored at –80°C until further use.

Following Northern and/or Western blot analyses, one clone out of four of Tb-Isa1, Tblsa2 and Tblsa1/2 RNAi knock-downs were used for further experiments. In the *T. brucei* PF and BF cells RNAi was induced by the addition of 1 μ g ml⁻¹ tetracycline to the SDM-79 and HMI-9 medium respectively. Cell density was measured every 24 h using the Beckman Z2 Coulter counter over a period of 12 days for PF and 7 days for BS after the induction of double stranded RNA synthesis. Cell morphology was analysed under the light microscope and by staining with DAPI and Giemsa.

Expression of recombinant Tblsa1, glycerol gradient and digitonin fractionation

The full-size Tblsa1 gene was amplified by PCR with primers Isa1-FP/O and Isa1-RP/O (containing the stop codon) (Table S1). The amplicon was gel-purified and cloned into the pET/100D expression vector (Invitrogen). The resulting expression plasmid encoding His₆-tagged Tblsa1 was transformed into the *E. coli* strain BL21 (star DE3) (Novagen). Insoluble protein was obtained from induced bacterial cells (incubation at 37°C for 3 h, and induced with 1 mM IPTG) under denaturing conditions using ProBond Ni-chelating resin (Invitrogen). Digitonin fractionation of the *T. brucei* PF and BF cells was performed following a protocol described

elsewhere (Smid *et al.*, 2006). Glycerol gradient of the PF cells was performed as described previously (Hashimi *et al.*, 2008).

Preparation of antibodies and Western blot analyses

Polyclonal antibody against the Tblsa1 protein was prepared by immunizing a rat at two-week intervals with the purified recombinant *Isa1* protein by Cocalico Biologicals (Reamstown, PA, USA). In the case of Tblsa2, a synthetic oligopeptide (QPKSQELRTVAEGEC) corresponding to amino acids 97–110 of the *T. brucei* protein was used to raise polyclonal antibodies in a rabbit, which were subsequently affinity-purified by GeneScript. Cell lysates corresponding to 5×10^6 cells/lane of the PF cells, or 1.5×10^7 cells of the BF cells were separated on a 15% SDS-polyacrylamide gel, transferred to membranes and probed. The anti-Tblsa1 polyclonal rat antibodies and the anti-Tblsa2 rabbit antibodies were used at 1:1000 and 1:25 dilutions respectively. The polyclonal antibodies against MRP2 (Vondrušková *et al.*, 2005), frataxin (Long *et al.*, 2008a), IscS and IscU (Smid *et al.*, 2006), enolase (provided by P.A.M. Michels), aconitase (provided by M. Boshart), and human *Isa2* (provided by H. Puccio) were used at 1:1000, 1:1500, 1:500, 1:1000, 1:200 000, 1:500 and 1:1000 dilutions respectively. Antibodies against TbRGG1 and KREL1 were used as described elsewhere (Hashimi *et al.*, 2008). The HA₃- or TAP-tagged *in vivo* expressed Tblsa proteins were determined by Western blot analysis using corresponding polyclonal antibodies followed by appropriate secondary antibodies conjugated with horse radish peroxidase (Sigma), and visualized using ECL substrates (Pierce) (Hashimi *et al.*, 2008; Long *et al.*, 2008a). For quantification of signals in Western blots, the program ImageJ 1.44p (NIH) was used.

Measurement of intracellular iron

Cytosolic and mitochondrial fractions were prepared by digitonin fractionation as described above. After protein concentration was estimated with the Bradford reagent (Bio-Rad), the volume of the fractions was decreased using a vacuum centrifuge, but the protein pellet was kept wet. Iron content was quantified by the ferene method (Hennesy and Reid, 1984; Pieroni *et al.*, 2001). Briefly, 3–5 mg protein per sample was resuspended in 100 µl of phosphate buffered saline, treated with 50 µl concentrated HCl in 100°C for 15 min, the sample was centrifuged and supernatant was transferred to a new tube. Fifty microlitres of the supernatant was mixed with 0.3 ml 1 M acetic acid-sodium acetate buffer (pH 5.5), then briefly treated with 5 µl thioglycolic acid with subsequent addition of 10 µl 6.25 mM ferene-S (Sigma). The reaction was incubated for 1 h at room temperature, and the absorbance was measured at 593 nm using a Tecan Spectrometer. To calculate the number of moles of iron bound to the protein, the molar extinction coefficient for ferene-S of $33\,850\text{ L cm}^{-1}\text{ mol}^{-1}$ was used. A standard iron solution was used as a control.

Measurement of mitochondrial ROS

After centrifugation, exponentially growing PF *T. brucei* (5×10^6 cells) were resuspended in 1 ml of fresh SDM-79

medium and ROS were measured by oxidation of dihydroethidium (Sigma), added to the final concentration $5\text{ }\mu\text{g ml}^{-1}$, in the time frame of 30 min at 27°C (Long *et al.*, 2008a). After staining, the cells were resuspended in Iso-flow buffer and instantly measured by flow cytometry using an Epics XL flow cytometer (Coulter) with excitation and emission settings of 488 and 620 nm. Dihydroethidium can be oxidized by superoxide to fluorescent ethidium, which interacts with DNA (Carter *et al.*, 1994).

Measurement of enzymatic activities

The activities of fumarase, aconitase and threonine dehydrogenase were measured in cytosolic and mitochondrial fractions obtained with digitonin fractionation, the purity of which was controlled by compartment-specific antibodies against MRP2 and enolase using Western blot analysis. The activities of fumarase and aconitase were determined spectrophotometrically at 240 nm as the rate of production of fumarate and *cis*-aconitate respectively. The activity of threonine dehydrogenase was established at 340 nm as the rate of NAD⁺ reduction as described elsewhere (Saas *et al.*, 2000). The activity of succinate dehydrogenase was measured in crude mitochondrial membrane extract as described elsewhere (Horváth *et al.*, 2005).

Rescue with human *Isa*

A 390-nt-long full-length cDNA of the human *Isa1* (*hIsa1*) gene fragment (AAH02675) with the stop codon (or without the stop codon in case of tagging) were amplified from a commercial human liver cDNA library (Invitrogen) using primers hFxn-*hIsa1*, hFxn-*hIsa1*-M and *hIsa1*-R-RP or *hIsa1*-HA₃, and cloned into the pABPURO vector with or without HA₃ tag in their 3' end, respectively, following a strategy described previously (Long *et al.*, 2008b). Next, the mitochondrial targeting peptide (1–13 amino acids) of *hIsa1* predicted by MitoProt II (0.9807) was replaced with mitochondrial targeting peptide of human frataxin (amino acids 1–55), which is known to efficiently import proteins in the *T. brucei* organelle (Long *et al.*, 2008b), using primers hFxn-*hIsa1* and *hIsa1*-R-RP or *hIsa1*-HA₃ (Table S1). A 465-nt-long full-length cDNA (AAH15771) was amplified from a commercial *hIsa2* construct (NITE BioResource Center) using primers *hIsa2*-R-FP and *hIsa2*-R-RP, and cloned into the pFC4 vector with blasticidin resistance, producing pFC4-*hIsa2*. All constructs were verified by sequencing. pABPURO- and pFC4-based constructs were linearized with BstXI and NotI, respectively, and used for transfection of the PF cells, in which RNAi against Tblsa1, Tblsa2 and Tblsa1/2 can be induced. In these cells, the activities of mitochondrial fumarase and aconitase were measured as described above.

Rescue with *Blastocystis Isa*

A partial sequence of the *Isa2* gene was identified among the expressed sequence tags of *Blastocystis* sp. (Stechmann *et al.*, 2008). The full-length sequence of this gene was obtained using RACE techniques as described previously (Stechmann *et al.*, 2008). The 498-nt-long full-length cDNA of

the *Blastocystis* Isa2 (Bhlsa2) gene was cloned into the pABPURO vector (using primers Bhlsa-F and Bhlsa-R; Table S1), following the cloning strategy described above for hlsa. A putative mitochondrial targeting peptide of the *Blastocystis* Isa2 protein, predicted by MitoProt II with high probability (> 0.99), was retained in the construct for the rescue experiments. The linearized construct was introduced into the inducible knock-downs PF cells for Tblsa1 and Tblsa2. In the obtained cell lines, the activities of fumarase, aconitase, succinate dehydrogenase and threonine dehydrogenase were measured in total cell lysates, as well as in subcellular fractions as described above.

Acknowledgements

We thank members of our laboratories for discussions, Gabriela Ridvanová for technical assistance, Helene Puccio (Université de Strasbourg) and Michael Boshart (Ludwig-Maximilians-Universität München) for the donation of anti-hlsa2 and anti-aconitase antibodies, respectively, and André Schneider (University of Berne) for providing the pFC4 vector. This work was supported by the Grant Agency of the Czech Republic 204/09/1667, the Ministry of Education of the Czech Republic (LC07032, 2B06129 and 6007665801) and the Praemium Academiae award to J.L. A.D.T. was supported by an EMBO fellowship and travel grant from the Canadian Institute for Advanced Research to visit Czech Republic.

References

- Besteiro, S., Barrett, M.P., Rivière, L., and Bringaud, F. (2005) Energy generation in insect stages of *Trypanosoma brucei*: metabolism in flux. *Trends Parasitol* **21**: 185–191.
- Bilder, P.W., Ding, H., and Newcomer, M.E. (2004) Crystal structure of the ancient Fe-S scaffold IscA reveals a novel protein fold. *Biochemistry* **43**: 133–139.
- Blouin, C., Perry, S., Lavell, A., Susko, E., and Roger, A.J. (2009) Reproducing the manual annotation of multiple sequence alignments using a SVM classifier. *Bioinformatics* **25**: 3093–3098.
- Carter, W.O., Narayanan, P.K., and Robinson, J.P. (1994) Intracellular hydrogen peroxide and superoxide anion detection in endothelial cells. *J Leukoc Biol* **55**: 253–258.
- Comini, M.A., Retting, J., Dirdjaja, N., Hanschmann, E.M., Berndt, C., and Krauth-Siegel, R.L. (2008) Monothiol glutaredoxin-1 is an essential iron-sulfur protein in the mitochondrion of African trypanosomes. *J Biol Chem* **283**: 27785–27798.
- Córaz-Castellano, I., Machargo, M., Trujillo, E., Arteaga, M.F., González, T., Martín-Vasallo, P., and Avila, J. (2004) hIsca: a protein implicated in the biogenesis of iron-sulfur clusters. *Biochim Biophys Acta* **1700**: 179–188.
- Coustou, V., Biran, M., Besteiro, S., Rivière, L., Baltz, T., Franconi, J.M., and Bringaud, F. (2006) Fumarate is an essential intermediary metabolite produced by the procyclic *Trypanosoma brucei*. *J Biol Chem* **281**: 26832–26846.
- Cupp-Vickery, J.R., Silberg, J.J., Ta, D.T., and Vickery, L.E. (2004) Crystal structure of IscA, an iron-sulfur cluster assembly protein from *Escherichia coli*. *J Mol Biol* **16**: 127–137.
- Ding, H., and Clark, R.J. (2004) Characterization of iron binding in IscA, an ancient iron-sulfur cluster assembly protein. *Biochem J* **379**: 433–440.
- Ding, H., Clark, R.J., and Ding, B. (2004) IscA mediates iron delivery for assembly of iron-sulfur clusters in IscU under the limited accessible free iron conditions. *J Biol Chem* **279**: 37499–37504.
- Djaman, O., Outten, F.W., and Imlay, J.A. (2004) Repair of oxidized iron-sulfur clusters in *Escherichia coli*. *J Biol Chem* **279**: 44590–44599.
- Estévez, A.M., Haile, S., Steinbuechel, M., Quijada, L., and Clayton, C. (2004) Effects of depletion and overexpression of the *Trypanosoma brucei* ribonuclease L inhibitor homologue. *Mol Biochem Parasitol* **133**: 137–141.
- Fontecave, M. (2006) Iron-sulfur clusters: ever-expanding roles. *Nature Chem Biol* **2**: 171–174.
- Fontecave, M., and Ollagnier-de-Choudens, S. (2008) Iron-sulfur cluster biosynthesis in bacteria: Mechanisms of cluster assembly and transfer. *Arch Biochem Biophys* **474**: 226–237.
- Gelling, C., Dawes, I.W., Richhardt, N., Lill, R., and Mühlenhoff, U. (2008) Mitochondrial Iba57 is required for Fe-S cluster formation on aconitase and activation of radical SAM enzyme. *Mol Cell Biol* **28**: 1851–1861.
- Hashimi, H., Zíková, A., Panigrahi, A.K., Stuart, K.D., and Lukeš, J. (2008) TbRGG1, a component of a novel multi-protein complex involved in kinetoplast RNA editing. *RNA* **14**: 970–980.
- Hashimi, H., Benkovičová, V., Čermáková, P., Lai, D.-H., Horváth, A., and Lukeš, J. (2010) The assembly of F₁F₀-ATP synthase is disrupted upon interference of RNA editing in *Trypanosoma brucei*. *Int J Parasitol* **40**: 45–54.
- Hennesy, J.D., and Reid, R.G. (1984) Ferene – a new spectrophotometric reagent for iron. *Can J Chem* **62**: 721–724.
- Horváth, A., Horáková, E., Dunajčíková, P., Verner, Z., Pravadová, E., Šlapetová, I., et al. (2005) Down-regulation of the nuclear-encoded subunits of the complexes III and IV disrupts their respective complexes but not complex I in procyclic *Trypanosoma brucei*. *Mol Microbiol* **58**: 116–130.
- Jensen, L.T., and Culotta, V.C. (2000) Role of *S. cerevisiae* ISA1 and ISA2 in iron homeostasis. *Mol Cell Biol* **20**: 3918–3927.
- Johnson, D.C., Dean, D.R., Smith, A.D., and Johnson, M.K. (2005) Structure, function, and formation of biological iron-sulfur clusters. *Annu Rev Biochem* **74**: 247–281.
- Johnson, D.C., Unciuleac, M.C., and Dean, D.R. (2006) Controlled expression of nif and isc iron-sulfur protein maturation components reveals target specificity and limited functional replacement between the two systems. *J Bacteriol* **188**: 7551–7561.
- Katoh, K., Misawa, K., Kuma, K., and Miyata, T. (2002) MAFFT: a novel method for rapid multiple sequence alignment based on fast Fourier transform. *Nucleic Acids Res* **30**: 3059–3066.
- Kaut, A., Lange, H., Diekert, K., Kispal, G., and Lill, R. (2000) Isa1p is a component of the mitochondrial machinery for maturation of cellular iron-sulfur proteins and requires conserved cysteine residues for function. *J Biol Chem* **275**: 15955–15961.
- Kispal, G., Sipos, K., Lange, H., Fekete, Z., Bedekovics, T., Janáky, T., et al. (2005) Biogenesis of cytosolic ribosomes

- requires the essential iron-sulfur protein Rli1 and mitochondria. *EMBO J* **24**: 589–598.
- Kořený, L., Lukeš, J., and Oborník, M. (2010) Evolution of the heme synthetic pathway in kinetoplastid flagellates: an essential pathway that is not essential after all? *Int J Parasitol* **40**: 149–156.
- Krebs, C., Agar, J.N., Smith, A.D., Frazzon, J., Dean, D.R., Huynh, B.H., and Johnson, M.K. (2001) IscA, an alternate scaffold for Fe-S cluster biosynthesis. *Biochemistry* **40**: 14069–14080.
- Lill, R. (2009) Function and biogenesis of iron-sulfur proteins. *Nature* **460**: 831–838.
- Lill, R., and Mühlenhoff, U. (2005) Iron-sulfur-protein biogenesis in eukaryotes. *Trends Biochem Sci* **30**: 133–141.
- Lill, R., and Mühlenhoff, U. (2008) Maturation of iron-sulfur proteins in eukaryotes: Mechanisms, connected processes and diseases. *Annu Rev Biochem* **77**: 669–700.
- Long, S., Jirků, M., Mach, J., Ginger, M.L., Sutak, R., Richardson, D., *et al.* (2008a) Ancestral roles of eukaryotic frataxin: mitochondrial frataxin function and heterologous expression of hydrogenosomal *Trichomonas* homologs in trypanosomes. *Mol Microbiol* **69**: 94–109.
- Long, S., Jirků, M., Ayala, F.J., and Lukeš, J. (2008b) Mitochondrial localization but not processing of human frataxin is essential for a rescue of frataxin deficiency in the excavate flagellate *Trypanosoma brucei*. *Proc Natl Acad Sci USA* **105**: 13468–13473.
- Lu, J., Yang, J., Tan, G., and Ding, H. (2008) Complementary roles of SufA and IscA in the biogenesis of iron-sulfur clusters in *Escherichia coli*. *Biochem J* **409**: 535–543.
- Lu, J., Bitoun, P.J., Tan, G., Wang, W., Min, W., and Ding, H. (2010) Iron-binding activity of human iron-sulfur cluster assembly protein hIscA1. *Biochem J* **428**: 125–131.
- Lukeš, J., Hashimi, H., and Zíková, A. (2005) Unexplained complexity of the mitochondrial genome and transcriptome in kinetoplastid flagellates. *Curr Genet* **48**: 277–299.
- Mühlenhoff, U., Gerber, J., Richhardt, N., and Lill, R. (2003) Components involved in assembly and dislocation of iron-sulfur clusters on the scaffold protein Isu1p. *EMBO J* **22**: 4815–4825.
- Mühlenhoff, U., Gerl, M.J., Flauger, B., Pirner, H.M., Balsler, S., Richhardt, N., *et al.* (2007) The ISC proteins Isa1 and Isa2 are required for the function but not for the de novo synthesis of Fe/S cluster of biotin synthase in *Saccharomyces cerevisiae*. *Eukaryot Cell* **6**: 495–504.
- Nakamura, M., Saeki, K., and Takahashi, Y. (1999) Hyperproduction of recombinant ferredoxins in *Escherichia coli* by coexpression of the ORF1-ORF2-iscS-iscU-iscA-hscB-hscA-fdx-ORF3 gene cluster. *J Biochem* **126**: 10–18.
- Nilsson, R., Schultz, I.J., Pierce, E.L., Soltis, K.A., Naranuntarat, A., Ward, D.M., *et al.* (2009) Discovery of genes essential for heme biosynthesis through large-scale gene expression analysis. *Cell Metab* **10**: 119–130.
- Nishio, K., and Nakai, M. (2000) Transfer of iron-sulfur cluster from NifU to apoferredoxin. *J Biol Chem* **275**: 22615–22618.
- Ollagnier-de-Choudens, S., Mattioli, T., Tagahashi, Y., and Fontecave, M. (2001) Iron-sulfur cluster assembly – characterization of IscA and evidence for a specific and functional complex with ferredoxin. *J Biol Chem* **276**: 22604–22607.
- Ollagnier-de-Choudens, S., Sanakis, Y., and Fontecave, M. (2004) SufA/IscA: reactivity studies of a class of scaffold proteins involved in [Fe-S] cluster assembly. *J Biol Inorg Chem* **9**: 828–838.
- Paris, Z., Changmai, P., Rubio, M.A.T., Zíková, A., Stuart, K.D., Alfonzo, J.D., and Lukeš, J. (2010) The Fe/S cluster assembly protein Isd11 is essential for tRNA thiolation in *Trypanosoma brucei*. *J Biol Chem* **285**: 22394–22402.
- Pelzer, W., Mühlenhoff, U., Diekert, K., Siegmund, K., Kispal, G., and Lill, R. (2000) Mitochondrial Isa2p plays a crucial role in the maturation of cellular iron-sulfur proteins. *FEBS Lett* **476**: 134–139.
- Pieroni, L., Khalil, L., Charlotte, F., Poynard, T., Piton, A., Hainque, B., and Imbert-Bismut, F. (2001) Comparison of bathophenanthroline sulfonate and ferene as chromogens in colorimetric measurement of low hepatic iron concentration. *Clin Chem* **47**: 2059–2061.
- Poliak, P., Van Hoewyk, D., Oborník, M., Zíková, A., Stuart, K.D., Tachezy, J., *et al.* (2010) Functions and cellular localization of cysteine desulfurase and selenocysteine lyase in *Trypanosoma brucei*. *FEBS J* **277**: 383–393.
- Rouault, T.A., and Tong, W.H. (2005) Iron-sulfur cluster biogenesis and mitochondrial iron homeostasis. *Nat Rev Mol Cell Biol* **6**: 345–351.
- Saas, J., Ziegelbauer, K., von Haeseler, A., Fast, B., and Boshart, M. (2000) A developmentally regulated aconitase related to iron-regulatory protein-1 is localized in the cytoplasm and in the mitochondrion of *Trypanosoma brucei*. *J Biol Chem* **275**: 2745–2755.
- Schneider, A. (2001) Unique aspects of mitochondrial biogenesis in trypanosomatids. *Int J Parasitol* **31**: 1403–1415.
- Smid, O., Horáková, E., Vilímová, V., Hrdý, I., Cammack, R., Horváth, A., *et al.* (2006) Knock-downs of mitochondrial iron-sulfur cluster assembly proteins IscS and IscU down-regulate the active mitochondrion of procyclic *Trypanosoma brucei*. *J Biol Chem* **281**: 28679–28686.
- Song, D., Tu, Z., and Lee, F.S. (2009) Human ISCA1 interacts with IOP1/NARFL and functions in both cytosolic and mitochondrial iron-sulfur protein biogenesis. *J Biol Chem* **284**: 35297–35307.
- Stamatakis, A., Ludwig, T., and Meier, H. (2005) RAxML-III: a fast program for maximum likelihood-based inference of large phylogenetic trees. *Bioinformatics* **21**: 456–463.
- Stechmann, A., Hamblin, K., Perez-Brocal, V., Gaston, D., Richmond, G.S., van der Giezen, M., *et al.* (2008) Organelles in *Blastocystis* that blur the distinction between mitochondria and hydrogenosomes. *Curr Biol* **18**: 580–585.
- Tan, G., Lu, J., Bitou, J.P., Huang, H., and Ding, H. (2009) ISA/SufA paralogs are required for the [4Fe-4S] cluster assembly in enzyme sof multiple physiological pathways in *Escherichia coli* under aerobic growth conditions. *Biochem J* **420**: 463–472.
- Tielens, A.G.M., and van Hellemond, J.J. (1998) Differences in energy metabolism between Trypanosomatidae. *Parasitol Today* **14**: 265–271.
- Tokumoto, U., and Takahashi, Y. (2001) Genetic analysis of the isc operon in *Escherichia coli* involved in the biogenesis of cellular iron-sulfur proteins. *J Biochem* **130**: 63–71.
- Vinella, D., Brochier-Armanet, C., Loiseau, L., Talla, E., and Barras, F. (2009) Iron-sulfur (Fe/S) protein biogenesis: phy-

- logenomic and genetic studies of A-type carriers. *PLoS Genet* **5**: e1000497.
- Vondrušková, E., van den Burg, J., Zíková, A., Ernst, N.L., Stuart, K., Benne, R., and Lukeš, J. (2005) RNA interference analyses suggest a transcript-specific regulatory role for MRP1 and MRP2 in RNA editing and other RNA processing in *Trypanosoma brucei*. *J Biol Chem* **280**: 2429–2438.
- Wang, W., Huang, H., Tan, G., Si, F., Liu, M., Landry, P.A., et al. (2010) *In vivo* evidence for the iron binding activity of an iron-sulfur cluster assembly protein ISA in *Escherichia coli*. *Biochem J* **432**: 429–436.
- Wingert, R.A., Galloway, J.L., Barut, B., Foott, H., Fraenkel, P., Axe, J.L., et al. (2005) Deficiency of glutaredoxin 5 reveals Fe-S clusters are required for vertebrate haem synthesis. *Nature* **436**: 1035–1039.
- Wohlgamuth-Benedum, J.M., Rubio, M.A.T., Paris, Z., Long, S., Poliak, P., Lukeš, J., and Alfonzo, J.D. (2009) Thiolation controls cytoplasmic tRNA stability and acts as a negative determinant for tRNA editing in mitochondria. *J Biol Chem* **284**: 23947–23953.
- Wollenberg, M., Berndt, C., Bill, E., Schwenn, J.D., and Seidler, A. (2003) A dimer of the FeS cluster biosynthesis protein IscA from cyanobacteria binds a [2Fe2S] cluster between two protomers and transfers it to [2Fe2S] and [4Fe4S] apo proteins. *Eur J Biochem* **270**: 1662–1671.
- Wu, G., Mansy, S.S., Hemann, C., Hille, R., Surerus, K.K., and Cowan, J.A. (2002) Iron-sulfur cluster biosynthesis: characterization of *Schizosaccharomyces pombe* Isa1. *J Biol Inorg Chem* **7**: 526–532.
- Zheng, L., White, R.H., Cash, V.L., Jack, R.F., and Dean, D.R. (1993) Cysteine desulfurase activity indicates a role for NIFS in metallocluster biosynthesis. *Proc Natl Acad Sci USA* **90**: 2754–2758.
- Zheng, L., Cash, V.L., Flint, D.H., and Dean, D.R. (1998) Assembly of iron-sulfur clusters. Identification of an iscSUA-hscBA-fdx gene cluster from *Azotobacter vinelandii*. *J Biol Chem* **273**: 13264–13272.

Supporting information

Additional supporting information may be found in the online version of this article.

Please note: Wiley-Blackwell are not responsible for the content or functionality of any supporting materials supplied by the authors. Any queries (other than missing material) should be directed to the corresponding author for the article.

3.3 Both human ferredoxins equally efficiently rescue ferredoxin deficiency in *Trypanosoma brucei*

(reprint of Molecular Microbiology 89: 135–51)

Both human ferredoxins equally efficiently rescue ferredoxin deficiency in *Trypanosoma brucei*

Piya Changmai,^{1,2} Eva Horáková,¹ Shaojun Long,^{1†}
Eva Černotíková-Stříbrná,¹ Lindsay M. McDonald,^{1‡}
Esteban J. Bontempi^{1§} and Julius Lukeš^{1,2*}

¹Institute of Parasitology, Biology Centre and ²Faculty of Science, University of South Bohemia, Branišovská 31, 37005 České Budějovice (Budweis), Czech Republic.

Summary

Ferredoxins are highly conserved proteins that function universally as electron transporters. They not only require Fe-S clusters for their own activity, but are also involved in Fe-S formation itself. We identified two homologues of ferredoxin in the genome of the parasitic protist *Trypanosoma brucei* and named them *TbFdxA* and *TbFdxB*. *TbFdxA* protein, which is homologous to other eukaryotic mitochondrial ferredoxins, is essential in both the procyclic (= insect-transmitted) and bloodstream (mammalian) stage, but is more abundant in the active mitochondrion of the former stage. Depletion of *TbFdxA* caused disruption of Fe-S cluster biogenesis and lowered the level of intracellular haem. However, *TbFdxB*, which is present exclusively within kinetoplastid flagellates, was non-essential for the procyclic stage, and double knock-down with *TbFdxA* showed this was not due to functional redundancy between the two homologues. Heterologous expressions of human orthologues HsFdx1 and HsFdx2 fully rescued the growth and Fe-S-dependent enzymatic activities of *TbFdxA* knock-down. In both cases, the genuine human import signals allowed efficient import into the *T. brucei* mitochondrion. Given the huge evolutionary distance between trypanosomes and humans, ferredoxins clearly have ancestral and highly conserved function in eukaryotes and both human orthologues have

retained the capacity to participate in Fe-S cluster assembly.

Introduction

Iron-sulphur (Fe-S) clusters are ancient cofactors found in every domain of life. They can function as electron donors and/or acceptors, sulphur donors and sensors for specific molecular conditions and in a typical cell are likely to serve numerous other, as yet unknown functions (Lill, 2009). In eukaryotic cells, well over a hundred proteins requiring Fe-S clusters for their function have been identified so far, of which mitochondrial respiratory complexes I through III, ferredoxin, aconitase and DNA repair enzymes are among the best known (Rouault, 2012). Although well studied for decades, the eukaryotic DNA polymerases I through IV were only very recently shown to contain Fe-S clusters (Netz *et al.*, 2012). Hence, it is reasonable to anticipate that the importance of Fe-S cofactors is still underestimated.

In the yeast *Saccharomyces cerevisiae*, in which it has been studied extensively, the Fe-S cluster (ISC) assembly takes place in mitochondria with the participation of at least a dozen proteins. Core participants include the cysteine desulphurase complex (Nfs-Isd11), which provides sulphur to the scaffold protein IscU (Zheng *et al.*, 1993; Adam *et al.*, 2006; Wiedemann *et al.*, 2006; Shi *et al.*, 2009) and frataxin, generally considered to be an iron donor, although direct evidence for this function is still lacking (Stemmler *et al.*, 2010). In addition to these core proteins, ferredoxin and its reductase provide electrons, while a number of other proteins including Isa1/2 and Iba57 perform more specialized functions (Lange *et al.*, 2000; Li *et al.*, 2001; Mühlhoff *et al.*, 2007; Long *et al.*, 2011).

A number of distinct systems exist for the biogenesis of Fe-S clusters: the sulphur assimilation (SUF) machinery of prokaryotes and a handful of eukaryotes; the bacterial and mitochondrial ISC system, the prokaryotic nitrogen-fixing (NIF) machinery and, finally, the eukaryotic cytosolic (CIA) pathway (Py and Barras, 2010; Tsoulos *et al.*, 2012). With the exception of the SUF pathway, all of these machineries contain a system for electron transfer (Lill,

Accepted 13 May, 2013. *For correspondence. E-mail jula@paru.cas.cz; Tel. (+420) 387775416; Fax (+420) 385310388. Present addresses: [†]Institute for Cell and Molecular Biosciences, Faculty of Medical Science, Newcastle University, Newcastle, UK; [‡]Institute of Immunology & Infection Research, University of Edinburgh, Edinburgh, UK; [§]Instituto Nacional de Parasitología 'Dr. M. Fatala Chabén', Ministerio de Salud, Buenos Aires, Argentina.

2009). The ISC machinery acquires NADH-derived electrons via the ferredoxin and ferredoxin-reductase complex for the reduction of cysteine-bound S^0 to the Fe-S cluster component S^{2-} (Kakuta *et al.*, 2001; Mühlenhoff *et al.*, 2003). *In vitro* experiments revealed that in the bacterium *Azotobacter vinelandii* ferredoxin also acts as a reductant in the formation of a single $[4Fe-4S]^{2+}$ cluster from two $[2Fe-2S]^{2+}$ clusters on the homodimeric IscU scaffold (Chandramouli *et al.*, 2007).

Saccharomyces cerevisiae contains only one homologue of ferredoxin (Yah1), while there are two homologues in humans, namely ferredoxins 1 (HsFdx1) and 2 (HsFdx2) (Shi *et al.*, 2012). Surprisingly, although HsFdx1 and Yah1 belong to type II ferredoxins, which contain the Pro-His motif while HsFdx2 belongs to type I ferredoxins (Seeber, 2002), only HsFdx2 is able to complement Yah1-depleted yeast cells (Sheftel *et al.*, 2010). Both HsFdx1 and HsFdx2 are expressed ubiquitously, with the former being highly expressed in the adrenal cortex and medulla, while the latter is abundant in the central nervous system (Sheftel *et al.*, 2010; Shi *et al.*, 2012). Investigation of the relevance of each homologue to Fe-S cluster assembly has produced conflicting results. While Sheftel *et al.* (2010) found only HsFdx2 to be involved in this process, Shi *et al.* (2012) determined both homologues to be necessary. Numerous other important roles have been identified for ferredoxins. Using electrons from NADPH-dependent ferredoxin reductase, HsFdx1 also participates in mammalian steroid hormone biosynthesis as a reductant of mitochondrial cytochrome P450 enzymes (Ewen *et al.*, 2011). In yeast, Yah1 together with Arh1 and Cox15p have a role in hydroxylation of haem *o* to haem *a* (Barros *et al.*, 2001) and coenzyme Q biosynthesis (Pierrel *et al.*, 2010). Hence, the depletion of Yah1 leads to defects in ISC assembly, haem synthesis and iron homeostasis (Lange *et al.*, 2000; Sheftel *et al.*, 2010; Miao *et al.*, 2011; Shi *et al.*, 2012).

In this study we identified two homologues of ferredoxin in the genome of the parasitic protist *Trypanosoma brucei*, a causative agent of highly pathogenic African sleeping sickness of humans and other diseases of animals. During their life cycle, trypanosomes alternate between the procyclic stage (PC), with a fully active reticulated mitochondrion, and the bloodstream stage (BS), for which an organelle highly reduced in morphology and function is characteristic (Besteiro *et al.*, 2002; Lukeš *et al.*, 2005). Since this excavate model flagellate is amenable to various methods of reverse genetics, we undertook functional analysis of both ferredoxins, termed here *TbFdxA* and *TbFdxB*. These analyses revealed that *TbFdxA* but not *TbFdxB* is essential for PC *T. brucei*, where it participates in Fe-S biogenesis. This feature makes trypanosomes suitable for heterologous functional analysis of human

ferredoxins. Interestingly, *TbFdxA* knock-down was efficiently rescued by both human orthologues, which restored the viability of the cells and their ability to form Fe-S clusters.

Results

Identification and phylogenetic analysis of ferredoxins in T. brucei

A BLAST search using the Yah1 sequence of *S. cerevisiae* as a query produced two significant hits within the genome of *T. brucei*. The corresponding small proteins, which we call *TbFdxA* (Tb927.7.890) and *TbFdxB* (Tb927.4.4980), have calculated molecular weights 19.71 kDa and 17.62 kDa respectively. Both *TbFdxA* and *TbFdxB* were predicted to have mitochondrial localization by MitoProtII, with 0.9829 and 0.8525 probabilities, respectively, and with similarly high probabilities predicted by pSORT.

At the protein level, *TbFdxA* and *TbFdxB* respectively share 39% and 33% identity with the yeast orthologue Yah1, while the identity between the two trypanosome proteins is 40%. Both *TbFdxA* and *TbFdxB* contain a conserved fer2 superfamily domain with a 2Fe-2S binding domain and a catalytic loop that may participate in catalysing electron transfer in redox reactions (Marchler-Bauer *et al.*, 2011). Conserved homologues of both proteins containing cysteine residues proposed to be responsible for the ligation of Fe or Fe-S clusters and other conserved motifs (Fig. 1A), were also found in the genomes of related kinetoplastid flagellates, including *Trypanosoma cruzi*, *Leishmania major*, *Leishmania braziliensis* and *Leishmania infantum* (Fig. S1A).

In order to reveal the phylogenetic position of the *T. brucei* ferredoxins within eukaryotes, we constructed a maximum likelihood phylogenetic tree (Fig. 1B). Unexpectedly, *TbFdxA* and *TbFdxB* are not closely related to one another. Neither is specifically related to any of the major eukaryotic groups. Although the clade containing *TbFdxA* is more closely related to the human and yeast ferredoxins than *TbFdxB* (Fig. 1B), its position is rather unstable and dependent on the taxon sampling (Fig. S1B). On the other hand, our analyses consistently reveal that *TbFdxB* belongs to the basal-most eukaryotic ferredoxin clade known so far. Interestingly, this clade contains a single trypanosomatid paralogue, whereas four *Leishmania* paralogues are present. Although the branching support was rather weak, the topology shown in Fig. 1B hints at the presence of at least one additional trypanosomatid paralogue that was lost during evolution. It also suggests the existence of a specific selective pressure that retains multiple paralogues present in the transcriptome of *Leishmania* spp.

A

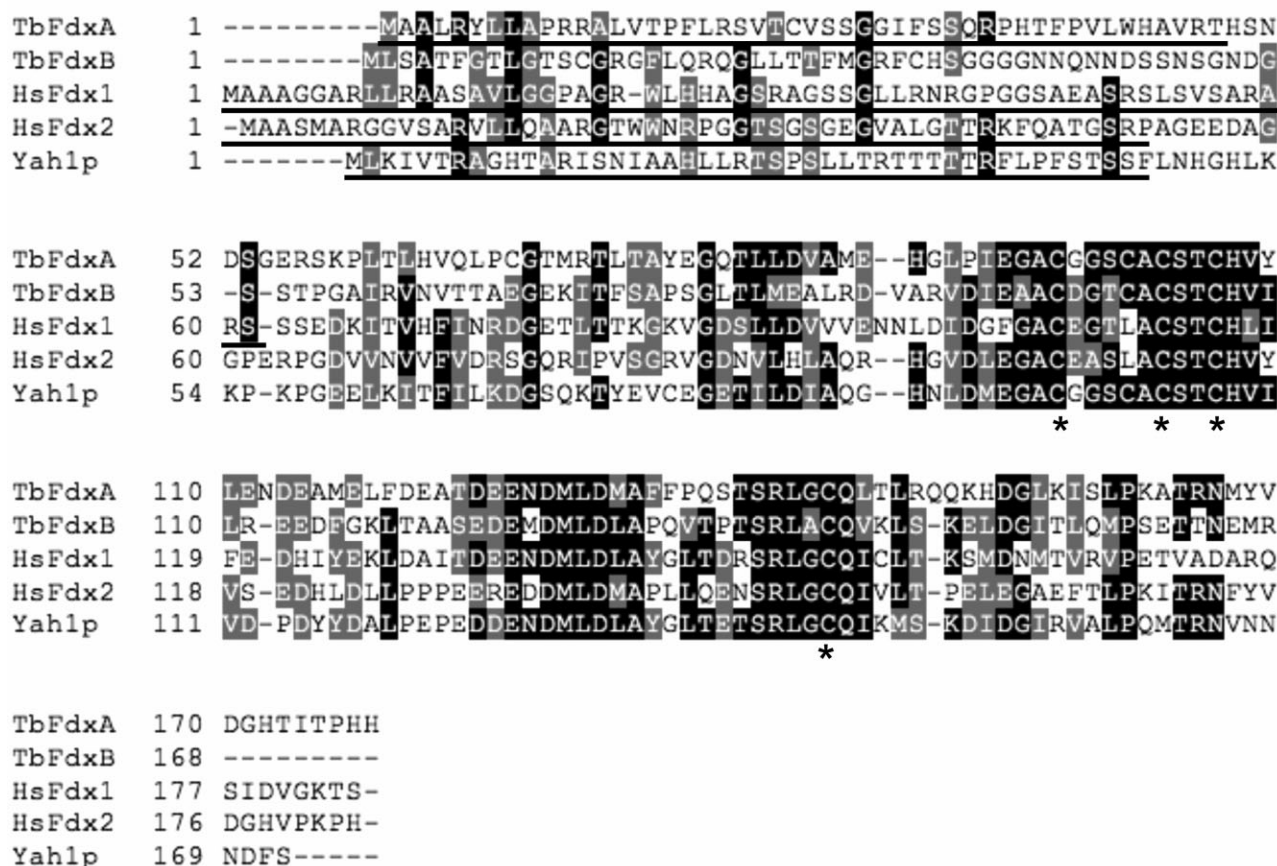


Fig. 1. Phylogenetic analysis of *TbFdxA* and *TbFdxB*.

A. Multiple sequence alignment of ferredoxins in *T. brucei*, *H. sapiens* and *S. cerevisiae*. The alignment was generated using CLUSTALW (<http://www.ch.embnet.org/software/ClustalW.html>) and Boxshade (http://www.ch.embnet.org/software/BOX_form.html). Identical residues are highlighted in black and conserved residues in grey. Conserved cysteine residues of the Fe-S motif are marked with asterisks. Underlines represent predicted mitochondrial targeting sequences by MitoProtII.

B. Maximum likelihood phylogenetic analysis of ferredoxins inferred using RAxML and Γ -corrected LG matrix (LG+ Γ model). Branching support is expressed via non-parametric bootstrap support and Bayesian posterior probabilities. See *Experimental procedures* for details.

Localization of ferredoxins in *T. brucei*

Although both ferredoxins (*TbFdxA* and *TbFdxB*) were predicted to have mitochondrial localization with similarly high probabilities, we tested their localization experimentally. Having specific polyclonal antibody only against *TbFdxA* (see below), we decided to fused both proteins on their C-terminus with V5 tag. The resulting tetracyclin (Tet)-inducible constructs *TbFdxA*_pT7_V5 and *TbFdxB*_pT7_V5 were electroporated into wild-type PC and clonal cell lines were selected using puromycin. Two clones from each cell line were examined 2 days after the addition of Tet using indirect immunofluorescence. As shown in Fig. 2A, both ferredoxins fully colocalized with Mitotracker Red, confirming their mitochondrial localization.

TbFdxA is essential for cell growth of the procyclic stage

To establish protein expression and depletion levels of the *TbFdxA* and *TbFdxB* proteins, we expressed both full-size His₆-tagged proteins in *Escherichia coli*, from which the abundantly expressed insoluble brown proteins were purified. Specific polyclonal antibodies generated in rats against the expressed *TbFdxA* and *TbFdxB* proteins did immunodecorate *TbFdxA*, but failed to recognize the latter protein (data not shown). Therefore, we compared the abundance of only *TbFdxA* in individual life stages. As shown in Fig. 2B, the protein is highly expressed in the PC trypanosomes, but is much less abundant in the BS cells.

In order to assess the function of individual ferredoxins in PC, we used RNAi to selectively deplete the mRNA

B



Fig. 1. cont.

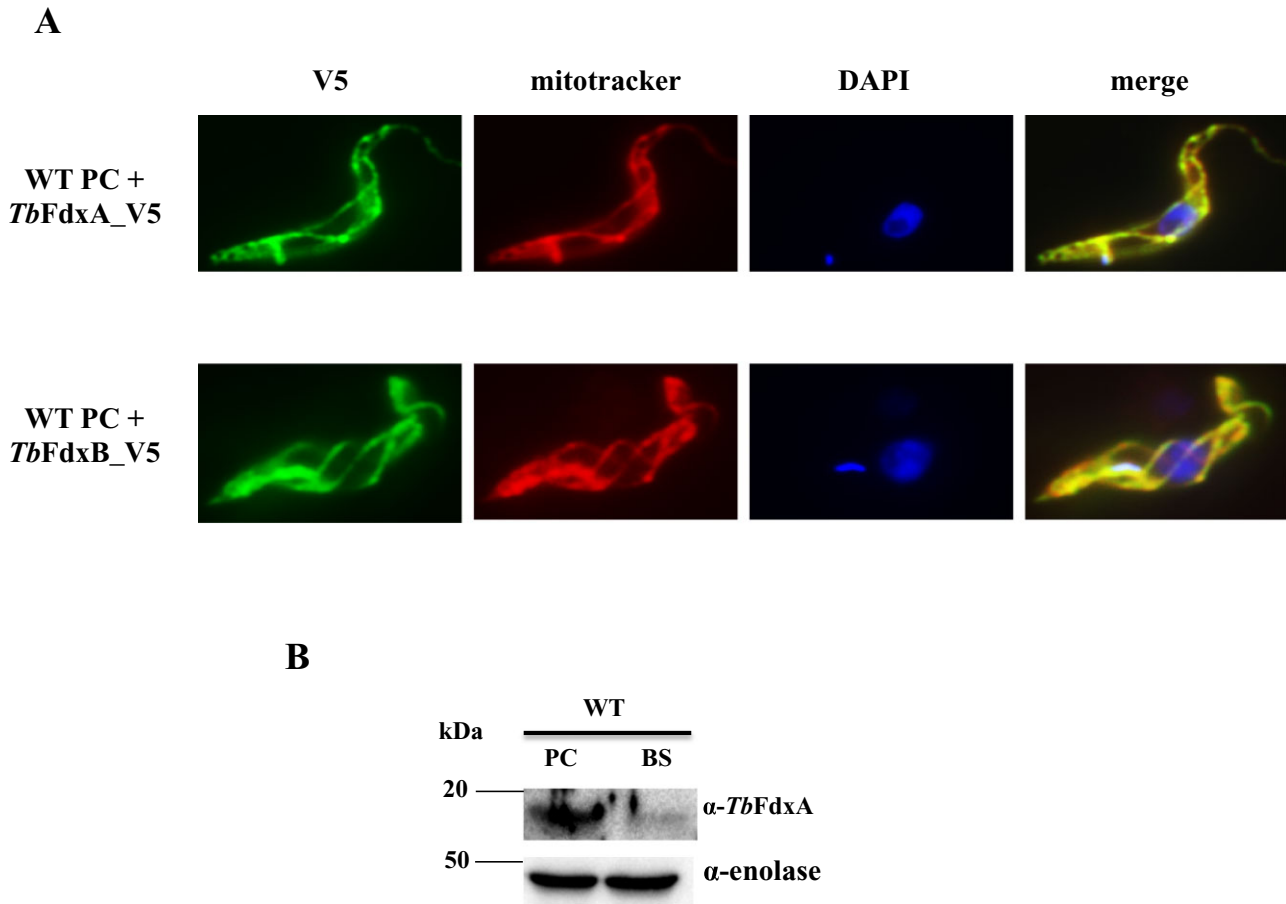


Fig. 2. *TbFdxA* and *TbFdxB* localize to the mitochondrion of *T. brucei*.

A. Fluorescence microscopy of the wild-type PC cell line expressing *TbFdxA_V5* or *TbFdxB_V5* fusion protein. Mitotracker Red staining visualizes the mitochondrion. 4,6-diamidino-2-phenylindole (DAPI) stains nuclear and mitochondrial DNA.

B. Western analysis of protein level of *TbFdxA* in the wild-type PC and BS.

levels of *TbFdxA* and/or *TbFdxB*. Fragments of both genes were cloned into the p2T7-177 vector containing opposing Tet-regulatable promoters. Another construct was also generated with fragments of the *TbFdxA* and *TbFdxB* genes cloned in tandem to allow their parallel ablation. Parental *T. brucei* 29-13 cells were transfected with the NotI-linearized p2T7-177 constructs, and clonal cell lines were obtained by limiting dilution using phleomycin as a selectable marker.

RNAi induction impacted the studied cell lines differently: single *TbFdxA* and double *TbFdxA+B* knock-downs showed significantly reduced proliferation (Fig. 3A and C), whereas the growth of the *TbFdxB* RNAi cell line was not affected at all (Fig. 3B). The depletion of the target proteins was monitored by Western blot analysis using α -*TbFdxA* antibodies and in the case of *TbFdxB* by quantitative real-time PCR (Fig. 3). In the *TbFdxA* and *TbFdxA+B* RNAi cell lines where *TbFdxA* mRNA was targeted, a total elimination of the *TbFdxA* protein occurred (Fig. 3A and C). The target mRNA was also efficiently

depleted in the single *TbFdxB* knock-down as well as in the double knock-down (Fig. 3D). Western blot analysis also showed that the depletion of *TbFdxA* had no effect on the levels of other component of the ISC pathway namely Nfs, IscU and frataxin (Fig. S2). These results demonstrate that *TbFdxA*, but not *TbFdxB*, is essential for the viability of PC *T. brucei*.

TbFdxA is indispensable for the bloodstream stage

The BS of *T. brucei* harbours a mitochondrion which is substantially reduced in terms of morphology and metabolism, lacking the respiratory chain, fumarase and other activities (Tielens and van Hellemond, 1998; Besteiro *et al.*, 2005; Lukeš *et al.*, 2005; Coustou *et al.*, 2006). Consequently this stage relies on glycolysis for its fast growth. While the mitochondrial Fe-S cluster-containing proteins may therefore theoretically be bypassed in this life stage, this is not the case for numerous cytosolic and nuclear proteins requiring clusters for their activities.

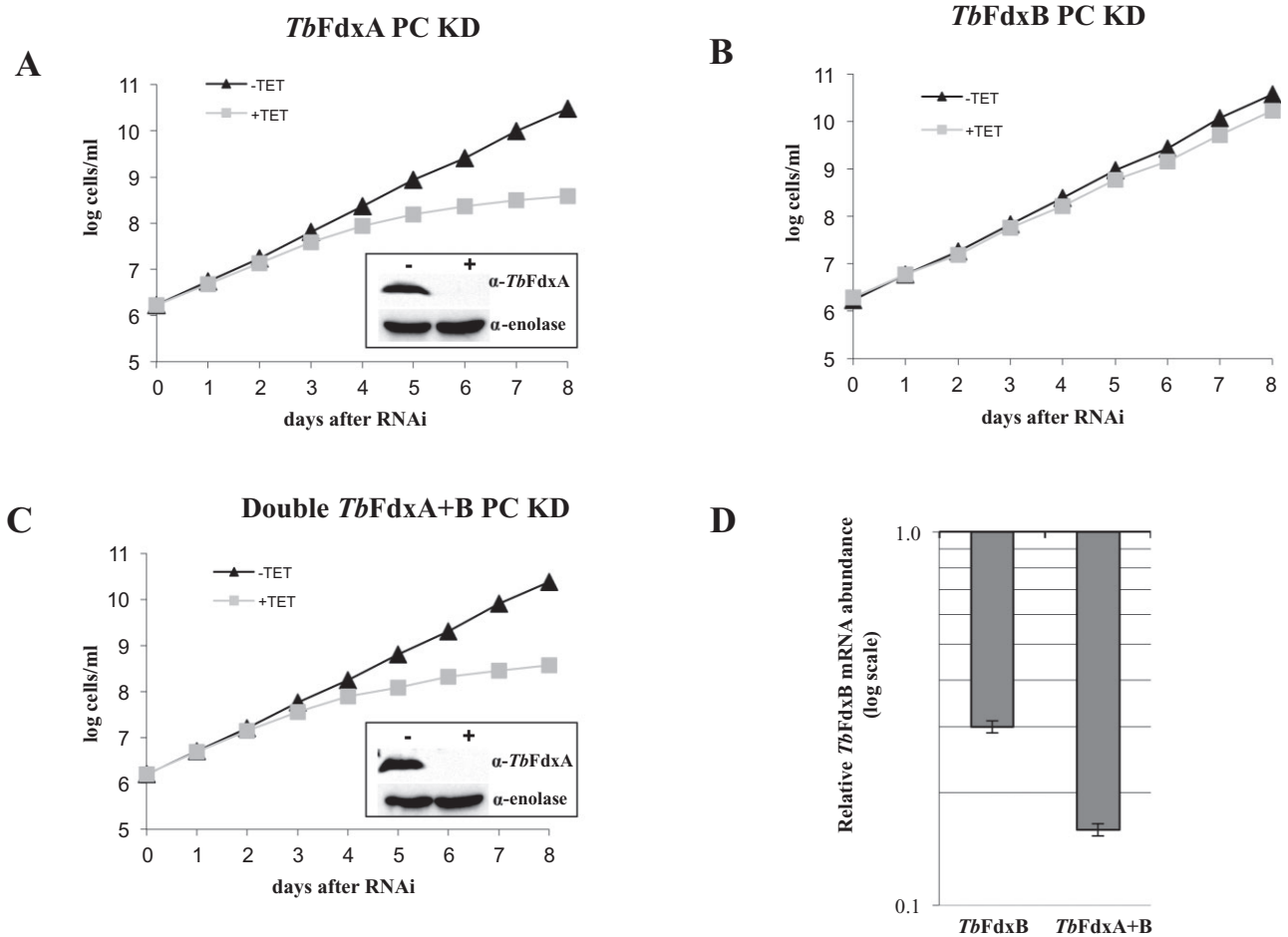


Fig. 3. *TbFdxA* but not *TbFdxB* is essential for growth of PC *T. brucei*.

A–C. Growth curves represent numbers of non-induced (triangles; black line) and RNAi-induced (squares; grey line) cell lines for single *TbFdxA* (A), single *TbFdxB* (B) and double *TbFdxA+B* knock-down PC cells (C). The y-axis represents the log scale product of cell density and total dilution. The data show a single representative experiment of biological triplicates. *TbFdxA* protein levels were analysed by Western blot analysis with α -*TbFdxA* antibody in whole-cell lysates from non-induced (–) and RNAi-induced (+) single *TbFdxA* (A) and double *TbFdxA+B* knock-downs (C) after 5 days of induction. Enolase was used as a loading control.

D. Quantitative real-time PCR analysis of *TbFdxB* mRNA was performed on cDNAs generated from the non-induced and RNAi-induced single *TbFdxB* and double *TbFdxA+B* knock-down cells 5 days after RNAi induction. The relative change in *TbFdxB* mRNA abundance upon tetracycline addition was determined by using 18S rRNA as internal reference. The means and SD values of three independent experiments are shown.

Indeed, Fe-S cluster-containing DNA polymerase and RNase L inhibitor (RLI), highly conserved proteins required for genomic DNA replication and cytosolic translation respectively, are clearly essential for both *T. brucei* stages (Estévez *et al.*, 2004; Bruhn *et al.*, 2011). Comparative Western blot analysis of the PC and BS cells revealed that the level of *TbFdxA* protein in the latter stage is less than 17% of that in the insect dwelling stage (Fig. 2B).

We further investigate the role of *TbFdxA* in the BS, using the same RNAi strategy as for the PC. Surprisingly, we did not observe any growth defect in this knock-down even if the level of *TbFdxA* protein dropped by 96% as shown by Western analysis (Fig. S3). This result did not allow us to adequately distinguish as to whether *TbFdxA* was insuffi-

ciently depleted to cause a growth phenotype, or whether this protein is non-essential for the BS cells. Therefore, we resorted to a knockout strategy via homologous recombination (Fig. 4A and B), which leads to the disruption of both alleles of a single-copy gene, such as *TbFdxA*, resulting in total elimination of the corresponding protein. The presence of a regulatable copy of *TbFdxA* allows us to conclusively address whether the protein is indispensable for the BS of *T. brucei*. A previously described knockout strategy (Schnauffer *et al.*, 2001) was followed by replacing one allele of *TbFdxA* with a hygromycin-resistance cassette. Next, a plasmid allowing ectopic expression of the *TbFdxA* protein under the control of a Tet-responsive element was introduced into the single knockouts (1KO). This allows

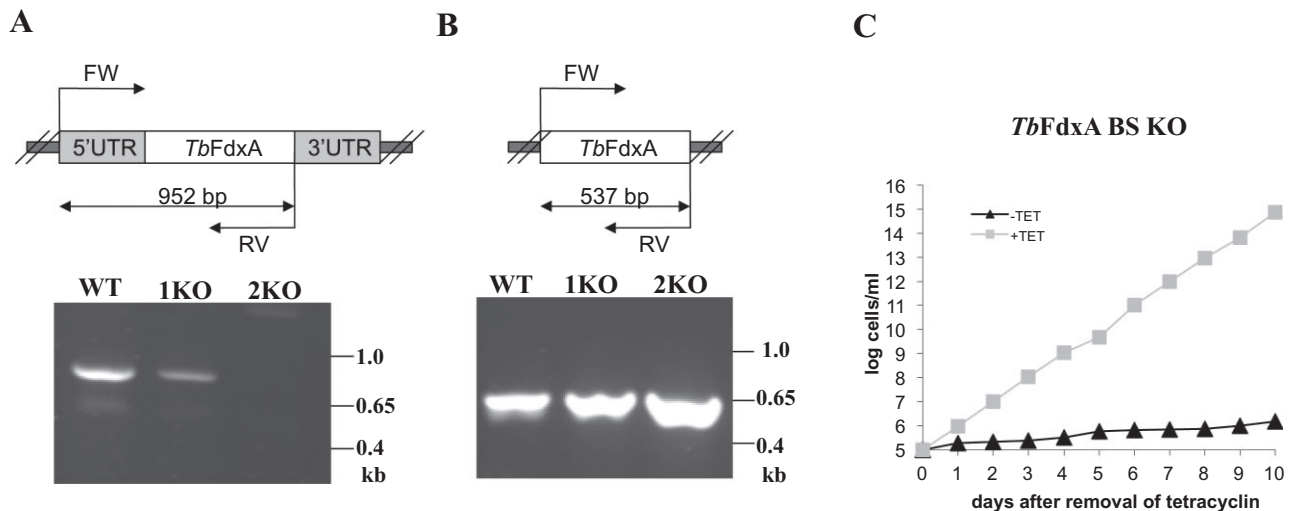


Fig. 4. *TbFdxA* is indispensable for viability of BS *T. brucei*.

A and B. PCR showing the absence of the endogenous *TbFdxA* gene in *TbFdxA* knockout cell line (A) and presence of the ectopic copy of *TbFdxA* (B). DNA was isolated from wild-type (WT), single allele replacement (1KO) and second allele replacement (2KO) BS cell lines. C. Growth curve represents numbers of *TbFdxA* knockout cell line grown in the presence (squares; grey line) or absence of tetracycline (triangles; black line). The data show a single representative experiment of biological triplicates.

proliferation of cells in the presence of Tet even when an essential gene is lost. Indeed, even when the second *TbFdxA* allele was subsequently disrupted by a neomycin-resistance cassette (2KO), the BS cells remained alive while the medium was supplemented with Tet. However, they immediately and completely lost viability when the drug was withdrawn (Fig. 4C), strongly indicating that the expression of an ectopic *TbFdxA* is vital for the survival of these flagellates. Elimination of the endogenous *TbFdxA* was confirmed using specific forward and reverse primers, annealing to the 5'UTR and part of the *TbFdxA* ORF, resulting in a 952-bp-long amplicon (Fig. 4A), confirmed by sequencing. Presence of the ectopic copy was verified by PCR with specific primers for full-length *TbFdxA* producing a 537 bp amplicon (Fig. 4B). All in all, the results obtained from the conditional knockout confirmed the essentiality of *TbFdxA* for the BS cells, although this stage seems to contain a far lower amount of the protein relative to PC (Fig. 2B). Consequently, despite the presence of only a rudimentary mitochondrion in the mammalian stage, the obtained results are compatible with active Fe-S cluster assembly in the organelle.

TbFdxA is required for synthesis of cytosolic and mitochondrial Fe-S proteins

Early studies suggested that the yeast and human ferredoxins are involved in mitochondrial *de novo* Fe-S cluster assembly, most likely functioning as electron donors (Lange *et al.*, 2000). We examined the effect of depletion of both ferredoxins on selected cytosolic and mitochondrial Fe-S enzymes in the PC trypanosomes.

In *T. brucei*, about 70% and 30% of aconitase, which is encoded by a single gene, is distributed in the cytosol and mitochondrion respectively (Saas *et al.*, 2000). This feature allows us to monitor its activity separately in both compartments (Fig. 5). The purity of each cell compartment, obtained by digitonin fractionation, was controlled by Western blot using antibodies specific for mitochondrial Hsp70 and cytosolic enolase (Fig. S4). As shown in Fig. 5A and C, both cytosolic and mitochondrial aconitase dropped by about 70% upon triggering RNAi of *TbFdxA* and *TbFdxA+B*. However, no decrease was observed in cytosolic and mitochondrial aconitase activities upon ablation of *TbFdxB* (Fig. 5B). The activity of succinate dehydrogenase (complex II), a Fe-S cluster-containing enzyme that is confined to the mitochondrion, followed the pattern observed for aconitase (Fig. 5D), whereas the reduction in activity of another Fe-S enzyme, cytochrome *c* reductase (complex III), was less pronounced, decreasing only by ~30% (Fig. 5E). These altered enzymatic activities demonstrate the importance of *TbFdxA*, but not *TbFdxB*, in the formation of both mitochondrial and cytosolic Fe-S cluster proteins. Threonine dehydrogenase, which lacks Fe-S clusters and was used as a control, remained unaffected in studied cell lines (Fig. S5).

Haem content is decreased in *TbFdxA* knock-down

Haem *a* is a prosthetic group of eukaryotic mitochondrial cytochrome *c* oxidase (complex IV) and some prokaryotic cytochrome oxidases. Complex IV is the only known eukaryotic protein containing haem *a* (Michel *et al.*, 1998;

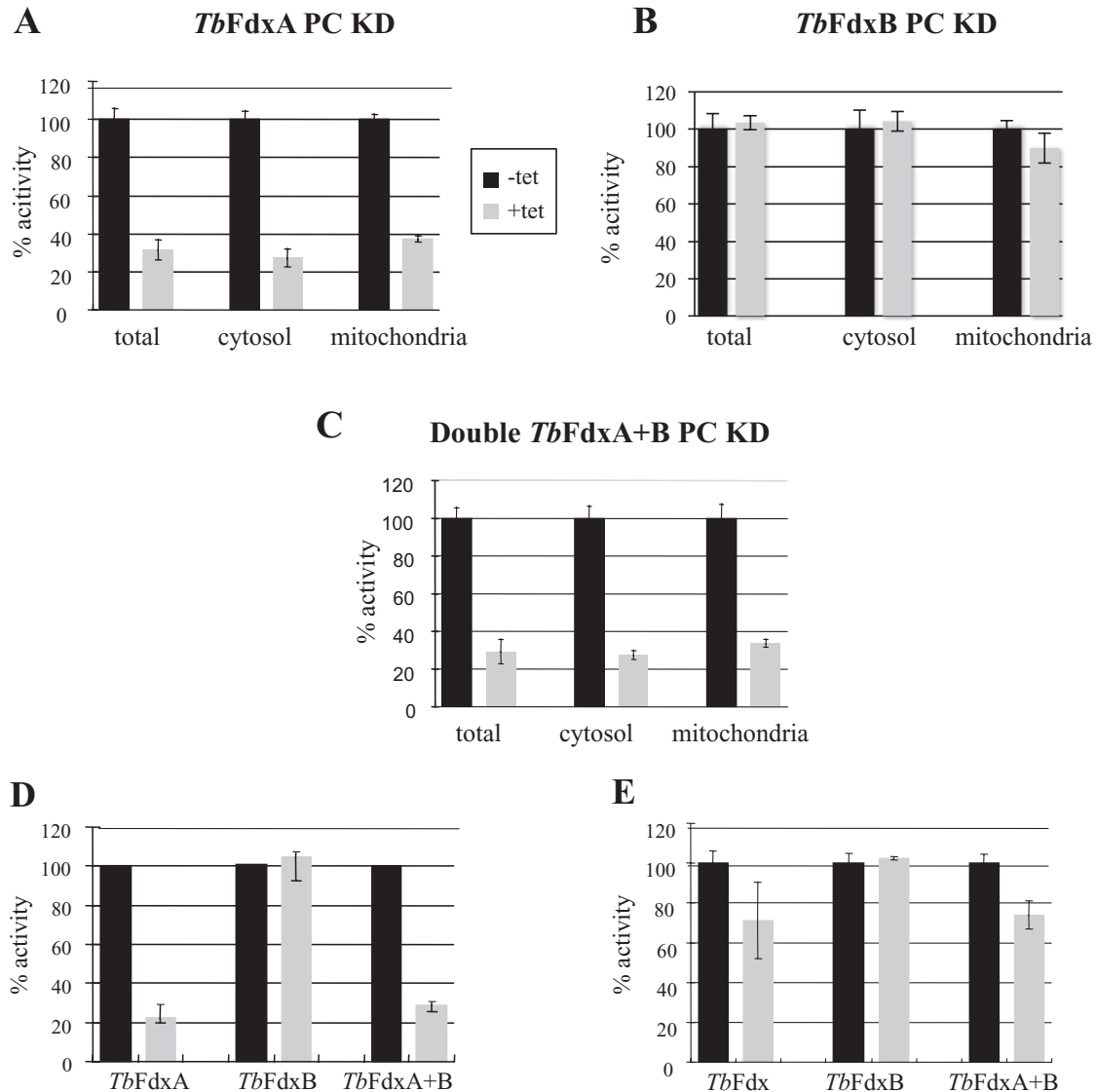


Fig. 5. Effect of *TbFdxA* and *TbFdxB* depletion in PC on Fe-S proteins. Aconitase activities of non-induced (black column) (-Tet) and RNAi-induced (grey column) (+Tet) of single *TbFdxA* (A), single *TbFdxB* (B) and double *TbFdxA+B* knock-down PC cells (C) were measured in whole cell, cytosolic and mitochondrial compartments 5 days after RNAi. Enzymatic activities of succinate dehydrogenase (complex II) (D) and cytochrome *c* reductase (complex III) (E) were measured in crude mitochondrial membrane extract. Specific activities are shown as a percentage of activities in non-induced cells. The means and SD values of three independent experiments are shown.

Barrientos *et al.*, 2009) and as such, bovine heart complex IV was used as a haem *a* standard for HPLC analysis (Fig. 6A). Since in *S. cerevisiae* ferredoxin together with ferredoxin reductase and Cox15 are required for the biosynthesis of haem *a* from the more abundant cellular haem *b* (Barros *et al.*, 2002), we measured the concentrations of haem *a* and haem *b* in the PC trypanosomes with ablated *TbFdxA*. We detected a 20% decrease of both haem *a* and haem *b* as compared with the non-induced cells (Fig. 6B), with the *P*-values being very close to the significant value (haem *b* *P* = 0.0682; haem *a* *P* = 0.0702).

TbFdxA knock-down alters mitochondrial biology

In the PC cells appropriate function of all respiratory complexes is required to maintain mitochondrial inner membrane potential (Besteiro *et al.*, 2005). Membrane potential was drastically reduced in *TbFdxA*-depleted cells, as measured by flow cytometry via quantification of TMRE uptake (Fig. S6A). Furthermore, the same cells accumulated ROS, as followed by dihydroethidium oxidation (Fig. S6B). Extensive disruption of the overall mitochondrial metabolism was reflected in alterations in levels of metabolic end-products upon *TbFdxA* RNAi induction. The

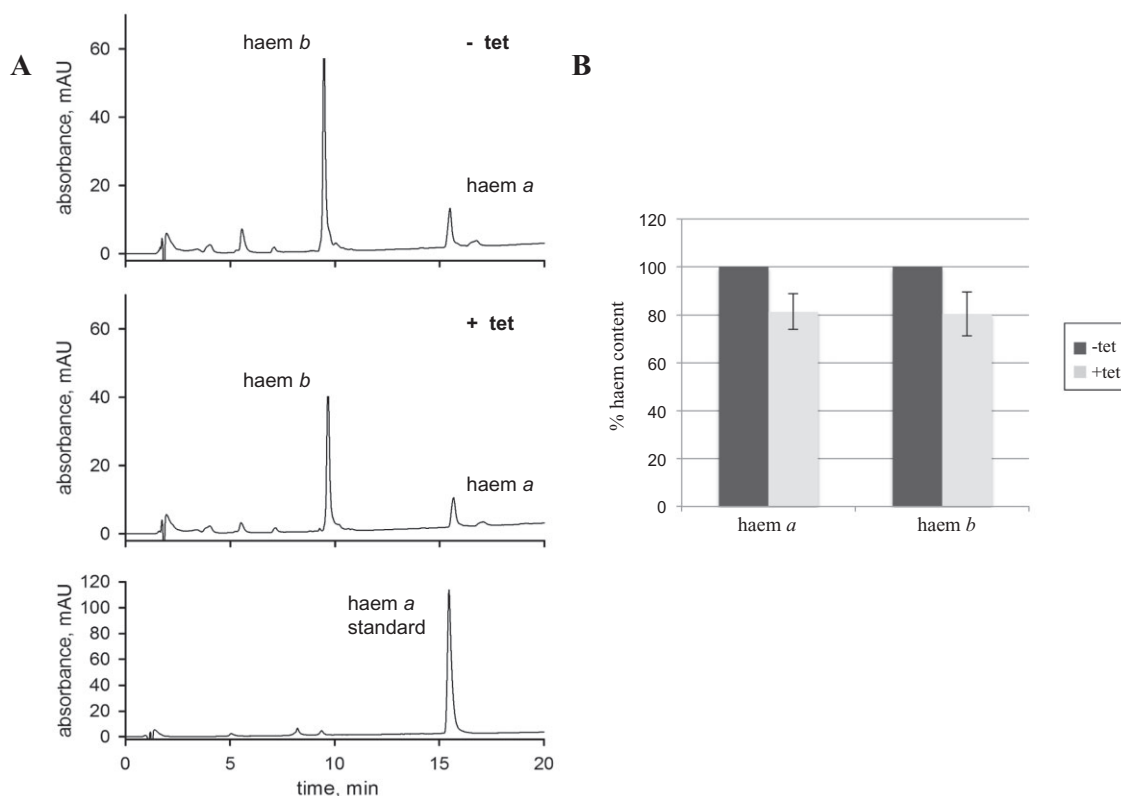


Fig. 6. Haem is decreased in PC *TbFdxA*-depleted cell.

A. Representative measurement of haem of non-induced (–Tet) and RNAi-induced (+Tet) single *TbFdxA* knock-down PC cells. Peaks at 10th and 16th min. represent haem *b* and haem *a* respectively.

B. Amount of haem *a* and haem *b* shown as a percentage with the level in the non-induced cells set to 100%. Dark grey and light grey columns represent per cent haem content of non-induced and RNAi-induced *TbFdxA* PC cells (day 7 post induction) respectively. The means and SD values of four independent RNAi inductions are shown. Haem was extracted from 2×10^9 cells, separated by HPLC and detected by diode array detector. *P*-values were calculated with a non-parametric Student's *t*-test (haem *b* *P* = 0.0682; haem *a* *P* = 0.0702).

most prominent change was an eightfold increase in pyruvate production. In contrast, excretion of succinate and acetate significantly lowered in the induced cells (Fig. S6C and Table S1).

Human ferredoxin homologues rescue *TbFdxA* knock-down

Taking advantage of the *T. brucei* model to gain insight into the controversial function of both human ferredoxin homologues, we tested the ability of each to compensate for the loss of *TbFdxA*. To this end, two rescue cell lines were generated, each constitutively expressing one of the two human ferredoxin genes fused to a C-terminal EGFP tag, which enabled us to monitor their expression (Fig. 7A). In both cell lines, the tagged human ferredoxins (HsFdx1 and HsFdx2) showed a strong signal which colocalized with Mitotracker Red (Fig. 7B). The exclusive mitochondrial localization of these human proteins demonstrated the ability of their respective human mitochondrial targeting

sequences to efficiently mediate import of the downstream protein into the trypanosome mitochondrion (Fig. 7B).

Following RNAi induction, both HsFdx1 and HsFdx2 were able to rescue cell growth, with no growth defect observed throughout the 8-day period for which growth was measured (Fig. 8A), in contrast to the parental *TbFdxA* RNAi line (Fig. 3A). Hence, the presence of either HsFdx1 or HsFdx2 was sufficient to support, in the absence of *TbFdxA*, the growth of PC at wild-type level. Furthermore, aconitase activity in the *TbFdxA*-depleted cells was rescued by HsFdx1 to almost wild-type level in both cytosolic and mitochondrial compartments (Fig. 8B). In the case of HsFdx2, the total aconitase activity was rescued completely, and the mitochondrially localized fraction was even slightly overexpressed (Fig. 8B). Western blot analysis confirmed that about 95% of *TbFdxA* was eliminated within 2 days of RNAi (Fig. 7A). These data demonstrate that either human ferredoxin homologue is sufficient to compensate for the essential Fe-S biosynthetic function of *TbFdxA* in *T. brucei*.

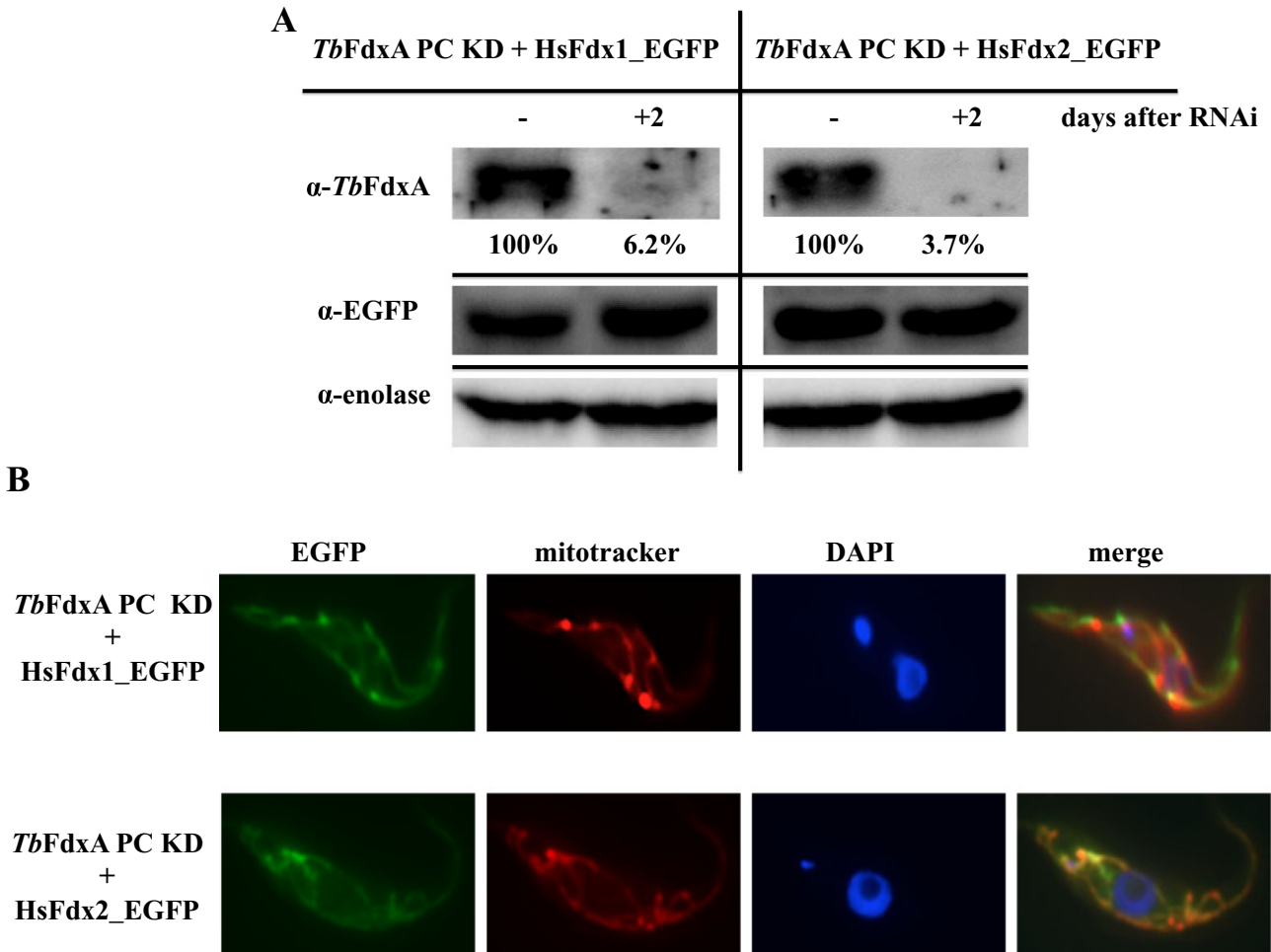


Fig. 7. HsFdx1 and HsFdx2 are expressed in PC *TbFdxA* RNAi cell lines and imported into the *T. brucei* mitochondrion.

A. Western blot analysis with α -*TbFdxA* antibody determines level of endogenous *TbFdxA* 2 days upon RNAi induction. Expression of HsFdx1-EGFP or HsFdx2-EGFP in the *TbFdxA* knock-down cells was followed by α -EGFP antibody. Enolase was used as a loading control. Western blots were quantified with Image J software, enolase was used as a normalizer.

B. Fluorescence microscopy of *TbFdxA* knock-down cell lines expressing HsFdx1-EGFP or HsFdx2-EGFP. Mitotracker Red staining visualizes the mitochondrion. 4,6-diamidino-2-phenylindole (DAPI) stains nuclear and mitochondrial DNA.

Discussion

Ever since ferredoxin was first isolated from *Clostridium pasteurianum* in the early 1960s (Mortenson *et al.*, 1962), this protein highly conserved across the prokaryotic and eukaryotic domains has emerged as a multifunctional protein involved in electron transport, biosynthesis of coenzyme Q, steroid hormone and haem *a* synthesis (Barros *et al.*, 2002; Pierrel *et al.*, 2010; Ewen *et al.*, 2011). Moreover, as both a [2Fe-2S] cluster-containing protein and a Fe-S biosynthetic enzyme, it has the converse properties of being both dependent on and essential for cluster assembly (Barros and Nobrega, 1999; Lange *et al.*, 2000; Tokumoto and Takahashi, 2001).

Here, we have identified two mitochondrial ferredoxin homologues in *T. brucei*, named *TbFdxA* and *TbFdxB*,

and experimentally verified their localization within the organelle. Phylogenetic analysis of ferredoxins across the eukaryotic supergroups revealed that both trypanosome homologues are only distantly related to other ferredoxins and that *TbFdxB* and its homologues in other kinetoplasts constitute the basal branch of the tree. Moreover, this approach detected amplification of ferredoxins in the genomes of *Leishmania* species.

In a recent global RNAi analysis in *T. brucei*, *TbFdxA* was found to be essential in both PC and BS cells, unlike *TbFdxB* which was essential only in the former stage (Alford *et al.*, 2011). Contradictory to this high-throughput screen, the separate and tandem RNAi silencing of ferredoxins presented here showed that *TbFdxA* is essential in both life cycle stages while *TbFdxB*, which we studied only in the PC cells, is dispensable. Moreover, the experi-

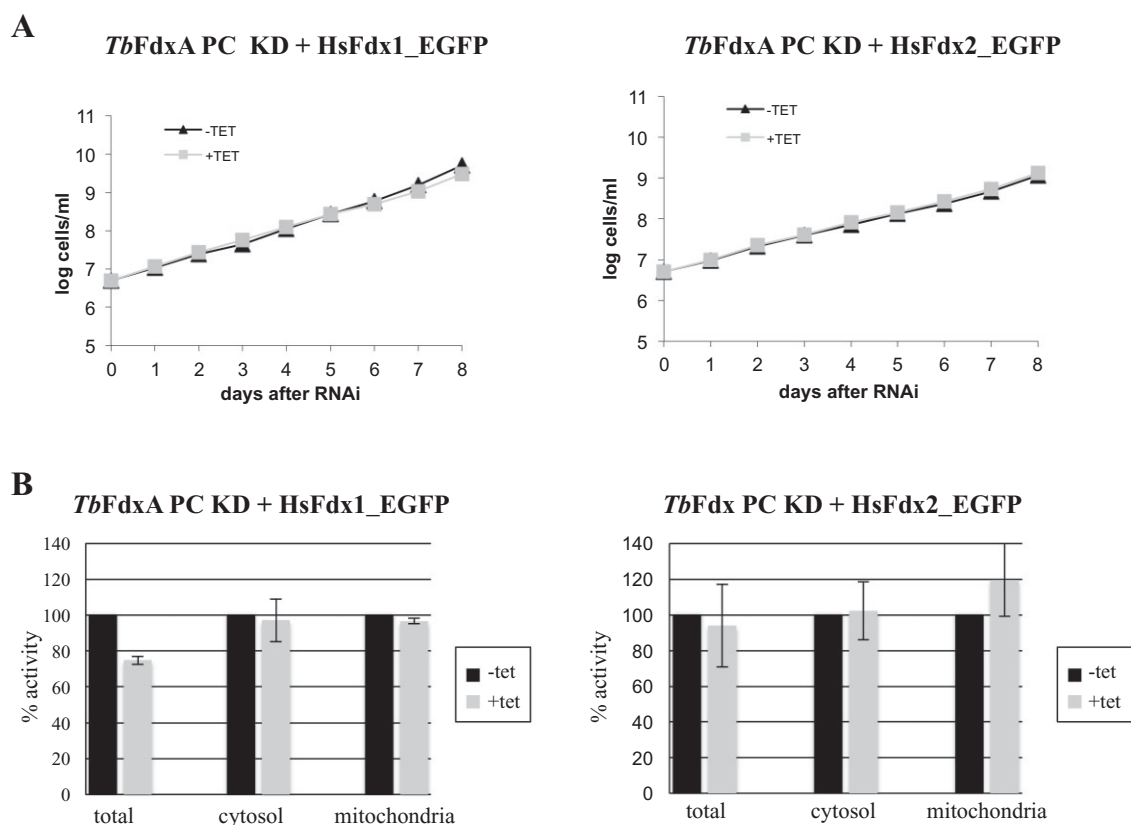


Fig. 8. Expression of either human ferredoxin rescues *TbFdxA* depletion in PC.

A. Growth curves of non-induced (triangle; black line) and RNAi-induced (square; grey line) *TbFdxA* knock-down PC cells constitutively expressing HsFdx1 (left) or HsFdx2 (right). The y-axis represents the log scale product of cell density and total dilution. The data show a single representative experiment of biological triplicates.

B. Aconitase activities in whole cell lysates as well as, cytosolic and mitochondrial compartments of *TbFdxA* knock-down PC cells expressing HsFdx1 (left) or HsFdx2 (right) 5 days post induction. Specific activities are shown for non-induced (black columns) and RNAi-induced cells (grey columns) as a percentage of activity of non-induced cells. The means and SD values of three independent experiments are shown.

mental set-up enabled us to rule out the possibility of redundancy between both homologues.

Upon depletion of *TbFdxA* in the PC cells, the activities of Fe-S cluster-containing cytosolic and mitochondrial aconitase, as well as respiratory complex II were dramatically decreased. Respiratory complex III activity was also reduced, although to a lesser extent. The alterations in the respiratory chain likely caused the decrease of mitochondrial membrane potential and a direct transfer of electrons from complex III to oxygen, with the concomitant production of ROS as was reported recently (Gnipová *et al.*, 2012). These activity measurements confirmed the indispensability of *TbFdxA* in Fe-S cluster biogenesis in both compartments, which is in good correlation with other eukaryotes (Lange *et al.*, 2000; Shi *et al.*, 2012). Since its depletion does not affect levels of frataxin, IscU or Nfs and it was not detected in the IscU/Nfs/Isc11 complex (Paris *et al.*, 2010), *TbFdxA* most likely functions as a solo player that does not stably associate with other ISC assembly proteins. Indeed, exactly how ferredoxin participates in

the Fe-S biosynthesis remains largely unknown. Available data support its function in an electron transfer chain, in which ferredoxin reductase receives electrons from NADH and transfers them to ferredoxin, which in turn donates electrons for the reduction of cysteine-derived sulphur in order to produce the sulphide component of the clusters (Mühlenhoff *et al.*, 2003). Since ablation of *TbFdxB* in PC did not cause any visible phenotype, the function of this unusual ferredoxin, representative of a kinetoplastid-specific branch distinct from all other eukaryotic ferredoxins, remains to be established.

Trypanosomes are unusual among eukaryotes in that they have lost the capacity to synthesize haem *b*, which must consequently be imported from the host or from the medium (Kořený *et al.*, 2010). Conversion of haem *b* to haem *a* has been described for *T. cruzi* and likely also occurs in *T. brucei* (Tripodi *et al.*, 2011). An additional role for ferredoxin in haem *a* synthesis has been demonstrated in yeast (Barros *et al.*, 2002; Moraes *et al.*, 2004), and as HsFdx2 was able to rescue this function in yeast

cells (Sheftel *et al.*, 2010), we examined the effects of *TbFdxA* depletion on haem levels. HPLC analysis of the *TbFdxA* knock-downs showed that haem *a* and surprisingly also haem *b* levels were decreased by approximately a quarter in the RNAi-induced cells as compared with the non-induced ones. The decrease of haem *a* was expected, on the other hand the level of haem *b* should stay unaffected (Barros *et al.*, 2001). We can only speculate that there may be feedback machinery in *T. brucei* that is providing haem *a*/haem *b* equilibrium. It can be particularly important in the mitochondrion, since respiratory complexes are the main consumers of both haems. Disruption of haem homeostasis can lead to increased ROS production with devastating consequences to the cell. Since the change in haem content is rather low, it seems that in *T. brucei*, as in other organisms (Barros *et al.*, 2002), other players participate in haem *a* biosynthesis apart from ferredoxin. In summary, it seems likely that in bridging the two major mitochondrial iron-consuming pathways, namely haem *a* synthesis and Fe-S cluster assembly, this protein is also perfectly positioned to impact on cellular iron homeostasis, as has been observed upon ferredoxin disruption in both yeast and humans (Sheftel *et al.*, 2010; Miao *et al.*, 2011; Shi *et al.*, 2012).

Although the PC trypanosomes rely on L-proline and other amino acids as a source of energy inside the tsetse fly, they will preferentially consume glucose in a glucose-rich medium (Bringaud *et al.*, 2006). Under such conditions, pyruvate is produced glycolytically and subsequently converted to the metabolic end-products succinate, acetate and lactate. In the *TbFdxA*-depleted PC cells, the production of pyruvate dramatically increases. This can be well explained by a compensatory upregulation of glycolysis in response to reduced mitochondrial substrate level ATP production (Bochud-Allemann and Schneider, 2002). Similar phenotype was observed in the PC cells depleted for other Fe-S assembly proteins (Smíd *et al.*, 2006). By decreasing acetate and ATP production, mitochondria of these genetically modified PC act like metabolically suppressed organelles in the BS flagellates. The parallel decrease in succinate production, meanwhile, may result from depletion of its fumarate precursor due to impaired function of the Fe-S-dependent enzyme fumarase, which is required for the conversion of malate to fumarate. Because we observed loss of membrane potential in *TbFdxA* PC KD, pyruvate cannot enter the organelle since it requires H⁺ symport. Nevertheless, even if pyruvate reached the mitochondrial matrix, it cannot be converted to acetyl-CoA, as this reaction requires available NAD⁺. It is unlikely that mitochondrion lacking Fe-S production possesses enough capacity to regenerate this cofactor having respiratory chain off-line. Tentatively, the production of acetate is diminished as a consequence of pyruvate not

being able to reach the mitochondrion and the lack of NAD⁺ available for the pyruvate-acetyl-CoA reaction.

Since the rudimentary mitochondrion of the BS trypanosomes lacks both respiratory chain and tricarboxylic acid cycle (Grant and Sargent, 1960), it is not surprising that its levels of *TbFdxA* are greatly reduced. In fact, the only Fe-S cluster-containing proteins we are aware of in this organelle are monothiol glutaredoxin-1 and aconitase expressed at a very low level (Saas *et al.*, 2000; Comini *et al.*, 2008), while the cytosol of BS contains numerous indispensable proteins, the function of which depends on clusters, such as RLI and nuclear DNA polymerases (Estévez *et al.*, 2004; Netz *et al.*, 2012). Initially, the absence of any growth defect following RNAi-mediated depletion called into question the essentiality of *TbFdxA* for the BS. However, conditional knockout cells provided evidence that even in this life cycle stage, canonical Fe-S cluster assembly takes place within the repressed mitochondrion and the whole pathway thus remains essential. Indeed, ferredoxins are known to be retained in mitochondrion-derived reduced organelles of anaerobic protists, such as the hydrogenosomes of *Trichomonas vaginalis* (Sutak *et al.*, 2004) and the mitosomes of *Giardia intestinalis* (Tovar *et al.*, 2003). Thus, Fe-S cluster biosynthesis clearly remains one of the fundamental processes of mitochondria and mitochondrion-like organelles, the role of which in energy production has been diminished or lost altogether.

Our next aim was to shed light, via complementation studies in trypanosomes, on the function of the human ferredoxins, the role of which still remains to some extent controversial. A recent study in yeast demonstrated that only HsFdx2 but not HsFdx1 can complement the defect in Fe-S cluster assembly in the yeast Yah1 mutant (Sheftel *et al.*, 2010). In contrast, another group showed that both human ferredoxins together with ferredoxin reductase are involved in Fe-S cluster assembly (Shi *et al.*, 2012). We took advantage of the PC knock-downs to perform complementation assays with two EGFP-tagged human ferredoxins, equipped with their endogenous mammalian mitochondrial import signals. Interestingly, both human proteins mediated a full rescue in terms of growth defect and aconitase activity. These successful rescues strongly support the view that the human ferredoxins are functional homologues that evolved by gene duplication.

The highly efficient import of both human proteins via their genuine import signals is unexpected and exciting on its own right, since trypanosomes and humans shared the last common ancestor perhaps over 1 billion years ago, and these flagellates qualify for one of the earliest offshoots of the eukaryotic tree (Cavalier-Smith, 2010). Moreover, trypanosomes and related flagellates are characterized by generally very short mitochondrial import presequences (Schneider *et al.*, 2008) and elusive trans-

porters of the inner and outer membrane complexes. This may be caused by either genuine absence of most key subunits (Pusnik *et al.*, 2009), divergence obscuring their recognition (Žárský *et al.*, 2012), or the existence of transporter complexes that are mostly composed of novel proteins (Singha *et al.*, 2012). It has been shown previously in *T. brucei* that the mitochondrial presequence of human frataxin is sufficient for import and processing of human frataxin (Long *et al.*, 2008) and human Isa1/2 proteins (Long *et al.*, 2011). Our corresponding finding for HsFdx1 and HsFdx2 suggests that the *T. brucei* mitochondrion is capable of importing proteins with complex organellar import signals.

Experimental procedures

Phylogenetic analysis

Maximum likelihood phylogeny of the aligned data set was created using RAxML 7.3a (Stamatakis, 2006) employing Γ -corrected LG substitution matrix. The highest scoring topology was chosen from 100 independent runs each starting with a different starting tree. Branching support was assessed using non-parametric bootstrapping (RAxML LG+ Γ ; 500 replicates) and Bayesian posterior probabilities as estimated in Phylobayes 3.2 (Lartillot *et al.*, 2009) under the empirical mixture model C40 combined with substitution rates derived from the LG matrix. For this, two independent chains were run until their maximum observed discrepancy was lower than 0.1 (i.e. they converged) and effective sample size of model parameters was equal to 150 or higher.

Preparation of pT7V5-FdxA and pT7V5-FdxB constructs

Gene constructs were prepared to contain *TbFdxA* (Tb927.7.890) and *TbFdxB* (Tb927.4.4980) ORFs lacking stop codons followed by V5 tags. They were amplified from the total genomic DNA of *T. brucei* strain 29-13 using primer pairs *TbFdxA_V5-FP* (5'-CGCAAAGCTTATGGCTGCTTTA CGCTACTT) and *TbFdxA_V5-RP* (5'-CGCGGATCCGTGA TGAGGGTTATGGTGT), and *TbFdxB_V5-FP* (5'-CGCAA GCTTATGCTTTCCGCAACTTTCGG) and *TbFdxB_V5-RP* (5'-CGCGGATCCCGCATTTCATTTCGTTGTTT) (added BamHI and HindIII restriction sites are underlined).

PCR product were cloned into pT7V5 vector and verified by sequencing. The pT7V5-FdxA and pT7V5-FdxB were linearized with NotI and electroporated into wild-type PC *T. brucei* strain 29-13. The transfected cell lines were selected on puromycin (1 $\mu\text{g ml}^{-1}$) and expression of the tagged protein was induced by addition of Tet (1 $\mu\text{g ml}^{-1}$).

RNAi constructs, transfections, cloning, RNAi induction and cultivation

To prepare *TbFdxA* (Tb927.7.890) and *TbFdxB* (Tb927.4.4980) RNA interference (RNAi) constructs, 537-nt-long and 504-nt-long fragments of *TbFdxA* and *TbFdxB* respectively, were amplified using primer pairs *TbFdxA-FP* (5'-GAAG

CTTATGGCTGCTT TACGCTACTT) and *TbFdxA-RP* (5'-GACTAGTTCAGTGATGAGGGTTATGG), and *TbFdxB-FP* (5'-GAAGCTTATGCTTTCCG CAACTTTCGG) and *TbFdxB-RP* (5'-GACTAGTTCACCGCATTTCATTTCGTTG) (added HindIII and SpeI restriction sites are underlined) and total genomic DNA of *T. brucei* strain 29-13 as a template. Both amplicons were separately cloned into the p2T7-177 vector which was, upon NotI-mediated linearization, introduced into PC *T. brucei* 29-13 cells using a BTX electroporator and selected as described elsewhere (Vondrušková *et al.*, 2005). The double knock-down was prepared by cloning the amplicon produced by the primers *TbFdxB2KD-FP* (5'-GATCGAT ATGCTTTCCGCAACTTTCGG) and *TbFdxB2KD-RP* (5'-GCTCGAGTCAACCGCATTTCATTTCGTTG) (added ClaI and XhoI restriction sites are underlined), into the p2T7-177 + *TbFdxA* construct, which was then stably integrated into the PC cells as described above. The p2T7-177 + *TbFdxA* construct was also transfected into BS *T. brucei* 427 cells using the Amaxa Nucleofector II electroporator, with transfectants maintained in HMI-9 medium and selected following a protocol described previously (Hashimi *et al.*, 2008). PC and BS trypanosomes were cultivated in SDM-79 medium at 27°C and HMI-9 medium at 37°C respectively. RNAi was initiated by the addition of 1 $\mu\text{g ml}^{-1}$ tetracycline (Tet) to the medium and growth measurements were made using the Beckman Z2 Coulter counter at 24 h intervals, for 9 days in the case of PC and 7 days for BS cells.

Generation of *TbFdxA* conditional knockout

A *TbFdxA* conditional knockout was generated in BS cells strain 427 following a strategy described by Schnauer *et al.* (2001). Fragments of the 5'UTR and 3'UTR of *TbFdxA* were amplified from *T. brucei* genomic DNA using primer pairs 5'UTR-FP (5'-AGTGCGGCCGAGTGGGGCCTGTGGTGT) and 5'UTR-RP (5'-AGTACGCGCTCGAGTGCCCCGCTCA CCT), and 3'UTR-FP (5'-CACTCTAGAATTTAAATCGCAC CCGCCGTAG) and 3'UTR-RP (5'-AGTAGGCCTGCGGC CGCTGGGTGCCTCGCTCA). The amplicons were cloned into the T7RNP/NEO cassette of pLew13. This construct (designated pFdxA-KO1) was then transfected to generate the first allele replacement. Next, pLew79 with full-length *TbFdxA*, PCR-amplified from genomic DNA using primers *FdxAORF-FP* (5'-CACGATTTCATGGCTGCTTTAC) and *FdxAORF-RP* (5'-CACAAGCTTTCAGTGATGAGG), was transfected in order to express an ectopic copy of *TbFdxA* in the presence of Tet. Lastly, pFdxA-KO2 was created by replacing the T7RNP/NEO cassette in pFdxA-KO1 with the TETR/HYG cassette from pLew90. Integration of this plasmid generated the second allele replacement. PCR using primers 5'UTR-FP, *FdxAORF-FP* and *FdxAORF-RP* were used to confirm proper integration in the conditional knockout cells.

Preparation of antibodies and Western blot analysis

The full-size *TbFdxA* and *TbFdxB* genes were amplified by PCR with primers *TbFdxA-FP/O* (5'-CACCATGGCTGCTT TACGCTACTT) and *TbFdxA-RP/O* (5'-TCAGTGATGAGG GGTTATGG), and *TbFdxB-FP/O* (5'-CACCATGCTTTCCGC AACTTTCGG) and *TbFdxB-RP/O* (5'-TCACCGCATTCA

TTCGTTG). The amplicons were gel-purified and cloned into the pET/100D expression vector (Invitrogen). The resulting expression plasmids encoding His₆-tagged *TbFdxA* and *TbFdxB* were transformed into the *E. coli* strain BL21 star (DE3) (Invitrogen). Insoluble proteins were obtained from induced bacterial cells (incubation at 37°C for 3 h; induced with 1 mM IPTG) under denaturing conditions using ProBond Ni-chelating resin (Invitrogen). Polyclonal antibodies against the *TbFdxA* protein were prepared by Cocalico Biologicals (Reamstown, PA, USA) by immunizing a rat at 2-week intervals with the purified recombinant *TbFdxA* protein. Cell lysates corresponding to 5×10^6 cells per lane were separated on a 15% SDS-polyacrylamide gel, transferred to a PVDF membrane and probed. α -*TbFdxA* polyclonal rat antibodies, polyclonal antibodies against enolase (provided by Paul A. M. Michels) and monoclonal antibodies against GFP (Invitrogen) were used at 1:1000, 1:200 000 and 1:1000 dilutions respectively, followed by appropriate secondary antibodies conjugated with horseradish peroxidase (Sigma), then visualized using an ECL kit (Pierce).

Quantitative real-time PCR

Total RNA from induced and non-induced cells was isolated using TRIzol (Sigma). The turbo DNA-free DNase kit (Ambion) was used to remove residual DNA. Reverse transcription using the SuperScript III reverse transcriptase (Invitrogen) and Oligo (dT)₂₀ primer (Invitrogen) was performed to obtain cDNAs. Quantitative real-time PCR reactions were performed as described elsewhere (Hashimi *et al.*, 2008). The primer pair for detecting of *TbFdxB* mRNA is *FdxB-qPCR-FW* (5'-TGCCAGGTAAAGCTCAGCAA) and *TbFdxB_V5-RP*. The primer pair for the internal reference 18S rRNA was described previously (Carnes *et al.*, 2005). The relative *TbFdxB* mRNA abundance between induced and non-induced cells was determined by the Pfaffl method (Pfaffl, 2001).

Digitonin fractionation and enzymatic activities measurement

Cytosolic and mitochondrial fractions for aconitase activity measurements were obtained by digitonin fractionation, performed as described elsewhere (Smíd *et al.*, 2006). Total cell fraction was obtained by treating cell suspension in Hanks' balanced salt solution with 0.1% Triton X-100 and incubating for 5 min. After centrifugation the supernatant was collected as total cell fraction. Aconitase activity was measured spectrophotometrically at 240 nm as production of *cis*-aconitate. The activity of threonine dehydrogenase was measured at 340 nm as a rate of NAD reduction. The activities of succinate dehydrogenase and cytochrome *c* reductase were measured in crude mitochondrial membrane extract as described elsewhere (Horváth *et al.*, 2005).

Measurement of mitochondrial inner membrane potential and ROS

Approximately 5×10^6 cells of exponentially growing PC *T. brucei* were harvested and centrifuged, and the pellet was

resuspended in 1 ml fresh SDM-79 medium. Membrane potential was measured by monitoring uptake of tetramethylrhodamine ethyl ester (TMRE) (Molecular Probes) as described previously (Horváth *et al.*, 2005). Reactive oxygen species (ROS) were measured by oxidation of dihydroethidium (Sigma) as described elsewhere (Long *et al.*, 2008). After staining with $5 \mu\text{g ml}^{-1}$ dihydroethidium for 30 min at 27°C, cells were resuspended in 5 ml iso-flow buffer. Intracellular ROS were detected by an Epics XL flow cytometer (Beckman Coulter) with excitation and emission settings of 488 nm and 620 nm respectively.

Determination of metabolic end-products

Approximately 8×10^7 cells were washed with incubation buffer (PBS supplemented with 11 mM glucose and 24 mM NaHCO₃, pH 7.3). After incubation for 2 h at 27°C, cells were centrifuged for 10 min at 3000 r.p.m. The supernatant was collected and analysed by HPLC in a PL Hi-Plex H column as described elsewhere (Vaňáčová *et al.*, 2001).

Immunofluorescence assay

Approximately 1×10^7 PC cells were collected, centrifuged, resuspended in fresh medium and stained with 200 nM of the mitochondrion-selective dye Mitotracker Red (Invitrogen). After 30 min incubation at 27°C, the cells were centrifuged for 5 min at 3000 r.p.m. at room temperature. The pellet was washed and resuspended in 1 ml PBS with 4% paraformaldehyde and 1.25 mM NaOH. Two hundred and fifty microlitres of the suspension was applied to a microscopic slide and incubated for 10 min at room temperature. The slides were washed with PBS, incubated in ice-cold methanol for an additional 20 min and washed briefly with PBS. Primary anti-V5 antibody (Invitrogen) was added at 1:100 dilution in PBS-Tween (0.05%) with 5% milk and incubated at 4°C overnight. Slides were washed with PBS. Alexa Fluor® 488 goat anti-mouse IgG (Molecular Probes) was used at 1:1000 dilution for 1 h at room temperature. The samples were mounted with antifade reagent with DAPI (Invitrogen). After incubation in the dark for 30 min, the sample was visualized using an Axioplan2 imaging (Zeiss) fluorescent microscope.

Human ferredoxin rescues and growth curves

To prepare constructs expressing human ferredoxin, the *HsFdx1* and *HsFdx2* genes, each conjugated to C-terminal enhanced green fluorescent protein (EGFP), were amplified from the *HsFdx1*-EGFP-N3 and *HsFdx2*-EGFP-N3 plasmids respectively (kindly provided by Antonio Pierik and Roland Lill). PCR was performed using primer *huFdx1-1* (5'-AAGCTTATGGCTGCCGCTGGGGCGC) or *huFdx2-F* (5'-AAGCTTGCTACCGGACTCAGATCTAC) in combination with common *huFdx-R* (5'-GATATCTTTACTTGACAGCTCGTCCA) (added restriction sites HindIII and EcoRV are underlined). Each product was cloned into the pABPURO constitutive expression vector. The *HsFdx1*-EGFP-pABPURO and *HsFdx2*-EGFP-pABPURO constructs were separately transfected into PC cells carrying the inducible *TbFdxA* RNAi construct. Transformants were selected with puromycin and

clonal cell lines were obtained by limiting dilution. RNAi was induced with the addition of Tet and growth measurements were made using the Beckman Z2 Coulter counter at 24 h intervals for 8 days.

Haem measurement

A total of 2×10^9 PC cells were harvested, centrifuged at 3000 r.p.m. for 5 min and washed three times with PBS. The cell pellet was then resuspended in 200 μ l H₂O and extracted with 400 μ l acetone/0.2% HCl. The supernatant was collected after centrifugation for 5 min at 12 000 r.p.m. The pellet was resuspended in 300 μ l acetone/0.2% HCl and spun again for 5 min at 12 000 r.p.m. Both supernatants were combined and 150 μ l of each sample was separated by HPLC on a Nova-Pak C18 column using linear gradient 25–100% acetonitrile/0.1% trifluoroacetic acid at a flow rate of 1.1 ml min⁻¹ at 40°C. Haem was detected by diode array detector Agilent 1200 (Agilent Technologies).

Acknowledgements

We thank Roman Sobotka (Institute of Microbiology, Třeboň) for valuable help with the HPLC experiment, Antonio Pierik and Roland Lill (Philipps University, Marburg) for kindly sharing plasmids with tagged human ferredoxins, Aleš Horák (Biology Centre, České Budějovice) for help with phylogenetic analysis, Ivan Hrdý (Charles University, Prague) for end-product measurement, Luděk Kořený (University of Cambridge, Cambridge) and Zdeněk Verner (Comenius University, Bratislava) for helpful discussions and Paul A. M. Michels (Universidad de los Andes, Mérida) for the gift of α -enolase antibodies. This work was supported by the Grant Agency of the Czech Republic (P305/11/2179), Czech Ministry of Education (AMVIS LH12104), and the Praemium Academiae award to J.L., who is also a Fellow of the Canadian Institute for Advanced Research.

References

- Adam, A.C., Bornhvd, C., Prokisch, H., Neupert, W., and Hell, K. (2006) The Nfs1 interacting protein Isd11 has an essential role in Fe/S cluster biogenesis in mitochondria. *EMBO J* **25**: 174–183.
- Alsford, S., Turner, D.J., Obado, S.O., Sanchez-Flores, A., Glover, L., Berriman, M., *et al.* (2011) High-throughput phenotyping using parallel sequencing of RNA interference targets in the African trypanosome. *Genome Res* **21**: 915–924.
- Barrientos, A., Gouget, K., Horn, D., Soto, I.C., and Fontanesi, F. (2009) Suppression mechanisms of COX assembly defects in yeast and human: insights into the COX assembly process. *Biochim Biophys Acta* **1793**: 97–107.
- Barros, M.H., and Nobrega, F.G. (1999) YAH1 of *Saccharomyces cerevisiae*: a new essential gene that codes for a protein homologous to human adrenodoxin. *Gene* **233**: 197–203.
- Barros, M.H., Carlson, C.G., Glerum, D.M., and Tzagoloff, A. (2001) Involvement of mitochondrial ferredoxin and Cox15p in hydroxylation of heme O. *FEBS Lett* **492**: 133–138.
- Barros, M.H., Nobrega, F.G., and Tzagoloff, A. (2002) Mitochondrial ferredoxin is required for heme A synthesis in *Saccharomyces cerevisiae*. *J Biol Chem* **277**: 9997–10002.
- Besteiro, S., Biran, M., Biteau, N., Coustou, V., Baltz, T., Canioni, P., and Bringaud, F. (2002) Succinate secreted by *Trypanosoma brucei* is produced by a novel and unique glycosomal enzyme, NADH-dependent fumarate reductase. *J Biol Chem* **277**: 38001–38012.
- Besteiro, S., Barrett, M., Riviere, L., and Bringaud, F. (2005) Energy generation in insect stages of *Trypanosoma brucei*: metabolism in flux. *Trends Parasitol* **21**: 185–191.
- Bochud-Allemann, N., and Schneider, A. (2002) Mitochondrial substrate level phosphorylation is essential for growth of procyclic *Trypanosoma brucei*. *J Biol Chem* **277**: 32849–32854.
- Bringaud, F., Riviere, L., and Coustou, V. (2006) Energy metabolism of trypanosomatids: adaptation to available carbon sources. *Mol Biochem Parasitol* **149**: 1–9.
- Bruhn, D.F., Sammartino, M., and Klingbeil, M.M. (2011) Three mitochondrial DNA polymerases are essential for kinetoplast DNA replication and survival of bloodstream form *Trypanosoma brucei*. *Eukaryot Cell* **10**: 734–743.
- Carnes, J., Trotter, J.R., Ernst, N.L., Steinberg, A., and Stuart, K. (2005) An essential RNase III insertion editing endonuclease in *Trypanosoma brucei*. *Proc Natl Acad Sci USA* **102**: 16614–16619.
- Cavalier-Smith, T. (2010) Deep phylogeny, ancestral groups and the four ages of life. *Philos Trans R Soc Lond B Biol Sci* **365**: 111–132.
- Chandramouli, K., Unciuleac, M.C., Naik, S., Dean, D.R., Huynh, B.H., and Johnson, M.K. (2007) Formation and properties of [4Fe-4S] clusters on the IscU scaffold protein. *Biochemistry* **46**: 6804–6811.
- Comini, M.A., Rettig, J., Dirdjaja, N., Hanschmann, E.M., Berndt, C., and Krauth-Siegel, R.L. (2008) Monothiol glutaredoxin-1 is an essential iron-sulfur protein in the mitochondrion of African trypanosomes. *J Biol Chem* **283**: 27785–27798.
- Coustou, V., Biran, M., Besteiro, S., Riviere, L., Baltz, T., Franconi, J.M., and Bringaud, F. (2006) Fumarate is an essential intermediary metabolite produced by the procyclic *Trypanosoma brucei*. *J Biol Chem* **281**: 26832–26846.
- Estévez, A.M., Haile, S., Steinbuchel, M., Quijada, L., and Clayton, C. (2004) Effects of depletion and overexpression of the *Trypanosoma brucei* ribonuclease L inhibitor homologue. *Mol Biochem Parasitol* **133**: 137–141.
- Ewen, K.M., Kleser, M., and Bernhardt, R. (2011) Adrenodoxin: the archetype of vertebrate-type [2Fe-2S] cluster ferredoxins. *Biochim Biophys Acta Proteins Proteomics* **1814**: 111–125.
- Gnipová, A., Panicucci, B., Paris, Z., Verner, Z., Horváth, A., Lukeš, J., and Zíková, A. (2012) Disparate phenotypic effects from the knockdown of various *Trypanosoma brucei* cytochrome *c* oxidase subunits. *Mol Biochem Parasitol* **184**: 90–98.
- Grant, P.T., and Sargent, J.R. (1960) Properties of L- α -glycerophosphate oxidase and its role in the respiration of *Trypanosoma rhodesiense*. *Biochem J* **76**: 229–237.
- Hashimi, H., Zíková, A., Panigrahi, A.K., Stuart, K.D., and Lukeš, J. (2008) TbRGG1, an essential protein involved in

- kinetoplastid RNA metabolism that is associated with a novel multiprotein complex. *RNA* **14**: 970–980.
- Horváth, A., Horáková, E., Dunajčíková, P., Verner, Z., Pravdová, E., Šlapetová, I., et al. (2005) Downregulation of the nuclear-encoded subunits of the complexes III and IV disrupts their respective complexes but not complex I in procyclic *Trypanosoma brucei*. *Mol Microbiol* **58**: 116–130.
- Kakuta, Y., Horio, T., Takahashi, Y., and Fukuyama, K. (2001) Crystal structure of *Escherichia coli* Fdx, an adrenodoxin-type ferredoxin involved in the assembly of iron-sulfur clusters. *Biochemistry* **40**: 11007–11012.
- Kořený, L., Lukeš, J., and Oborník, M. (2010) Evolution of the haem synthetic pathway in kinetoplastid flagellates: an essential pathway that is not essential after all? *Int J Parasitol* **40**: 149–156.
- Lange, H., Kaut, A., Kispal, G., and Lill, R. (2000) A mitochondrial ferredoxin is essential for biogenesis of cellular iron-sulfur proteins. *Proc Natl Acad Sci USA* **97**: 1050–1055.
- Lartillot, N., Lepage, T., and Blanquart, S. (2009) PhyloBayes 3: a Bayesian software package for phylogenetic reconstruction and molecular dating. *Bioinformatics* **25**: 2286–2288.
- Li, J., Saxena, S., Pain, D., and Dancis, A. (2001) Adrenodoxin reductase homolog (Arh1p) of yeast mitochondria required for iron homeostasis. *J Biol Chem* **276**: 1503–1509.
- Lill, R. (2009) Function and biogenesis of iron-sulphur proteins. *Nature* **460**: 831–838.
- Long, S., Jirků, M., Ayala, F.J., and Lukeš, J. (2008) Mitochondrial localization of human frataxin is necessary but processing is not for rescuing frataxin deficiency in *Trypanosoma brucei*. *Proc Natl Acad Sci USA* **105**: 13468–13473.
- Long, S.J., Changmai, P., Tsaousis, A.D., Skalický, T., Verner, Z., Wen, Y.Z., et al. (2011) Stage-specific requirement for Isa1 and Isa2 proteins in the mitochondrion of *Trypanosoma brucei* and heterologous rescue by human and *Blasotocystis* orthologues. *Mol Microbiol* **81**: 1403–1418.
- Lukeš, J., Hashimi, H., and Ziková, A. (2005) Unexplained complexity of the mitochondrial genome and transcriptome in kinetoplastid flagellates. *Curr Genet* **48**: 277–299.
- Marchler-Bauer, A., Lu, S., Anderson, J.B., Chitsaz, F., Derbyshire, M.K., DeWeese-Scott, C., et al. (2011) CDD: a Conserved Domain Database for the functional annotation of proteins. *Nucleic Acids Res* **39**: 225–229.
- Miao, R., Holmes-Hampton, G., and Lindahl, P.A. (2011) Biophysical Investigation of the Iron in Aft1-1(up) and Gal-YAH1 *Saccharomyces cerevisiae*. *Biochemistry* **50**: 2660–2671.
- Michel, H., Behr, J., Harrenga, A., and Kannt, A. (1998) Cytochrome C oxidase: structure and spectroscopy. *Annu Rev Biophys Biomol Struct* **27**: 329–356.
- Moraes, C.T., Diaz, F., and Barrientos, A. (2004) Defects in the biosynthesis of mitochondrial heme c and heme a in yeast and mammals. *Biochim Biophys Acta Bioenerg* **1659**: 153–159.
- Mortenson, L.E., Carnahan, J.E., and Valentine, R.C. (1962) An electron transport factor from *Clostridium pasteurianum*. *Biochem Biophys Res Commun* **7**: 448–452.
- Mühlenhoff, U., Gerber, J., Richhardt, N., and Lill, R. (2003) Components involved in assembly and dislocation of iron-sulfur clusters on the scaffold protein Isu1p. *EMBO J* **22**: 4815–4825.
- Mühlenhoff, U., Gerl, M.J., Flauger, B., Pimer, H.M., Balsler, S., Richhardt, N., et al. (2007) The iron-sulfur cluster proteins Isa1 and Isa2 are required for the function but not for the *de novo* synthesis of the Fe/S clusters of biotin synthase in *Saccharomyces cerevisiae*. *Eukaryot Cell* **6**: 753–753.
- Netz, D.J.A., Stiith, C.M., Stumpfig, M., Kopf, G., Vogel, D., Genau, H.M., et al. (2012) Eukaryotic DNA polymerases require an iron-sulfur cluster for the formation of active complexes. *Nature Chem Biol* **8**: 125–132.
- Paris, Z., Changmai, P., Rubio, M.A., Ziková, A., Stuart, K.D., Alfonzo, J.D., and Lukeš, J. (2010) The Fe/S cluster assembly protein Isd11 is essential for tRNA thiolation in *Trypanosoma brucei*. *J Biol Chem* **285**: 22394–22402.
- Pfaffl, M.W. (2001) A new mathematical model for relative quantification in real-time RT-PCR. *Nucleic Acids Res* **29**: e45.
- Pierrel, F., Hamelin, O., Douki, T., Kieffer-Jaquinod, S., Mühlenhoff, U., Ozeir, M., et al. (2010) Involvement of mitochondrial ferredoxin and para-aminobenzoic acid in yeast coenzyme Q biosynthesis. *Chem Biol* **17**: 449–459.
- Pusnik, M., Charrière, F., Mäser, P., Waller, R.F., Dagley, M.J., Lithgow, T., and Schneider, A. (2009) The single mitochondrial porin of *Trypanosoma brucei* is the main metabolite transporter in the outer mitochondrial membrane. *Mol Biol Evol* **26**: 671–680.
- Py, B., and Barras, F. (2010) Building Fe-S proteins: bacterial strategies. *Nat Rev Microbiol* **8**: 436–446.
- Rouault, T.A. (2012) Biogenesis of iron-sulfur clusters in mammalian cells: new insights and relevance to human disease. *Dis Model Mech* **5**: 155–164.
- Saas, J., Ziegelbauer, K., von Haeseler, A., Fast, B., and Boshart, M. (2000) A developmentally regulated aconitase related to iron-regulatory protein-1 is localized in the cytoplasm and in the mitochondrion of *Trypanosoma brucei*. *J Biol Chem* **275**: 2745–2755.
- Schnauffer, A., Panigrahi, A.K., Panicucci, B., Igo, P., Wirtz, E., Salavati, R., and Stuart, K. (2001) An RNA ligase essential for RNA editing and survival of the bloodstream form of *Trypanosoma brucei*. *Science* **291**: 2159–2162.
- Schneider, A., Bursac, D., and Lithgow, T. (2008) The direct route: a simplified pathway for protein import into the mitochondrion of trypanosomes. *Trends Cell Biol* **18**: 12–18.
- Seeber, F. (2002) Eukaryotic genomes contain a [2Fe-2S] ferredoxin isoform with a conserved C-terminal sequence motif. *Trends Biochem Sci* **27**: 545–547.
- Sheftel, A.D., Stehling, O., Pierik, A.J., Elsasser, H.P., Mühlenhoff, U., Webert, H., et al. (2010) Humans possess two mitochondrial ferredoxins, Fdx1 and Fdx2, with distinct roles in steroidogenesis, heme, and Fe/S cluster biosynthesis. *Proc Natl Acad Sci USA* **107**: 11775–11780.
- Shi, Y.B., Ghosh, M.C., Tong, W.H., and Rouault, T.A. (2009) Human ISD11 is essential for both iron-sulfur cluster assembly and maintenance of normal cellular iron homeostasis. *Hum Mol Genet* **18**: 3014–3025.
- Shi, Y.B., Ghosh, M., Kovtunovych, G., Crooks, D.R., and Rouault, T.A. (2012) Both human ferredoxins 1 and 2 and ferredoxin reductase are important for iron-sulfur cluster

- biogenesis. *Biochim Biophys Acta Mol Cell Res* **1823**: 484–492.
- Singha, U.K., Hamilton, V., Duncan, M.R., Weems, E., Tripathi, M.K., and Chaudhuri, M. (2012) Protein translocase of mitochondrial inner membrane in *Trypanosoma brucei*. *J Biol Chem* **287**: 14480–14493.
- Smíd, O., Horáková, E., Vilimová, V., Hrdý, I., Cammack, R., Horváth, A., *et al.* (2006) Knock-downs of iron-sulfur cluster assembly proteins IscS and IscU down-regulate the active mitochondrion of procyclic *Trypanosoma brucei*. *J Biol Chem* **281**: 28679–28686.
- Stamatakis, A. (2006) RAxML-VI-HPC: maximum likelihood-based phylogenetic analyses with thousands of taxa and mixed models. *Bioinformatics* **22**: 2688–2690.
- Stemmler, T.L., Lesuisse, E., Pain, D., and Dancis, A. (2010) Frataxin and mitochondrial FeS cluster biogenesis. *J Biol Chem* **285**: 26737–26743.
- Sutak, R., Doležal, P., Fiumera, H.L., Hrdý, I., Dancis, A., Delgadillo-Correa, M., *et al.* (2004) Mitochondrial-type assembly of FeS centers in the hydrogenosomes of the amitochondriate eukaryote *Trichomonas vaginalis*. *Proc Natl Acad Sci USA* **101**: 10368–10373.
- Tielens, A.G., and Van Hellemond, J.J. (1998) The electron transport chain in anaerobically functioning eukaryotes. *Biochim Biophys Acta* **1365**: 71–78.
- Tokumoto, U., and Takahashi, Y. (2001) Genetic analysis of the *isc* operon in *Escherichia coli* involved in the biogenesis of cellular iron-sulfur protein. *J Biochem (Tokyo)* **130**: 63–71.
- Tovar, J., Leon-Avila, G., Sanchez, L.B., Šuták, R., Tachezy, J., van der Giezen, M., *et al.* (2003) Mitochondrial remnant organelles of *Giardia* function in iron-sulphur protein maturation. *Nature* **426**: 172–176.
- Tripodi, K.E., Menendez, S.M., and Cricco, J.A. (2011) Role of heme and heme-proteins in trypanosomatid essential metabolic pathways. *Enzyme Res* **2011**: 873230.
- Tsaousis, A.D., de Choudens, S.O., Gentekaki, E., Long, S.J., Gaston, D., Stechmann, A., *et al.* (2012) Evolution of Fe/S cluster biogenesis in the anaerobic parasite *Blastocystis*. *Proc Natl Acad Sci USA* **109**: 10426–10431.
- Vaňáčová, S., Rasoloson, D., Razga, J., Hrdý, I., Kulda, J., and Tachezy, J. (2001) Iron-induced changes in pyruvate metabolism of *Tritrichomonas foetus* and involvement of iron in expression of hydrogenosomal proteins. *Microbiology* **147**: 53–62.
- Vondrušková, E., van den Burg, J., Zíková, A., Ernst, N.L., Stuart, K., Benne, R., and Lukeš, J. (2005) RNA interference analyses suggest a transcript-specific regulatory role for mitochondrial RNA-binding proteins MRP1 and MRP2 in RNA editing and other RNA processing in *Trypanosoma brucei*. *J Biol Chem* **280**: 2429–2438.
- Wiedemann, N., Urzica, E., Guiard, B., Muller, H., Lohaus, C., Meyer, H.E., *et al.* (2006) Essential role of Isd11 in mitochondrial iron-sulfur cluster synthesis on Isu scaffold proteins. *EMBO J* **25**: 184–195.
- Žárský, V., Tachezy, J., and Doležal, P. (2012) Tom40 is likely common to all mitochondria. *Curr Biol* **22**: R479–R481.
- Zheng, L.M., White, R.H., Cash, V.L., Jack, R.F., and Dean, D.R. (1993) Cysteine desulfurase activity indicates a role for Nifs in metallocluster biosynthesis. *Proc Natl Acad Sci USA* **90**: 2754–2758.

Supporting information

Additional supporting information may be found in the online version of this article at the publisher's web-site.

3.4 Mitochondrial and nucleolar localization of cysteine desulfurase Nfs and the scaffold protein Isu in *Trypanosoma brucei*

(submitted to Eukaryotic Cell)

Mitochondrial and nucleolar localization of cysteine desulfurase Nfs and the scaffold protein Isu in *Trypanosoma brucei*

Julie Kovářová ^{*}, Eva Horáková, Piya Changmai, Marie Vancová and Julius Lukeš [#]

Biology Center, Institute of Parasitology, Czech Academy of Sciences and Faculty of Sciences, University of South Bohemia, České Budějovice (Budweis), Czech Republic

[#] To whom correspondence should be addressed: Institute of Parasitology, Branišovská 31, 37005 České Budějovice, Czech Republic; Tel: +420 38 777 5481; Fax: +420 38 531 0388; E-mail: jula@paru.cas.cz

Running Title: Fe-S cluster synthesis in bloodstream *T. brucei*

Keywords: mitochondrion; *Trypanosoma*; Fe-S cluster; bloodstream stage; cysteine desulfurase, scaffold protein

^{*} Present address: Institute of Infection, Immunity and Inflammation, College of Medical, Veterinary and Life Sciences, University of Glasgow, Glasgow, United Kingdom

ABSTRACT

Trypanosoma brucei has a complex life cycle during which its single mitochondrion is subject to major metabolic and morphological changes. While the procyclic stage (PS) of the insect vector contains a large and reticulated mitochondrion, its counterpart in the bloodstream stage (BS) parasitizing mammals is highly reduced and seems to be devoid of most functions. We show here that key Fe-S cluster assembly proteins are still present and active in this organelle, and produced clusters are incorporated into over-expressed enzymes. Importantly, the cysteine desulfurase Nfs, equipped with the nuclear localization signal, was detected in the nucleolus of both *T. brucei* life stages. The scaffold protein Isu, an interacting partner of Nfs, was also found to have a dual localization in the mitochondrion and the nucleolus, while frataxin and both ferredoxins are confined to the mitochondrion. Moreover, upon depletion of Isu, cytosolic tRNA thiolation dropped in the PS but not BS flagellates.

INTRODUCTION

Trypanosoma brucei is a protozoan parasite causing serious human African trypanosomiasis and related diseases in cattle, camels, water buffalos and horses. The bloodstream stage (BS) infects mammalian blood and subcutaneous tissues and is transmitted to another host via a tse-tse fly vector, where it prospers as the so-called procyclic stage (PS) (1). As an adaptation to the distinct host environments, these two major life stages differ significantly in their morphology and metabolism. One of the most striking differences between them rests in the single mitochondrion, which is large and reticulated in the PS, maintaining all canonical functions, whereas the same organelle in the BS is significantly reduced with only a few pathways detected so far. In order to recapitulate the situation, we bring here a short summary of known and verified mitochondrial pathways in the BS.

Out of all 14 mitochondrial-encoded genes, only subunit A6 of ATPase is translated and utilized in the BS as an indispensable part of the respiratory complex V, which is present and active, even though not fulfilling its standard function (2, 3). Hence, translation is indispensable (4, 5). Since the A6 transcript undergoes extensive RNA editing, the entire RNA processing machinery is active and essential in the BS as well (6, 7). In addition, since no tRNAs are encoded in the mitochondrial (kinetoplast; k) DNA, their import from the cytosol and modifications are mandatory for mitochondrial translation (4, 8). Ultimately, the import of hundreds of nuclear-encoded mitochondrial proteins involved in protein import and processing, kDNA replication and maintenance, kRNA transcription and processing, as well as translation are indispensable in the BS (3, 4, 9, 10). In contrast to a typical mitochondrion, the BS organelle does not serve as the main energy source. Instead of the canonical respiratory chain, glycerol-3-phosphate dehydrogenase supplies electrons to trypanosome alternative oxidase as a terminal electron acceptor (11). While cytochrome *c*-dependent respiratory complexes III and IV are altogether missing from the BS, complex II probably remains active. Moreover, complex I is expressed, yet its enzymatic activity is not significant and its real function remains elusive (12–15). Complex V (ATP synthase) is present, but its F1 part rotates in reverse direction, as compared to the PS, cleaving ATP and pumping H⁺ out of the mitochondrion in order to create membrane potential required for protein import (2).

The efficiency of fatty acids synthesis in the BS organelle via type II pathway is unclear, since its main product, lipoic acid, is present only in a very low amount and there is no apparent usage for it (16), although, its down-regulation caused defects in the kDNA segregation (17). Furthermore, the degradation of fatty acids was transferred from the mitochondrion into the glycosomes in all trypanosomatid flagellates (15).

In most eukaryotic cells, mitochondria have a central role in Ca^{2+} homeostasis, yet in trypanosomes this key role is questionable due to the presence of acidocalcisomes (15, 18). Although the mitochondrial calcium uniporter is present in both stages (19), its role in the BS mitochondrion, devoid of citric acid cycle and respiratory chain, remains elusive (15, 19, 20). On the other hand, K^+ ion homeostasis is essential for the mitochondrion and subsequently for the whole cell (20). Other typical mitochondrial functions such as citric acid cycle, urea cycle, role in apoptosis, biosynthesis of ubiquinol and heme are likely absent from the reduced BS mitochondrion (3, 15, 21–23).

Finally, all mitochondria studied so far harbor biosynthesis of Fe-S clusters, ubiquitous and very ancient enzymatic cofactors (24). Their capacity to transfer electrons is used in complexes I thru III of the respiratory chain or metabolic enzymes such as aconitase, fumarase and lipoate synthase (25, 26). In addition, Fe-S clusters are utilized in iron metabolism, serve in DNA replication and have structural or other functions (25). These cofactors are synthesized via a complex pathway composed of more than twenty enzymes, and as detailed below, most of them are present in *T. brucei* (27–31).

Cysteine desulfurase (Nfs) abstracts sulfur from cysteine producing alanine, while ferredoxin provides electrons obtained from NADH by ferredoxin reductase (24). Frataxin is supposed to supply an iron atom, however, this role has still not been convincingly confirmed (26, 32, 33). The assembly of a new Fe-S cluster occurs on a large protein complex composed of Nfs, its indispensable interacting partner Isd11 and a scaffold protein Isu (24). In mammals, frataxin is also present in this complex (34), yet this was not confirmed for trypanosomes (27). The newly formed cofactors are transferred by numerous chaperons and scaffold proteins, which either transfer them to the mitochondrial apoproteins or export a so far unknown intermediate

from the organelle, where it is further processed and exploited for the cytosolic and nuclear Fe-S dependent proteins (24–26).

Most key components of the mitochondrial Fe-S biosynthetic pathway are essential for the PS of *T. brucei*. RNAi depletion of Nfs, Isd11, Isu, Isa1, Isa2, and frataxin resulted in serious growth phenotypes, decrease in the activity of several Fe-S enzymes and other downstream effects (27–29, 31, 35). In addition, Nfs and Isd11 are also indispensable for tRNA thiolation (27). Two homologues of electron donor protein ferredoxin were identified in the genomes of trypanosomatid flagellates, but only ferredoxin A is essential for the Fe-S cluster assembly (31).

However, no functional data is available on this pathway in the BS other than that the level of its components is much lower as compared to the PS, as was so far shown for frataxin (35), Isd11 (27), ferredoxin (31) and Isa1 and Isa2 (29). In general, the (in)dispensability of Fe-S machinery in the BS mitochondrion is questionable, since the bulk of Fe-S clusters produced in the organelle of a typical eukaryotic cell are utilized for its respiratory chain complexes, which are either repressed or absent in this life stage of *T. brucei*. To the best of our knowledge, the only Fe-S dependent proteins still expressed are ferredoxin and glutaredoxin 1, and both are involved in the Fe-S pathway itself (31, 36), which implies they are present only in a very low amount and pose the problem of ‘chicken-egg’ situation. Moreover, there is Fe-S dependent lipoic acid synthetase but, as mentioned above, the relevance of lipoic acid synthesis for the BS remains to be established (16, 17).

We scrutinized the localization of three core Fe-S assembly components, Nfs, Isu and frataxin, using cell lines with tagged proteins and examined them by immunofluorescent microscopy, digitonin fractionation followed by Western blot analysis and electron microscopy. We were able to show that these proteins are located in the mitochondrion, yet in the case of Nfs and Isu, a substantial amount was detected in the nucleolus, suggesting that cysteine desulfurase

with its scaffold protein must have a so far unknown function in this cell compartment. Since there is no detectable activity of the Fe-S dependent enzymes aconitase and fumarase in the BS, we created cell lines overexpressing these marker Fe-S enzymes, which enabled us to verify that Fe-S proteins are produced in this unusual organelle and are capable of fulfilling their standard functions.

MATERIALS AND METHODS

Preparation of pT7-v5 constructs

Gene constructs with Nfs (Tb927.7.890), Isu (Tb927.4.4980) and frataxin (Tb927.3.1000) ORFs lacking stop codons, followed by v5 or HA₃ tags were prepared using the following primer pairs:

Nfs-v5-FP (5' GGAAGCTTATGTTTAGTGGTGTTCGCGTAC) and

Nfs-v5-RP (5' TTAGATCTCCGCCACTCCACGTCTTTAAGG);

Isu-v5-FP (5' AGGAAAGCTTATGCGGCGACTGATATCATC) and

Isu-v5-RP (5' AGGGATCCGCTTGACACCTCACC);

Frat HA FP- (5' ATAAAAGCTTATGCGGCGCACATGTTGCGC) and

Frat HA RP- (5' AGACTCGAGTTCGGTTTCTCCAGCCCCTG)

(added *Bam*HI and *Hind*III restriction sites are underlined).

PCR products amplified from the total genomic DNA of *T. brucei* PS 29-13 strain were cloned into pT7-v5 or pT7-HA₃ vectors and verified by sequencing. The obtained constructs were linearized by *Not*I, electroporated into the parental PS 29-13 cells and the single-marker BS cells, the transfected cell lines were selected using puromycin (1 µg/ml) and expression of the tagged protein was induced by the addition of tetracycline (1 µg/ml). Cell line expressing the v5-tagged ferredoxin A was described elsewhere (31).

Immunofluorescence assay

Approximately 1×10^7 PS or BS cells were collected, centrifuged, resuspended in fresh medium and stained with 200 nM or 20 nM, respectively, of the mitochondrion-selective dye Mitotracker Red (Invitrogen). After 30 min incubation at 27 °C or 37 °C, the cells were centrifuged for 5 min at $1,300 \times g$ at room temperature, the pellet was washed and resuspended in 1 ml phosphate buffered saline (PBS) with 4 % formaldehyde and 1.25 mM NaOH. The suspension (250 μ l) was applied to a microscopic slide and incubated for 10 min at room temperature. The slides were washed with PBS, incubated in ice-cold methanol for an additional 20 min and briefly washed with PBS. Next, primary anti-v5 or anti-HA₃ antibodies (Invitrogen) were added at 1:100 dilution in PBS-Tween (0.05 %) with 5 % milk and incubated at 4 °C overnight. Slides were washed with PBS prior to the application of Alexa Fluor® 488 goat anti-mouse IgG (Molecular Probes) at 1:1,000 dilution for 1hr at room temperature. Finally, the samples were mounted with Antifade reagent with DAPI (Invitrogen) and after incubation in the dark for 30 min were visualized using an Axioplan2 imaging fluorescent microscope (Zeiss).

Digitonin fractionation and Western blot analysis

In order to compare protein expression in the PS versus BS, cell lysates corresponding to 5×10^6 cells per lane were separated on a 12 % SDS-polyacrylamide gel, transferred to a PVDF membrane and probed with different antibodies: chicken anti-Nfs, rat anti-Isu and anti-enolase polyclonal antibodies were used at 1:1,000, 1:1,000 and 1:50,000 dilutions, respectively, followed by appropriate secondary antibodies conjugated with horseradish peroxidase (Sigma), and then visualized using the Pierce ECL kit (Thermo Scientific).

For the digitonin fractionation, 10^7 cells per sample were collected, incubated in STE-NaCl buffer with 0.04, 0.16, 0.32, 0.4, 0.8 and 1.2 mM digitonin, respectively, for 4 min at 27 °C.

Subsequently, samples were centrifuged ($16,000 \times g$ for 2 min) and obtained supernatants were used for Western blot analysis. For decorating of tagged proteins, monoclonal anti-mouse antibody (Sigma) was used at 1:2,000 dilution. As controls, antibodies against the following proteins were used: outer mitochondrial membrane protein VDAC (37), mitochondrial intermembrane sulfhydryl oxidase (38), mitochondrial matrix protein MRP2 (39), nuclear protein La (40), glycosomal triosephosphate isomerase TIM424 and cytosolic enolase (both provided by Paul A. M. Michels).

Electron microscopy

Cells were fixed either with 4 % formaldehyde or 4 % formaldehyde with 0.1 % glutaraldehyde in 0.1 M sodium phosphate buffer, pH 7.2, for 1 hr at room temperature. After centrifugation at $1,300 \times g$ for 10 min, cells were washed three times in 0.1 M phosphate buffer containing 0.01 M glycine. The pellet was resuspended in 10 % gelatin dissolved in water at 37 °C, centrifuged and solidified on ice. Slices of gelatin-embedded pellet were immersed in 2.3 M sucrose and left for 6 days on a rotating wheel at 4 °C. Infiltrated samples were immersed in liquid nitrogen and cryosectioned using ultramicrotome Leica EM FCS (Leica) equipped with cryochamber (UCT, Leica) at -100 °C. Cryosections were picked up using a mixture of 1 % methyl cellulose and 1.15 M sucrose and thawed in PBS. Grids were placed on drops of blocking solution containing 5 % low fat milk and 0.02 M glycine in PBS for 2 hrs. Antibody against v5-tag was diluted 1:10 in blocking solution and left overnight at 4 °C. Grids were washed in blocking solution, diluted 1:10 in PBS, and transferred to drops of goat anti-mouse IgG conjugated to 10 nm gold particles (Aurion) diluted 1:40 in blocking solution for 1 hr. Grids were then washed in PBS, distilled water, contrasted and dried using 2 % methyl cellulose with 3 % aqueous uranyl acetate solution

diluted at 9:1. Sections were examined in 80 kV JEOL 1010 and 200 kV 2100F transmission electron microscopes.

Quantification of gold labeling

Electron micrographs of randomly selected areas were taken at the same magnification. Using ImageJ software, points at constant distance 1 nm were applied and counted for each compartments. Observed densities of labeling (LD_{obs}) were expressed for each compartment separately as sum of gold particles per sum of points. In order to statistically evaluate labeling of individual compartments, total expected numbers of gold particles for each compartment were calculated as total expected density (all gold particles divided by total counts of hits; total LD_{exp}) multiplied by total counts of points of each cell line. Chi-squared test was calculated as $(LD_{obs} - LD_{exp})^2 / LD_{exp}$. The relative labeling index (RLI) was counted for each compartments as ratio of values of labeling density observed and labeling density expected (41).

RNAi construct, transfection, cloning, RNAi induction and cultivation

To prepare Isu (Tb927.4.4980) RNAi construct, fragment of Isu ORF was amplified using primer pairs IscU-F1 (5-CACCTCGAGCAGCCTCACTTCGGTCACT) and IscU-R1 (5-TGCACGGATCCCCAACAGCCTCGGACTTAG) from total genomic DNA of *T. brucei* PS 29-13 strain. Amplicon was cloned into the p2T7-177 vector which was, upon *NotI*-mediated linearization, introduced into the BS *T. brucei* single-marker cells using a BTX electroporator and selected as described elsewhere (42). The BS trypanosomes were cultivated in HMI-9 medium at 37 °C in the presence of G418 (2.5 µg/ml) and phleomycin (2.5 µg/ml). RNAi was initiated by the addition of 1 µg/ml tetracycline to the medium and growth measurements were made using the Beckman Z2 Coulter counter.

tRNA thiolation assay

Total and mitochondrial RNA was electrophoretically separated on 8 M urea 8 % acrylamide gels cast with 50 μ M [(*N*-acryloylamino)-phenyl] mercuric chloride (APM). The samples were denatured by heating at 72 °C for 2 min and equal amounts (10 μ g) of RNA were loaded per lane. After electrophoresis the gels were stained with ethidium bromide for visualization under UV light, soaked in Tris/Borate/EDTA (TBE) buffer containing 200 μ M β -mercaptoethanol and blotted onto a Zetaprobe membrane (BioRad) for Northern blot analysis. The hydrogen peroxide treatment was carried out as a non-thiolated control as described elsewhere (27).

Expression and measurement of aconitase and fumarase in BS

The ORFs of fumarase (Tb927.3.4500) and aconitase (Tb927.10.14000) were PCR amplified from the total genomic DNA of *T. brucei* PS 29-13 strain using the primer pairs TbAco-FW (GGGTCTAGAATGCTCAGCACGATGAAGTT) and TbAco-RV (GCGCTCGAGCTACTACAAATTACCCTTGAT) (added *Xba*I and *Xho*I restriction sites are underlined), Tbcy-Fum-FW (AGGAAAGCTTATGAGTCTCTGCGAAAACTG) and Tbcy-Fum-RV (ATATCTAGAGACGAGTTTAGCATAGAA) (added *Bam*HI and *Hind*III restriction sites are underlined) and the PCR products were cloned into pT7-v5 vector. The obtained vectors were linearized by *Not*I and electroporated into BS *T. brucei* single-marker cells using the Amaxa Nucleofector II electroporator, with puromycin (1 μ g/ml) used as a selectable marker. Expression of the ectopic proteins was induced by the addition of 1 μ g/ml tetracycline.

Cytosolic and mitochondrial fractions were obtained by digitonin fractionation following the protocol described elsewhere (28). The aconitase and fumarase activities were measured

spectrophotometrically at 240 nm as the production rate of *cis*-aconitase and fumarate, respectively. L-Malic acid (Serva) and DL-Isocitric acid trisodium salt hydrate (Sigma) were used as substrates of the aconitase and fumarase activity assays, respectively, as described previously (35).

RESULTS

Nfs contains nuclear localization signal

The cysteine desulfurase Nfs is a common mitochondrial protein found in almost all eukaryotes. An alignment of protein sequences of nine species from different eukaryotic supergroups revealed high conservation of key domains (Fig. S1). A nuclear localization signal RRRPR was determined in the *Saccharomyces cerevisiae* Nfs protein sequence (43), which is also present in the *T. brucei* sequence (Fig. 1). Even though nuclear targeting sequence in trypanosomes was described only in a few cases (44–48), and no consensus sequence was defined so far, the general rules postulating high content of positively charged amino acids such as arginine, seems to be universal. Thus, we expect the sequence RRRPR to function as a nuclear targeting signal in *T. brucei* as well. Moreover, the alignment showed absolute conservation of this motif in six out of nine compared eukaryotes, including human, with positively charged residues predominating in all aligned putative nuclear targeting signals (Fig. 1).

Fe-S assembly proteins are present in the BS mitochondrion

In order to establish localization of the Fe-S assembly machinery in the BS, we created cell lines overexpressing tagged versions of Nfs, Isu and frataxin. Each of these genes was cloned into the pT7-v5 vector and the obtained constructs were separately electroporated into the BS *T. brucei*. Since such an approach may cause non-physiologically high expression of the tagged proteins

resulting in possible misslocalization within the cell, we transfected the same constructs also into the PS cells, where these proteins are known to localize to the mitochondrion (27, 28, 30). Upon decoration with monoclonal anti-v5 antibody and examination by immunofluorescent microscopy, in both the PS and BS trypanosomes expressing the v5-tagged Nfs, the signal was confined exclusively to the mitochondrion (Fig. 2A, B).

The same approach was used to detect the Isu protein in both life stages. Indeed, the fluorescent signal corresponded to the large reticulated or dwindled sausage-shaped mitochondrion of the PS and BS cells, respectively (Fig. 2D, E). In order to eliminate potential artifacts caused by the v5-tagging strategy, an additional cell line was produced containing a HA₃-tagged Isu. As with the other tag, the monoclonal anti- HA antibody decorated again solely the mitochondrion (Fig. 2C). Frataxin, the presumed iron donor for Fe-S clusters, was functionally analyzed in the PS (35), but not in the BS *T.brucei*. Therefore, we created a BS cell line expressing frataxin with added HA₃ tag and showed by immunofluorescent microscopy its localization in the reduced mitochondrion of this life stage (Fig. 2F).

Digitonin fractionation reveals dual localization of Nfs

An alternative approach to interrogate intracellular localization of a target protein is treatment of cells with the detergent digitonin that disrupts phospholipid membranes and allows to distinguish between subcellular compartments. For each cell line, subcellular fractions were obtained using increasing concentrations of digitonin (0.04 – 1.2 mM). As shown by Western blot analyses, the mitochondrial proteins were released only when 0.8 mM or higher concentration of digitonin was used. All fractions were also treated with antibodies against the following control proteins: i/ voltage dependent anion channel (VDAC) of the outer mitochondrial membrane (37); ii/ sulfhydryl oxidase Erv1 of the intermembrane space (38); iii/ mitochondrial RNA-binding protein

MRP2 present in the mitochondrial matrix (39); iv/ glycosomal triose-phosphate isomerase (TIM424); v/ nuclear protein La (40) and finally, vi/ cytosolic enolase.

Using the Nfs-v5 expressing cells, the signal acquired with anti-v5 antibody differed from the pattern obtained with antibodies against the available mitochondrial markers (Fig. 3). Substantial fraction of the v5 signal was consistent with much earlier release of the tagged Nfs protein, suggesting localization also outside of the double membrane-bound mitochondrion. Identical result was obtained when the specific anti-*T. brucei* Nfs antibody was used (data not shown). Although in both PS and BS cells the target protein was detected in overlapping fractions, much stronger signal was present in the last two PS fractions, strongly suggesting that in this life stage the majority of the Nfs protein is located in the mitochondrion. However, in the BS the extra-mitochondrial signal was as strong as the organellar one (Fig. 3).

Western blot analysis of the PS lysates expressing the v5-tagged Isu revealed two separate bands, even though a monoclonal anti-v5 antibody was used (Fig. 3). Since the upper band corresponds to the double size of the lower band, we interpret these bands as Isu dimer and monomer, respectively. Dimerization of components of the Fe-S assembly machinery was described for the mammalian cells (49) and apparently the complex was not effectively separated under the used polyacrylamide gel conditions. Strong signal of the 50 kDa band is present in the mitochondrial fractions, while much weaker, yet distinct signal in other fractions suggests the presence of Isu in additional subcellular compartments. The weak 25 kDa is confined to the mitochondrial fractions (Fig. 3).

Finally, the BS cells containing HA₃-tagged frataxin were analyzed by digitonin fractionation. The results were fully consistent with localization solely in the mitochondrial matrix (Fig. 3), which is in agreement with the data from the PS flagellates (30). Taken together,

these results strongly indicate that Nfs and Isu are localized predominantly in the mitochondrion, but also in an additional subcellular compartment, possibly the nucleus.

Nfs and Isu are also present in the nucleolus

Next, we subjected the tagged cell lines to immunostaining with colloidal gold-labelled antibodies followed by transmission electron microscopy. This sensitive approach confirmed the presence of Nfs in the mitochondrion and the nucleolus of both the PS (Fig. 4A- C) and BS (Fig. 4G, H) *T. brucei*. Nfs was detected in the mitochondrial lumen, with most signal present in the vicinity of the kDNA disk, and the nucleolus (Fig. 5). The same approach was applied to the PS cells expressing v5-tagged Isu, ferredoxin A and ferredoxin B. Similarly, Isu was detected in the mitochondrial lumen and in the nucleolus (Figs. 4D-F, 5, S2). In contrast, ferredoxin A and ferredoxin B were present solely in the mitochondrion with only a slight enrichment in the region around the kDNA (Figs. 4I, 5, S2).

Observed and expected counts of gold particles were compared in order to distinguish preferential labeling ($RLI > 1$) from the random one ($RLI = 1$) and the data was examined using chi-squared (χ^2) analysis (Table S1). We calculated partial (for each compartment and cell line) and total χ^2 values (sum of partials) to test the null hypothesis (no difference between distributions). Values of partial χ^2 indicate responsibility of these compartments for the difference (preferential versus random distribution). Proportions of observed labeling densities over the mitochondria, nuclei and nucleoli are summarized in Fig. 5. Thorough analysis of formaldehyde-fixed cryosections confirmed that Nfs and Isu are localized in the nucleolus, while in their dual presence in the mitochondrion only the former protein is significantly enriched in the

vicinity of the kDNA disk. On the contrary, both ferredoxins are confined to the mitochondrion (Fig. 5, S2).

Fe-S cluster assembly is an essential function of the BS mitochondrion

With regards to the differences between the large reticulated versus the reduced sausage-shaped mitochondria of the two life stages, it is not surprising that in the BS *T. brucei*, frataxin (35), ferredoxin A (31) and Isa1 and Isa2 proteins (29) are significantly less abundant than in the PS trypanosomes. The situation is very similar in the cases of Nfs and Isu, which are decreased two and five times, respectively, in the mammalian BS as compared to the insect-dwelling PS (Fig. 6A).

Importantly, the significance of the Fe-S cluster assembly in the disease-causing BS has not been established thus far. In order to address this issue, a BS Isu RNAi cell line was constructed, where the depletion of Isu resulted in a severe growth phenotype (Fig. 6B). The efficiency of RNAi-mediated ablation of the target protein was confirmed by Western blot analysis (Fig. 6B; inset). Since except for its scaffold role in the Fe-S cluster synthesis, no other function is known for the Isu protein, we resorted to test its possible function in tRNA thiolation (see below).

Cytosolic thiolation is downregulated in Isu PS but not in BS knock downs

Since Isu is a binding partner of Nfs, which in *T. brucei* is also known as a source of sulfur for tRNA thiolation (27), we decided to study its potential role in this process as well. To our surprise the thiolation of several cytosolic tRNAs remained unaltered upon the ablation of Isu in the BS (Fig. 7A). Therefore, we decided to study the modification also in the PS Isu RNAi knock downs, which was previously generated in our lab (28). Contrary to the BS data, thiolation is very

sensitive to the loss of Isu with apparent phenotype showing up already two days after RNAi induction (Fig. 7B). It is known that this tRNA modification and tRNA import are used equally in both life cycle stages (4), meaning that the resulting growth inhibition in the BS depleted for Isu is most likely a consequence of a perturbation of the Fe-S synthesis pathway rather than tRNA thiolation.

Fe-S cluster assembly is active in the BS

Finally, we addressed the question whether the Fe-S assembly pathway is complete and active in the highly reduced BS mitochondrion. A standard approach of scrutinizing the availability of the Fe-S clusters is the activity assay for the Fe-S-containing metabolic enzymes aconitase and fumarase. As in other eukaryotes, this method is suitable for the PS (27, 29, 31), but activities of both enzymes are undetectable in the wild-type BS (Fig. 8A, B). To overcome this lack of measurable Fe-S-dependent activities in BS, we created BS cell lines overexpressing either fumarase or aconitase from a pT7-v5 vector. Upon induction with tetracycline, aconitase or the cytosolic form of fumarase were strongly expressed and the relevant activity was measured in a given cell compartment. In all cases, a strong activity of the overexpressed enzyme, almost reaching its level in the PS, was obtained (Fig. 8A, B). Separate measurement of the aconitase activity in either the cytosol or the mitochondrion confirmed that the Fe-S clusters are available in both compartments (Fig. 8B). These results confirm that the whole Fe-S synthetic pathway is not only present but indeed active in the BS and that the functional cofactors are available in both the organelle and the cytosol.

DISCUSSION

Combined, the data provide a comprehensive overview of the Fe-S assembly machinery in the BS *T. brucei*. We focused at its key components, namely the cysteine desulfurase Nfs, the scaffold protein Isu and frataxin. Several lines of evidence are consistent with the conclusion that even in the highly suppressed BS mitochondrion, the Fe-S clusters are efficiently build, regardless of the low abundance of the following proteins. Importantly, Nfs and Isu are also present in the nucleolus, while frataxin and both ferredoxins were detected solely in the mitochondrion.

It was of interest to thoroughly examine the subcellular localization of Nfs, Isu and frataxin proteins in the BS *T. brucei*. Indeed, Nfs has a dual localization in the mitochondrion and the nucleolus, which is in line with the results obtained from yeast (50, 51). The same dual localization was demonstrated for Isu, but unlike Nfs, no nuclear localization signal can be detected in the Isu sequence. However, noncanonical and bipartite nuclear localization signals were reported from trypanosomes, which are notoriously difficult to determine (45). Furthermore, in yeast Nfs is first imported into the mitochondrion and only afterwards transferred to the nucleus (43). The possibility that the whole protein complex is formed in the mitochondrion and only subsequently imported into the nucleolus, the nuclear localization signal of Nfs being responsible for such targeting, has to be tested.

As we showed previously, same as in other eukaryotes, in *T. brucei*, Isd11 is a partner of the Nfs, which participates in both Fe-S biosynthesis and tRNA thiolation (27). Mimicking the situation in the mitochondrion, a functional complex of Nfs, Isd11 and Isu may also be formed in the nucleolus in order to effectively abstract sulfur from cysteine and exploit it for a different use than incorporation into the Fe-S clusters. In contrast to mammals (34), trypanosomes do not appear to have frataxin as part of this complex (27), and the protein is strictly detected in the mitochondrion (30, this work).

To the best of our knowledge, here we provide first direct evidence of localization of Nfs and Isu in the nucleolus. Both Western blot analysis and transmission electron microscopy showed that the bulk of these proteins is present in the mitochondrion as compared to the nucleolus, due to which similar dual localization may have got overlooked in other organisms. In yeast, it was detected by means of α -complementation assay (43), which is highly sensitive, but is hardly applicable in other eukaryotes. In fact, a signal in the nucleolus of *T. brucei* was undetectable by immunofluorescence, although this may be due to technical reasons, such as the nucleolar localization being masked in the PS by the extensively reticulated mitochondrion. Another reason may be a limited penetration of the specific antibody into the nucleus during the applied staining protocol.

While function of the mitochondrial Nfs is well known, we know close to nothing about its nucleolar version. It is apparently essential, since mutation of its nuclear localization signal caused a severe growth phenotype in yeast, yet depletion of the nuclear Nfs did not affect maturation of the Fe-S containing proteins neither in the mitochondrion, nor in the nucleus (50, 51). The authors consequently predicted that the nuclear Nfs must be involved in tRNA thiolation. However, this possibility was excluded by showing that Nfs lacking mitochondrial targeting sequence cannot complement thiolation of both the cytosolic and mitochondrial tRNAs (52). In mammalian cells, Nfs was also detected in the cytosol (49) and was shown to be involved in the biosynthesis of the molybdenum co-factor (53). We can speculate that such a role may be also attributed to the mitochondrial Nfs in the studied protist, since the molybdenum co-factor synthetase of *T. brucei* (Tb11.01.3750) has, according to Mitoprot (54), 0.99 probability of mitochondrial localization.

Interestingly, a role in phosphorothioation was recently proposed for bacterial Nfs (55). This DNA modification is unique in directly altering the DNA backbone by exchanging oxygen

of phosphate for sulfur (56–58). Phosphorothioation seems to be widespread among diverse bacteria, but data about its presence in eukaryotes is lacking (56). While the DNA of *E. coli* depleted for IscS (bacterial homolog of Nfs) is broken into a characteristic smear (55), exactly the same experiment performed in wild type and Nfs-depleted *T. brucei* did not result in a DNA degradation phenotype (Fig. S3).

It is of interest to note that almost half of the mitochondrial Nfs is situated in or around the kDNA disk, which is located right next to the basal body of the single flagellum. The remaining signal was more or less evenly distributed throughout the lumen of the reticulated organelle, while Isu and both ferredoxins did not show similarly skewed distribution. This indicates possible association of a fraction of Nfs with the mitochondrial DNA. Since the nuclear localization signal must be evolutionary ancient, as it is carried by the family of Nfs-related cysteine desulfurases throughout the eukaryotic domain, the so far elusive nucleolar function is also likely to be ancestral.

Although the current paradigm postulates that the Fe-S clusters are in some form essential for every extant eukaryotic cell (24, 25), we wondered whether the mitochondrial branch of the Fe-S assembly pathway is producing clusters in the BS organelle, which uniquely lacks respiratory complexes. The only components of the Fe-S biosynthetic pathway studied so far in the BS are the scaffold proteins Isa1 and Isa2, which are dispensable in this stage in contrast to the PS (29). Nevertheless, they were shown to function as scaffolds for the synthesis of only 4Fe-4S clusters (59), thus their dispensability in the reduced organelle is not surprising.

Since the Fe-S cluster assembly was detected in the mitochondrion-derived mitosomes and hydrogenosomes of *Giardia* and *Entamoeba*, respectively (60, 61), it was anticipated that it is also active in the highly functionally down-regulated mitochondrion of African trypanosomes. Genes encoding components of this ancestral α -proteobacterial pathway were in the course of

evolution transferred into the nucleus and retargeted to the organelle via acquired mitochondrial localization signals (62). Retention of the Fe-S cluster assembly in the hydrogenosomes is meaningful since they possess an alternative pathway producing acetyl-CoA and hydrogen (61), and three enzymes involved in this pathway contain Fe-S clusters. The essentiality of Isu and the measured activities of over-expressed aconitase and fumarase provide evidence that these ancient clusters are made in the repressed organelle of the BS *T. brucei*.

In the BS mitochondrion, these cofactors may be incorporated into the non-essential respiratory complexes I and II (12), as well as ferredoxin, glutaredoxin and lipoate synthase, all of which are expressed at a very low level, however (31, 63). Therefore, we propose that in this life cycle stage the bulk of cofactors is exported outside of the mitochondrion, where in these fast dividing parasites a high demand for them exists in the catalytic subunits of DNA polymerases (25) and other cytosolic and nuclear proteins.

In conclusion, all the presented results indicate that the key components of the Fe-S biosynthetic pathway are present in the minimalistic mitochondrion of the BS *T. brucei*, where they are essential and produce functional cofactors, even though the demand for Fe-S clusters within this organelle is significantly lower than in the PS mitochondrion. In addition we have shown that a significant fraction of Nfs and Isu is present in the nucleolus. Nonetheless, their role in this compartment remains elusive, since all so far tested putative functions, such as Fe-S cluster synthesis (50), tRNA thiolation (52), and phosphorothioation of DNA (this work) provided negative results.

ACKNOWLEDGEMENTS

We thank Shaojun Long (Washington University, St. Louis) and De-Hua Lai (Sun Yat-Sen University, Guanqzhou, China) for their contribution in the early stages of this project, and Hassan Hashimi for helpful discussions. We also thank Paul A. M. Michels (Universidad de los Andes, Mérida/University of Edinburgh, Edinburgh) and André Schneider (University of Bern, Bern) for sharing antibodies.

This work was supported by the Czech Grant Agency P305/11/2179, the Bioglobe grant CZ.1.07/2.3.00/30.0032, the AMVIS LH12104 grant and the Praemium Academiae award to J. L., who is also a Fellow of the Canadian Institute for Advanced Research.

REFERENCES

1. **Fenn K, Matthews KR.** 2007. The cell biology of *Trypanosoma brucei* differentiation. *Curr. Opin. Microbiol.* **10**:539–46.
2. **Schnauffer A, Clark-Walker GD, Steinberg AG, Stuart K.** 2005. The F1-ATP synthase complex in bloodstream stage trypanosomes has an unusual and essential function. *EMBO J.* **24**:4029–40.
3. **Schnauffer A, Domingo GJ, Stuart K.** 2002. Natural and induced dyskinetoplastic trypanosomatids: how to live without mitochondrial DNA. *Int. J. Parasitol.* **32**:1071–84.
4. **Cristodero M, Seebeck T, Schneider A.** 2010. Mitochondrial translation is essential in bloodstream forms of *Trypanosoma brucei*. *Mol. Microbiol.* **78**:757–69.
5. **Alfonzo JD, Lukeš J.** 2011. Assembling Fe/S-clusters and modifying tRNAs: ancient co-factors meet ancient adaptors. *Trends Parasitol.* **27**:235–8.
6. **Halbig K, Nova-Ocampo MDE, Cruz-Reyes J.** 2004. Complete cycles of bloodstream trypanosome RNA editing *in vitro*. *RNA* **10**: 914–20.

7. **Kafková L, Ammerman ML, Faktorová D, Fisk JC, Zimmer SL, Sobotka R, Read LK, Lukeš J, Hashimi H.** 2012. Functional characterization of two paralogs that are novel RNA binding proteins influencing mitochondrial transcripts of *Trypanosoma brucei*. *RNA* **18**:1846–61.
8. **Schneider A, Martin JAY, Agabian N.** 1994. A nuclear encoded tRNA of *Trypanosoma brucei* is imported into mitochondria. *Mol. Cell. Biol.* **14**:2317–22.
9. **Schneider A.** 2001. Unique aspects of mitochondrial biogenesis in trypanosomatids. *Int. J. Parasitol.* **31**:1403–15.
10. **Lukeš J, Archibald JM, Keeling PJ, Doolittle WF, Gray MW.** 2011. How a neutral evolutionary ratchet can build cellular complexity. *IUBMB Life* **63**:528–37.
11. **Chaudhuri M, Ott RD, Hill GC.** 2006. Trypanosome alternative oxidase: from molecule to function. *Trends Parasitol.* **22**:484–91.
12. **Surve S, Heestand M, Panicucci B, Schnauffer A, Parsons M.** 2012. Enigmatic presence of mitochondrial complex I in *Trypanosoma brucei* bloodstream forms. *Eukaryot. Cell* **11**:183–93.
13. **Timms MW, Deursen FJ Van, Hendriks EF, Matthews KR.** 2002. Mitochondrial development during life cycle differentiation of African trypanosomes : Evidence for a kinetoplast-dependent differentiation control point. *Mol. Biol. Cell.* **13**:3747–59.
14. **Tasker M, Timms M, Hendriks E, Matthews K.** 2001. Cytochrome oxidase subunit VI of *Trypanosoma brucei* is imported without a cleaved presequence and is developmentally regulated at both RNA and protein levels. *Mol. Microbiol.* **39**:272–85.
15. **Hannaert V, Bringaud F, Opperdoes FR, Michels PAM.** 2003. Evolution of energy metabolism and its compartmentation in Kinetoplastida. *Kinetopl. Biol. Dis.* **30**:1–30.

16. **Stephens JL, Lee SH, Paul KS, Englund PT.** 2007. Mitochondrial fatty acid synthesis in *Trypanosoma brucei*. *J. Biol. Chem.* **282**:4427–36.
17. **Clayton AM, Guler JL, Povelones ML, Gluenz E, Gull K, Smith TK, Jensen RE, Englund PT.** 2011. Depletion of mitochondrial acyl carrier protein in bloodstream-form *Trypanosoma brucei* causes a kinetoplast segregation defect. *Eukaryot. Cell* **10**:286–92.
18. **Xiong Z, Ridgley EL, Enis D, Olness F, Ruben L.** 1997. Selective transfer of calcium from an acidic compartment to the mitochondrion of *Trypanosoma brucei*. *J. Biol. Chem.* **272**:31022–8.
19. **Vercesi AE, Docampo R, Moreno SN.** 1992. Energization-dependent Ca²⁺ accumulation in *Trypanosoma brucei* bloodstream and procyclic trypomastigotes mitochondria. *Mol. Biochem. Parasitol.* **56**:251–7.
20. **Hashimi H, McDonald L, Stříbrná E, Lukeš J.** 2013. Trypanosome Letm1 protein is essential for mitochondrial potassium homeostasis. *J. Biol. Chem.*, in press
21. **Hellemond JJ Van, Bakker BM, Tielens AGM.** 2005. Energy metabolism and its compartmentation in *Trypanosoma brucei*. *Adv. Microb. Physiol.* **50**:199–226.
22. **Docampo R, Lukeš J.** 2012. Trypanosomes and the solution to a 50-year mitochondrial calcium mystery. *Trends Parasitol.* **28**:31–7.
23. **Schnauffer A, Panigrahi AK, Panicucci B, Igo RP, Salavati R, Stuart K.** 2001. An RNA ligase essential for RNA editing and survival of the bloodstream form of *Trypanosoma brucei*. *Science* **291**:2159–62.
24. **Lill R.** 2009. Function and biogenesis of iron–sulphur proteins. *Nature* **460**:831–838.
25. **Pierik AJ, Netz DJA, Lill R.** 2009. Analysis of iron-sulfur protein maturation in eukaryotes. *Nat. Protoc.* **4**:753–66.

26. **Rouault TA.** 2012. Biogenesis of iron-sulfur clusters in mammalian cells: new insights and relevance to human disease. *Dis. Mod. Mech.* **5**:155–64.
27. **Paris Z, Changmai P, Rubio MAT, Zíková A, Stuart KD, Alfonso JD, Lukeš J.** 2010. The Fe/S cluster assembly protein Isd11 is essential for tRNA thiolation in *Trypanosoma brucei*. *J. Biol. Chem.* **285**:22394–402.
28. **Smíd O, Horáková E, Vilímová V, Hrdy I, Cammack R, Horváth A, Lukeš J, Tachezy J.** 2006. Knock-downs of iron-sulfur cluster assembly proteins IscS and IscU down-regulate the active mitochondrion of procyclic *Trypanosoma brucei*. *J. Biol. Chem.* **281**:28679–86.
29. **Long S, Changmai P, Tsaousis AD, Skalický T, Verner Z, Wen Y-Z, Roger AJ, Lukeš J.** 2011. Stage-specific requirement for Isa1 and Isa2 proteins in the mitochondrion of *Trypanosoma brucei* and heterologous rescue by human and *Blastocystis* orthologues. *Mol. Microbiol.* **81**:1403–18.
30. **Long S, Jirků M, Ayala FJ, Lukeš J.** 2008. Mitochondrial localization of human frataxin is necessary but processing is not for rescuing frataxin deficiency in *Trypanosoma brucei*. *Proc. Natl. Acad. Sci. USA* **105**:13468–73.
31. **Changmai P, Horáková E, Long S, Cernotíková-Stříbrná E, McDonald LM, Bontempi EJ, Lukeš J.** 2013. Both human ferredoxins equally efficiently rescue ferredoxin deficiency in *Trypanosoma brucei*. *Mol. Microbiol.* **89**:135–51.
32. **Yoon T, Cowan JA.** 2003. Iron-sulfur cluster biosynthesis. Characterization of frataxin as an iron donor for assembly of [2Fe-2S] clusters in ISU-type proteins. *J. Am. Chem. Soc.* **125**:6078–84.

33. **Gentry LE, Thacker MA, Doughty R, Timkovich R, Busenlehner LS.** 2013. His86 from the N-terminus of frataxin coordinates iron and is required for Fe–S cluster synthesis. *Biochemistry*, in press.
34. **Schmucker S, Martelli A, Colin F, Page A, Wattenhofer-Donzé M, Reutenauer L, Puccio H.** 2011. Mammalian frataxin: An essential function for cellular viability through an interaction with a preformed ISCU/NFS1/ISD11 Iron-Sulfur assembly complex. *PLoS One* **6**:e16199.
35. **Long S, Jirků M, Mach J, Ginger ML, Sutak R, Richardson D, Tachezy J, Lukeš J.** 2008. Ancestral roles of eukaryotic frataxin: mitochondrial frataxin function and heterologous expression of hydrogenosomal *Trichomonas* homologues in trypanosomes. *Mol. Microbiol.* **69**:94–109.
36. **Comini MA, Rettig J, Dirdjaja N, Hanschmann E-M, Berndt C, Krauth-Siegel RL.** 2008. Monothiol glutaredoxin-1 is an essential iron-sulfur protein in the mitochondrion of African trypanosomes. *J. Biol. Chem.* **283**:27785–98.
37. **Pusnik M, Charrière F, Mäser P, Waller RF, Dagley MJ, Lithgow T, Schneider A.** 2009. The single mitochondrial porin of *Trypanosoma brucei* is the main metabolite transporter in the outer mitochondrial membrane. *Mol. Biol. Evol.* **26**:671–80.
38. **Basu S, Leonard JC, Desai N, Mavridou DAI, Tang KH, Goddard AD, Ginger ML, Allen JWA, Lukeš J.** 2013. Divergence of Erv1-associated mitochondrial import and export pathways in trypanosomes and anaerobic protists. *Eukaryot. Cell* **12**:343–55.
39. **Zíková A, Panigrahi AK, Uboldi AD, Dalley R, Handman E, Stuart K.** 2008. Structural and functional association of *Trypanosoma brucei* MIX protein with cytochrome *c* oxidase complex. *Eukaryot. Cell* **7**:1994–2003.

40. **Foldynová-Trantírková S, Paris Z, Sturm NR, Campbell DA, Lukeš J.** 2005. The *Trypanosoma brucei* La protein is a candidate poly(U) shield that impacts spliced leader RNA maturation and tRNA intron removal. *Int. J. Parasitol.* **35**:359–66.
41. **Mayhew TM, Lucocq JM, Griffiths G.** 2002. Relative labelling index: a novel stereological approach to test for non-random immunogold labelling of organelles and membranes on transmission electron microscopy thin sections. *J. Microsc.* **205**:153–64.
42. **Vondrušková E, Van den Burg J, Zíková A, Ernst NL, Stuart K, Benne R, Lukeš J.** 2005. RNA interference analyses suggest a transcript-specific regulatory role for mitochondrial RNA-binding proteins MRP1 and MRP2 in RNA editing and other RNA processing in *Trypanosoma brucei*. *J. Biol. Chem.* **280**:2429–38.
43. **Naamati A, Regev-Rudzki N, Galperin S, Lill R, Pines O.** 2009. Dual targeting of Nfs1 and discovery of its novel processing enzyme, Icp55. *J. Biol. Chem.* **284**:30200–8.
44. **Westergaard GG, Bercovich N, Reinert MD, Vazquez MP.** 2010. Analysis of a nuclear localization signal in the p14 splicing factor in *Trypanosoma cruzi*. *Int. J. Parasitol.* **40**:1029–35.
45. **Marchetti MA, Tschudi C, Kwon H, Wolin SL, Ullu E.** 2000. Import of proteins into the trypanosome nucleus and their distribution at karyokinesis. *J. Cell Sci.* **113**:899–906.
46. **Boucher N, Dacheux D, Giroud C, Baltz T.** 2007. An essential cell cycle-regulated nucleolar protein relocates to the mitotic spindle where it is involved in mitotic progression in *Trypanosoma brucei*. *J. Biol. Chem.* **282**:13780–90.
47. **Hellman K, Prohaska K, Williams N.** 2007. *Trypanosoma brucei* RNA binding proteins p34 and p37 mediate NOPP44/46 cellular localization via the exportin 1 nuclear export pathway. *Eukaryot. Cell* **6**:2206–13.

48. **Cámara MDLM, Bouvier LA, Canepa GE, Miranda MR, Pereira CA.** 2013. Molecular and functional characterization of a *Trypanosoma cruzi* nuclear adenylate kinase isoform. *PLoS Negl. Trop. Dis.* **7**:e2044.
49. **Li K, Tong W-H, Hughes RM, Rouault TA.** 2006. Roles of the mammalian cytosolic cysteine desulfurase, ISCS, and scaffold protein, ISCU, in iron-sulfur cluster assembly. *J. Biol. Chem.* **281**:12344–51.
50. **Nakai Y, Nakai M, Hayashi H, Kagamiyama H.** 2001. Nuclear localization of yeast Nfs1p is required for cell survival. *J. Biol. Chem.* **276**:8314–20.
51. **Mühlenhoff U, Balk J, Richhardt N, Kaiser JT, Sipos K, Kispal G, Lill R.** 2004. Functional characterization of the eukaryotic cysteine desulfurase Nfs1p from *Saccharomyces cerevisiae*. *J. Biol. Chem.* **279**:36906–15.
52. **Nakai Y, Nakai M, Lill R, Suzuki T, Hayashi H.** 2007. Thio modification of yeast cytosolic tRNA is an iron-sulfur protein-dependent pathway. *Mol. Cell. Biol.* **27**:2841–7.
53. **Marelja Z, Stöcklein W, Nimtz M, Leimkühler S.** 2008. A novel role for human Nfs1 in the cytoplasm: Nfs1 acts as a sulfur donor for MOCS3, a protein involved in molybdenum cofactor biosynthesis. *J. Biol. Chem.* **283**:25178–85.
54. **Claros MG, Vincens P.** 1996. Computational method to predict mitochondrially imported proteins and their targeting sequences. *Eur. J. Biochem.* **241**:779–86.
55. **An X, Xiong W, Yang Y, Li F, Zhou X, Wang Z, Deng Z, Liang J.** 2012. A novel target of IscS in *Escherichia coli*: participating in DNA phosphorothioation. *PloS One* **7**:e51265.
56. **Wang L, Chen S, Vergin KL, Giovannoni SJ, Chan SW, DeMott MS, Taghizadeh K, Cordero OX, Cutler M, Timberlake S, Alm EJ, Polz MF, Pinhassi J, Deng Z, Dedon PC.** 2011. DNA phosphorothioation is widespread and quantized in bacterial genomes. *Proc. Natl. Acad. Sci. USA* **108**:2963–8.

57. **Eckstein F.** 2007. Phosphorothioation of DNA in bacteria. *Nat. Chem. Biol.* **3**:689–690.
58. **Wang L, Chen S, Xu T, Taghizadeh K, Wishnok JS, Zhou X, You D, Deng Z, Dedon PC.** 2007. Phosphorothioation of DNA in bacteria by *dnd* genes. *Nat. Chem. Biol.* **3**:709–10.
59. **Mühlenhoff U, Richter N, Pines O, Pierik AJ, Lill R.** 2011. Specialized function of yeast *Isa1* and *Isa2* proteins in the maturation of mitochondrial [4Fe-4S] proteins. *J. Biol. Chem.* **286**:41205–16.
60. **Sa LB, Tovar J, Leo G.** 2003. Mitochondrial remnant organelles of *Giardia* function in iron-sulphur protein maturation. *Nature* **426**:172-6.
61. **Sutak R, Dolezal P, Fiumera HL, Hrdy I, Dancis A, Delgadillo-Correa M, Johnson PJ, Müller M, Tachezy J.** 2004. Mitochondrial-type assembly of FeS centers in the hydrogenosomes of the amitochondriate eukaryote *Trichomonas vaginalis*. *Proc. Natl. Acad. Sci. USA* **101**:10368–73.
62. **Tachezy J, Sánchez LB, Müller M.** 2001. Mitochondrial type iron-sulfur cluster assembly in the amitochondriate eukaryotes *Trichomonas vaginalis* and *Giardia intestinalis*, as indicated by the phylogeny of *IscS*. *Mol. Biol. Evol.* **18**:1919–28.
63. **Nilsson D, Gunasekera K, Mani J, Osteras M, Farinelli L, Baerlocher L, Roditi I, Ochsenreiter T.** 2010. Spliced leader trapping reveals widespread alternative splicing patterns in the highly dynamic transcriptome of *Trypanosoma brucei*. *PLoS Pathog.* **6**:e1001037.

FIGURES

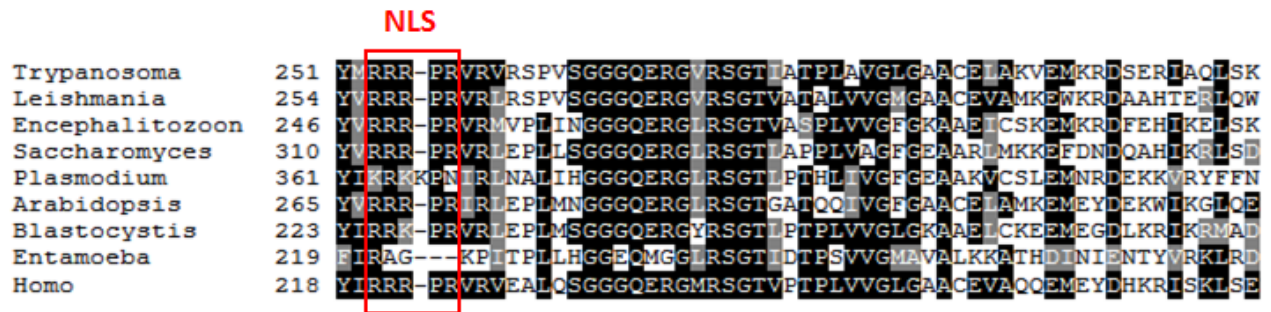


Fig. 1. Nuclear localization signal is present in Nfs from *T. brucei* and other eukaryotes.

Multiple sequence alignment of the Nfs proteins from distantly related eukaryotes. The alignment was generated using ClustalW (<http://www.ch.embnet.org/software/ClustalW.html>) and

Boxshade (http://www.ch.embnet.org/software/BOX_form.html). Identical residues are depicted in black and conserved residues in grey. Nuclear localization signal (NLS) identified in yeast is

highlighted (38). The following sequences were used: *Trypanosoma brucei* Tb927.11.1670 , *Homo*

sapiens NP_001185918.1, *Saccharomyces cerevisiae* NP_009912.2, *Arabidopsis thaliana*

NP_201373.1, *Leishmania mexicana* XP_003876680.1, *Plasmodium falciparum*

XP_001349169.1, *Blastocystis hominis* CBK24185.2, *Encephalitozoon cuniculi* NP_586483.1

and *Entamoeba histolytica* XP_655257.1.

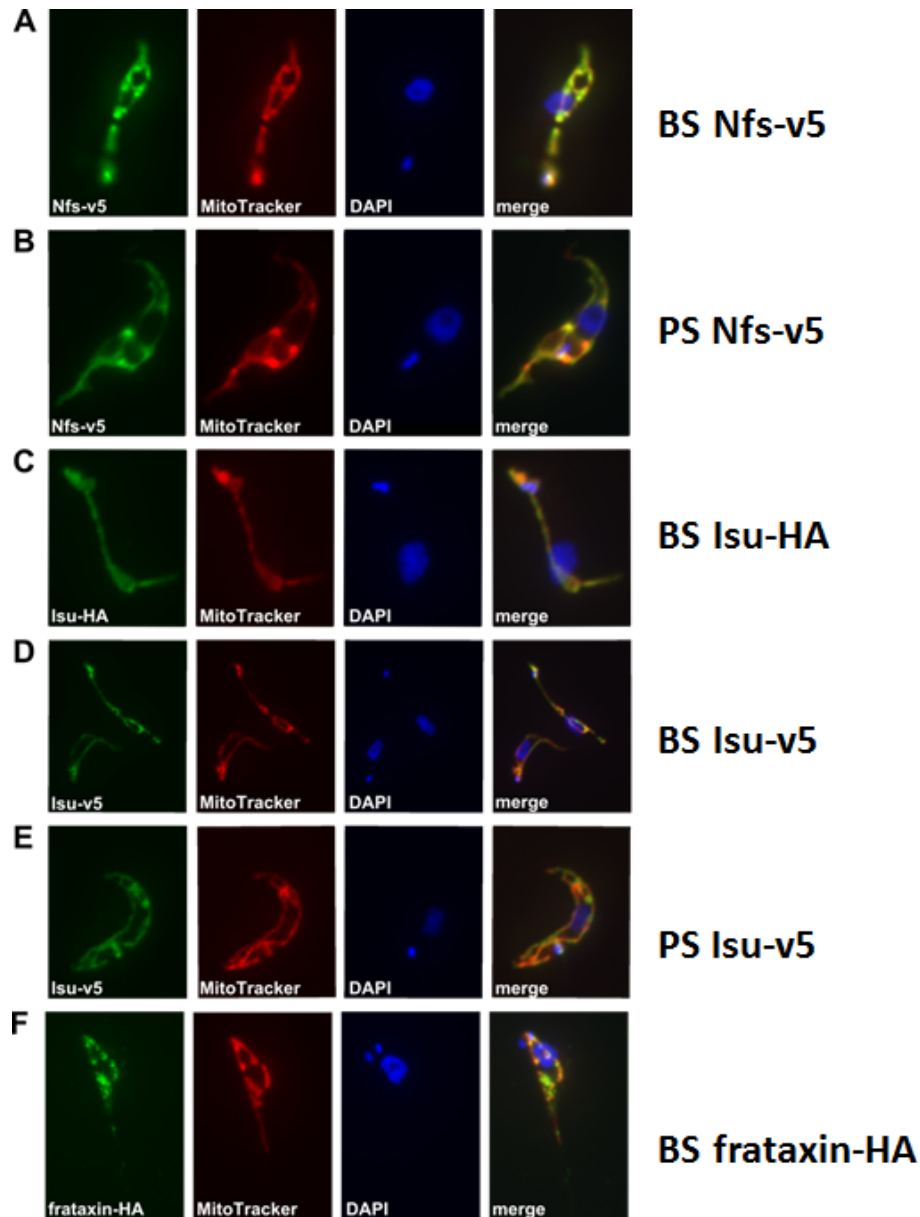


Fig. 2. Immunofluorescence analysis of tagged proteins in *T. brucei* BS and PS. The cells were stained with monoclonal anti-v5 and anti-HA antibodies (green), mitotracker (red) and DAPI (blue). All target proteins were detected in mitochondria as confirmed by colocalization with the mitotracker signal. Identical results were obtained for the BS and PS cells and for the v5 and HA tags.

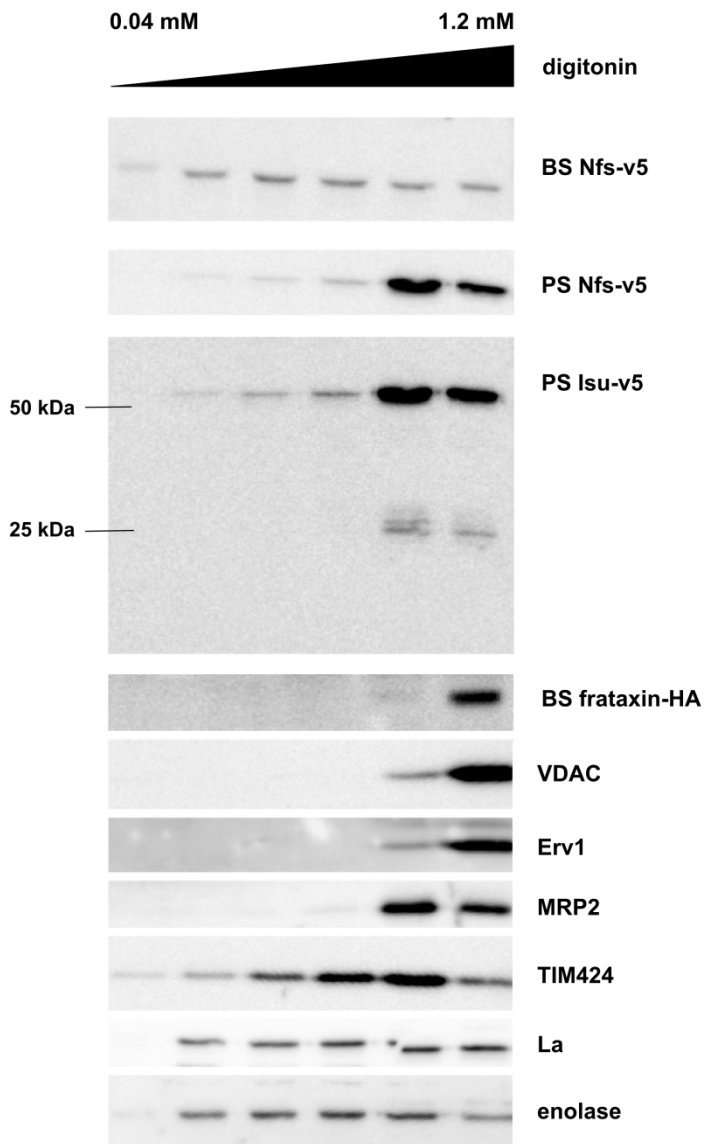


Fig. 3. Nfs and Isu proteins are present in the mitochondrion and in another subcellular compartment. Six samples were prepared from each cell line, incubated with increasing amount of digitonin, centrifuged and obtained supernatants were used for Western blot analyses. Monoclonal anti-v5 and anti-HA antibodies were used for detection of the tagged proteins. Mitochondrial membrane channel VDAC, intermembrane protein Erv1 and mitochondrial matrix protein MRP2 were used as mitochondrial controls; TIM424, the La protein and enolase were

used as glycosomal, nuclear and cytosolic controls, respectively. These controls determined that mitochondrial proteins are present only in the two last fractions, but Nfs was released by lower concentrations of digitonin in both the BS and PS samples. Isu-v5 was detected in both monomeric (25 kDa) and dimeric forms (50 kDa). Again, fraction of the signal was extramitochondrial. In the PS, the bulk of both proteins is present in the mitochondrion. The HA-tagged frataxin was detected solely in the mitochondria-containing fractions.

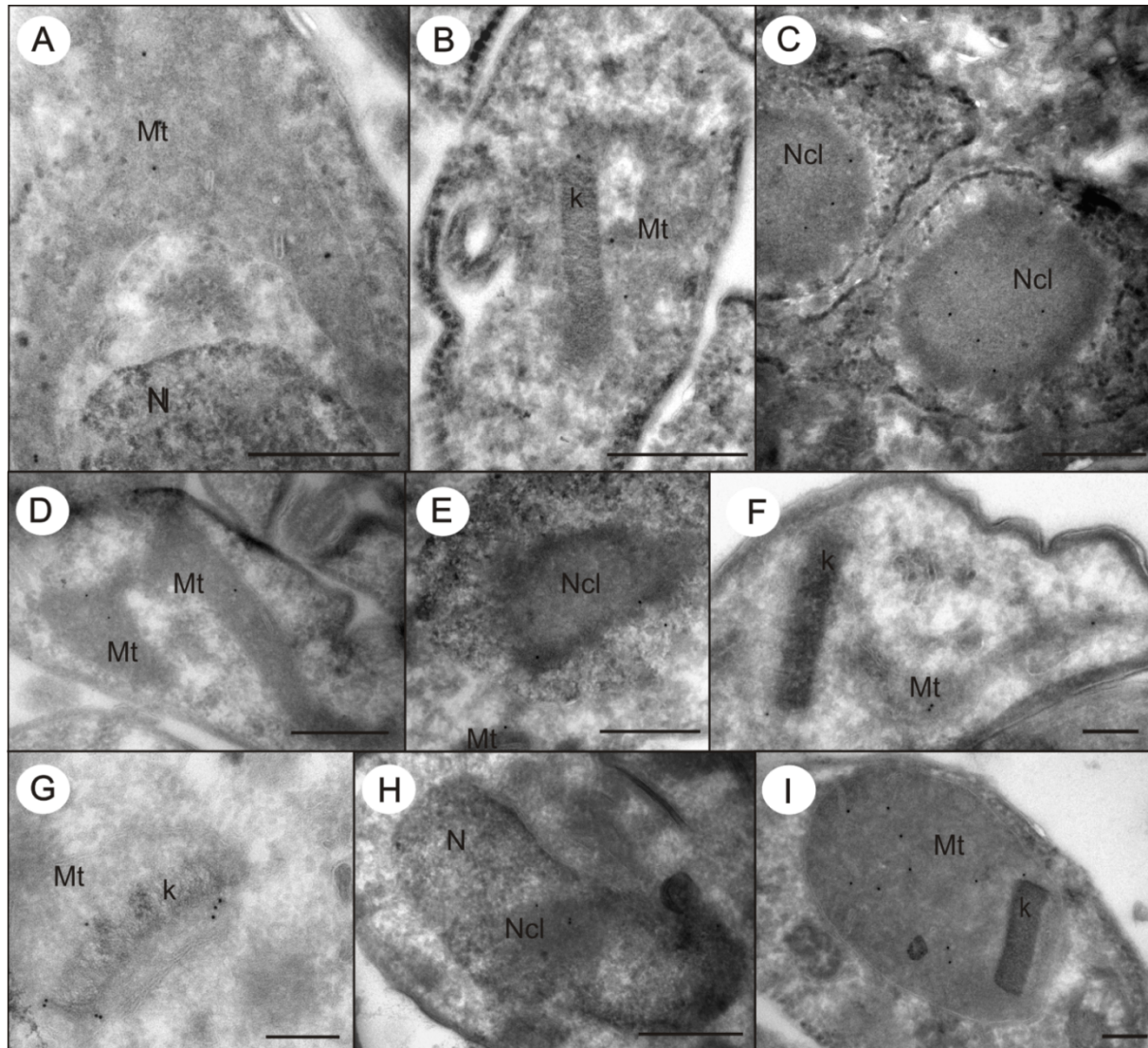


Fig. 4. Nfs and Isu are present in the mitochondrion and the nucleolus. Immunolocalization of Nfs (A-C, G, H) and Isu (D-F) in ultrathin cryosections of PS (A-F, I) and BS (G,H). The gold particles were detected in the mitochondrion (A, D), often associated with kDNA (B, F, G) and nucleolus (C, E, H). Ferredoxin B (I) was localized only in the mitochondrion of PS. Mitochondrion (Mt), nucleolus (Nc), nucleus (N), kDNA (k). Bar 500 nm (A-E, H); bar 200 nm (F, G, I).

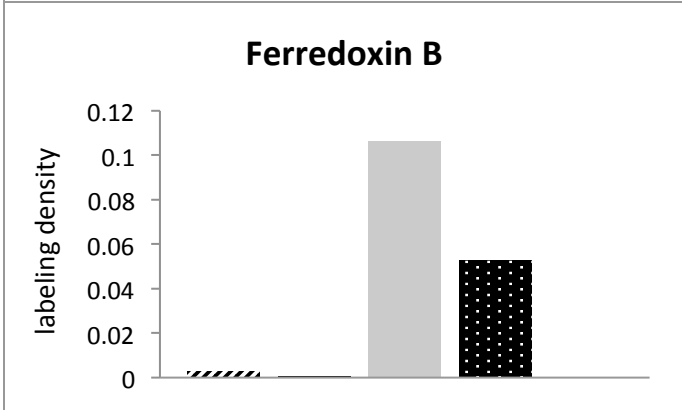
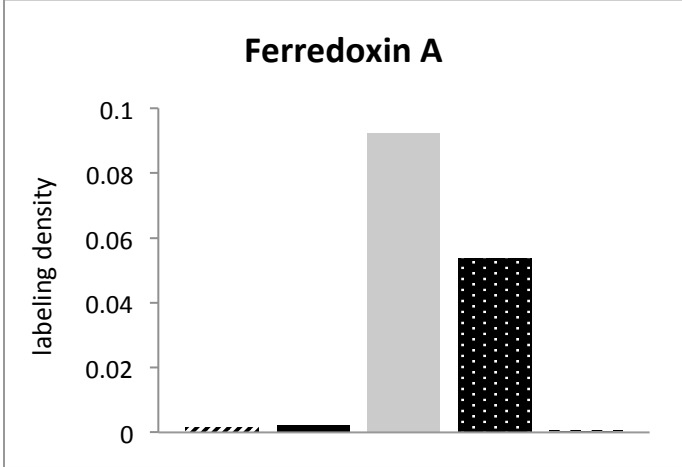
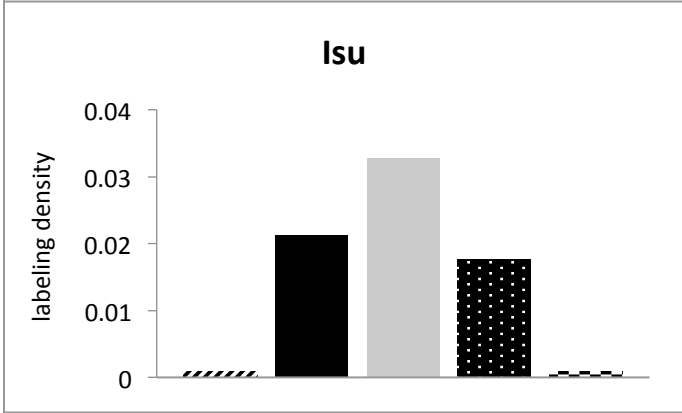
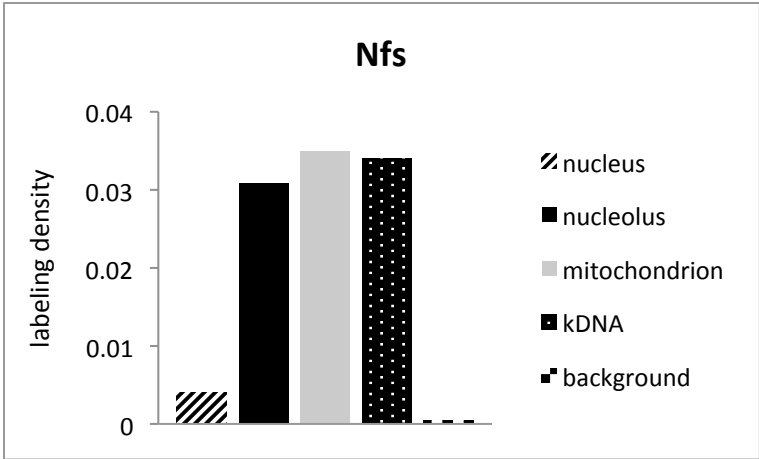


Fig. 5. Statistical analysis of immunogold labeling on cryosections of PS. Nfs is present in the nucleolus and the mitochondrion, where half of the protein is associated with the kDNA. Similarly, Isu is present in the nucleolus and the mitochondrion, but with somewhat lower affinity for the kDNA. Ferredoxins A and B are present solely in the mitochondrion.

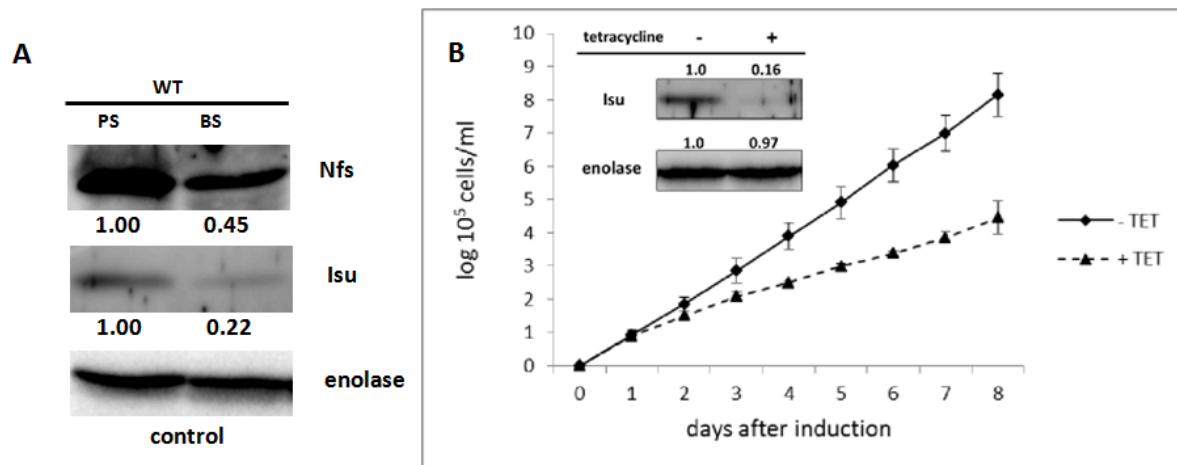


Fig. 6. Fe-S cluster assembly is diminished but essential in BS. (A) Samples containing the same cell number were prepared from the PS and BS cells and analyzed by Western blot analysis. Nfs and Isu are expressed at 45 % and 22 %, respectively, in the BS as compared to the PS. Enolase was used as a loading control. (B) Growth of the BS Isu RNAi cells in the absence (solid line) or presence (dashed line) of tetracycline was examined. After the induction, a significant growth defect was observed. The efficiency of RNAi was verified by Western blot analysis using anti-Isu antibody and enolase as a loading control (inset).

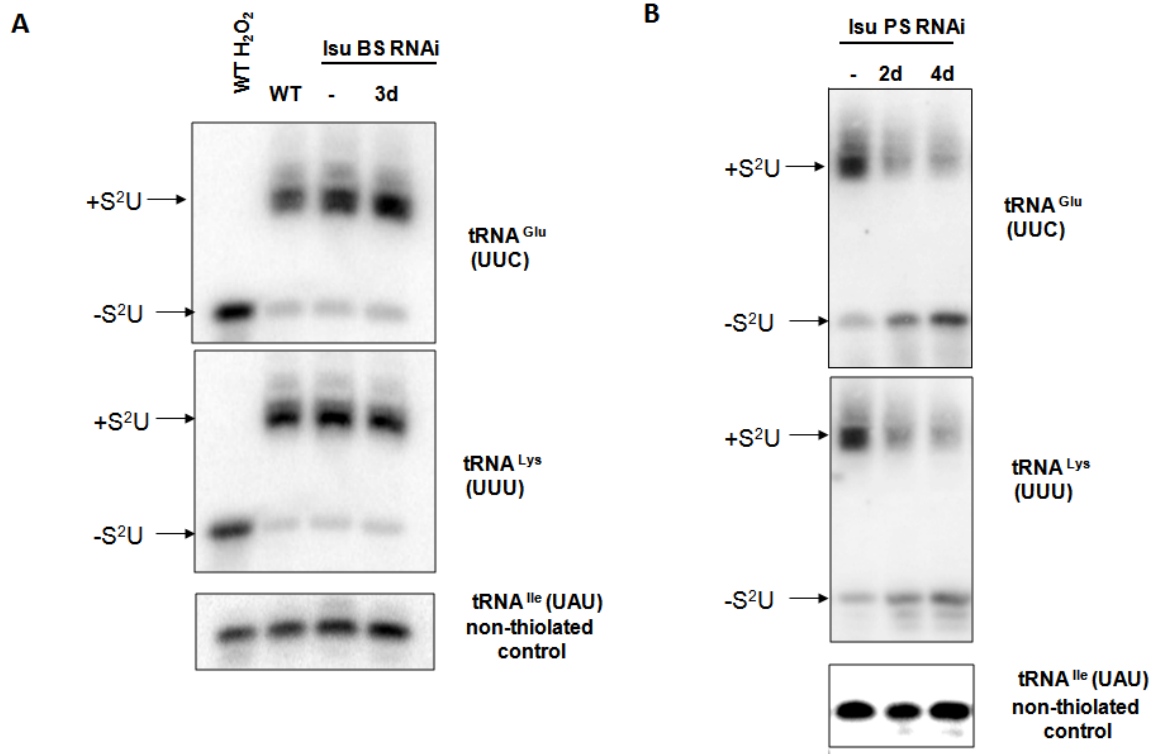


Fig. 7. Cytosolic thiolation in the BS (A) or PS (B) depleted for Isu. RNA isolated from different cell lines was separated on an APM gel followed by Northern blot analysis. Bands corresponding to thiolated (+S²U) and non-thiolated (-S²U) tRNAs are indicated. H₂O₂ was used in wild type cells as a control of complete oxidation of thiolation, eliminating the mobility shift.

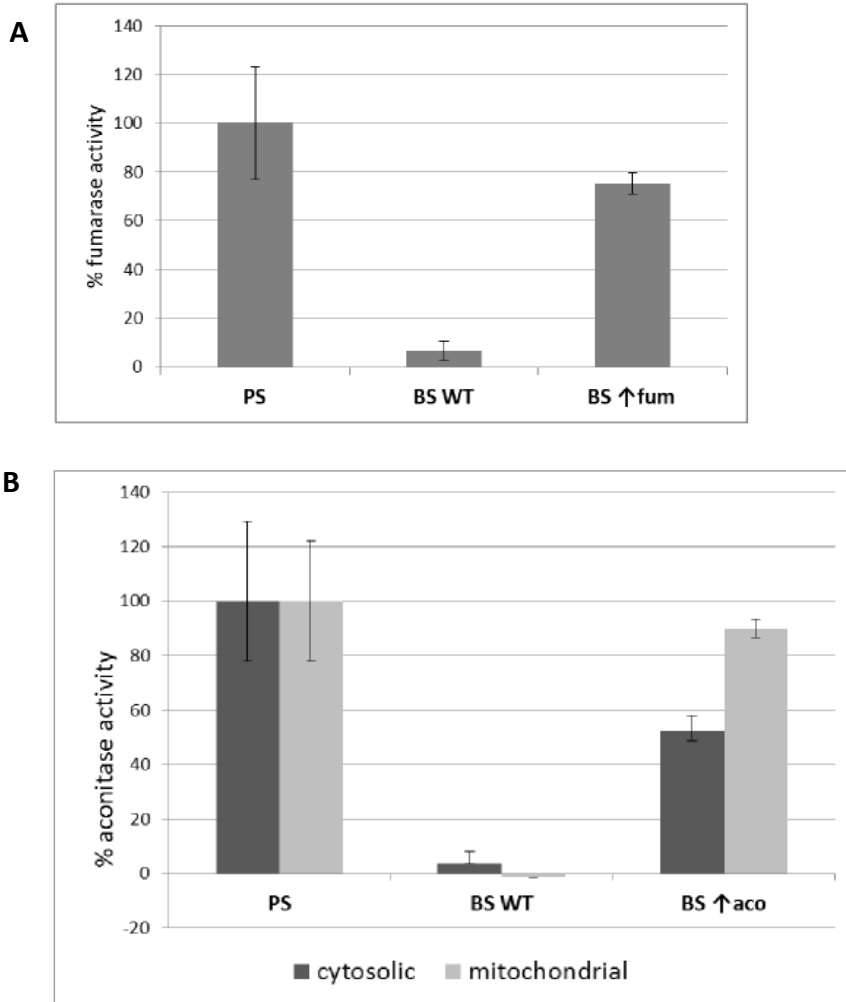


Fig. 8. Enzymatic activities of fumarase (A) and aconitase (B) in PS and BS. Aconitase was measured in cytosolic (dark grey column) and mitochondrial fractions (light grey columns), fumarase was measured only in the cytosol. Activities of both Fe-S dependent enzymes were measured in the wild type PS and BS flagellates and in the BS with inducible overexpression of the target proteins (BS ↑fum, BS ↑aco). The activity obtained in the PS was set as 100%. Whereas in the wild type BS, the activities are almost undetectable, levels comparable with the PS were reached after overexpression of each enzyme. These results confirm that functional Fe-S clusters are produced even in the BS in both cytosolic and mitochondrial compartments. The means and SD values of three independent experiments are shown.

Trypanosoma 1 -----
 Leishmania 1 -----
 Encephalitozoon 1 -----
 Saccharomyces 1 -----MLKSTATRSITRL
 Plasmodium 1 MKFLQI IKHLKLQNKKNALDNFVNCRTYEHISNINKLFLNNFSSTKEHSEHGQVKHENFL
 Arabidopsis 1 -----
 Blastocystis 1 -----
 Entamoeba 1 -----
 Homo 1 -----

Trypanosoma 1 -----MFSGVRVLLCAACGSAS
 Leishmania 1 -----MWRASRVFFCAAASTAN
 Encephalitozoon 1 -----MIGGLKSCIEQPSLPKPTLLPQD----
 Saccharomyces 14 SQVYNVPAATYRACLVSRRFYSPPAAGVKLDDNFSLEHTDIAAAKAQASARASASGTT
 Plasmodium 61 NSTLKYEENSQNGSTNNLKNQKYNMYVSEGNVINEEKYKDNNISSNNTQYNNNSNSGS
 Arabidopsis 1 -----MASKVISATIRRTLTKPHGTFRCRYLS
 Blastocystis 1 -----
 Entamoeba 1 -----
 Homo 1 -----MLLRAAWRRRAVAVTAAPGPKPAAPTRGLRLR

Trypanosoma 18 ---AISQGVSSVGGAGRPFKRDPRLYLIDLSSTTPLDPRVLEKMLPYMTEMYGNPHSRT
 Leishmania 18 GAGAVSKAAAAVAAPSSTLPVFKTRPTIYMDNQATTPLDPRVLDAMLPMTEEYGNPNSRT
 Encephalitozoon 25 -----KACDTGGKRLFLDVGSTTFLDPRVLDAMLPEYTTVIGNPHSRT
 Saccharomyces 74 PDAVVASGSTAMSHAYQENTGFGTRFLYLDLQATTPLDPRVLEMLKEYTGLYGNPHSRT
 Plasmodium 121 LNDEGPLWKEHIDDVVNENKKKKMNRFYLSQATTMLDPRVLEKMLPYMTYIYGNPHSRT
 Arabidopsis 29 TAAATEVNYEDESIMMKGVRI SGRPLYLDLQATTPLDPRVLEAMNASQIHEYGNPHSRT
 Blastocystis 1 -----MSFTWMQAYLLDLPHNQATSRDPRVLEMLPYFTEDYGNPHSRT
 Entamoeba 1 -----MQSTLSVYLDLNNATTMLDPEVLNSMLPYFSEIYGNPNS-L
 Homo 33 VGDRAPQS AVPADTAAAPEVGPVLRPLYMDVQATTPLDPRVLEAMLPLYLINYGNPHSRT

~~~~~  
 Beta strand S1  
 ↓ conserved methionine

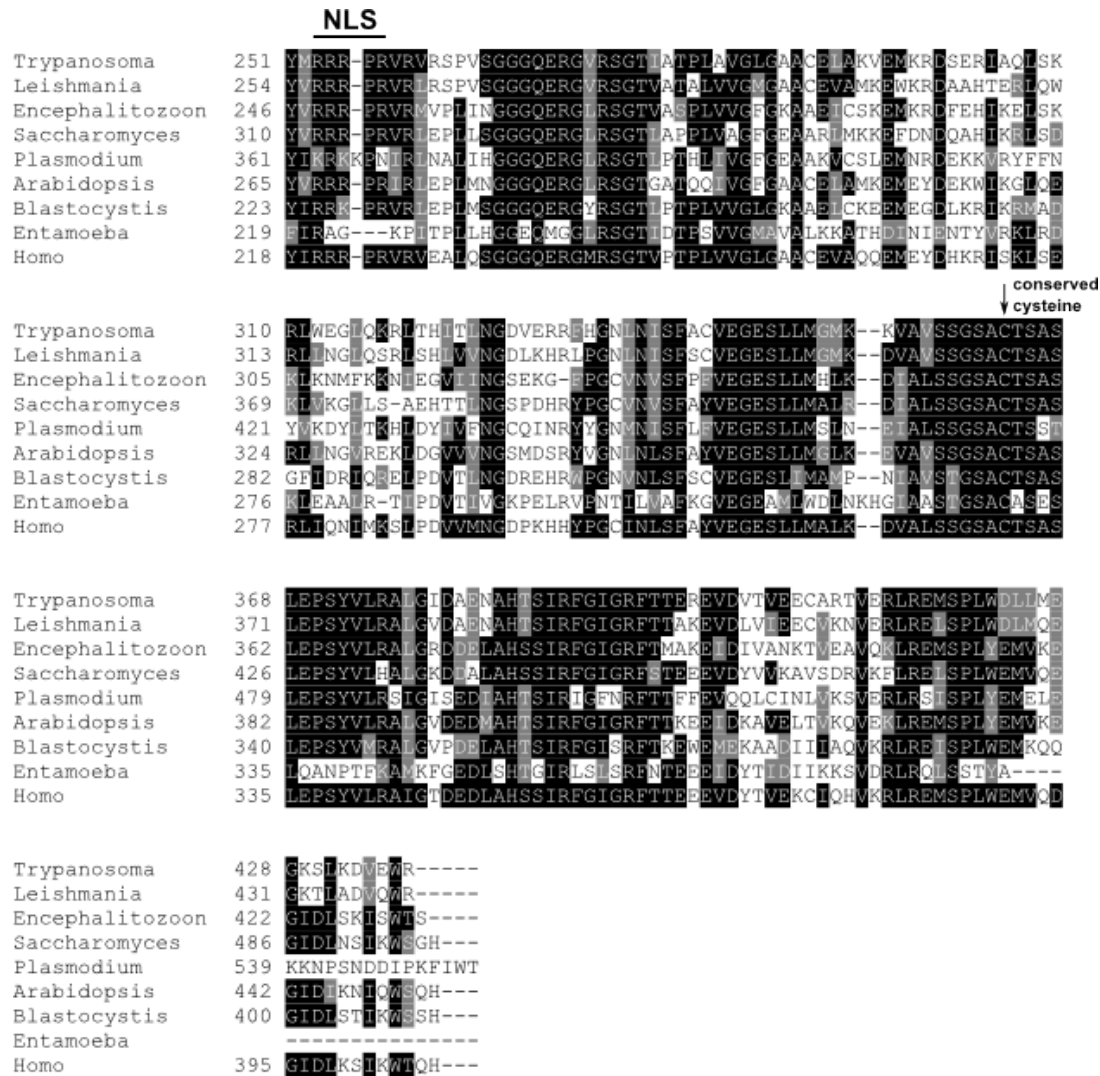
Trypanosoma 75 HSYGWTAEEAVEKARTQVADLIR-ASEPKGVEFTSGATESNNIAIKGVANYNKEK---KNH  
 Leishmania 78 HQYGWSAEBAVEKARKQVADLIG-ASEPKEIFFTSGATPCNNIAIKGVGNFLKAK---KNH  
 Encephalitozoon 68 HRYGWQAEEAVEKARSQVAVSLIG-CDPKIIFFTSGATESNNIAIKGVSGFKLKEGK-AAH  
 Saccharomyces 134 HSYGWETNTAVENARAHVAKIIN-ADPEKIIFFTSGATESNNI VIKGVPRFYKKT---KKH  
 Plasmodium 181 HFFGWSESEKAVEDARTNLMLINGKNNKEIIFFTSGATESNNIALIGICTYYNKLNKQKNH  
 Arabidopsis 89 HLYGWEAENAVENARNOVAQLIE-ASEKEIIFVSGATBANMMAKGVMHFYKDT---KKH  
 Blastocystis 47 HIFGWSAAQAVEKAREQVAQLIG-ASAKEIIFFTSGATPCNNIAIKGVVAQFYKKG---KNH  
 Entamoeba 40 HAFGQKARKALSDSLDIIEYECIGASDDDTVITANSLEGNNITVTKTMLARYETMKG-RNK  
 Homo 93 HAYGWSEBAAMERARQVAVSLIG-ADPREIIFFTSGATESNNIAIK-----

Trypanosoma 131 LITLQTEHKCVLDSCRYLEMEGFVETLVPVEKNGIVNLQKLEBAIRFETALVLSQMYVNVNE  
 Leishmania 134 IITLQTEHKCVLDSCRYLEMEGFVETLVPVQKNGILDVLEBAIKPFTSLVSCVAAHNE  
 Encephalitozoon 126 IITLQTEHKCILDTCRNLEENGVEVETLVPVNDGVVDIDVKKSIKENTVLSVIGAVNSE  
 Saccharomyces 190 IITRTEHKCVLEAARAMMKEGFVETFLNVDDQGLIDLKELEPAIREDTGLVSMVAVNNE  
 Plasmodium 241 IITSQIEHKCILTQCRFLQTKGFVETLKPDTNGLVKLDDIKNSIKDNTIMASFIHFVNNE  
 Arabidopsis 145 VITLQTEHKCVLDSCRHLQEGFVETLVPVKT DGLVDLEMLREAIRFDTGLVSLVAVNNE  
 Blastocystis 103 IITLQTEHKCVLDSCRWLSEGFVETLVPVQKNGILNLDLENAITDKTSLVSMGVNNE  
 Entamoeba 99 IIVSQIEHPSISESEKYLKERGIEVIKMPVNE DGVVDPKLERLIDDKTALVSCMYVNVNE  
 Homo 137 -----ELEBAIQPDTSLVSMVTVNNE

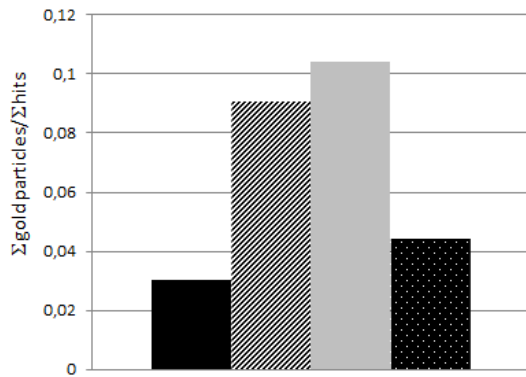
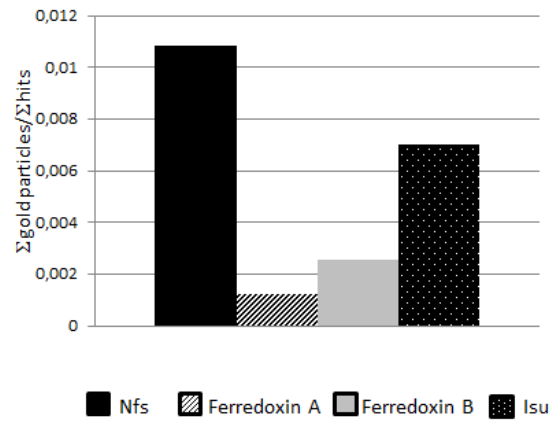
PLP binding domain

Trypanosoma 191 IGVVQPIGEIGKICRKKVLFHTDAAQAVGKIDIDVDRDNIDLMSVSSHKIYGPKGCGAL  
 Leishmania 194 IGVVQPIREIGALCHSKKVLFFHTDAAQALGKIKLDVNDNIDAMSSSHKIYGPKGCGAL  
 Encephalitozoon 186 IGVVQPIKEIGMICKERGVLFHTDAAQAVGKIQIDVNEBNNIDLSMCAHKIYGPKGIGAL  
 Saccharomyces 250 IGVVQPIKEIGAI CRKNKIYFHTDAAQAVGKIHTDVEBNNIDLSISSHKIYGPKGIGAI  
 Plasmodium 301 IGVVQPIENIGNICKENLFFHTDAAQAVGKIPIDVKNMIDLMSVSGHKIYGPKGIGAL  
 Arabidopsis 205 IGVVQPMEEIGMICKEHNVFFHTDAAQALGKIPVDVKKNNVALMSVSSHKIYGPKGVGAL  
 Blastocystis 163 IGVVQPIKEIGAI CRKHGVFFHTDCAQMFGLIFLDVDAMNIDLMSVSGHKCYGPKGVGAL  
 Entamoeba 159 TGVVQPIAEIGRICSSRKKVYFHTDAAQAVGKIFLDVNDMKNIDLMSVSGHKIYGPKGVGAI  
 Homo 158 IGVVQPIAEIGRICSSRKKVYFHTDAAQAVGKIFLDVNDMKNIDLMSVSGHKIYGPKGVGAI

↑ conserved lysine



**Fig. S1. Multiple sequence alignment of Nfs proteins from different distantly related eukaryotes.** The same sequences as in Fig. 1 were used. The alignment was generated using ClustalW (<http://www.ch.embnet.org/software/ClustalW.html>) and Boxshade ([http://www.ch.embnet.org/software/BOX\\_form.html](http://www.ch.embnet.org/software/BOX_form.html)). Identical residues are depicted in black and conserved residues in grey. The wavy line indicates trypanosomal mitochondrial targeting sequence, conserved domains and amino acid residues are labeled.

**A****B**

**Fig. S2. Comparison of gold labeling densities in cryosections.** The signal in the mitochondrion and the kDNA is shown in (A), while labeling in the nucleus and nucleolus is shown in (B). Nfs, ferredoxin A, ferredoxin B and Isu in the PS trypanosomes expressing v5 tag and fixed in 4% formaldehyde were analyzed.



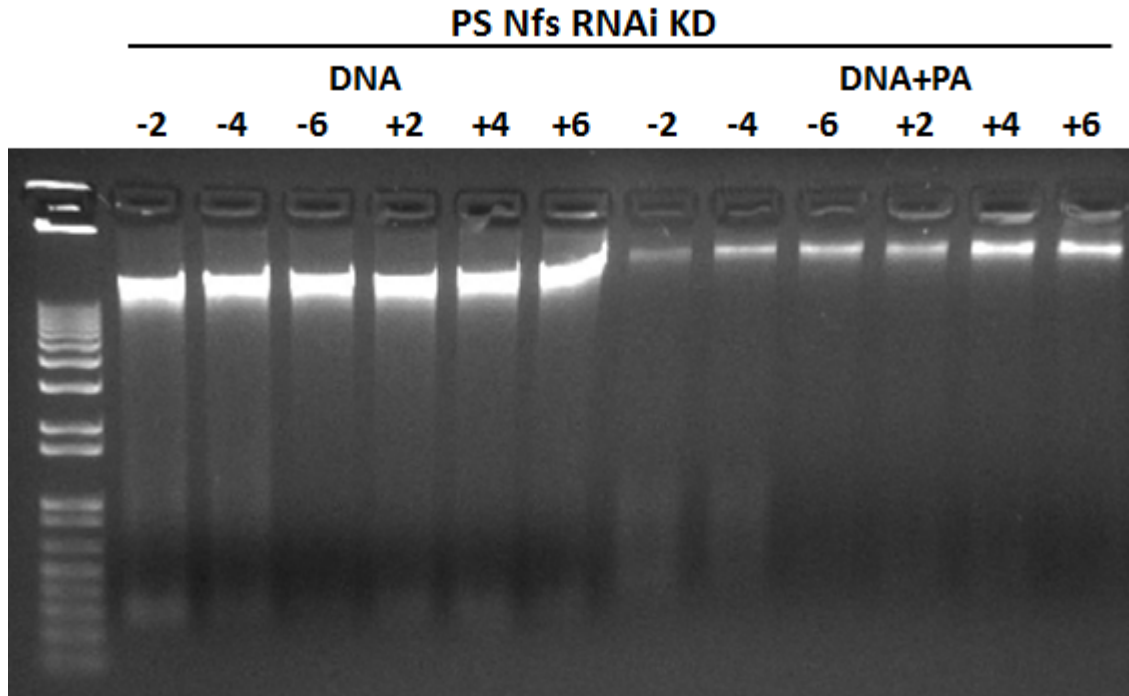


**Fig. S3. DNA phoshothioation is missing in *T. brucei*.** Ethidium bromide-stained agarose gels containing *T. brucei* total genomic DNA, separated in Tris-acetate EDTA buffer. Untreated samples were loaded into six lanes to the left, while identical DNA samples after incubation in TAE containing 2% per-acetic acid (PA) were loaded into the six lanes to the right. In each set, the first three lines represents the non-induced RNAi of Nfs, whereas the other three samples induced for 2, 4 and 6 days, respectively.

Tab. 1. Distribution of gold particles in thawed cryosections of trypanosoma cells expressed v5 tag.

| Compartment             | NFS                     |      |                     | FdxA                    |      |                  | FdxB                    |      |                    | Isu                     |      |                    |
|-------------------------|-------------------------|------|---------------------|-------------------------|------|------------------|-------------------------|------|--------------------|-------------------------|------|--------------------|
|                         | $N_{obs} (N_{exp}) / P$ | RLI  | $\chi^2$ (%)        | $N_{obs} (N_{exp}) / P$ | RLI  | $\chi^2$ (%)     | $N_{obs} (N_{exp}) / P$ | RLI  | $\chi^2$ (%)       | $N_{obs} (N_{exp}) / P$ | RLI  | $\chi^2$ (%)       |
| Nucleus                 | 10 (10.05) / 2869       | 1    | 0 (0)               | 2 (61.4) / 1684         | 0.03 | 57.4 (8.16)      | 5 (75) / 1780           | 0.07 | 65.4 (7.8)         | 2 (34.8) / 2397         | 0.06 | 30.8 (41.6)        |
| Nucleolus               | 39 (5.82) / 1662        | 6.7  | 189 (21.7)          | 1 (27.8) / 763          | 0.04 | 25.8 (3.67)      | 1 (23.8) / 566          | 0.04 | 21.9 (2.6)         | 22 (14.98) / 1034       | 1.47 | 3.28 (4.43)        |
| Mitochondrion           | 74 (8.79) / 2510        | 8.4  | 483.8 (55.6)        | 141 (55.8) / 1531       | 2.53 | 130.1 (18.49)    | 153 (60.7) / 1440       | 2.52 | 140.3 (16.8)       | 55 (24.26) / 1674       | 2.27 | 38.96 (52.51)      |
| kDNA                    | 11 (1) / 285            | 11.1 | 100.2 (11.5)        | 3 (2) / 56              | 1.47 | 0.5 (0.06)       | 3 (2.4) / 57            | 1.25 | 0.2 (0.02)         | 4 (3.29) / 227          | 1.22 | 0.15 (0.21)        |
| Background <sup>a</sup> | 12 (120.35) / 34366     | 0.1  | 97.5 (11.2)         | 8 (506) / 13886         | 0.02 | 490.1 (69.62)    | 4 (617) / 14637         | 0.01 | 609 (72.8)         | 29 (34.73) / 2397       | 0.83 | 0.95 (1.27)        |
| Column totals           | 146 / 41692             |      | 870.73 <sup>b</sup> | 147 / 4034              |      | 704 <sup>b</sup> | 162 / 3843              |      | 836.8 <sup>b</sup> | 112 / 7729              |      | 74.19 <sup>b</sup> |

The labeling is preferential when RLI value is higher than 1 and its partial  $\chi^2$  makes a substantial contribution to the total  $\chi^2$  (highlighted in gray).

<sup>a</sup> Background: gold particles and points present elsewhere than on observed compartments.

<sup>b</sup> Distribution of gold particles is not random,  $df = 4$ ,  $P < 0.001$ .

$N_{obs}$ = number of gold particles observed

$N_{exp}$ =(points for compartment\*total  $N_{obs}$ )/total points; e.g.  $6=(1662*146)/41692$

P= points

$RLI = N_{obs}/N_{exp}$

partial  $\chi^2$  value for compartment=  $(N_{obs}-N_{exp})^2/N_{exp}$

**Table S1. Counts and statistical analysis of the distribution of gold particles in cryosections of v5-tagged PS cell lines.**

### **3.5 Simultaneous depletion of Atm1 and Mdl in *Trypanosoma brucei* offsets the Fe-S cluster assembly in cytosol**

(manuscript in preparation)

work in progress: Due to unexpected phenomena when *TbAtm1* and *TbMdl* were depleted simultaneously, the *Atm1* and *Mdl2* double knockout are being generated in *Saccharomyces cerevisiae* in order to see the effect of the simultaneous depletion of these two genes in a different organism.

# Simultaneous depletion of Atm1 and Mdl in *Trypanosoma brucei* offsets the Fe-S cluster assembly in cytosol

Piya Changmai<sup>1,2</sup>, Eva Horáková<sup>1</sup>, Zdeněk Paris<sup>1,\*</sup>, Didier Salmon<sup>3</sup> and Julius Lukeš<sup>1,2,#</sup>

<sup>1</sup>Biology Centre, Institute of Parasitology, and <sup>2</sup>Faculty of Sciences, University of South Bohemia, České Budějovice (Budweis), Czech Republic, <sup>3</sup>Institute of Medical Biochemistry, Centro de Ciências e da Saude, Federal University of Rio de Janeiro, Rio de Janeiro, Brazil

# Corresponding author

\* Present address: Department of Microbiology, Center for RNA Biology, The Ohio State University, Columbus, Ohio 43210, USA

## Abstract

Atm1 and Mdl are putative ABC transporters. While Atm1 is supposed to transport an unknown component from the mitochondrion, which is required for iron-sulfur (Fe-S) protein maturation in the cytosol, the function of Mdl remains elusive. We identified one homolog of each in *Trypanosoma brucei*, called here *TbAtm1* and *TbMdl*, which we down-regulated either separately or simultaneously using RNA interference. The separate depletion of *TbAtm1* and *TbMdl* led to limited growth defects. In cells ablated for *TbAtm1*, the enzymatic activities of Fe-S cluster proteins aconitase and fumarase decreased in the cytosol by 60% and 50%, respectively, while the same activities in the mitochondrion remained unaltered. These results corroborate the key role of Atm1 in the mitochondrial and cytosolic Fe-S cluster biogenesis.

Downregulation of *TbMdl* did not cause any change in activities of these Fe-S proteins. Surprisingly, the simultaneous ablation of *TbAtm1* and *TbMdl* did not cause any growth defect. Furthermore, the Fe-S protein activities were unaltered in both the cytosolic and mitochondrial compartments. We hypothesize that *TbAtm1* and *TbMdl* transport some molecules that need to be in balance, resulting in a negative effect only

when this balance is disrupted. *TbAtm1* and *TbMdl* were able to partially restore the growth of *S. cerevisiae* *Atm1* and *Mdl2* null mutant. ABCB10, the mammalian homolog of *Mdl*, was recently postulated to export  $\delta$ -aminolevulinic acid (ALA), an intermediate in early step of heme biosynthesis, yet in *T. brucei*, which completely lost heme biosynthesis, such function for *TbMdl* can be excluded. Since *TbMdl* was able to partially rescue the growth defect of *Mdl2* null mutant in yeast, both proteins might transport the same substrate, which is, however, not ALA.

## Introduction

Every extant prokaryotic and eukaryotic cell contains dozens of so-called iron-sulfur (Fe-S) proteins, which carry one or more of these ancient inorganic cofactors. Well over one hundred different Fe-S proteins have been described so far, which are involved in DNA repair, oxidative phosphorylation, DNA/RNA metabolism, sensing and other cellular processes, and prominent examples include mitochondrial respiratory complexes I-III, ferredoxin, aconitase, and DNA polymerases (Lill, 2009; Netz *et al.*, 2011). Even though Fe-S clusters can be spontaneously assembled *in vitro* under specific chemical conditions (Malkin and Rabinowitz, 1966), their assembly *in vivo* requires complex mechanism and regulation (for review see Lill and Mühlenhoff, 2008).

In eukaryotes, mitochondria had inherited the ISC (iron-sulfur cluster) machinery from bacteria, while plastids are equipped with the SUF (sulfur mobilization) pathway. Since they have many Fe-S proteins in the cytosol and nucleus, eukaryotes evolved an exclusive mechanism for maturation of the cytosolic Fe-S clusters, the so-called CIA (cytosolic iron-sulfur cluster assembly) machinery for these compartments (for review see Lill, 2009).

In a typical eukaryote, such as *Saccharomyces cerevisiae*, the mitochondrial ISC machinery is composed of the cysteine desulfurase complex Nfs-Isd11, a putative sulfur donor, which converts cysteine to alanine and provides sulfur to the scaffold protein Isu (Zheng *et al.*, 1993; Lill, 2009; Netz *et al.*, 2011), while ferredoxin is the source of electrons for the reduction of  $S^0$  in cysteine to  $S^{2-}$  in the Fe-S cluster (Kakuta *et al.*, 2001; Mühlenhoff, 2003). Frataxin and glutathione were proposed to serve as iron donors (Yoon and Cowan, 2003; Kondapalli *et al.*, 2008; Hider and

Kong, 2011). Although the former protein was found to enhance the Fe-S formation in eukaryotes (Bedekovics *et al.*, 2007), it seems to inhibit the same reaction in prokaryotes (Adinolfi *et al.*, 2009). Apart from these key components, other proteins such as Isa1, Isa2 and Iba57 participate in transportation of the Fe-S clusters to specific mitochondrial proteins (Mühlenhoff *et al.*, 2007; Long *et al.*, 2011; Sheftel *et al.*, 2012).

The extra-mitochondrial Fe-S proteins require CIA machinery for maturation of their clusters. In *S. cerevisiae*, Fe-S biogenesis in the cytosol and nucleus depends on the mitochondrial ISC machinery. Cytosolic IscU in mammalian cells was reported to have function in recovery of the cytosolic Fe-S proteins after oxidative damage and iron chelation, yet its role in *de novo* Fe-S synthesis is still questioned (Tong and Rouault, 2006). The cytosolic Nfs1 was not able to maintain Fe-S protein activities (Biederbick *et al.*, 2006). Since the extra-mitochondrial Fe-S assembly most likely depends on the mitochondrial ISC machinery, an export machinery that transports some substrate from the mitochondria to the cytosol is needed.

Atm1 is a putative transporter of an unknown component, labelled “X”, which is essential for maturation of the cytosolic and nuclear Fe-S proteins. “X” is believed to be a sulfur compound (Kuhnke *et al.*, 2006). It is a half-transporter, which assembles as a homodimer and contains trans-membrane domain and nucleotide-binding domains (Chloupková *et al.*, 2004). Atm1 is localized in the mitochondrial inner membrane, with its C-terminus exposed into the mitochondrial matrix, being important for coupling energy from ATP hydrolysis (Leighton, 1995). ABCB7 (ATP-binding cassette sub-family B member 7), the human ortholog of Atm1, was found to have an interaction with the Fe-S containing ferrochelatase, the enzyme that inserts ferrous ion into protoporphyrin IX in the terminal step of heme biosynthesis (Taketani *et al.*, 2003). Apart from the “X” component, *Arabidopsis thaliana* homolog Atm3 also transports cyclic pyranopterin monophosphate from the mitochondrion to the cytosol, where it is converted into molybdopterin, an intermediate in molybdenum cofactor biosynthesis (Teschner *et al.*, 2010).

Lack of Atm1 in *S. cerevisiae* under aerobic conditions causes iron accumulation in the mitochondria, decrease of Fe-S clusters and heme in both the mitochondria and the cytosol collectively lead to oxidative damage. However, during anaerobiosis, neither Fe-S clusters nor heme levels were affected. Furthermore, the Atm1-depleted yeasts exhibited normal level of mitochondrial iron. In contrast to

aerobic condition, the activity of only cytosolic, but not mitochondrial Fe-S proteins was impaired (Miao *et al.*, 2009). In humans, mutations in ABCB7 are responsible for X-linked sideroblastic anemia with ataxia (Bekri *et al.*, 2000). The depletion of ABCB7 in HeLa cells caused a decrease of cell proliferation, iron accumulation in mitochondria, increase in protoporphyrin IX and decrease in the activity of the cytosolic Fe-S proteins (Cavadini *et al.*, 2007).

*A. thaliana* has three homologs of Atm1 (AtAtm1 thru AtAtm3). AtAtm3 seems to be the functional homolog of Atm1 (Chen *et al.*, 2007), as its mutant showed a decrease of the cytosolic Fe-S protein activities, while those in the mitochondrion and plastid remained unaltered (Bernard *et al.*, 2009). Activity of nitrate reductase, which is a molybdenum cofactor-containing enzyme, was decreased. The activity of catalase, a heme containing enzyme, was unaltered and the heme itself was not accumulated in the mitochondrion (Bernard *et al.*, 2009).

Mdl1, an ABC transporter in *S. cerevisiae*, which localizes to the mitochondrial inner membrane, has a role in the export of ~ 6 to 21 kDa peptides, generated by the m-AAA protease in the mitochondrial matrix (Young, 2001). The exact role of Mdl2, another Mdl homolog found in the genome of *S. cerevisiae*, which does not transport the same proteolytic breakdown products as Mdl1 remains to be established (Young, 2001). Overexpression of Mdl1 in  $\Delta$ Atm1 yeast cells was able to reduce iron accumulation in mitochondria, while expression of Mdl1 in wild-type cells did not affect the level of organellar iron (Chaloupková *et al.*, 2003).

ABCB10, the mammalian Mdl homolog was shown to interact with mitochondrial iron importer mitoferrin-1 (Mfrn1) in differentiated mouse erythroleukemia cells (Chen *et al.*, 2009). ABCB10 not only enhanced the stability of Mfrn1, but it also potentiated mitochondrial iron import. The ABCB10-Mfrn1 complex was found to transiently interact with ferrochelatase (Chen *et al.*, 2010). Recently, it was proposed that ABCB10 may have a specific role in heme biosynthesis by facilitating the export or even exporting  $\delta$ -aminolevulinic acid (ALA) (Bayeva *et al.*, 2013).

*Trypanosoma brucei* is a parasitic flagellate that causes sleeping sickness in humans, and a host of other diseases in cold and warm-blooded vertebrates. It is transmitted by tse-tse fly, in the midgut of which the parasite proliferates as a so-called procyclic stage (PS), characterized by a single fully active mitochondrion (Besteiro *et al.*, 2005). However, when *T. brucei* enters the mammalian host, its

morphology and metabolism transform into a bloodstream stage (BS), with most functions of its mitochondrion being repressed (Hellemond *et al.*, 2005). Here we studied the function of *T. brucei* homologues of Atm1 (*TbAtm1*) and Mdl (*TbMdl*) in the PS of this model protist. RNAi depletion of either *TbAtm1* or *TbMdl* led to the moderate growth defect, yet unexpectedly, in case of *TbAtm1*+Mdl double knock-down, the growth remained unaltered. The depletion of *TbAtm1* resulted in reduced activities of cytosolic, but not mitochondrial aconitase and fumarase, whereas this phenotype was absent in cells ablated for either *TbMdl* or in the *TbAtm1*+*TbMdl* double knock-downs.

## Results

### *Identification of TbAtm1 and TbMdl*

Using *S. cerevisiae* Atm1 gene as a query, we identified its single homolog in *T. brucei* (Tb927.11.16930) and named it *TbAtm1*. The *TbAtm1* gene codes for 719 amino acid-long protein with calculated molecular weight 79.10 kDa. MitoprotII predicted its mitochondrial localization with 0.991 probability, with the cleavage site at position 54. *TbAtm1* shares 38%, 42% and 43% identity with yeast Atm1p, human ABCB7 and *A. thaliana* Atm3 orthologues, respectively. The gene contains conserved ABC transporter trans-membrane and ATPase regions.

The same strategy was applied for Mdl, resulting in the identification of a single homolog (Tb927.11.540), labelled *TbMdl*. The 691 amino acid-long *TbMdl* of calculated molecular weight 76.25 kDa, contains conserved trans-membrane and ATPase regions, and is likely mitochondrial (MitoprotII score of 0.9484 probability) with position 97 as the predicted cleavage site. *TbMdl* shares 38%, 37% and 37% sequence similarity with human ABCB10 and *S. cerevisiae* Mdl1p and Mdl2p orthologues, respectively. The presence of a single Mdl gene in most eukaryotes including *T. brucei* indicates that the two orthologues found in yeast resulted from a rather unique and late duplication event, unlike in green algae where the gene was duplicated earlier.

Phylogenetic analysis based on the amino acid sequence of *TbAtm1* and *TbMdl* was performed using the maximum likelihood approach (Fig. 1A and B). Both



genes are highly conserved and present in most eukaryotic supergroups except for alveolata.

### ***Localization of TbAtm1***

High probability predicted by MitoprotII for mitochondrial localization of *TbAtm1* is corroborated by its mass spectrometry-based identification in the *T. brucei* mitochondrial proteome (Panigrahi *et al.*, 2009). We decided to experimentally investigate *in situ* localization of the GFP-tagged version of *TbAtm1* using immunofluorescence assay. Full-length *TbAtm1* was cloned into the pET-GFP vector with a GFP-tag at the C-terminus (Devaux *et al.*, 2007). The construct was linearized by *XhoI* and transfected into the *T. brucei* ProAnv PS cell. Flagellates expressing the endogenously tagged gene were selected using phleomycin as a selectable marker. As expected, the immunofluorescence assay showed clearly co-localization with the mitochondrial marker tetramethylrhodamine ethyl ester (TMRE) (Fig. 2), confirming the predicted mitochondrial localization of *TbAtm1*. The protein seems to be evenly distributed throughout the reticulated mitochondrion of the PS trypanosomes.

### ***Individual but not simultaneous depletion of TbAtm1 and TbMdl affects viability***

In order to investigate the functions of both ABCB transporters, we used the advantage of RNAi-mediated gene silencing in *T. brucei*. Fragments of *TbAtm1* and *TbMdl* were cloned into the opposing Tet-regulatable promoter-containing p2T7-177 plasmid, and the *TbAtm1+TbMdl* double knock-down was generated by cloning both gene fragments in tandem. The constructs were *NotI*-linearized, transfected into the *T. brucei* 29-13 PS cells, and RNAi was induced in phleomycin-resistant cell line by the addition of tetracycline to the medium.

Upon RNAi induction, the *TbAtm1*-depleted cells showed slightly reduced proliferation (Fig. 3A), while the ablation of *TbMdl* resulted in growth defect of a greater extent (Fig. 3B). Surprisingly, when *TbAtm1* and *TbMdl* were down-regulated at the same time, the growth remained unaltered. Indeed, repeated and prolonged cultivation of the non-induced and RNAi-induced double knock-downs confirmed the absence of any growth phenotype (Fig. 3C).

The ablation of *TbAtm1* in both the *TbAtm1* single knock-down and the *TbAtm1+Mdl* double knock-down cells was monitored by Western blot analysis using specific polyclonal antibodies against *TbAtm1*. The elimination in the *TbAtm1* single

knock-down was efficient with the protein being virtually undetectable on day 3 post-induction, while the lack of any leaky transcription is exemplified by same levels of the protein in the wild type and the non-induced cell (Fig. 3D). Western blot analysis using the same polyclonal antibody with lysates from the non-induced and RNAi-induced *TbMdl* single and *TbAtm1+TbMdl* double knock-downs confirmed unaltered level of *TbAtm1* in the former cells and its efficient depletion in the latter ones (Fig. 3D). In the absence of a specific antibody, down regulation of *TbMdl* was followed by quantitative real-time PCR. As shown in Fig. 3E, the *TbMdl* mRNA decreased by ~70% in the *TbMdl* single knock-down, whereas ablation of the same transcript in the *TbAtm1+TbMdl* double knock-down was even more efficient, lowering it by 85%.

### ***TbAtm1 is required for cytosolic but not mitochondrial Fe-S proteins***

In order to investigate the role of *TbAtm1* in the mitochondrial and cytosolic Fe-S cluster assembly, enzymatic activities of selected Fe-S enzymes have been measured in both cellular compartments. Aconitase, a marker Fe-S protein, is in *T. brucei* encoded by a single gene, with about 70% and 30% of the protein being targeted to the cytosol and mitochondrion, respectively (Saas *et al.*, 2000), while the studied flagellate encodes in its genome two fumarases, the cytosolic and mitochondrial one (Coustou *et al.*, 2006). The dual localization of both enzymes makes them particularly suitable to examine the effects of *TbAtm1* depletion in each compartment of *T. brucei*.

The activities of cytosolic aconitase and fumarase in the *TbAtm1*-depleted cells dropped to 40% and 50%, respectively (Fig. 4A). The unaltered activity of the mitochondrial threonine dehydrogenase was used as a Fe-S cluster-lacking control. Similar to *S. cerevisiae*, *A. thaliana* and humans (Cavadini *et al.*, 2007; Bernard *et al.*, 2009), activities of both of these enzymes were upon the depletion of *TbAtm1* changed in the mitochondrial compartment. As expected, in the PS flagellates ablated for *TbMdl*, neither aconitase nor fumarase activities were affected in the cytosole and mitochondrion (Fig. 4B). Surprisingly, when *TbAtm1* and *TbMdl* were down-regulated at the same time, the enzymatic activities of aconitase and fumarase remained unaltered in both the cytosolic and mitochondrial compartments (Fig. 4C). Again, threonine dehydrogenase remained on wild type level in each studied cell line, regardless of RNAi induction (Fig. 4).

### ***TbAtm1 partially rescues $\Delta$ Atm1 in *S. cerevisiae****

Haploid Atm1 null mutant of *S. cerevisiae* is not able to grow on a minimal medium and barely grows on a rich medium (Leighton and Schatz, 1995). Thus in order to investigate whether *TbAtm1* was able to complement the growth defect of Atm1 null mutant in *S. cerevisiae* we first generated a  $\Delta$ Atm1 diploid strain by disruption of Atm1 with the *kan<sup>r</sup>* gene in strain  $\Sigma$ 1278b (Grenson *et al.*, 1966). We checked that upon sporulation the heterozygous  $\Delta$ Atm1 exhibits Mendelian 2:2 segregation in a tetrad. Next, Atm1, Mdl1, and *TbAtm1* were cloned respectively into the pRS426Met25 (URA3) vector, and the resulting constructs were subsequently introduced into the  $\Delta$ Atm1 diploid mutant by homologous recombination (Guldener *et al.*, 1996). After sporulation, haploid cells were grown in minimal medium lacking uracil. As expected for mutant cells expressing the ectopic copies of yeast Atm1, the growth was restored to wild-type level (Fig. 5A). When the same mutant cells expressed yeast Mdl1, the growth was partially rescued, which is in agreement with previous work (Chloupková *et al.*, 2003). Similarly, complementation with the trypanosome homologue *TbAtm1* was able to support only limited growth, at about the same level as the mutant expressing yeast Mdl1 (Fig. 5A).

### ***TbMdl partially rescues $\Delta$ Mdl2 in *S. cerevisiae****

$\Delta$ Mdl2 *S. cerevisiae* grows normally in a glucose-rich fermentable medium, while this mutant fails to proliferate on non-fermentable sources, such as a glycerol-rich medium. We tested whether the above-mentioned growth defect of yeast lacking Mdl2 in the BY4742 background (YPL270w, Euroscarf) can be rescued by *TbMdl* expressed from the high-copy pRS426Met25 vector. As shown in Fig. 5B, in a glucose-rich medium (YPD= 868 medium), the yeast Mdl2 null mutant expressing *TbMdl* grows as well as the wild-type cells containing empty plasmid and the  $\Delta$ Mdl2 strain, proving that *TbMdl* is not toxic to *S. cerevisiae*. Moreover, expression of the heterologous *T. brucei* protein in the yeast Mdl2 null mutants is able to restore the growth in a glycerol-rich medium, although not to the wild-type level (Fig. 5B).

### ***Double $\Delta$ Atm1+Mdl2 in *S. cerevisiae****

Experiment currently in progress. (Fig.6)

## Discussion

Despite intense research in the last decade, the mitochondrial machinery responsible for the export of the so-called “X” component remains elusive. Although several studies implicated the conserved and evolutionary widespread Atm1 protein in this process (Kuhnke *et al.*, 2006; Bernard, 2013; Haynes, 2010; Kispal, 1999), the identity of this hypothetical component, proposed to be involved not only in the cytosolic and nuclear Fe-S protein maturation, but also in iron homeostasis (Kispal *et al.*, 1997; 1999) is still unknown. Ambiguous results are partially responsible for this situation. In *S. cerevisiae* grown under aerobic conditions and in mammalian cells, depletion of Atm1 causes accumulation of mitochondrial iron, whereas the same phenotype is absent from *A. thaliana* and anaerobic *S. cerevisiae* (Miao *et al.*, 2009; Rouault and Tong, 2008). Thus, the “X” component itself or a deficiency in the cytosolic Fe-S maturation might be a signal for iron homeostasis only under specific conditions and/or in some organisms.

We are also far from understanding the function(s) of Mdl and its homologs. The *S. cerevisiae* Mdl1 as well as the Mdl homolog in *C. elegans* (HAF-1) have been proposed to serve as exporters of proteolytic oligopeptides resulting from misfolded proteins outside the mitochondrial matrix (Young, 2001; Haynes *et al.*, 2010). However, the *S. cerevisiae* Mdl2 is not involved in such an export and must have a different function (Young, 2001). In most eukaryotes, the only homologue of Mdl is ABCB10, which was lately postulated to transport ALA from mitochondria in cardiac cells (Bayeva *et al.*, 2013), while in differentiated mouse erythroleukemia cells, it interacts with Mfrn-1 in order to stabilize and promote heme import into the organelle (Chen *et al.*, 2009). The recently described transient interaction between ABCB10-Mfrn-1 complex and ferrochelatase (Chen *et al.*, 2010) has to be further investigated, yet it further implicates Mdl with heme metabolism.

Both *T. brucei* homologues (*TbAtm1* and *TbMdl*) contain mitochondrial targeting sequence, transmembrane and nucleotide binding domains, and have been previously found in the PS mitochondrial proteome (Panigrahi *et al.*, 2009). For *TbAtm1*, we have confirmed localization in the organelle by immunofluorescence microscopy using the GFP-tagging strategy. For functional analysis, single and

double knock-down cell lines of the PS have been generated. In *S. cerevisiae*,  $\Delta$ Atm1 results in *petite* phenotype and inability to grow on a minimal medium (Leighton, 1995). In *A. thaliana*, Atm3 deficiency causes a host of defects in chlorophyll content, seed establishment, decreased root growth and dwarfism (Kushnir *et al.*, 2001; Bernard *et al.*, 2009). Moreover, mutations in ABCB7 in humans cause X-linked sideroblastic anemia with ataxia. Hence, at least one Atm homologue is essential for these model organisms, and cross-complementation studies confirmed that human ABCB7 and *A. thaliana* AtAtm3, and to lesser extent AtAtm1, are able to rescue not only growth defect in the yeast Atm1 deficiency, but also suppress iron accumulation in the mitochondria and restore respiration and activity of the cytosolic Fe-S proteins (Bekri *et al.*, 2000; Chen *et al.*, 2007). Similarly, the overexpression of Mdl1 partially complemented growth defect and reduced iron accumulation in the mitochondria of  $\Delta$ Atm1 *S. cerevisiae* (Chaloupková *et al.*, 2003).

Given the general essentiality of Atm1, the relatively mild growth phenotype caused by its efficient ablation in *T. brucei* was rather unexpected, especially when the depletion of *TbMdl* led to a more pronounced growth defect. This latter phenotype is not surprising, since deletion of ABCB10, its mammalian homolog, caused death of mouse embryos by day 12, a consequence of increased ROS, mitochondrial protein oxidation and apoptosis (Hyde *et al.*, 2012). ABCB10 was proposed to export ALA, an early precursor of heme synthesis, from human mitochondrion (Bayeva *et al.*, 2013), yet such a function in *T. brucei* is hardly reconcilable with earlier and well as our data. The ability of *TbMdl* to restore growth of yeast  $\Delta$ Mdl2 on a non-fermentable carbon source is quite informative in this context, as *T. brucei* lacks entire heme biosynthesis pathway (Kořený *et al.*, 2010; 2012) and hence certainly cannot transport ALA. Therefore, this result implies that not only *TbMdl* but also yeast Mdl2 likely transports other substrate than ALA.

Due to the position of the export machinery between the cytosolic and mitochondrial Fe-S cluster biogenesis, processes upstream of Atm1 should not be affected upon its depletion. Indeed, in the PS trypanosomes ablated for *TbAtm1*, activities of the Fe-S cluster-containing mitochondrial aconitase and fumarase remained unaltered. In contrast, activities of the same enzymes located in the cytosol were substantially decreased. This result confirms the notion that the cytosolic Fe-S protein maturation depends, at least to some extent, on the mitochondrial ISC

machinery and that *Atm1* is the key link of the maturation pathway between both these cellular compartments (Lill 2009; Lill and Mühlenhoff, 2008). The ability of *TbAtm1* to partially complement the growth defect of the yeast knock-down is in line with this interpretation.

Interestingly, no significant changes in the enzymatic activities of fumarase and aconitase in both compartments were observed in the *TbMdl*-depleted cells, strongly indicating that this protein does not have a direct role in the Fe-S cluster biogenesis. However, its true function, reflected by a significant growth defect upon its ablation, remains unknown.

To our surprise, the simultaneous depletion of *TbAtm1* and *TbMdl* did not cause any growth phenotype, even though single knock-downs of each gene resulted in an altered growth. Furthermore, the enzymatic activities of aconitase and fumarase in the cytosolic and mitochondrial compartments were unaltered, which is in contradiction with the results obtained with the *TbAtm1* knock-downs, in which this protein is clearly needed for the Fe-S cluster maturation in the cytosol. This result is highly reproducible, allowing us to conclude that in the background of concurrently missing *TbMdl*, *TbAtm1* is no longer needed for the cytosolic Fe-S assembly. At this point we can only speculate that in cells depleted for both *TbAtm1* and *TbMdl*, an as yet unknown mechanism is triggered, which is able to compensate for the lack of both transporters. Another hypothesis postulates that *TbAtm1* and *TbMdl* transport molecule with opposing function, and the lack of one transporter can therefore be outweighed by the absence of its opponent. In such case, cells depleted for *TbAtm1* lack a signal transported via this protein, while another signal or molecule carried by *TbMdl* become excessive. However, an unknown compensatory mechanism would have to be in place. Further studies are needed to shed light on this intriguing and highly reproducible observation.

### **Acknowledgements**

We thank Shaojun Long (Washington University School of Medicine, St. Louis) and Aurélie Wertz (Université Libre de Bruxelles, Gosselies) for initial experiments, Aleš Horák (Biology Centre, České Budějovice) for phylogenetic analysis, Luděk Kořený (Cambridge University, Cambridge) for discussions, Bruno André and Catherine Jauniaux ( Université Libre de Bruxelles, Gosselies) for advice and help with yeast experiments and Paul A. M. Michels (Universidad de los Andes, Mérida/University of

Edinburgh, Edinburgh) for the gift of  $\alpha$ -enolase antibody. This work was supported by the Czech Grant Agency (P305/11/2179), Czech Ministry of Education (AMVIS LH12104), and the Praemium Academiae award to J.L., who is also a Fellow of the Canadian Institute for Advanced Research.

## References

- Bayeva, M., Khechaduri, A., Wu, R., Burke, M.A., Wasserstrom, J.A., Singh, N., *et al.* (2013) ABCB10 regulates early steps of heme synthesis. *Circ Res* **113**:279-87.
- Bekri, S., Kispal, G., Lange, H., Fitzsimons, E., Tolmie, J., Lill, R., and Bishop, D.F. (2000) Human ABC7 transporter: gene structure and mutation causing X-linked sideroblastic anemia with ataxia with disruption of cytosolic iron-sulfur protein maturation. *Blood* **96**: 3256–3264.
- Bernard, D.G., Cheng, Y., Zhao, Y., and Balk, J. (2009) An allelic mutant series of ATM3 reveals its key role in the biogenesis of cytosolic iron-sulfur proteins in *Arabidopsis*. *Plant Physiol* **151**: 590–602.
- Bernard, D.G., Netz, D.J.A., Lagny, T.J., Pierik, A.J., Balk, J. (2013). Requirements of the cytosolic iron-sulphur cluster assembly pathway in *Arabidopsis*. *Phil Trans Roy Soc B* **368**: 20120259 .
- Besteiro, S., Barrett, M.P., Rivière, L., and Bringaud, F. (2005) Energy generation in insect stages of *Trypanosoma brucei*: metabolism in flux. *Trends Parasitol* **21**: 185–191.
- Biederbick, A., Stehling, O., Rösser, R., Niggemeyer, B., Nakai, Y., Elsässer, H.-P., and Lill, R. (2006) Role of human mitochondrial Nfs1 in cytosolic iron-sulfur protein biogenesis and iron regulation. *Mol Cell Biol* **26**: 5675–5687.
- Cavadini, P., Biasiotto, G., Poli, M., Levi, S., Verardi, R., Zanella, I., *et al.* (2007) RNA silencing of the mitochondrial ABCB7 transporter in HeLa cells causes an iron-deficient phenotype with mitochondrial iron overload. *Blood* **109**: 3552–3559.

- Chen, S., Sánchez-Fernández, R., Lyver, E.R., Dancis, A., and Rea, P.A. (2007) Functional characterization of AtATM1, AtATM2, and AtATM3, a subfamily of *Arabidopsis* half-molecule ATP-binding cassette transporters implicated in iron homeostasis. *J Biol Chem* **282**: 21561–21571.
- Chen, W., Dailey, H.A., and Paw, B.H. (2010) Ferrochelatase forms an oligomeric complex with mitoferrin-1 and Abcb10 for erythroid heme biosynthesis. *Blood* **116**: 628–630.
- Chen, W., Paradkar, P.N., Li, L., Pierce, E.L., Langer, N.B., Takahashi-Makise, N., *et al.* (2009) Abcb10 physically interacts with mitoferrin-1 (Slc25a37) to enhance its stability and function in the erythroid mitochondria. *Proc Natl Acad Sci USA* **106**: 16263–16268.
- Chloupková, M., LeBard, L.S., and Koeller, D.M. (2003) MDL1 is a High Copy Suppressor of ATM1: Evidence for a role in resistance to oxidative stress. *J Mol Biol* **331**: 155–165.
- Chloupková, M., Reaves, S.K., LeBard, L.M., and Koeller, D.M. (2004) The mitochondrial ABC transporter Atm1p functions as a homodimer. *FEBS Letters* **569**: 65–69.
- Coustou, V., Biran, M., Besteiro, S., Rivière, L., Baltz, T., Franconi, J.-M., and Bringaud, F. (2006) Fumarate is an essential intermediary metabolite produced by the procyclic *Trypanosoma brucei*. *J Biol Chem* **281**: 26832–26846.
- Grenson, M., Mousset, M., Wiame, J.M., and Bechet, J. (1966). Multiplicity of the amino acid permeases in *Saccharomyces cerevisiae*. I. Evidence for a specific arginine-transporting system. *Biochim. Biophys. Acta* **127**: 325–338.
- Güldener, U., Heck, S., Fielder, T., Beinhauer, J. and Hegemann, J. H. (1996). A new efficient gene disruption cassette for repeated use in budding yeast. *Nucleic Acids Res* **24**: 2519-2524.
- Haynes, C.M., Yang, Y., Blais, S.P., Neubert, T.A., and Ron, D. (2010) The matrix peptide exporter HAF-1 signals a mitochondrial UPR by activating the transcription factor ZC376.7 in *C. elegans*. *Mol Cell* **37**: 529–540.



Hellemond, J.J.V., Bakker, B.M., and Tielens, A.G.M. (2005) Energy metabolism and its compartmentation in *Trypanosoma brucei*. *Adv Microb Physiol* **50**: 199–226.

Hider, R.C., and Kong, X.L. (2011) Glutathione: a key component of the cytoplasmic labile iron pool. *Biometals* **24**: 1179–1187.

Hyde, B.B., Liesa, M., Elorza, A.A., Qiu, W., Haigh, S.E., Richey, L., *et al.* (2012) The mitochondrial transporter ABC-me (ABCB10), a downstream target of GATA-1, is essential for erythropoiesis *in vivo*. *Cell Death Differ* **19**: 1117–1126.

Kakuta, Y., Horio, T., Takahashi, Y., and Fukuyama, K. (2001) Crystal structure of *Escherichia coli* Fdx, an adrenodoxin-type ferredoxin Involved in the assembly of iron–sulfur clusters. *Biochemistry* **40**: 11007–11012.

Kispal, G., Csere, P., Guiard, B., Lill, R. (1997) The ABC transporter Atm1p is required for mitochondrial iron homeostasis. *FEBS Lett* **418**: 346–35.

Kispal, G., Csere, P., Prohl, C., Lill, R. (1999) The mitochondrial proteins Atm1p and Nfs1p are essential for biogenesis of cytosolic Fe/S proteins. *EMBO J* **18**: 3981–3989.

Kondapalli, K.C., Kok, N.M., Dancis, A., and Stemmler, T.L. (2008) *Drosophila* frataxin: an iron chaperone during cellular Fe-S cluster bioassembly. *Biochemistry* **47**: 6917–6927.

Kořený, L., Lukeš, J., and Oborník, M. (2010) Evolution of the haem synthetic pathway in kinetoplastid flagellates: An essential pathway that is not essential after all? *Int J Parasitol* **40**: 149–156.

Kořený, L., Sobotka, R., Kovářová, J., Gnipová, A., Flegontov, P., Horváth, A., Oborník, M., Ayala, F.J., and Lukeš J. (2012) Aerobic kinetoplastid flagellate *Phytomonas* does not require heme for viability. *Proc Natl Acad Sci USA* **109**: 3808–3813.

Kuhnke, G., Neumann, K., Mühlenhoff, U., and Lill, R. (2006) Stimulation of the ATPase activity of the yeast mitochondrial ABC transporter Atm1p by thiol compounds. *Mol Membr Biol* **23**: 173–184.

- Kushnir, S., Babiychuk, E., Storozhenko, S., Davey, M.W., Papenbrock, J., De Rycke, R., *et al.* (2001) A mutation of the mitochondrial ABC transporter Sta1 leads to dwarfism and chlorosis in the *Arabidopsis* mutant starik. *Plant Cell* **13**: 89–100.
- Leighton, J and Schatz G. (1995) An ABC transporter in the mitochondrial inner membrane is required for normal growth of yeast. *EMBO J* **14**: 188-195.
- Lill, R. (2009) Function and biogenesis of iron–sulphur proteins. *Nature* **460**: 831–838.
- Lill, R., and Mühlenhoff, U. (2008) Maturation of iron-sulfur proteins in eukaryotes: mechanisms, connected processes, and diseases. *Annu Rev Biochem* **77**: 669–700.
- Long, S., Changmai, P., Tsaousis, A.D., Skalický, T., Verner, Z., Wen, Y.-Z., *et al.* (2011) Stage-specific requirement for Isa1 and Isa2 proteins in the mitochondrion of *Trypanosoma brucei* and heterologous rescue by human and *Blastocystis* orthologues. *Mol Microbiol* **81**: 1403–1418.
- Malkin, R. and Rabinowitz, J.C. (1966) The reconstitution of clostridial ferredoxin. *Biochem Biophys Res Commun* **23**: 822–827.
- Miao, R., Kim, H., Koppolu, U.M.K., Ellis, E.A., Scott, R.A., and Lindahl, P.A. (2009) Biophysical characterization of the iron in mitochondria from Atm1p-depleted *Saccharomyces cerevisiae*. *Biochemistry* **48**: 9556–9568.
- Mühlenhoff, U. (2003) Components involved in assembly and dislocation of iron-sulfur clusters on the scaffold protein Isu1p. *EMBO J* **22**: 4815–4825.
- Mühlenhoff, U., Gerl, M.J., Flauger, B., Pirner, H.M., Balser, S., Richhardt, N., *et al.* (2007) The iron-sulfur cluster proteins Isa1 and Isa2 are required for the function but not for the de novo synthesis of the Fe/S clusters of biotin synthase in *Saccharomyces cerevisiae*. *Eukaryot Cell* **6**: 495–504.
- Netz, D.J.A., Stith, C.M., Stümpfig, M., Köpf, G., Vogel, D., Genau, H.M., *et al.* (2011) Eukaryotic DNA polymerases require an iron-sulfur cluster for the formation of active complexes. *Nat Chem Biol* **8**: 125–132.
- Panigrahi, A.K., Ogata, Y., Zíková, A., Anupama, A., Dalley, R.A., Acestor, N., *et al.*

(2009) A comprehensive analysis of *Trypanosoma brucei* mitochondrial proteome. *Proteomics* **9**: 434–450.

Rouault, T.A., Tong, W.H. (2008) Iron-sulfur cluster biogenesis and human disease. *Trends Genet* **24**:398–407.

Saas, J., Ziegelbauer, K., Haeseler, von, A., Fast, B., and Boshart, M. (2000) A developmentally regulated aconitase related to iron-regulatory protein-1 is localized in the cytoplasm and in the mitochondrion of *Trypanosoma brucei*. *J Biol Chem* **275**: 2745–2755.

Sheftel, A.D., Wilbrecht, C., Stehling, O., Niggemeyer, B., Elsässer, H.-P., Mühlhoff, U., and Lill, R. (2012) The human mitochondrial ISCA1, ISCA2, and IBA57 proteins are required for [4Fe-4S] protein maturation. *Mol Biol Cell* **23**: 1157–1166.

Taketani, S., Kakimoto, K., Ueta, H., Masaki, R., and Furukawa, T. (2003) Involvement of ABC7 in the biosynthesis of heme in erythroid cells: interaction of ABC7 with ferrochelatase. *Blood* **101**: 3274–3280.

Teschner, J., Lachmann, N., Schulze, J., Geisler, M., Selbach, K., Santamaria-Araujo, J., *et al.* (2010) A Novel Role for *Arabidopsis* mitochondrial ABC transporter ATM3 in molybdenum cofactor biosynthesis. *Plant Cell* **22**: 468–480.

Tong, W.-H., and Rouault, T.A. (2006) Functions of mitochondrial ISCU and cytosolic ISCU in mammalian iron-sulfur cluster biogenesis and iron homeostasis. *Cell Metabol* **3**: 199–210.

Yoon, T., and Cowan, J.A. (2003) Iron-sulfur cluster biosynthesis. Characterization of frataxin as an iron donor for assembly of [2Fe-2S] clusters in ISU-type proteins. *J Am Chem Soc* **125**: 6078–6084.

Young, L. (2001) Role of the ABC transporter Mdl1 in peptide export from mitochondria. *Science* **291**: 2135–2138.

Zheng, L., White, R.H., Cash, V.L., Jack, R.F., and Dean, D.R. (1993) Cysteine

desulfurase activity indicates a role for NIFS in metallocluster biosynthesis. *Proc Natl Acad Sci USA* **90**: 2754–2758.

## Figure legends

### **Fig. 1. Phylogenetic analysis of *TbAtm1* and *TbMdl***

Maximum likelihood phylogenetic analysis of *Atm1* (A) and *Mdl* (B) inferred using RAxML and  $\Gamma$ -corrected LG matrix (LG+ $\Gamma$  model). Branching support is expressed via non-parametric bootstrap support and Bayesian posterior probabilities. See *Experimental procedures* for details.

### **Fig. 2. *TbAtm1* is localized in the mitochondrion of *T. brucei***

Fluorescence microscopy of wild type live cell expressing *TbAtm1*-GFP tagged protein. Phase shows picture from Nomarski contrast microscopy, TMRE visualizes the mitochondrion.

### **Fig. 3. Each *TbAtm1* and *TbMdl* depletion caused growth defect, but not when the both genes were depleted simultaneously**

Growth curves of non-induced (triangles; black line) and RNAi-induced (squares; grey line) cell lines for (A) single *TbAtm1*, (B) *TbMdl* and (C) double *TbAtm1*+*Mdl* knock downs. The *y*-axis represents the log scale product of cell density and total dilution. (D) The depletion of *TbAtm1* in each KD was confirmed by western blot Enolase was used as loading control. (E) Quantitative real-time PCR shows relative *TbMdl* mRNA abundance of the single *TbMdl* and *TbAtm1*+*Mdl* RNAi induced cells compared to non-induced cells. 18S rRNA transcript was used as internal reference.

### **Fig. 4. Effect of *TbAtm1* and *TbMdl* depletion on Fe-S proteins activities.**

Enzymatic activities of aconitase (dark grey columns) and fumarase (light grey column) in *TbAtm1* (A), *TbMdl* (B) and *TbAtm1*+*Mdl* (C) depleted cells were measured in the whole cell lysate (total), cytosolic (cyto) and mitochondrial (mito)

fractions. Graphs represent relative percentage of the activities in RNAi induced compared to the non-induced cells. Enzymatic activity of thereonine dehydrogenase (white columns), non Fe-S protein, was used as control.

**Fig. 5. Complementation of *TbAtm1* and *TbMdl* in *S. cerevisiae***

(A) The picture represent viability of *S. cerevisiae* Atm1 null haploid strain (haploid strain  $\Delta atm1$ ), wild type, Atm1 single allele deleted diploid strain (diploid strain ATM1/atm1), Atm1 null haploid strain expressing yeast Mdl1 (haploid strain  $\Delta atm1+MDL1$ ), Atm1 null haploid strain expressing *TbAtm1* (haploid strain  $\Delta atm1+TbATM1$ ) and Atm1 null haploid strain expressing yeast Atm1 (haploid strain  $\Delta atm1+ATM1$ ). Cells were grown on synthetic minimal medium lacking uracil and methionine.

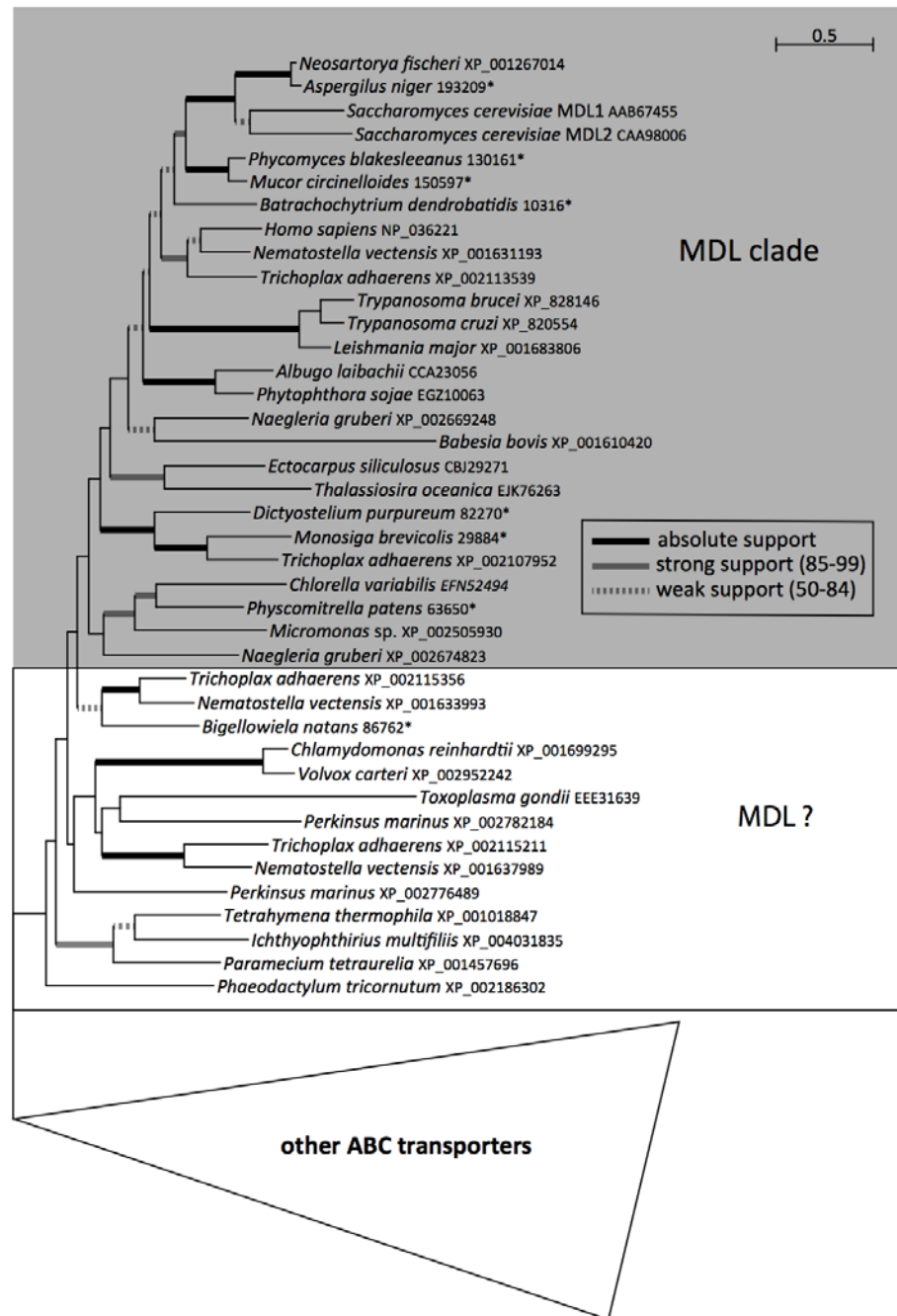
(B) *S. cerevisiae* WT, Mdl2 null expressing *TbMdl* ( $\Delta mdl2+TbMdl$ ) and Mdl2 null mutant with empty pRS426Met vector ( $\Delta mdl2$ ) were grown on glucose rich medium (fermentable carbon source, upper panel) and glycerol rich medium (non-fermentable carbon source, lower panel).

A

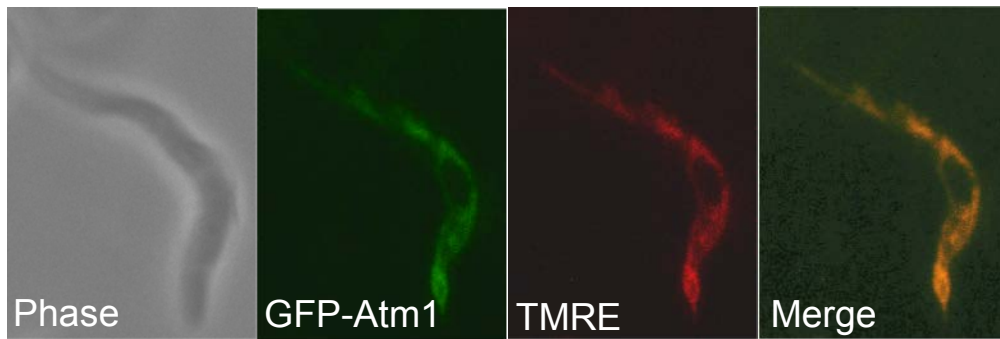


Fig. 1

**B**

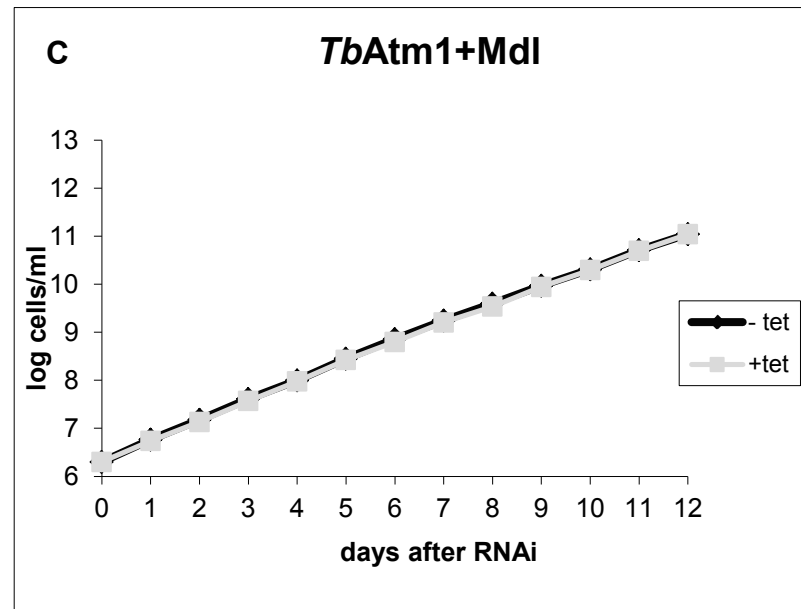
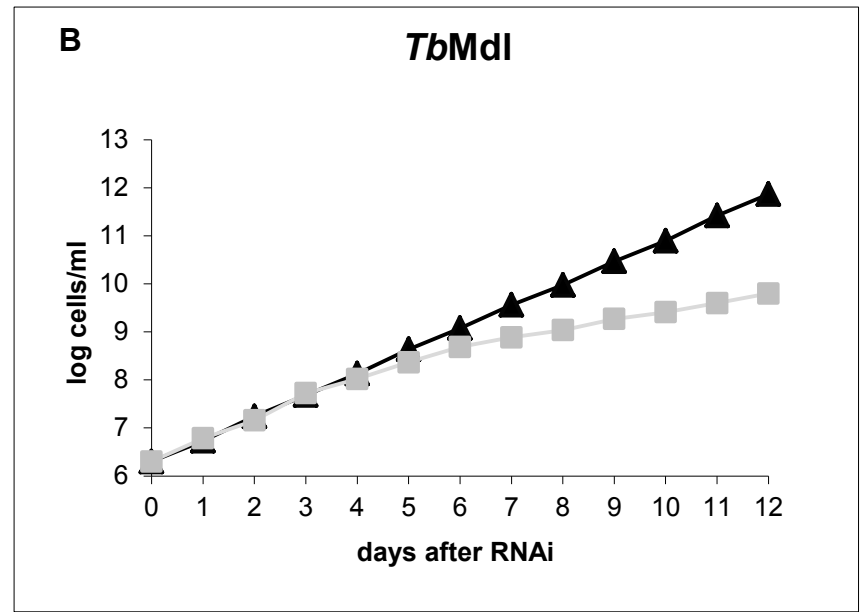
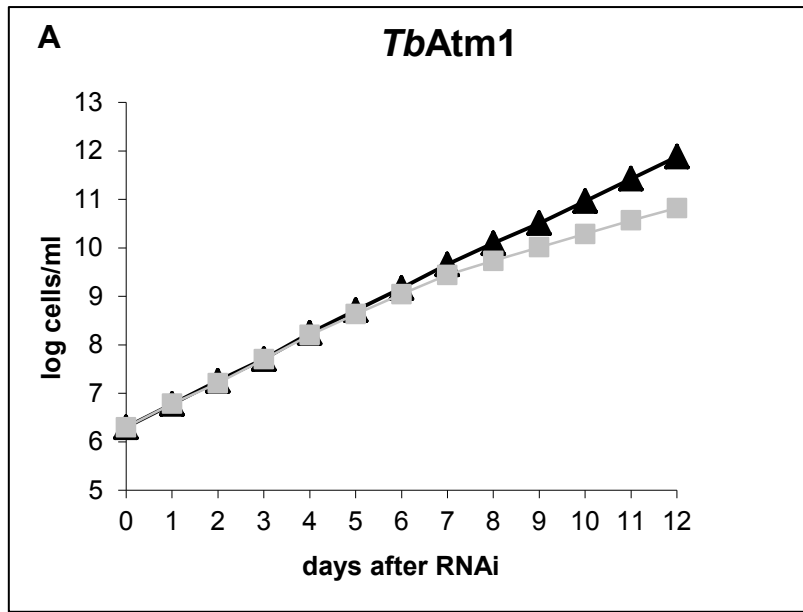


**Fig. 1**

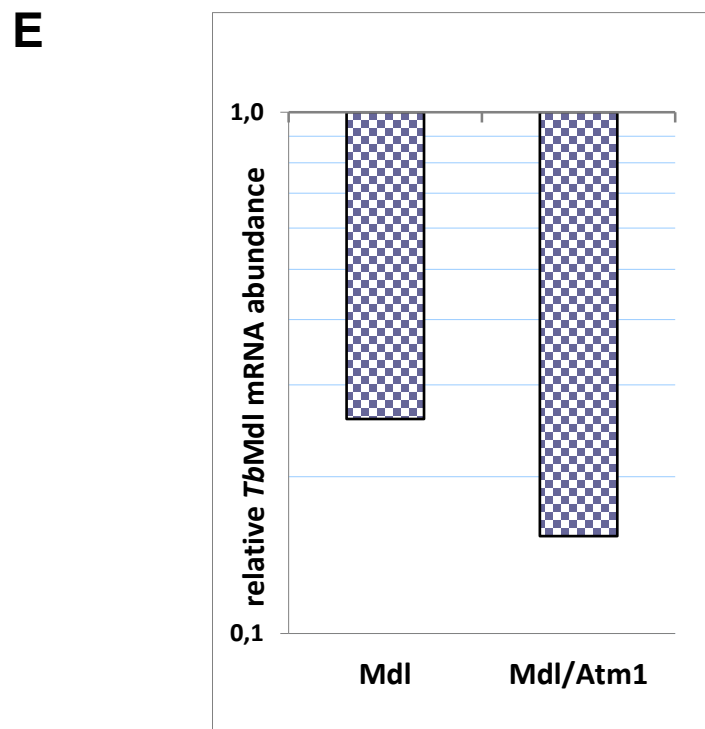
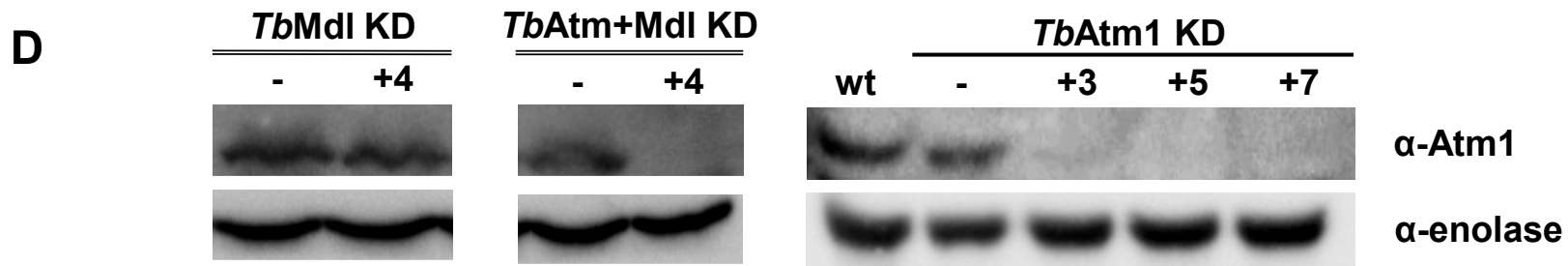


**Fig. 2**

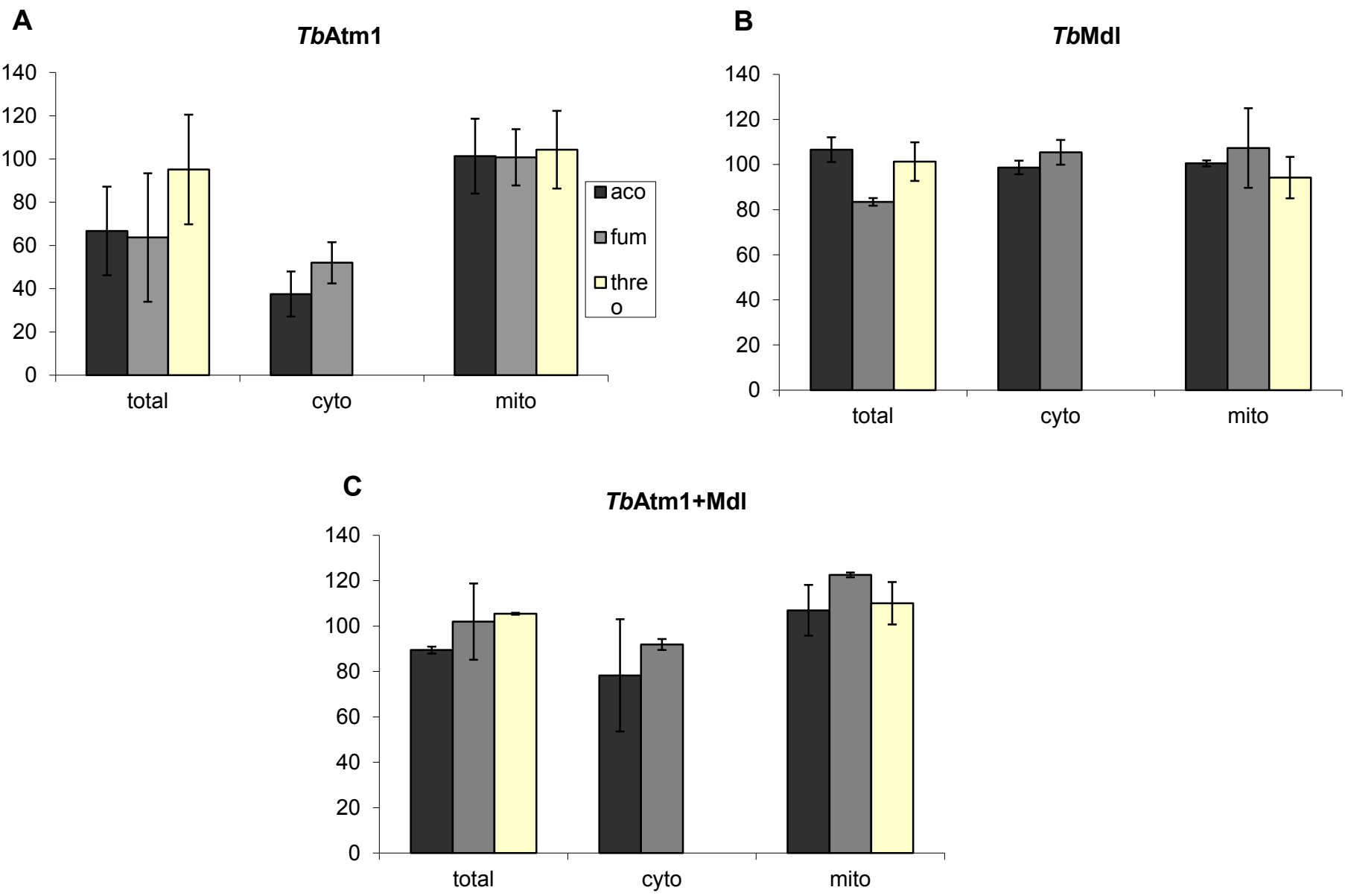




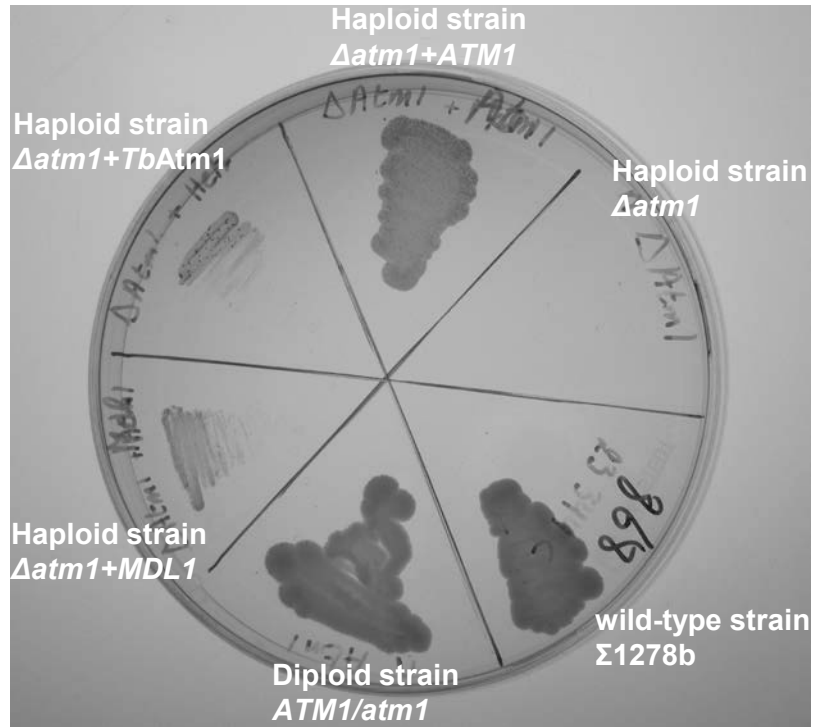
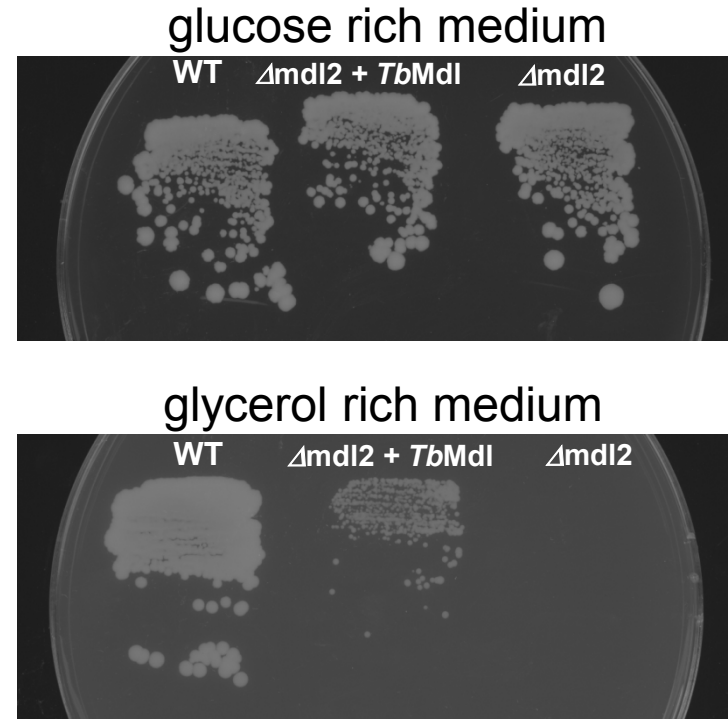
**Fig. 3**



**Fig. 3**



**Fig. 4**

**A****B****Fig. 5**

### **3.6 Functional analysis of putative heme transporter *TbHrg* in *T.brucei***

(unpublished data)

## Functional analysis of putative heme transporter *TbHrg* in *T.brucei*

In 2012 Huynh and colleagues identified a putative heme transporter gene in the genome of *Leishmania amazonensis* genome (Lhr1, *leishmania heme response 1*) (Huynh *et al.*, 2012). They also found homologs in other trypanosomatids including *T. brucei* (Tb927.8.6010). We decided to study the function of this gene in *T. brucei* and dissect its putative function as a heme transporter in our model organism.

### Characterization of heme transporter in *T. brucei*

Here we named the putative heme transporter in *T.brucei* *TbHrg* (trypanosome heme responsive gene). The *TbHrg* has 26% identity and 42% similarity with *L.amazonensis* Lhr1. Amino acid sequences analysis by MINOU (<http://minnou.cchmc.org/>) reveals four predicted transmembrane domains (TMD) similarly to *Leishmania* Lhr1 and CeHrg-4 from *C. elegans* (Fig. 1). Even though the *TbHrg* lacks the conserved histidine residue between TMD 3 and 4, it contains conserved histidine in the TMD 2, which is essential for heme transportation in *C. elegans* as well as in humans (Yuan *et al.*, 2012).

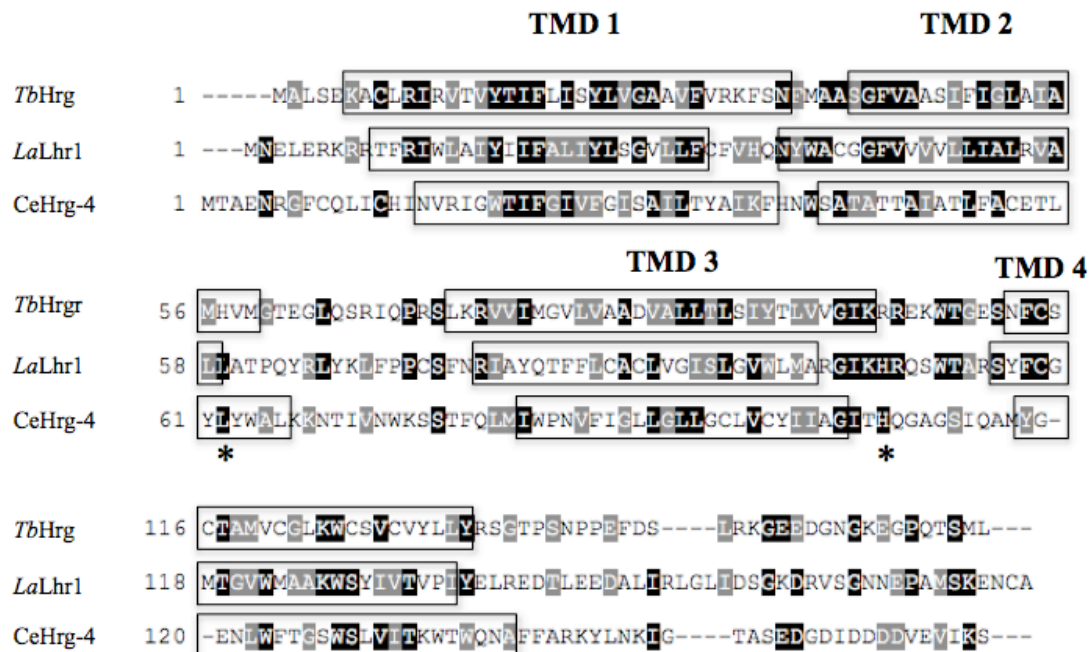


**Fig.1. Multiple sequence alignment of heme responsive genes.**

Sequence of *T. brucei* (*TbHrg*, TriTrypDB accession # Tb927.8.6010), *L. amazonensis* (Lhr1, Genbank accession # CBZ27556) and *C. elegans* (Hrg-4, WormBase Gene ID WBGene00009493) were used in this alignment generated by ClustalW (<http://www.ch.embnet.org/software/ClustalW.html>). Boxshade ([http://www.ch.embnet.org/software/BOX\\_form.html](http://www.ch.embnet.org/software/BOX_form.html)) was used to highlight the identical domains. Rectangular frames shows transmembrane domains (TMD) predicted by

MINOU(<http://minnou.cchmc.org/>) in *TbHrg*. The TMDs in LaLhr1 and CeHrg-4 are adapted from Huynh *et al.*, 2012. Asterisks indicate conserved histidine residues.

### *Depletion of TbHrg causes growth defect in limited heme B*

In order to explore the function(s) of *TbHrg*, we generated inducible *TbHrg*-depleted RNAi cell lines. Fragment of *TbHrg* was cloned into the vector P2T7-177 containing opposing T7 promoters. The construct was linearized by *NotI* and subsequently electroporated into *T. brucei* 29-13 (PS) and *T. brucei* Lister 427 (BS). RNAi was induced by the addition of tetracycline to the medium. Based on previous studies from *C. elegans* (Rajagopal *et al.*, 2008), we decided to test the viability of the cells in two different conditions: i/ in the high heme medium, where the cells are cultivated in standard SDM 79, which contains 7.5 mg/l hemin (=heme B; +hemin) and ii/ in the low heme (-hemin) medium with no hemin added. It has to be mentioned here, that the low heme medium does not completely lack heme B, since 10%FBS routinely added to the medium supplements at least trace amount of heme B.

When cultured in the high heme medium, the PS cells depleted for *TbHrg* did not show any significant growth defect as compared to the non-induced control (Fig. 2A). In contrast, the proliferation of the same cell line was significantly reduced in the low heme medium after tetracycline induction (Fig. 2B).

Functionality of RNAi was monitored by Northern blot analysis (Fig. 2C). The *TbHrg* transcript was undetectable using a radioactively labeled probe, with only double stranded RNA present in the RNAi-induced cells. This represents only an indirect prove of functional RNAi, as the actual decrease of *TbHrg* mRNA could not have been detected. Therefore, we decided to confirm the depletion of *TbHrg* by quantitative real time PCR (Fig. 2D). At day 4, almost 80% drop in *TbHrg* mRNA level upon RNAi induction cells as compared to the non-induced level, was deemed sufficient for the follow-up phenotypical studies.

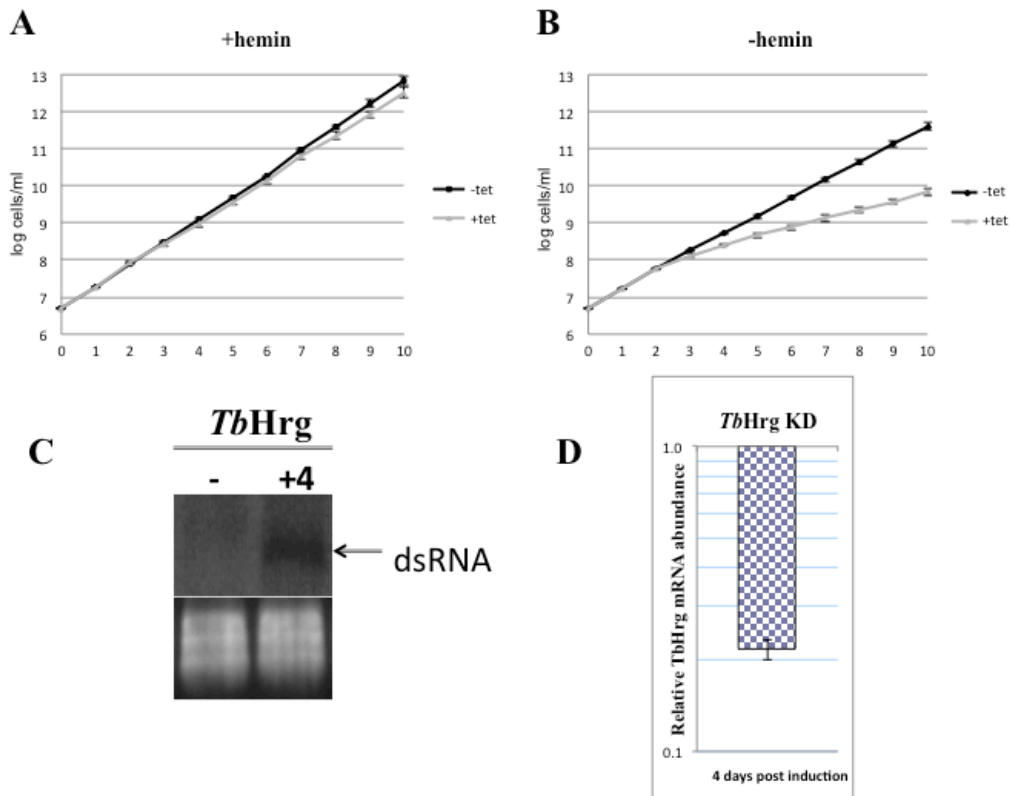


**Fig. 2. Missing *TbHrg* affects viability of cells in low heme medium**

Growth curves of the non-induced (-tet; black line) and t RNAi- induced (+tet; grey line) cells. The cells were grown in high heme medium (A; +hemin) or in low heme medium (B; -hemin). Cell densities were measured every day using the Beckman Z2 cell counter. Total RNA from the induced and non-induced cells was harvested 4 days after the induction. The presence of double stranded RNA (dsRNA) in the RNAi-induced cells was visualized by Northern blot analysis (C), ethidium bromide stained rRNA was used as a loading control. Quantitative real-time PCR was performed in order to analyze relative change in *TbHrg* mRNA abundance upon tetracycline induction (D). 18S rRNA was used as an internal reference.

#### *Depletion of TbHrg decreases cellular heme content*

Due to the lack of heme biosynthesis in *T. brucei*, the cells have to acquire heme from an external source. *T. brucei* obtains heme A most likely by taking up heme B from the environment, which is then converted to heme O and subsequently to heme A in the mitochondrion (Kořený *et al.*, 2013). This pathway was reported only in closely related *T. cruzi*, (Buchensky *et al.*, 2010; Tripodi *et al.*, 2011), but never directly in *T. brucei*. In order to investigate effect on cellular hemes upon the depletion of *TbHrg*, we employed HPLC analysis, following a protocol described elsewhere (Kořený *et al.*, 2012). This enables us to measure the amount of heme A and heme B separately. Heme B was decreased by 30% in *TbHrg*-depleted cells grown in the high heme medium, and the drop was even more pronounced in the low heme medium, where it went down by 60% (Fig. 3A.). Interestingly, the amount of heme A in the high heme medium was unaltered in the *TbHrg* knock-down, while in



the low heme medium a significant decrease by 60 % occurred (Fig. 3A.). Such a discrepancy can be explained by two considerations. First, even though heme B is lower in the high heme medium, there is still sufficient amount of heme A being produced in the cell (Fig. 3B), which may not be the case in the low heme medium, where there is simply not enough heme B as a substrate for heme A synthesis. It may also explain the lack of growth defect in *TbHrg* depleted cells in the former condition. We also hypothesize that the cells may have some control mechanism monitoring the proportion of heme A to heme B. The ratio of heme A/ heme B is quite stable in both heme conditions (around 10 and 35, respectively), regardless of whether the cells are ablated for *TbHrg* or not (Fig. 3C.).

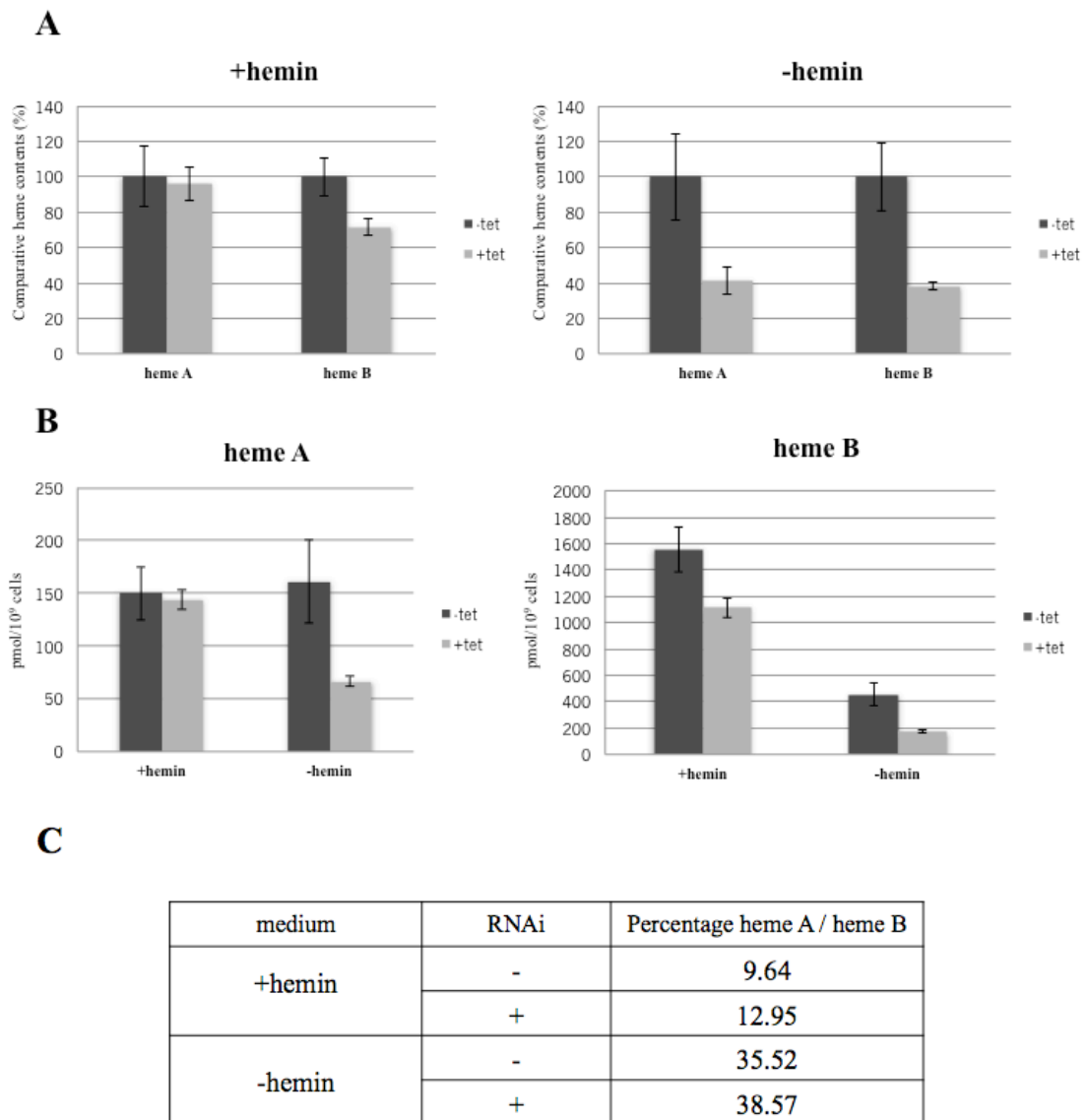


Fig. 3. Effect of *TbHrg* depletion on heme A and heme B content, monitored by HPLC.

A. Relative heme content in the non-induced (dark grey columns) and RNAi-induced (light grey columns) cells. Heme content in the non-induced cells was set as 100%. Heme content of cells grown in high heme and in low heme condition is showed in the left panel and the right panel, respectively.  
B. Heme A (left panel) and heme B (right panel) content represented in pmol/10<sup>9</sup> cells.  
C. Percentage of heme A/heme B in each sample.

### Preliminary conclusions

In this work we studied a putative heme transporter *TbHrg* in *T. brucei*, a homolog of *L. amazonensis* heme transporter Lhr1. Even though similarity of those two homologs is rather low, the preliminary results indicated that *TbHrg* is fulfilling its putative function as a heme transporter in *T. brucei*. Although depletion of *TbHrg* did not cause growth defect when cells were grown in the high heme medium, the heme B content was decreased. In the low heme medium, the depletion of *TbHrg* led to reduced proliferation together with decreased heme content. Since this is project in progress, more experiments are needed to consolidate the data and validate the role of *TbHrg* in heme transportation. In order to explore the localization of this protein, we have prepared cell lines expressing the ectopic copy of V5-tagged *TbHrg*. We are also going to monitor the affect on growth phenotype and heme content in the *TbHrg* RNAi bloodstream stage. Moreover, we plan to examine the heme uptake using radioactive heme in both procyclic and bloodstream *TbHrg* RNAi cell lines.

### References

- Buchensky, C., Almirón, P., Mantilla, B.S., Silber, A.M., and Cricco, J.A. (2010) The *Trypanosoma cruzi* proteins TcCox10 and TcCox15 catalyze the formation of heme A in the yeast *Saccharomyces cerevisiae*. *FEMS Microbiol Lett* **312**: 133–141.
- Huynh, C., Yuan, X., Miguel, D.C., Renberg, R.L., Protchenko, O., Philpott, C.C., *et al.* (2012) Heme Uptake by *Leishmania amazonensis* is mediated by the transmembrane protein LHR1. *PLoS Pathog* **8**: e1002795.
- Kořený L., Sobotka R., Kovářová J., Gnipová A., Flegontov P., Horváth A., Oborník M., Ayala F.J., Lukeš J. (2012) Aerobic kinetoplastid flagellate *Phytomonas* does not require heme for viability. *PNAS* **109**: 3808-3813.
- Kořený L., Oborník M., Lukeš J. (2013) Make it, take it or leave it: heme metabolism of parasites. *PLoS Pathogens* **9**: e1003088.
- Rajagopal, A., Rao, A.U., Amigo, J., Tian, M., Upadhyay, S.K., Hall, C., *et al.* (2008) Haem homeostasis is regulated by the conserved and concerted functions of HRG-1 proteins. *Nature* **453**: 1127–1131.
- Tripodi, K.E.J., Menendez Bravo, S.M., and Cricco, J.A. (2011) Role of heme and

heme-proteins in trypanosomatid essential metabolic pathways. *Enzyme Research* **2011**: 1–12.

Yuan, X., Protchenko, O., Philpott, C.C., and Hamza, I. (2012) Topologically conserved residues direct heme transport in HRG-1-related proteins. *J Biol Chem* **287**: 4914–4924.

## 5. Conclusions

This Ph.D. thesis is composed of three published papers, one submitted paper and unpublished results. All presented data deal with proteins in the parasitic protist *Trypanosoma brucei* functioning in iron-sulfur (Fe-S) cluster biogenesis and related processes such as tRNA thiolation and iron and heme homeostasis. Fe-S cluster assembly in *T. brucei* as in other eukaryotes is a complex mechanism involving numerous players that function in the mitochondrion or in the cytoplasm, but possibly also in other compartments. I focused primarily on the Fe-S assembly proteins present in the organelle such as cysteine desulfurase Nfs, scaffold protein Isu, Isa1 and Isa2, Isd11, ferredoxins and the putative transporter Atm1. In collaboration with my colleagues, we show that Nfu, Isu and Isd11 are essential not only for the Fe-S cluster biogenesis, but also for tRNA thiolation in both the mitochondrion and the cytosol, unlike Isa1 and Isa2, the depletion of which has impact only on the mitochondrion. Atm1 seems to connect Fe-S assembly machineries in the mitochondrion and the cytosol.

Recently, contradicting results were published about the human ferredoxin 2 (hFdx2) and its role in Fe-S biogenesis. We provided evidence that the heterologously expressed human Fdx2 is able to rescue enzymatic activities of Fe-S proteins in *T. brucei* depleted for endogenous ferredoxin, strongly supporting the function of hFdx2 in Fe-S assembly. The thesis also demonstrates for the first time that the Fe-S clusters are efficiently assembled even in the bloodstream stage flagellates with rudimentary mitochondrion. Interestingly, we are able to detect Nfs and Isu proteins in the nucleolus in both life cycle stages, which represents a novel localization for both highly conserved and wide spread eukaryotic proteins. Finally, my preliminary results indicate that a putative transporter, *TbHrg*, has a potential to be a key player in heme uptake in heme auxotroph *T. brucei*.

## 6. References

- Adam, A.C., Bornhövd, C., Prokisch, H., Neupert, W., and Hell, K. (2006) The Nfs1 interacting protein Isd11 has an essential role in Fe/S cluster biogenesis in mitochondria. *EMBO J* **25**: 174–183.
- Alfonzo, J.D., and Lukeš, J. (2011) Assembling Fe/S-clusters and modifying tRNAs: ancient co-factors meet ancient adaptors. *Trends Parasitol* **27**: 235–238.
- Ali, V., Shigeta, Y., Tokumoto, U., Takahashi, Y., and Nozaki, T. (2004) An intestinal parasitic protist, *Entamoeba histolytica*, possesses a non-redundant nitrogen fixation-like system for iron-sulfur cluster assembly under anaerobic conditions. *J Biol Chem* **279**: 16863–16874.
- Anzenbacher, P., and Anzenbacherova, E. (2001) Cytochromes P450 and metabolism of xenobiotics. *Cell Mol Life Sci* **58**: 737–747.
- Balk, J., Aguilar Netz, D.J., Tepper, K., Pierik, A.J., and Lill, R. (2005) The essential WD40 protein Cia1 is involved in a late step of cytosolic and nuclear iron-sulfur protein assembly. *Mol Cell Biol* **25**: 10833–10841.
- Barros, M.H. (2002) Mitochondrial ferredoxin is required for heme A synthesis in *Saccharomyces cerevisiae*. *J Biol Chem* **277**: 9997–10002.
- Barton, R.M. and Worman, H.J. (1999) Prenylated prelamin A interacts with Narf, a novel nuclear protein. *J Biol Chem* **274**: 30008–30018.
- Bayeva, M., Khechaduri, A., Wu, R., Burke, M.A., Wasserstrom, J.A., Singh, N., et al. (2013) ABCB10 regulates early steps of heme synthesis. *Circ Res*.
- Beale, S.I. (1999) Enzymes of chlorophyll biosynthesis. *Photosynthesis Research* **60**: 43–73.
- Beinert, H. (1997) Iron-sulfur clusters: Nature's modular, multipurpose structures. *Science* **277**: 653–659.
- Beinert, H., Kennedy, M.C., and Stout, C.D. (1996) Aconitase as iron-sulfur protein, enzyme, and iron-regulatory protein. *Chem Rev* **96**: 2335–2374.
- Bernard, D.G., Cheng, Y., Zhao, Y., and Balk, J. (2009) An allelic mutant series of ATM3 reveals its key role in the biogenesis of cytosolic iron-sulfur proteins in *Arabidopsis*. *Plant Physiol* **151**: 590–602.
- Besteiro, S., Barrett, M.P., Rivière, L., and Bringaud, F. (2005) Energy generation in insect stages of *Trypanosoma brucei*: metabolism in flux. *Trends Parasitol* **21**: 185–191.
- Biederbick, A., Stehling, O., Rösser, R., Niggemeyer, B., Nakai, Y., Elsässer, H.-P., and Lill, R. (2006) Role of human mitochondrial Nfs1 in cytosolic iron-sulfur protein biogenesis and iron regulation. *Mol Cell Biol* **26**: 5675–5687.

- Booker, S.J., Cicchillo, R.M., and Grove, T.L. (2007) Self-sacrifice in radical S-adenosylmethionine proteins. *Curr Opin Chem Biol* **11**: 543–552.
- Braz, G.R., Coelho, H.S., Masuda, H., and Oliveira, P.L. (1999) A missing metabolic pathway in the cattle tick *Boophilus microplus*. *Curr Biol* **9**: 703–706.
- Bringaud, F., Rivière, L., and Coustou, V. (2006) Energy metabolism of trypanosomatids: Adaptation to available carbon sources. *Mol Biochem Parasitol* **149**: 1–9.
- Bych, K., Netz, D.J.A., Vigani, G., Bill, E., Lill, R., Pierik, A.J., and Balk, J. (2008) The essential cytosolic iron-sulfur protein Nbp35 acts without Cfd1 partner in the green lineage. *J Biol Chem* **283**: 35797–35804.
- Camaschella, C., Campanella, A., Falco, L. De, Boschetto, L., Merlini, R., Silvestri, L., *et al.* (2007) The human counterpart of zebrafish shiraz shows sideroblastic-like microcytic anemia and iron overload. *Blood* **110**: 1353–8
- Cavadini, P., Biasiotto, G., Poli, M., Levi, S., Verardi, R., Zanella, I., *et al.* (2007) RNA silencing of the mitochondrial ABCB7 transporter in HeLa cells causes an iron-deficient phenotype with mitochondrial iron overload. *Blood* **109**: 3552–3559.
- Changmai, P., Horáková, E., Long, S., Černotíková-Stříbrná, E., McDonald, L.M., Bontempi, E.J., and Lukeš, J. (2013) Both human ferredoxins equally efficiently rescue ferredoxin deficiency in *Trypanosoma brucei*. *Mol Microbiol* **89**: 135–151.
- Chaudhuri, M., Ott, R.D., and Hill, G.C. (2006) Trypanosome alternative oxidase: from molecule to function. *Trends Parasitol* **22**: 484–491.
- Chaloupková, M., Reaves, S.K., LeBard, L.M., and Koeller, D.M. (2004) The mitochondrial ABC transporter Atm1p functions as a homodimer. *FEBS Letters* **569**: 65–69.
- Chelikani, P., Fita, I., and Loewen, P.C. (2004) Diversity of structures and properties among catalases. *Cell Mol Life Sci* **61**: 192–208.
- Clayton, C.E. (2002) Life without transcriptional control? From fly to man and back again. *EMBO J* **21**: 1881–1888.
- Cuervo, P., Fernandes, N., and Jesus, J.B. de (2011) A proteomics view of programmed cell death mechanisms during host--parasite interactions. *Journal of Proteomics* **75**: 246–256.
- Duncan, R., Faggart, M.A., and Cornell, N.W. (1997) Phylogenetic analysis of the 5-aminolevulinate synthase gene. *Biol Bull* **193**: 247–248.
- Flannery, A.R., Huynh, C., Mitra, B., Mortara, R.A., and Andrews, N.W. (2011) LFR1 ferric iron reductase of *Leishmania amazonensis* is essential for the generation of infective parasite forms. *J Biol Chem* **286**: 23266–23279.

- Furuyama, K., Kaneko, K., and Vargas, P.D., V (2007) Heme as a magnificent molecule with multiple missions: heme determines its own fate and governs cellular homeostasis. *J exp med* **213**(1):1-16.
- Gari, K., León Ortiz, A.M., Borel, V., Flynn, H., Skehel, J.M., and Boulton, S.J. (2012) MMS19 links cytoplasmic iron-sulfur cluster assembly to DNA metabolism. *Science* **337**: 243–245.
- Gaud, A., Carrington, M., Deshusses, J., and Schaller, D.R. (1997) Polymerase chain reaction-based gene disruption in *Trypanosoma brucei*. *Mol Biochem Parasitol* **87**: 113–115.
- Gill, E.E., Diaz-Triviño, S., Barberà, M.J., Silberman, J.D., Stechmann, A., Gaston, D., *et al.* (2007) Novel mitochondrion-related organelles in the anaerobic amoeba *Mastigamoeba balamuthi*. *Mol Microbiol* **66**: 1306–1320.
- Goldberg, A.V., Molik, S., Tsaousis, A.D., Neumann, K., Kuhnke, G., Delbac, F., *et al.* (2008) Localization and functionality of microsporidian iron-sulphur cluster assembly proteins. *Nature* **452**: 624–628.
- Guerinot, M.L. (2000) The ZIP family of metal transporters. *Biochim Biophys Acta* **1465**: 190-198.
- Huynh, C., Sacks, D.L., and Andrews, N.W. (2006) A *Leishmania amazonensis* ZIP family iron transporter is essential for parasite replication within macrophage phagolysosomes. *J Exp Med* **203**: 2363–2375.
- Huynh, C., Yuan, X., Miguel, D.C., Renberg, R.L., Protchenko, O., Philpott, C.C., *et al.* (2012) Heme uptake by *Leishmania amazonensis* is mediated by the transmembrane protein LHR1. *PLoS Pathog* **8**: e1002795.
- Iannuzzi, C., Adinolfi, S., Howes, B.D., Garcia-Serres, R., Clémancey, M., Latour, J.-M., *et al.* (2011) The role of CyaY in iron sulfur cluster assembly on the *E. coli* IscU scaffold protein. *PLoS ONE* **6**: e21992.
- Ito, S., Tan, L.J., Andoh, D., Narita, T., Seki, M., Hirano, Y., *et al.* (2010) MMXD, a TFIIH-independent XPD-MMS19 protein complex involved in chromosome segregation. *Mol Cell* **39**: 632–640.
- Kakuta, Y., Horio, T., Takahashi, Y., and Fukuyama, K. (2001) Crystal structure of *Escherichia coli* Fdx, an adrenodoxin-type ferredoxin involved in the assembly of iron-sulfur clusters. *Biochemistry* **40**: 11007–11012.
- Kispal, G., Csere, P., Prohl, C., and Lill, R. (1999) The mitochondrial proteins Atm1p and Nfs1p are essential for biogenesis of cytosolic Fe/S proteins. *EMBO J* **18**: 3981–3989.
- Klinge, S., Hirst, J., Maman, J.D., Krude, T., and Pellegrini, L. (2007) An iron-sulfur domain of the eukaryotic primase is essential for RNA primer synthesis. *Nat Struct Mol Biol* **14**: 875–877.

- Kořený, L., Lukeš, J., and Oborník, M. (2010) Evolution of the haem synthetic pathway in kinetoplastid flagellates: An essential pathway that is not essential after all? *Int J Parasitol* **40**: 149–156.
- Kořený, L., Sobotka, R., Janouškovec, J., Keeling, P.J., and Oborník, M. (2011) Tetrapyrrole synthesis of photosynthetic chromerids is likely homologous to the unusual pathway of apicomplexan parasites. *The Plant Cell* **23**: 3454–3462.
- Kořený, L., Sobotka, R., Kovářová, J., Gnipová, A., Flegontov, P., Horváth, A., *et al.* (2012) Aerobic kinetoplastid flagellate *Phytomonas* does not require heme for viability. *Proc. Natl Acad. Sci. USA* **109**: 3808–3813.
- Kou, H., Zhou, Y., Gorospe, R.M.C., and Wang, Z. (2008) Mms19 protein functions in nucleotide excision repair by sustaining an adequate cellular concentration of the TFIIH component Rad3. *Proc. Natl Acad. Sci. USA* **105**: 15714–15719.
- K P Chang, C.S.C.S.S. (1975) Heme biosynthesis in bacterium-protozoon symbioses: enzymic defects in host hemoflagellates and complementary role of their intracellular symbiotes. *Proc Natl Acad Sci USA* **72**: 2979.
- Krishnamurthy, G., Vikram, R., Singh, S.B., Patel, N., Agarwal, S., Mukhopadhyay, G., *et al.* (2005) Hemoglobin receptor in *Leishmania* is a hexokinase located in the flagellar pocket. *J Biol Chem* **280**: 5884–5891.
- Krishnamurthy, P.C., Du, G., Fukuda, Y., Sun, D., Sampath, J., Mercer, K.E., *et al.* (2006) Identification of a mammalian mitochondrial porphyrin transporter. *Nature* **443**: 586–589.
- Kuhnke, G., Neumann, K., Mühlenhoff, U., and Lill, R. (2006) Stimulation of the ATPase activity of the yeast mitochondrial ABC transporter Atm1p by thiol compounds. *Mol Membr Biol* **23**: 173–184.
- Kumar, B., Chaubey, S., Shah, P., and Tanveer, A. (2011) Interaction between sulphur mobilisation proteins SufB and SufC: Evidence for an iron–sulphur cluster biogenesis pathway in the apicoplast of *Plasmodium falciparum*. *Int J Parasitol* **41**: 991–999.
- Lange, H., Lisowsky, T., Gerber, J., Mühlenhoff, U., Kispal, G., and Lill, R. (2001) An essential function of the mitochondrial sulfhydryl oxidase Erv1p/ALR in the maturation of cytosolic Fe/S proteins. *EMBO* **2**: 715–720.
- Lauder, S., Bankmann, M., Guzder, S.N., Sung, P., Prakash, L., and Prakash, S. (1996) Dual requirement for the yeast MMS19 gene in DNA repair and RNA polymerase II transcription. *Mol Cell Biol* **16**(12): 6783–93.
- Lukeš, J., Hashimi, H., and Zíková, A. (2005) Unexplained complexity of the mitochondrial genome and transcriptome in kinetoplastid flagellates. *Curr Genet* **48**: 277–299.



- Mach, J., Tachezy, J., and Šuťák, R. (2013) Efficient iron uptake via a reductive mechanism in procyclic *Trypanosoma brucei*. *J Parasitol* **99**: 363–364.
- Malkin, R., and Rabinowitz, J.C. (1966) The reconstitution of clostridial ferredoxin. *Biochem Biophys Res Commun.* **23(6)**: 822-7.
- Mauro Degli Esposti, E.F.D.Z. (1985) Functional characterization and partial purification of the ubiquinol-cytochrome *c* oxidoreductase from higher plant mitochondria (*Helianthus tuberosus*). *Plant Physiol* **77**: 758.
- Miao, R., Kim, H., Koppolu, U.M.K., Ellis, E.A., Scott, R.A., and Lindahl, P.A. (2009) Biophysical characterization of the iron in mitochondria from Atm1p-depleted *Saccharomyces cerevisiae*. *Biochemistry* **48**: 9556–9568.
- Moraes, C.T., Diaz, F., and Barrientos, A. (2004) Defects in the biosynthesis of mitochondrial heme *c* and heme *a* in yeast and mammals. *Biochimica et biophysica acta* **1659**: 153–9
- Mortenson, L.E., Valentine, R.C., and Carnahan, J.E. (1962) An electron transport factor from. *Biochem Biophys Res Commun.* **7**: 448–452.
- Mühlenhoff, U. (2003) Components involved in assembly and dislocation of iron-sulfur clusters on the scaffold protein Isu1p. *EMBO J* **22**: 4815–4825.
- Netz, D.J.A., Pierik, A.J., Stümpfig, M., Bill, E., Sharma, A.K., Pallesen, L.J., *et al.* (2012) A bridging [4Fe-4S] cluster and nucleotide binding are essential for function of the Cfd1-Nbp35 complex as a scaffold in iron-sulfur protein maturation. *J Biol Chem* **287**: 12365–12378.
- Netz, D.J.A., Pierik, A.J., Stümpfig, M., Mühlenhoff, U., and Lill, R. (2007) The Cfd1–Nbp35 complex acts as a scaffold for iron-sulfur protein assembly in the yeast cytosol. *Nat Chem Biol* **3**: 278–286.
- Netz, D.J.A., Stith, C.M., Stümpfig, M., Köpf, G., Vogel, D., Genau, H.M., *et al.* (2011) Eukaryotic DNA polymerases require an iron-sulfur cluster for the formation of active complexes. *Nat Chem Biol* **8**: 125–132.
- Nývltová, E., Šuťák, R., Harant, K., Šedinová, M., Hrdý, I., Pačes, J., Vlček, Č., Tachezy, J. (2013) NIF-type iron-sulfur cluster assembly system is duplicated and distributed in the mitochondria and cytosol of *Mastigamoeba balamuthi*. *Proc Natl Acad Sci USA* **110(18)**: 7371-6.
- Okada, K. (2009) The novel heme oxygenase-like protein from *Plasmodium falciparum* converts heme to bilirubin IX alpha in the apicoplast. *FEBS Letters* **583**: 313–319.
- Pal, J.K., and Joshi-Purandare, M. (2001) Dose-dependent differential effect of hemin on protein synthesis and cell proliferation in *Leishmania donovani* promastigotes cultured *in vitro*. *J Biosci* **26**: 225–231.

- Paris, Z., Changmai, P., Rubio, M.A.T., Zíková, A., Stuart, K.D., Alfonzo, J.D., and Lukeš, J. (2010) The Fe/S cluster assembly protein Isd11 is essential for tRNA thiolation in *Trypanosoma brucei*. *J Biol Chem* **285**: 22394–22402.
- Patel, N., Singh, S.B., Basu, S.K., and Mukhopadhyay, A. (2008) *Leishmania* requires Rab7-mediated degradation of endocytosed hemoglobin for their growth. *Proc Natl Acad Sci USA* **105**: 3980–3985.
- Pays, E. (2005) Regulation of antigen gene expression in *Trypanosoma brucei*. *Trends Parasitol* **21(11)**: 517-20.
- Perutz, M.F. (1942) X-ray analysis of haemoglobin. *Nature* **151**: 714-716.
- Pondarre, C. (2006) The mitochondrial ATP-binding cassette transporter Abcb7 is essential in mice and participates in cytosolic iron-sulfur cluster biogenesis. *Hum Mol Genet* **15**: 953–964.
- Py, B., and Barras, F. (2010) Building Fe–S proteins: bacterial strategies. *Nat Rev Micro* **8**: 436–446.
- Qi, W., Li, J., Chain, C.Y., Pasquevich, G.A., Pasquevich, A.F., and Cowan, J.A. (2012) Glutathione complexed Fe–S centers. *J Am Chem Soc* **134**: 10745–10748.
- R Cammack, J.M.P. (1977) Iron-sulphur centres in mitochondria from *Arum maculatum* spadix with very high rates of cyanide-resistant respiration. *Biochem J* **166**: 347–355.
- Rajagopal, A., Rao, A.U., Amigo, J., Tian, M., Upadhyay, S.K., Hall, C., *et al.* (2008) Haem homeostasis is regulated by the conserved and concerted functions of HRG-1 proteins. *Nature* **453**: 1127–1131.
- Rao, A.U., Carta, L.K., Lesuisse, E., and Hamza, I. (2005) Lack of heme synthesis in a free-living eukaryote. *Proc Natl Acad Sci USA* **102**: 4270–4275.
- Richards, T.A., and van der Giezen M. (2006) Evolution of the Isd11–IscS complex reveals a single  $\alpha$ -proteobacterial endosymbiosis for all eukaryotes. *Mol Biol Evol* **23(7)**:1341-4.
- Rodríguez-Manzaneque, M.T., Tamarit, J., Bellí, G., Ros, J., and Herrero, E. (2002) Grx5 is a mitochondrial glutaredoxin required for the activity of iron/sulfur enzymes. *Molecular biology of the cell* **13**: 1109–21
- Sah, J.F., Ito, H., Kolli, B.K., Peterson, D.A., Sassa, S., and Chang, K.-P. (2002) Genetic rescue of *Leishmania* deficiency in porphyrin biosynthesis creates mutants suitable for analysis of cellular events in uroporphyrin and for photodynamic therapy. *J Biol Chem* **277**: 14902–14909.
- Saiki, K., Mogi, T., Ogura, K., and Anraku, Y. *In vitro* heme O synthesis by the cyoE gene product from *Escherichia coli*. *J Biol Chem* **268**: 26041 -26045.

- Schenkman, J.B., and Jansson, I. (2003) The many roles of cytochrome b5. *Pharmacol Ther* **97**: 139–152.
- Schnauffer, A., Clark-Walker, G.D., Steinberg, A.G., and Stuart, K. (2005) The F1-ATP synthase complex in bloodstream stage trypanosomes has an unusual and essential function. *EMBO J* **24**: 4029–4040.
- Seeber, F., and Soldati-Favre, D. (2010) Metabolic pathways in the apicoplast of apicomplexa. *Int Rev Cell Mol Biol* **281**: 161–228.
- Sengupta, S., Tripathi, J., Tandon, R., Raje, M., Roy, R.P., Basu, S.K., and Mukhopadhyay, A. (1999) Hemoglobin endocytosis in *Leishmania* is mediated through a 46-kDa protein located in the flagellar pocket. *J Biol Chem* **274**: 2758–2765.
- Sipos, K. (2002) Maturation of cytosolic iron-sulfur proteins requires glutathione. *J Biol Chem* **277**: 26944–26949.
- Song, D., and Lee, F.S. (2008) A role for IOP1 in mammalian cytosolic iron-sulfur protein biogenesis. *J Biol Chem* **283**: 9231–9238.
- Srinivasan, V., Netz, D.J.A., Webert, H., Mascarenhas, J., Pierik, A.J., Michel, H., and Lill, R. (2007) Structure of the yeast WD40 domain protein Cia1, a component acting late in iron-sulfur protein biogenesis. *Structure* **15**: 1246–1257.
- Stehling, O., and Lill, R. (2013) The role of mitochondria in cellular iron-sulfur protein biogenesis: mechanisms, connected processes, and diseases. *Cold Spring Harb Perspect Biol* **5**.
- Stehling, O., Mascarenhas, J., Vashisht, A.A., Sheftel, A.D., Niggemeyer, B., Rösser, R., *et al.* (2013) Human CIA2A-FAM96A and CIA2B-FAM96B integrate iron homeostasis and maturation of different subsets of cytosolic-nuclear iron-sulfur proteins. *Cell Metabolism* **18**: 187–198.
- Stehling, O., Vashisht, A.A., Mascarenhas, J., Jonsson, Z.O., Sharma, T., Netz, D.J.A., *et al.* (2012) MMS19 assembles iron-sulfur proteins required for DNA metabolism and genomic integrity. *Science* **337**: 195–199.
- Suzuki, T., Akiyama, S., Fujimoto, S., Ishikawa, M., and Nakao, Y. (1976) The aconitase of yeast. IV. Studies on iron and sulfur in yeast aconitase. *J Biochem* **80**: 799–804.
- Takahashi, Y., and Tokumoto, U. (2002) A third bacterial system for the assembly of iron-sulfur clusters with homologs in archaea and plastids. *J Biol Chem* **277**: 28380–28383.
- Thon, G., Baltz, T., Giroud, C., and Eisen, H. (1990) Trypanosome variable surface glycoproteins: composite genes and order of expression. *Genes & Development* **4**: 1374–1383.
- Toh, S.Q., Glanfield, A., Gobert, G.N., and Jones, M.K. (2010) Heme and blood-feeding parasites: friends or foes? *Parasites & vectors*. **18**: 108.

- Tokumoto, U. (2004) Interchangeability and distinct properties of bacterial Fe-S cluster assembly systems: Functional replacement of the isc and suf operons in *Escherichia coli* with the nifSU-Like operon from *Helicobacter pylori*. *J Biochem* **136**: 199–209.
- Tong, W.-H., and Rouault, T.A. (2006) Functions of mitochondrial ISCU and cytosolic ISCU in mammalian iron-sulfur cluster biogenesis and iron homeostasis. *Cell Metabolism* **3**: 199–210.
- Tsai, C.-L., and Barondeau, D.P. (2010) Human frataxin is an allosteric switch that activates the Fe–S cluster biosynthetic complex. *Biochemistry* **49**: 9132–9139.
- Vanhollebeke, B., De Muylder, G., Nielsen, M.J., Pays, A., Tebabi, P., Dieu, M., *et al.* (2008) A haptoglobin-hemoglobin receptor conveys innate immunity to *Trypanosoma brucei* in humans. *Science* **320**: 677–681.
- Vernis, L., Facca, C., Delagoutte, E., Soler, N., Chanet, R., Guiard, B., *et al.* (2009) A newly identified essential complex, Dre2-Tah18, controls mitochondria integrity and cell death after oxidative stress in yeast. *PLoS ONE* **4**: e4376.
- Wang, Z. (2000) Inhibition of *Trypanosoma brucei* gene expression by RNA interference using an integratable vector with opposing T7 promoters. *J Biol Chem* **275**: 40174–40179.
- White, C., Yuan, X., Schmidt, P.J., Bresciani, E., Samuel, T.K., Campagna, D., *et al.* (2013) HRG1 is essential for heme transport from the phagolysosome of macrophages during erythrophagocytosis. *Cell Metabolism* **17**: 261–270.
- Wickstead, B., Ersfeld, K., and Gull, K. (2002) Targeting of a tetracycline-inducible expression system to the transcriptionally silent minichromosomes of *Trypanosoma brucei*. *Mol Biochem Parasitol* **125**: 211–216.
- Wiedemann, N., Urzica, E., Guiard, B., Müller, H., Lohaus, C., Meyer, H.E., *et al.* (2006) Essential role of Isd11 in mitochondrial iron-sulfur cluster synthesis on Isu scaffold proteins. *EMBO J* **25**: 184–195.
- Wingert, R.A., Galloway, J.L., Barut, B., Foott, H., Fraenkel, P., Axe, J.L., *et al.* (2005) Deficiency of glutaredoxin 5 reveals Fe-S clusters are required for vertebrate haem synthesis. *Nature* **436**: 1035–39
- Wirtz, E., Leal, S., Ochatt, C., and Cross, G.A. (1999) A tightly regulated inducible expression system for conditional gene knock-outs and dominant-negative genetics in *Trypanosoma brucei*. *Mol Biochem Parasitol* **99**: 89–101.
- Yoon, T., and Cowan, J.A. (2003) Iron-sulfur cluster biosynthesis. Characterization of frataxin as an iron donor for assembly of [2Fe-2S] clusters in ISU-type proteins. *J Am Chem Soc* **125**: 6078–6084.

Yuan, X., Protchenko, O., Philpott, C.C., and Hamza, I. (2012) Topologically conserved residues direct heme transport in HRG-1-related proteins. *J Biol Chem* **287**: 4914–4924.

Ye, H., Jeong, S.Y., Ghosh, M.C., Kovtunovych, G., Silvestri, L., Ortillo, D., *et al.* (2010) Glutaredoxin 5 deficiency causes sideroblastic anemia by specifically impairing heme biosynthesis and depleting cytosolic iron in human erythroblasts. *The Journal of clinical investigation* **120**: 1749–61

## 6. Curriculum vitae

Name: Piya Changmai

Date and place of birth: 23. October 1982

Email: jibjibboy@yahoo.com

### Education and employment

- 2001-2004 B.Sc. (Biotechnology), Faculty of Science, Mahidol University - Thailand
- April 2004 Internship, Applied Research Team, Effem food (Thailand)
- October 2004 – February 2005 Internship, Department of Molecular Genetics, Faculty of Biotechnology, Jagiellonian University- Kraków, Poland
- 2005 Research assistant, project “ Bioactive secondary metabolites from endophytic fungi of Thai medicinal plants”, Faculty of Science, Mahidol University and Faculty of Pharmaceutical Sciences, Chulalongkorn University.
- 2007-2009 M.Sc. (Molecular and cell biology) Faculty of Sciences, University of South Bohemia – České Budějovice, Czech Republic.
- 2010-present Ph.D. student (Molecular and cell biology) Faculty of Sciences, University of South Bohemia – České Budějovice, Czech Republic.

### Publications

- Paris, Z., **Changmai, P.**, Rubio, M.A.T., Zíková, A., Stuart, K.D., Alfonzo, J.D., and Lukeš, J. (2010) The Fe/S cluster assembly protein Isd11 is essential for tRNA thiolation in *Trypanosoma brucei*. *J Biol Chem* **285**: 22394–22402.
- Long S, **Changmai P**, Tsaousis AD, Skalicky T, Verner Z, Wen YZ, Roger AJ, Lukes J (2011) Stage-specific requirement for Isa1 and Isa2 proteins in the mitochondrion of *Trypanosoma brucei* and heterologous rescue by human and *Blastocystis* orthologues. *Mol Microbiol* **81**:1403–1418.
- **Changmai, P.**, Horáková, E., Long, S., Černotíková-Stříbrná, E., McDonald, L.M., Bontempi, E.J., and Lukeš, J. (2013) Both human ferredoxins equally efficiently rescue ferredoxin deficiency in *Trypanosoma brucei*. *Mol Microbiol* **89**: 135-151.

### Presentations

- Changmai, P., Paris, Z., Lukeš, J. Role in Fe-S cluster biogenesis of *TbAtm1* in *Trypanosoma brucei*. The 7<sup>th</sup> Mitochondrial Physiology conference (Oberurgl, Austria 27.09.10 – 1.10.10)
- Changmai, P., Salmon, D., Paris, Z., Lukeš. Functional analysis of *TbAtm1* and *TbMdl* in *Trypanosoma brucei*. 4<sup>th</sup> Congress of the BioIron society (Vancouver, Canada 22.05.11 – 26.05.13)
- Both human ferredoxins equally efficiently rescue ferredoxin deficiency in *Trypanosoma brucei*. 5<sup>th</sup> Congress of the BioIron society (London, UK 14.04.13 – 18.04.13)